Studies on selection of controlled variables

by

Vidar Alstad

A Thesis Submitted for the Degree of Dr. Ing.

Department of Chemical Engineering
Norwegian University of Science and Technology

March 2005

NTNU
Norwegian University of
Science and Technology

ISBN 82-471-7058-2 (printed)
ISBN 82-471-7057-4 (electronic)

Dr. Ing. thesis 2005:91

Abstract

Increased competition in the process industries requires optimal operation and better utilization of raw materials and energy. One strategy for achieving improved production is to use real-time optimization (RTO), based on measured disturbances and process measurements. The optimal solution is usually implemented by updating setpoints to the control system which task is to keep the controlled variables at the setpoint. Thus, the selection of controlled variables integrates the optimization and the control layer.

Selecting the right controlled variables can be of paramount importance. Many chemical processes are influenced by disturbances that are often *not* measured and where installing new measurements are not economically viable. Thus, finding controlled variables where the optimal value is insensitive to disturbances could eliminate the need of estimating these disturbances online and would reduce the need of frequent setpoint updates. The use of feedback control introduces implementation errors. It is important to select controlled variables that are insensitive to implementation errors. The "optimal" implementation would be to use a dynamic optimizer which, based on full information of the disturbances and the plant outputs, calculates the optimal inputs. In practice, control systems have a hierarchical structure, where different layers operate on different time scales. Thus, the selection of controlled variables (which links these layers together) is important.

The ideal situation is to have self-optimizing controlled variables where operation remains near-optimal in presence of disturbances and implementation errors using constant setpoints. This work puts emphasis on methods for selecting such self-optimizing controlled variables. We base the selection of controlled variables on an economic measure of the operation. We assume that the setpoints are nominally optimal, and we propose the null space method for selecting controlled variables as a combination of measurements. The selection of the controlled variables is based on the optimal sensitivity matrix from the disturbances to the measurements. This information can easily be provided by using experiments or a model of the plant. The main focus, is to find controlled variables that yield good self-optimizing properties with respect to disturbances. The method uses local information, however, several case studies have shown that the operation is near-optimal in a wider region of the disturbance space.

To generalize the null space method, we propose a method for selecting measurements that minimizes the effect of implementation errors on the economic performance for the resulting control structure. Based on the derivation of the null space method, we propose a simple procedure for finding controlled variables using the null space method. The procedure is split in two: First, we select measurements that are insensitive to measurement error. Second, we combine these measurements to form the self-optimizing control structure.

Further, we discuss how non-optimal nominal points affect the selection of controlled variables for self-optimizing control. We find that the selection of controlled variables is unaffected by non-optimal nominal points, and that the average increase in loss is independent of what we select to control.

Another contribution is to provide several case studies where the null space method is compared with previously proposed methods for selecting controlled variables. The null space method is illustrated on a Petlyuk distillation column for separation of ternary mixtures. We find that the null space method yields a control structure with acceptable steady-state and dynamic performance. Other cases studied are an evaporator process and oil and gas production networks.

Finally, we show that for the Petlyuk distillation column it is energetically optimal to over-fractionate one of the products. This surprising result is discussed and expressions for the possible savings are derived.

Acknowledgements

There are a lot of people who deserves credit for in some way or other helping me during my studies and to finish this thesis. I would like to gratefully acknowledge the enthusiastic supervision of professor Sigurd Skogestad during this work. Without his support and contributions, this thesis would never have emerged.

I thank my previous and present colleagues at the Process Control group for sharing their wisdom which has inspired and enlightened me. Special thanks go to Jens Strandberg and Vinay Kariwala for proof-reading and invaluable comments on the manuscript.

Sincere thanks go to Espen Storkaas, with whom I was fortunate to share office during my graduate studies.

The Research Council of Norway, Norsk Hydro ASA and ABB are acknowledged for financing this work and the support through the Petronics research programme.

Thanks to my family, for all their help and support and for always believing in me.

Finally, I would like to thank my wife Guri for the endless support and understanding during all these years. This thesis would not have been possible without you. Together we have become parents of the most loveliest child ever, Gaute. To him I dedicate this thesis.

Vidar Alstad

Trondheim, March, 2005

Table of Contents

Chapter 1

Introduction

In this chapter the thesis is restricted, the work motivated and placed in a wider perspective. An overview of the thesis and a list of the publications emerging from this thesis are given. Related work is discussed in Chapter 2.

1.1 Motivation and focus

Increasing demands for efficient operation and improved utilization of energy and raw materials in chemical processes require more knowledge and understanding of the dynamics and the steady-state operation of the processes. Increased efficiency often implies a more complex control system. Much work has gone into designing more complex controllers (i.e. H_∞/H_2-control, Model predictive control and Non-linear control) to improve the dynamics of a process. In most cases, the process outputs (controlled variables) are assumed known. However, in many systems it is not clear why specific outputs are controlled, and we need to ask questions such as: "Which variables should be controlled, which variables should be measured, which inputs should be manipulated, and which links should be made between them" (Foss, 1973).

In particular, the issue of selecting controlled variables has received little attention in the literature. The focus in this thesis is on the *implementation* of optimal operation, and the goal is to find a set of controlled variables which, when kept at constant setpoints, indirectly leads to near-optimal operation with acceptable steady-state economic performance (loss). This is denoted "self-optimizing control". We restrict the selection of controlled variables to the steady-state, since the economics in most cases are primarily decided by the steady-state operation (Skogestad, 2000).

Self-optimizing control follows the ideas of Morari et al. (1980) and Skogestad and Postlethwaite (1996). The basis is to define the quality of operation in terms of a scalar cost J. To achieve truly optimal operation, we would need to measure all disturbances, and we would need to solve the optimization problem online. This is unrealistic for many chemical processes, and the question is if it is possible to find a simpler implementation that retains satisfactory economic performance. The simplest operation would result if we could select controlled variables such that the operation remains acceptable with constant setpoints, thus turning the optimization problem into a simple feedback problem.

The main contribution of this thesis is a new method for selecting controlled variables which we denote as *the null space method*. The idea is to utilize the freedom of selecting controlled variables as combination of measurements, and to find the combination of measurements that yields near-optimal operation. The selection is based on defining a steady-state economic measure of the process to be minimized.

1.2 Thesis overview

In Chapter 2 we discuss previous work on self-optimizing control. We also discuss alternative methods for optimizing control.

Chapter 3 introduces the null space method for selecting controlled variables for self-optimizing control. The focus is on optimal selection of controlled variables in presence of unmeasured disturbances. We illustrate the method on a simple blending example. The null space method has been applied in several case studies later in the thesis, e.g. the Petlyuk distillation column (Chapter 8), an evaporator case (Chapter 11) and two cases related to offshore production of oil and gas (Chapter 10).

Chapter 4 generalizes the null space method to include implementation error. The focus is on reducing the sensitivity to measurement errors. We present a procedure for selecting the best subset of measurements for the null space method and illustrate the method on a CSTR-example. The case studies of Chapter 8 and Chapter 11 also illustrate the ideas presented in this chapter. Appendix B supplement this chapter. In Appendix C a paper on indirect control is included, where the candidate was third author. Indirect control can be seen as a sub-problem of self-optimizing control.

Chapter 5 discusses how to discriminate between important and unimportant disturbances for self-optimizing control and we present rules which can help discriminate between disturbances.

In Chapter 6 we discuss the effect of having non-optimal nominal setpoints, and how this affects the loss and internal rank between candidate controlled variables.

Chapter 7 discusses the dynamics of controlling measurement combinations. We show that controlling measurement combinations may lead to performance limitations such as right-half plane zeros, and we propose a simple rule for avoiding such behavior.

In Chapters 8 and 9 we discuss the Petlyuk distillation column. Chapter 8 focuses on the selection of controlled variables for self-optimizing control. The null space method is compared with alternative methods for selecting controlled variables. Dynamic simulations where we use a decentralized control structure are included.

In Chapter 8 we find that it is optimal to over-fractionate one of the product streams of the Petlyuk distillation column in order to *save* energy. This is discussed in Chapter 9, where we explain why this is possible and we derive expressions for the possible savings. We also discuss the possibility of bypassing some of the feed to further reduce the energy requirements.

In Chapter 10 and 11 we include additional case studies for self-optimizing control. In Chapter 10 we discuss the selection of control structures for two cases related to offshore oil and gas production. Appendix D supplements this chapter with the model equations. In Chapter 11 we discuss a simple evaporator case, which has been used in previous studies on self-optimizing control. Appendix E supplements this chapter with the model equations.

Chapter 12 sums up and concludes the thesis. Finally, we discuss directions for further work.

1.3 Publications

Chapter 3 and 8

Alstad, V. and Skogestad, S.: Robust Operation by controlling the right variable combination, AIChE Annual meeting, Paper 247g, Indianapolis, 3-8 Nov. 2002.

Alstad, V. and Skogestad, S.: Combinations of measurements as controlled variables: Application to a Petlyuk distillation column, International Symposium of Advanced Control of Chemical Processes (Adchem-2003), Hong Kong, 11-14 Jan. 2004.

Chapter 4

Alstad, V. and Skogestad, S.: Self-optimizing control: Optimal measurement selection, AIChE Annual Meeting, Austin, Texas, Nov. 2004, Poster 403e

Chapter 9

Alstad, V. and Skogestad, S.: Optimal operation of Petlyuk distillation column: Energy savings by over-fractionating, Proc. European Symposium on Computer Aided Process Engineering (ESCAPE-14), 16-19 May 2004, Lisbon, Portugal. Published by Elsevier, ISBN 0-444-51694-8, pp. 547-552.

Chapter 10

Case 1: Alstad, V. and Skogestad, S.: Combination of Measurements as Controlled Variables for Self-Optimizing Control, Proc. European Symposium on Computer Aided

Process Engineering (ESCAPE-13), 01-04 June 2003, Lappeenranta, Finland. Published by Elsevier, ISBN 0-444-51368-X, pp. 353-358.

Case 2: Presented at Petronics Workshop - 2004: "Joining Petroleum, Multiphase Flow, Chemical and Control Engineering", June 15-16, 2004, Trondheim, Norway.

Chapter 11

Presented at 12th Nordic Process Control Workshop (NPCW), August 19-22, Göteborg, Sweden.

Co-authored

Storkaas, E. , Skogestad, S. and Alstad, V.: Stabilizing of desired flow regimes in pipelines, AIChE Annual meeting, Paper 287d, Reno, Nevada, November 5-9, 2001.

Halvorsen, I.J., Skogestad, S., Morud, J.C. and Alstad, V.: Optimal selection of controlled variables, Ind. Eng. Chem. Res., 42 (14), 3273-3284 (2003).

Hori, E.S. , Skogestad, S. and Alstad, V.: Perfect steady-state indirect control,
Ind. Eng. Chem. Res, In press. (See Appendix C)

Bibliography

Foss, C. (1973). Critique of chemical process control theory. *AIChE Journal*, 19(2):209–214.

Morari, M., Stephanopoulos, G., and Arkun, Y. (1980). Studies in the synthesis of control structures for chemical processes. Part I: Formulation of the problem, process decomposition and the classification of the controller task. Analysis of the optimizing control structures. *AIChE Journal*, 26(2):220–232.

Skogestad, S. (2000). Plantwide control: The search for the self-optimizing control structure. *J. Proc. Control*, 10:487–507.

Skogestad, S. and Postlethwaite, I. (1996). *Multivariable Feedback Control*. John Wiley & Sons.

Chapter 2

Brief overview of control structure design and methods for ensuring optimal operation

This chapter contains a short overview of different methods for ensuring optimal operation with special emphasis on self-optimizing control. We discuss control structure design in general and how the control structure is linked to optimization.

2.1 Control structure design

Control structure design is the strategy of selecting which variables to control, which variables to measure, which inputs to manipulate and which links that should be made between them. Control structure design go back at least to the work of Foss (1973), where he criticized the control community for the gap between theory and practice. Later, the series of papers by Morari & co-workers (Morari et al., 1980a,b,c) on control structure design, hierarchical control and multilevel optimization, introduced new and exciting ideas and theories. While the area of control structure design has received some interest in the literature, it cannot be compared to the enormous amount of work on controller design, although control structure design is probably the most important in practice.

2.1.1 Plantwide control

Plantwide control deals with the overall control philosophy of the plant, with emphasis on structural decisions such as (Skogestad, 2000):

1. Selection of controlled variables and setpoints (c and c_s)
2. Selection of measured variables (y)
3. Selection of manipulated variables (u)
4. Selection of control configurations (the structure interconnecting measurements and manipulated variables)
5. Selection of type of controller (the control law)

The focus of this thesis is on selection of controlled variables and measurements. A typical control system is organized in a hierarchical structure, see Figure 2.1, divided

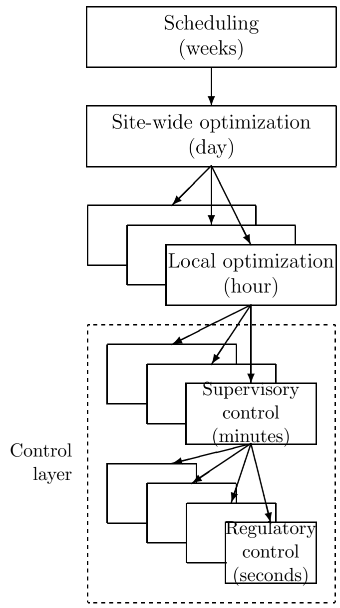

Figure 2.1: *Typical control system hierarchy in chemical plants (Skogestad and Postlethwaite, 1996)*

in several layers that operate on different time-scales:

1. *Scheduling* (weeks): Typically manual and offline, based on higher level economic models.
2. *Site-wide optimization* (days): Manual, semi-manual or fully automated. Often based on steady-state models. Typically a RTO (real-time optimizer).
3. *Local optimization* (hours): Manual, semi-manual or fully automated, often online.
4. *Control layer* (minutes and seconds): Often divided into two levels with *primary controlled variables* (supervisory control) and *secondary controlled variables* (regulatory control). The primary controlled variables deal with slow actions while the secondary controlled variables deal with stabilization and fast dynamics in order to achieve acceptable dynamic performance.

Control structure design is a subtask of the plantwide control procedure, see Larsson and Skogestad (2000) for a review on plantwide control. An important aspect of the control structure design is the selection of the controlled variables. Here, we focus on the interaction between the local optimization layer and the control layer as depicted in Figure 2.2. Typically, two classes of systems exist:

- *Constrained*: At the optimal point all degrees of freedom are used for satisfying constraints.
- *Fully of partially unconstrained*: One or more of the degrees of freedom are unconstrained for some or all disturbances.

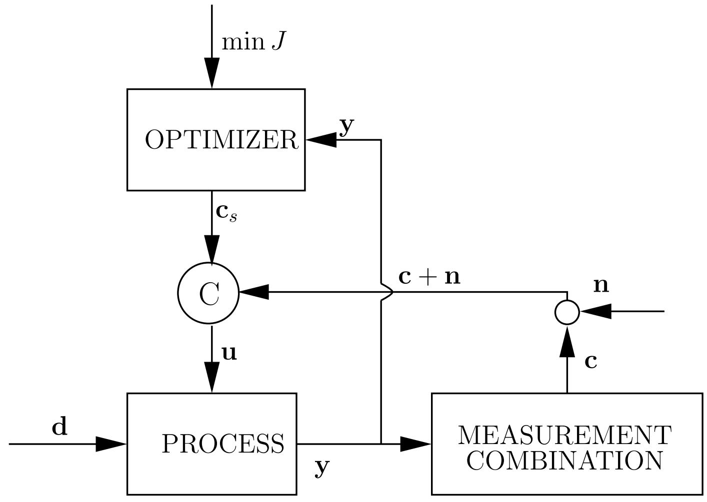

Figure 2.2: *A typical optimization structure incorporating local feedback. The process is disturbed (**d**) and the control system tries to keep the controlled variables (**c**) at their setpoints ($\mathbf{c}_s$) with accompanied noise* **n**. *The optimizer estimates the disturbance from the measurements and, based on a model of the plant, new optimal setpoints are found and implemented in the local feedback loop.*

For the constrained variables, active constraint control is used for controlling the optimally active constraints (Maarleveld and Rijnsdorp, 1970). If the constraints are not measurable, indirect measurements can be used to infer the actual value of the constraint, see Appendix C. For the active constraints, the optimal value does not change with respect to the disturbances. Examples of typical active constraints in chemical plants are:

- Maximum throughput of a unit (e.g. compressor load).
- Maximum temperature in reactor.
- Minimum composition for distillate products.

In case that the set of optimally active constraints change due to disturbances, an adaptive active constraint policy can be used (Arkun and Stephanopoulos, 1980). Constraints may be categorized, depending on the nature of the constraint. Typically we have:

- *Hard constraints*: Constraints that cannot be violated
- *Soft constraints*: Constraints that can be violated dynamically, while satisfied at steady-state.

For the unconstrained degrees of freedom, the optimal values are determined by an optimization of the plant and it is not clear what to control or what the control objectives are.

One approach is to adjust the inputs in an “open-loop” manner and use an online optimization to calculate new inputs based on a model of the plant and estimated disturbances. The alternative approach of self-optimizing control, is to use constant setpoints for the variables, that is, with no online optimization taking place. The idea is that the feedback from the process will detect the disturbances and adjust the remaining degrees of freedom in an optimal manner.

2.2 Policies for optimal operation for systems with uncertainty

Below we present a short overview of different methods for ensuring optimal operation for systems operating under uncertainty. This is by no means a complete review of all possible methods. For more information on each method see the references.

2.2.1 Experimental methods

For simple systems, experimental methods may be applied for finding the optimal operation of a system with uncertain and unknown parameters (Box, 1957). This requires carefully designed experiments and the possibility to measure or infer the objective function (Marlin, 2000). For most continuous systems, experimental methods are not applicable due to the disturbance frequency (require frequent experiments). The experiments are often resource intensive and disturb the normal operation. For systems with parametric uncertainties (model uncertainty) experimental methods may be applicable, e.g. for finding the degree of deactivation of catalysts.

Adaptive extremum seeking control

Adaptive extremum seeking control is an “experimental optimization” technique that, by imposing an excitation signal on the process, drives the process to the optimum. Thus, the identification of the state of the process and the optimal inputs to impose are combined. For an overview of extremum seeking control, see Ariyur and Krstic (2003).

Most of the work on extremum seeking control assume that the objective function is directly measurable. Guay and Zhang (2003) provide a new algorithm where the objective function is not measurable. However, they require explicit information on the structure of the objective function (how it depends on the states and disturbances).

In Guay and Zhang (2003) extremum seeking controllers are developed to drive the system states to the desired setpoints that optimize the value of an objective function. The proposed adaptive extremum seeking controller is ”inverse optimal” (El-Farra and Christofides, 2001) in the sense that it minimizes a meaningful cost function that incorporates a penalty on both the performance error and control action. Krstic and Wang (2000) consider systems where the structure of the objective function is not known.

Some fundamental requirements must be present in order to guarantee stability and extremum attenuation. The most important is the convexity of the disturbance space to guarantee that the estimation of the unknown parameters converge to the true value. A drawback of the proposed method is that an excitation signal must be introduced in the system in order for the extremum seeking controller to converge to the true optimal point. In effect, the excitation signal introduces a disturbance to the plant, with accompanying input usage, which may be undesirable. In addition, finding the excitation function is not trivial, nor is the assumption of state feedback.

2.2.2 Model based methods

Model based methods require a dynamic or static model of the plant. The type of model may range from pure empirical models (step responses) to first-principle models.

Optimal control

In optimal control, no distinction is made between optimization and control (Stengel, 1993). The trajectories of the optimal input are calculated based on state and disturbance estimates by the use of a dynamic model of the plant. Ideally, this approach is optimal, but has the following drawbacks (Cao, 2004):

1. The open-loop solution can be provided only if a perfect dynamic model is available.
2. It is assumed that the disturbances are measurable and predictable (future disturbances are known).

The structural information in the controller comes from the dynamic model of the plant. Thus, optimal controllers are often more sensitive to modeling uncertainty, as compared to decentralized control structures (Skogestad and Hovd, 1995). In a decentralized control structure, structural information is supplied through the linking of controlled variables and inputs, and is typically not that sensitive to modeling errors. In addition, the cost of acquiring a detailed dynamic model is often prohibitive.

Real-time optimizing control

Real-time optimizing control (RTO), where optimal setpoints are calculated online based on online measurements and a process model, is a much used implementation for ensuring optimal operation of chemical plants (Marlin and Hrymak, 1997), see Figure 2.3. Real-time optimization often utilize a stationary model for the parameter estimation and optimization steps (Zhang et al., 2002, 2001), but also dynamic versions of the RTO-framework have been presented (Kadam et al., 2003).

RTO is well suited for site-wide optimization, see Figure 2.1. While much of the work in the RTO-literature has focused on the estimation and the optimization layers (Loeblein and Perkins, 1998), less work has focused on the interaction between the optimization and control layer (the controlled variables) (Marlin and Hrymak, 1997). Typically, more manipulated variables than controlled variables exist and a common approach is to use a model based controlled (e.g. MPC) to implement the RTO output which is a combination of setpoints for the controlled variables and the inputs. Thus, the inputs without any accompanied control objective are controlled in an “open loop”

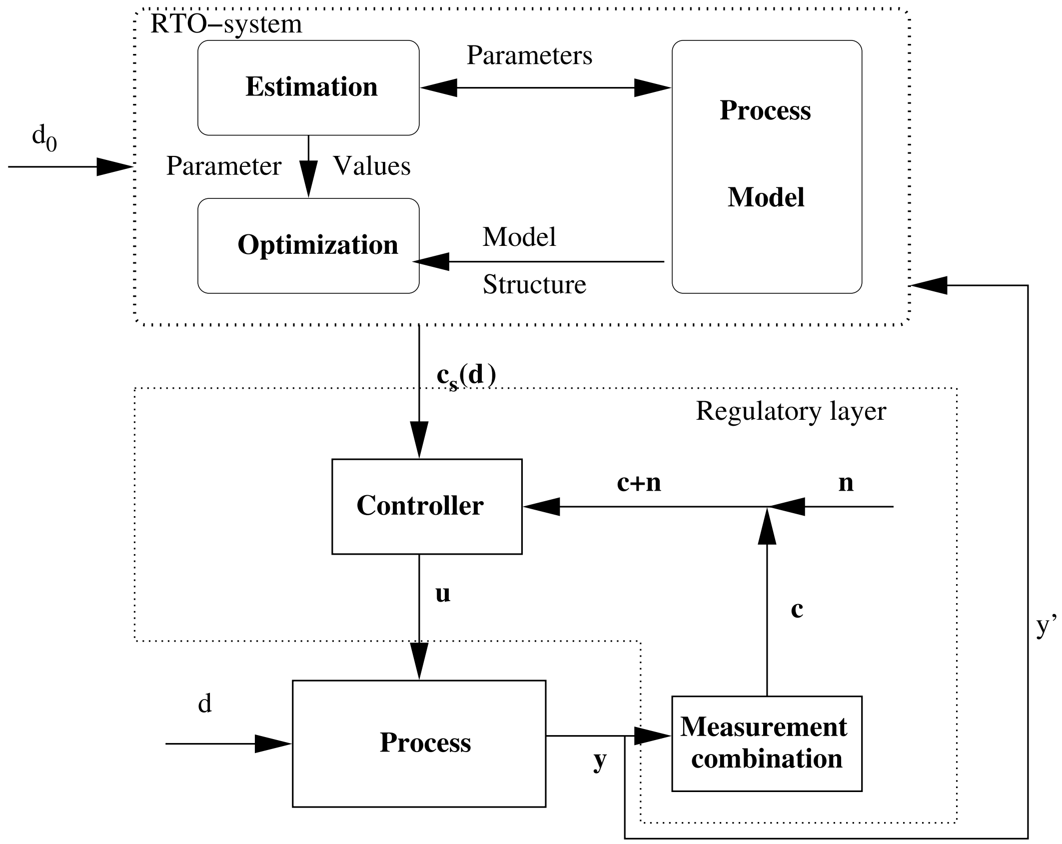

Figure 2.3: *Real-time optimization structure where, based on measurements from the process y' and a model of the process, uncertain parameters d are estimated and fed through the optimizer, which in turn calculates new optimal setpoints c_s.*

manner. The real-time optimization structure is complex since both the data reconciliation, the model update and the optimization must be performed online. In addition, the RTO requires a large and detailed model of the plant. If possible, a preferred structure would be to have a high-level model for the RTO, while the local optimization in each sub-unit could be achieved by the use of simple feedback control.

Model predictive control

Model predictive control (MPC) has received much attention in the control community over the last couple of decades and numerous industrial implementations exist (Qin and Badgwell, 2003). Traditional MPC is a real-time optimization implementation, where we need to solve an optimization online, and the same drawbacks as discussed above apply. The benefit of MPC is that a dynamic cost function is minimized online and an optimal input trajectory is calculated using a model of the plant.

The great flexibility in formulating the objective function for the MPC controller, gives a powerful method for optimizing control. However, MPC is usually used for setpoint control, where an optimization layer (RTO) gives the optimal setpoints to use for varying disturbances. If the disturbances are measured, this can be included in the MPC framework (Robust MPC, see Camacho and Bordons (1998)).

Recent work on explicit MPC (Pistikopoulos et al., 2000; Grancharova et al., 2004), where an explicit state feedback controller is calculated offline is a promising approach. The state space is divided into regions, where, in each region, a state feedback control law is valid. However, the need of state feedback and the fact that the method scales poorly, limits its applicability in typical chemical processes where the number of states can be large. One major advantage of explicit MPC is that no online optimization is necessary.

2.3 Self-optimizing control

Self-optimizing control follows the ideas of Morari et al. (1980a) and is the use of feedback to compensate and drive the process to the optimal steady-state. The key in self-optimizing control is to find controlled variables that, when kept at constant setpoints, indirectly keep the inputs optimal (indirect optimizing control). A model is most often needed in the analysis part, which can be performed offline. When the control structure has been decided, no model is needed online. This approach is fundamentally different from the RTO approach, where the optimal operation of the plant is achieved by changing the setpoints to the control system, and the information of the structure of the problem (cost function) is implemented online. In self-optimizing control, the structure of the optimization problem is utilized in making *structural* decisions on the controlled variables.

Self-optimizing control (Skogestad, 2000) *is when acceptable operation (small* ***loss****) can be achieved using constant setpoints* $\mathbf{c_s}$ *for the controlled variables* $\mathbf{c}$ *(without the need to re-optimize when disturbances occur).*

The loss is defined as the difference between the value of the objective function using constant setpoints and the true optimal value of the objective function:

$$L = J(\mathbf{c_s} + \mathbf{n}, \mathbf{d}) - J^{opt}(\mathbf{d}) \tag{2.1}$$

where $\mathbf{n}$ is the implementation error (measurement and setpoint error) in keeping the controlled variable at the setpoint $\mathbf{c} = \mathbf{c_s}$, J the cost function and $\mathbf{d}$ the disturbance. In general, the controlled variables can be expressed as

$$\mathbf{c}(\mathbf{u}, \mathbf{d}) = \mathbf{h}(\mathbf{y}(\mathbf{u}, \mathbf{d})) \tag{2.2}$$

where $\mathbf{h}$ is a vector valued function with respect to the measurements (y_i). The sources of uncertainties that contribute to the loss are:

1. **Disturbances** ($\mathbf{d}$): External unmeasured disturbances.

2. **Implementation error** ($\mathbf{n}$): Implementation error constitutes the measurement error and control error. Often the control error can be neglected if integral action is included in the controller.

Implementation error is always present in any control configuration; it is the error of implementing a certain policy. Thus, regardless of the method used for ensuring optimal operation (i.e. RTO or an optimal controller) the effect of implementation error must be taken into account. Often, an open-loop policy may give large losses since the difference between the calculated and implemented input may be large.

In self-optimizing control, we assume that optimally active constraints are controlled (Maarleveld and Rijnsdorp, 1970), and the problem is to find what to control for the remaining degrees of freedom (the optimization degrees of freedom, (Marlin, 2000)). We often simplify and call the optimally active constraints for the active constraints. For systems where the set of active constraints change with respect to the disturbances, special care must be taken to ensure that the active set of constraints are controlled (Arkun and Stephanopoulos, 1980; Cao, 2004).

2.3.1 Optimal operation

In general, the optimal input trajectory can be found by solving a non-linear dynamic optimization problem:

$$\min_{\mathbf{x}_0,\mathbf{u}_0} \int_{t=0}^{T} J(t,\mathbf{x}_0,\mathbf{u}_0,\mathbf{d})dt \tag{2.3}$$

subject to

$$\begin{aligned}
&\dot{\mathbf{x}}_0 = \mathbf{f}(\mathbf{x}_0,\mathbf{u}_0,\mathbf{d})\\
&\mathbf{g}(\mathbf{x}_0,\mathbf{u}_0,\mathbf{d}) \leq 0\\
&\mathbf{x}_{0|t=0} = \mathbf{x}_0^0\\
&\mathbf{y}_0 = \mathbf{f}_{y_0}(\mathbf{x}_0,\mathbf{u}_0,\mathbf{d})
\end{aligned} \tag{2.4}$$

where $\mathbf{x}_0 \in \mathcal{R}^{n_{x_0}}$ is the vector of internal dependent variables (states), $\mathbf{u}_0 \in \mathcal{R}^{n_{u_0}}$ the vector of manipulated variables, $\mathbf{d} \in \mathcal{R}^{n_d}$ vector of external disturbances, $\mathbf{y}_0 \in \mathcal{R}^{n_{y_0}}$ the measurements and J a scalar objective function (cost). The equality constraint vector ($\mathbf{f}$) corresponds to state equations (model equations), while the inequality constraint vector ($\mathbf{g}$) corresponds to process constraints (safety, environmental or process limitations).

In order to solve the dynamic optimization problem given in eqs. (2.3-2.4), one needs to have a prediction of the future disturbances. Here, the focus is on slow varying disturbances, and we make a pseudo steady-state assumption such that the dynamic optimization problem is reduced to its steady-state equivalent:

$$\min_{\mathbf{x}_0,\mathbf{u}_0} J_0(\mathbf{x}_0,\mathbf{u}_0,\mathbf{d}) \tag{2.5}$$

subject to

$$\begin{aligned} \mathbf{f}(\mathbf{x}_0, \mathbf{u}_0, \mathbf{d}) &= 0 \\ \mathbf{g}(\mathbf{x}_0, \mathbf{u}_0, \mathbf{d}) &\leq 0 \\ \mathbf{y}_0 &= \mathbf{f}_{y0}(\mathbf{x}_0, \mathbf{u}_0, \mathbf{d}) \end{aligned} \tag{2.6}$$

At the nominal optimum $(\mathbf{u}_0^*, \mathbf{d}^*)$, a subset $(\mathbf{g}')$ of the inequality constraints will be active (with $\mathbf{g}' = 0$). The considerations here are of local nature and we assume that the set of active constraints do not change (thus no additional constraints becomes active) and we can reduce the dimension of the problem by enforcing these inequality constraints $(\mathbf{g}' = 0)$.

Assumption: For all disturbances in the disturbance space $d \in \mathcal{D}$, it is assumed that the same set of inequality constraints $\mathbf{g}'$ is active, i.e. $\mathbf{g}' = 0 \ \forall \ \mathbf{d} \in \mathcal{D}$.

Clearly, for systems with a small disturbance window in which the set of active constraints remains constant, this assumption can be very restrictive.
Arkun and Stephanopoulos (1980) derive methods for handling varying active constraints in a decentralized control structure. Alternatively, a centralized approach can be used, e.g. model predictive control (Kadam et al., 2003).

We assume that the active constraints are measurable or that we can infer the constraints from indirect measurements. Thus, a subset of the available free variables (u_0's) is used to fulfill these active constraints and the optimization problem is reduced to:

$$\begin{aligned} \min_{\mathbf{u}} J_0(\mathbf{x}, \mathbf{u}, \mathbf{d}) \\ \mathbf{f}'(\mathbf{x}, \mathbf{u}, \mathbf{d}) = 0 \\ \mathbf{y}_0 = \mathbf{f}_{y_0}(\mathbf{x}, \mathbf{u}\, \mathbf{d}) \end{aligned} \tag{2.7}$$

where $\mathbf{f}'^T = \begin{bmatrix} \mathbf{f} & \mathbf{g}' \end{bmatrix}$, $\mathbf{x}^T = \begin{bmatrix} \mathbf{x_0} & \mathbf{u}' \end{bmatrix}$ where $\mathbf{u}' \in \mathcal{R}^{n_{u'}}$ is the subset of the inputs used to fulfill the active constraints and $\mathbf{u} \in \mathcal{R}^{n_u}$ denotes the remaining unconstrained reduced space degrees of freedom. In controlling the active constraints $(\mathbf{g}' = 0)$, the inputs $\mathbf{u}'$ bound to controlling the active constraints depends on the remaining inputs $\mathbf{u}$ and disturbances $\mathbf{d}$, i.e. $\mathbf{u}' = \mathbf{u}'(\mathbf{u}, \mathbf{d})$.

The solution of the reduced space problem in (2.7), may be categorized in two classes. Let $n_{f'} = dim(\mathbf{f}')$.

1. If $n_u = n_{u_0} + (n_{x_0} - n_{f'}) = 0$, all degrees of freedom must be used to fulfill the active constraints and implementation is usually simple by using the ideas of active constraint control (Maarleveld and Rijnsdorp, 1970). This can be achieved by direct measurement of the constraint (e.g. a pressure constraint) or an indirect measurement.

2. If $n_u > 0$, we have unconstrained degrees of freedom at the optimal point and implementing the remaining degrees of freedom is not straightforward. The task of selecting what to control for the remaining degrees of freedom will be the focus in this work.

By formally eliminating the states ($\mathbf{x}$) by using the equality constraints ($\mathbf{f}' = 0$), the remaining unconstrained problem becomes:

$$\min_{\mathbf{u}} J(\mathbf{u}, \mathbf{d}) \tag{2.8}$$

$$\mathbf{y}_0 = \mathbf{f}_{y_0}(\mathbf{u}, \mathbf{d}) \tag{2.9}$$

In general J is not a simple function in the variables $\mathbf{u}$ and $\mathbf{d}$. We assume that online information about the system behavior is available from the measurements in the plant:

$$\mathbf{y_0} = \mathbf{f}_{y_0}(\mathbf{u}, \mathbf{d}) \tag{2.10}$$

where $\mathbf{y}_0$ denotes the vector of all measurements in the plant. The measurement vector $\mathbf{y}_0 \in \mathbf{R}^{n_{y_0}}$ generally also include the input vector $\mathbf{u}_0$, while the measurements used for controlling the active constraints (either directly or indirectly) are not included due to zero gain from u to y (when the active constraint loops are closed).

2.3.2 Optimal controlled variables

From eq. (2.2) the vector of controlled variables is given by:

$$\mathbf{c} = \mathbf{h}(\mathbf{y}) \tag{2.11}$$

where the function $\mathbf{h}$ is free to choose and $\mathbf{y} = \mathbf{f}_y(\mathbf{u}, \mathbf{d})$ is a subset of the available measurements $\mathbf{y}_0$. Inserting into eq. (2.11) yields

$$\mathbf{c} = \mathbf{h}(\mathbf{f}_y(\mathbf{u}, \mathbf{d})) = \mathbf{f}_c(\mathbf{u}, \mathbf{d}) \tag{2.12}$$

We assume that the number of controlled variables equals the number of optimization degrees of freedom $\mathbf{u}$ and by assuming that $\mathbf{f}_c$ is invertible, we have

$$\mathbf{u} = \mathbf{f}_c^{-1}(\mathbf{u}, \mathbf{d}) \tag{2.13}$$

where $\mathbf{f}_c^{-1}$ exists and is unique. Examples of possible controlled variables are:

- *Difference*: $h(\mathbf{y}) = y_1 - y_2$
- *Ratio*: $h(\mathbf{y}) = \frac{y_1}{y_2}$
- *Linear combination*: $h(\mathbf{y}) = h_1 y_1 + h_2 y_2 + h_3 y_3$
- *Open-loop*: $h(y) = u$

With feedback, we adjust $\mathbf{u}$ such that $\mathbf{c} = \mathbf{c}_s + \mathbf{n}$, where $\mathbf{n}$ is the implementation error. More precisely, the actual value of the controlled variable $\mathbf{c}$ differs from the optimal value due to:

1. **Setpoint error**:

$$\mathbf{v}(\mathbf{d}) \overset{\text{def}}{=} \mathbf{c_s} - \mathbf{c}^{opt} \tag{2.14}$$

and if the nominal point is optimal ($\mathbf{v}(\mathbf{d}^*) = 0$), the setpoint error is only affected by the disturbance $\mathbf{d}$

2. **Implementation error**:
   Implementation error is defined as:
   $$\mathbf{n} \stackrel{\text{def}}{=} \mathbf{c} - \mathbf{c}_s \tag{2.15}$$
   and is the sum of the measurement error and the control error. In this work, we assume that the implementation error can be modeled as additive. In most cases, we assume that the controllers have integral action such that the control error is negligible at steady-state. The implementation error for the open-loop candidate is often large because the actual implemented input $\mathbf{u}$ deviates from the setpoint $\mathbf{u}_s$ since no feedback is used.

The total error is
$$\mathbf{e}_c = \mathbf{c} - \mathbf{c}^{opt} = \mathbf{v}(\mathbf{d}) + \mathbf{n} \tag{2.16}$$
where the disturbances and the implementation errors are assumed independent. Thus, in order for a candidate controlled variable to be a good self-optimizing variable, both of the errors need to be small (small $\mathbf{v}(\mathbf{d})$ and $\mathbf{n}$).

In eq. (2.16) we added noise on the controlled variable, which makes sense if the controlled variables correspond to single measurements. Here, we make no restrictions on the function $\mathbf{h}$ so
$$\mathbf{n} = \mathbf{h}(\mathbf{n}_y) \tag{2.17}$$
where n_y is the measurement error on the individual measurements. In general the optimal self-optimizing controlled variables (the function $\mathbf{h}$) can be found by solving the following optimization problem.
$$\min_{\mathbf{h}} \int \cdots \int_{d\in\mathcal{D},\ n\in\mathcal{N}} J(\mathbf{u}, \mathbf{d}) \ \mathrm{d}\mathcal{N}\mathrm{d}\mathcal{D} \tag{2.18}$$
$$\mathbf{h}(\mathbf{y} + \mathbf{n}_y) - \mathbf{c_s} = 0 \tag{2.19}$$
where $\mathbf{y} \in \mathbf{y_0}$ and $\mathbf{u}$ is an implicit function of $\mathbf{h}$, $\mathbf{d}$, $\mathbf{c_s}$ and $\mathbf{n}$ and $\mathbf{c}_s = \mathbf{h}(\mathbf{y}^*)$ where $\mathbf{y}^*$ denotes the nominal value. The goal is to find the vector function $\mathbf{h}$ interconnecting the measurements and the controlled variables that minimize some average measure of the cost (J) taken over the disturbance and implementation error space.

We assume in this work that we use nominally optimal setpoints, but this can be relaxed by computing robust optimal setpoints in which we add the setpoints $\mathbf{c}_s$ as additional degrees of freedom in eq. (2.18) (Govatsmark and Skogestad, 2002). Several strategies for selection of setpoints exist, i.e. for ensuring both feasibility and performance. Feasibility is achieved by using robust optimization (Glemmestad et al., 1999) in which the setpoints selected must be feasible for all disturbances and implementation errors. In practice, feasibility is achieved by back-off from the active constraints and by selecting setpoint for the unconstrained controlled variables that give feasible inputs for all disturbances and implementation errors.

Instead of minimizing the average cost as in eq. (2.18) we could minimize the average loss (L) (or the worst-case loss) which results in a min-max problem. The discussions hereafter will be of local nature and as assumed above, the set of active constraints remains constant.

Local Taylor Series Analysis

The following sections summarize the work of Halvorsen et al. (2003), otherwise noted. For small deviations from the nominal point we have from eq. (2.12) that

$$\Delta \mathbf{c} = \mathbf{G}\Delta \mathbf{u} + \mathbf{G}_d \Delta \mathbf{d} \tag{2.20}$$

where $\Delta \mathbf{c} = \mathbf{c} - \mathbf{c}^*$, $\Delta \mathbf{u} = \mathbf{u} - \mathbf{u}^*$, $\Delta \mathbf{d} = \mathbf{d} - \mathbf{d}^*$, $\mathbf{G} = \left(\frac{\partial \mathbf{f}_c}{\partial \mathbf{u}^T}\right)^*$ and $\mathbf{G}_d = \left(\frac{\partial \mathbf{f}_c}{\partial \mathbf{d}^T}\right)^*$. Similarly, we have for the measurements

$$\Delta \mathbf{y} = \mathbf{G}^y \Delta \mathbf{u} + \mathbf{G}_d^y \Delta \mathbf{d} \tag{2.21}$$

where $\Delta \mathbf{y} = \mathbf{y} - \mathbf{y}^*$ and $\mathbf{G}^y = \left(\frac{\partial \mathbf{f}_y}{\partial \mathbf{u}^T}\right)^*$ and $\mathbf{G}_d^y = \left(\frac{\partial \mathbf{f}_y}{\partial \mathbf{d}^T}\right)^*$. Linearization of eq. (2.19) yields

$$\Delta \mathbf{c} = \mathbf{H}\Delta \mathbf{y} \tag{2.22}$$

where the matrix $\mathbf{H} = (\frac{\partial \mathbf{h}}{\partial \mathbf{y}^T})$ is free to choose. Combining these equations yields

$$\mathbf{G} = \mathbf{H}\mathbf{G}^y \quad \text{and} \quad \mathbf{G}_d = \mathbf{H}\mathbf{G}_d^y \tag{2.23}$$

Expanding eq. (2.8) around the nominal point $(\mathbf{u}^*, \mathbf{d}^*)$ gives

$$\begin{aligned} J(\mathbf{u}, \mathbf{d}) = J^* + \mathbf{J}_u^T \Delta \mathbf{u} + \mathbf{J}_d^T \Delta \mathbf{d} + \frac{1}{2} \Delta \mathbf{u}^T \mathbf{J}_{uu} \Delta \mathbf{u} \\ + \frac{1}{2} \Delta \mathbf{d}^T \mathbf{J}_{dd} \Delta \mathbf{d} + \Delta \mathbf{d}^T \mathbf{J}_{du} \Delta \mathbf{u} + \mathcal{O}^3 \end{aligned} \tag{2.24}$$

where

$$J^* = J(\mathbf{u}^*, \mathbf{d}^*) \qquad \mathbf{J}_u = \left(\frac{\partial J}{\partial \mathbf{u}}\right)^* \qquad \mathbf{J}_d = \left(\frac{\partial J}{\partial \mathbf{d}}\right)^* \tag{2.25}$$

$$\mathbf{J}_{uu} = \left(\frac{\partial^2 J}{\partial \mathbf{u}^2}\right)^* \qquad \mathbf{J}_{dd} = \left(\frac{\partial^2 J}{\partial \mathbf{d}^2}\right)^* \qquad \mathbf{J}_{du} = \left(\frac{\partial^2 J}{\partial \mathbf{d} \partial \mathbf{u}^T}\right)^* \tag{2.26}$$

The Hessian matrices $\mathbf{J}_{uu}$ and $\mathbf{J}_{dd}$ are always symmetric and we have $\mathbf{J}_{du} = \mathbf{J}_{ud}^T$. If we assume that the nominal point is optimal (J is at a minimum) then the following applies:

1. $\mathbf{J}_u = 0$ since the gradient with respect to the independent variables must be zero at the optimal point
2. $\mathbf{J}_{uu}$ is positive definite, i.e. $\Delta \mathbf{u}^T \mathbf{J}_{uu} \Delta \mathbf{u} > 0 \ \forall \Delta \mathbf{u}$.

Optimal inputs with respect to d

Assume that the nominal point is optimal and that the objective function J is described by a second order function as given by eq. (2.24). By differentiation with respect to the input yields:

$$\frac{\partial J}{\partial \mathbf{u}} = \mathbf{J}_{uu}(\mathbf{u} - \mathbf{u}^*) + \mathbf{J}_{du}^T(\mathbf{d} - \mathbf{d}^*) \tag{2.27}$$

At the optimal input we have $\frac{\partial J}{\partial \mathbf{u}} = 0$ which yields:

$$\mathbf{u}^{opt}(\mathbf{d}) - \mathbf{u}^* = \Delta\mathbf{u}^{opt} = -\mathbf{J}_{uu}^{-1}\mathbf{J}_{ud}(\mathbf{d} - \mathbf{d}^*) \tag{2.28}$$

a second order accurate approximation of the sensitivity in the optimal input to disturbances. We can express the control error using eq. (2.20) which yields the first order accurate equation

$$\Delta\mathbf{c}^{opt} = \mathbf{G}\Delta\mathbf{u}^{opt} + \mathbf{G}_d\Delta\mathbf{d} = -\mathbf{v}(\mathbf{d}) = \left(\mathbf{G}\mathbf{J}_{uu}^{-1}\mathbf{J}_{ud} - \mathbf{G}_d\right)\Delta\mathbf{d} \tag{2.29}$$

In Appendix B we derive a second order function for the loss. This derivation is different from the one in Halvorsen et al. (2003). However, the resulting second order expansion of the loss function is equivalent:

$$\begin{aligned} L(\mathbf{u},\mathbf{d},\mathbf{n}_y) = \frac{1}{2}\left[\mathbf{u}(\mathbf{d},\mathbf{n}_y) - \mathbf{u}^{opt}(\mathbf{d},\mathbf{n}_y)\right]^T \mathbf{J}_{uu}\left[\mathbf{u}(\mathbf{d},\mathbf{n}_y) - \mathbf{u}^{opt}(\mathbf{d},\mathbf{n}_y)\right] \\ = \frac{1}{2}\mathbf{e}_u^T(\mathbf{d},\mathbf{n}_y)\mathbf{J}_{uu}\mathbf{e}_u(\mathbf{d},\mathbf{n}_y) \end{aligned} \tag{2.30}$$

which is a function of the disturbances and the implementation errors. From eq. (2.20) we have for a given disturbance

$$\mathbf{e}_c = \left(\mathbf{c} - \mathbf{c}^{opt}\right) = \mathbf{G}\left(\mathbf{u} - \mathbf{u}^{opt}\right) = \mathbf{G}\mathbf{e}_u \tag{2.31}$$

and if we assume that $\mathbf{G}$ is invertible and using eq. (2.29) the corresponding optimal change in the input is:

$$\mathbf{e}_u = \mathbf{G}^{-1}\left(\mathbf{v}(\mathbf{d}) + \mathbf{n}\right) \tag{2.32}$$

For the case of optimal nominal setpoints, inserting eq. (2.29) into eq. (2.32) yields

$$\mathbf{e}_u = \left(\mathbf{J}_{uu}^{-1}\mathbf{J}_{ud} - \mathbf{G}^{-1}\mathbf{G}_d\right)(\mathbf{d} - \mathbf{d}^*) + \mathbf{G}^{-1}\mathbf{n} \tag{2.33}$$

With this, the basic governing equations have been introduced which lay the basis for some of the results in this thesis. Next, we illustrate the effect of feedback on optimal operation.

2.3.3 Visualization of the effect of feedback

Halvorsen (2001) illustrates visually the idea of self-optimizing control and the effect of disturbances and implementation errors in the input space. Assume that we have $n_u = 2$ inputs (u_i), $n_d = 3$ disturbances d_i, and $n_c = n_u$ controlled variables. Further assume that the nominal point $\mathbf{u}^*$ is optimal, $\mathbf{u}^* = \mathbf{u}^{opt}(\mathbf{d}^*)$ where $\mathbf{d}^*$ is the nominal disturbance vector, and assume that the controlled variables ($\mathbf{c}$) are kept at the constant setpoint (or any setpoint) $\mathbf{c}_s$:

$$(\mathbf{c} + \mathbf{n}) - \mathbf{c}_s = 0 \tag{2.34}$$

where we assume additive implementation error. Let the process model be

$$\mathbf{c} = \mathbf{G}\mathbf{u} + \mathbf{G}_d\mathbf{d} \tag{2.35}$$

so the resulting input action is

$$\mathbf{u} = \mathbf{u}_s + \mathbf{G}^{-1}(\mathbf{c} + \mathbf{n} - \mathbf{c}_s) - \mathbf{G}^{-1}\mathbf{G}_d\mathbf{d} \tag{2.36}$$

Assume that the control error is eliminated, thus $\mathbf{c} - \mathbf{c}_s = 0$ and we have

$$\mathbf{u} = \mathbf{u}_s + \mathbf{G}^{-1}\mathbf{n} - \mathbf{G}^{-1}\mathbf{G}_d\mathbf{d} \tag{2.37}$$

The effect of implementation errors and disturbances are shown in Figure 2.4. For each possible disturbance we can map the resulting optimal input ($\mathbf{u}^{opt}(\mathbf{d})$) from the disturbances space to the input space. For the controlled variables kept at nominal setpoints, the corresponding input change is given through the mapping matrices $\mathbf{G}^{-1}\mathbf{G}_d$ which give an input which deviates from the optimal value. In addition, the measurement errors have an effect through $\mathbf{G}^{-1}$.

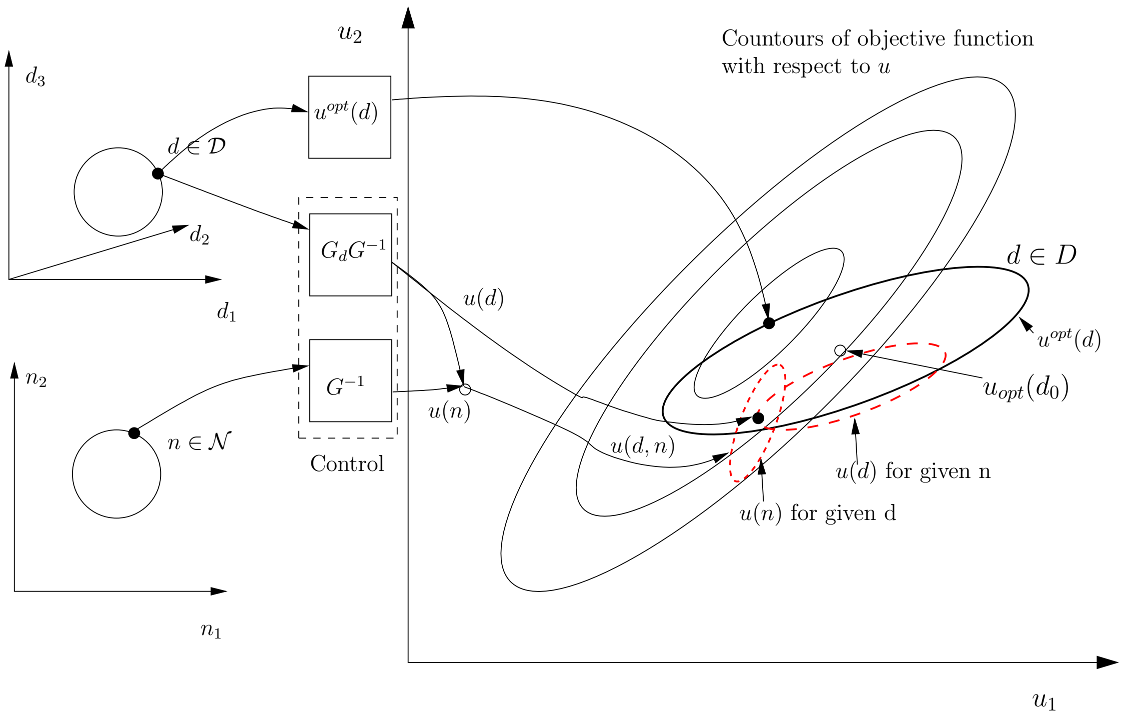

Figure 2.4: *Illustration of the effect of disturbances* $\mathbf{d}$ *and measurement noise* $\mathbf{n}$ *on the objective function. The control signal given by the larger of the dashed ellipses, shows the input as a function of the disturbance, while the smaller dashed ellipse shows the effect of the noise. The bold solid ellipse is the trajectory of the true optimal inputs in the disturbance space* $\mathbf{d} \in \mathcal{D}$ *(Halvorsen, 2001).*

2.3.4 Previously proposed methods for selection of self-optimizing controlled variables

Here, previously proposed methods for selecting self-optimizing controlled variables are discussed. For a detailed summary of the work on self-optimizing control, see Skogestad

(2000).

Qualitative requirements for self-optimizing controlled variables

Skogestad (2000) presents several qualitative requirements for a good self-optimizing controlled variable c:

Requirement 1: Its *optimal* value should be insensitive to disturbances, i.e. $\Delta\mathbf{c}^{opt}(\mathbf{d})$) small.

Requirement 2: It should be easy to measure and control accurately (its implementation error should be small).

Requirement 3: Its value should be sensitive to changes in the manipulated input ($\mathbf{u}$), that is, the gain from $\mathbf{u}$ to $\mathbf{c}$ should be large.

Requirement 4: For cases with two or more controlled variables, the selected controlled variables should not be closely correlated.

The first requirement deals with sensitivity to disturbances, while requirements 2-4 deal with the implementation errors. All these requirements need to be fulfilled in order to guarantee a good self-optimizing controlled variable. Note that requirement 1 says that the optimal value of $\mathbf{c}$, i.e. $\mathbf{c}^{opt}$ should be insensitive toward disturbances, not that $\mathbf{c}$ should be insensitive toward disturbances.

Minimum singular value rule

The minimum singular value rule (Skogestad and Postlethwaite, 1996; Halvorsen et al., 2003) bases the selection of the controlled variables on a scaled steady-state gain from the inputs to the candidate outputs. From eq. (2.30) we have that

$$L = \frac{1}{2}\mathbf{e}_u^T\mathbf{J}_{uu}\mathbf{e}_u = \frac{1}{2}\|\mathbf{z}\|_2^2 \tag{2.38}$$

where

$$\mathbf{z} = \mathbf{J}_{uu}^{1/2}\mathbf{e}_u = \mathbf{J}_{uu}^{1/2}\mathbf{G}^{-1}\mathbf{e}_c \tag{2.39}$$

where $\mathbf{J}_{uu}^{1/2}$ exists since $\mathbf{J}_{uu}$ is positive definite (Horn and Johnson, 1991), $\mathbf{e}_c = \mathbf{c} - \mathbf{c}^{opt}$ and $\|\mathbf{z}\|_2$ denotes the 2-norm of the vector. It is proposed to scale the variables as follows:

- Scale each candidate controlled variable c_i such that the sum of the optimal range v_i and implementation error n_i is unity. Then the combined error norm $\|e'_{c,i}\|_2 = \|c'_i - c_i^{opt'}\|_2 \leq 1$.
- Assume that each u_i is scaled such that a unit change in each input has the same effect on the cost function (J).

Now let $\mathbf{G}'$ be the scaled steady-state gain and from eq. (2.38) we have that the worst case loss is

$$\max_{\|\mathbf{e}_c'\|_2 \leq 1} L = \max_{\|\mathbf{e}_c'\|_2 \leq 1} \frac{1}{2}\|\mathbf{z}\|_2^2 = \frac{1}{2}\left(\bar{\sigma}\left(\mathbf{J}_{uu}^{1/2}\mathbf{G}'^{-1}\right)\right)^2 = \frac{1}{2}\left(\bar{\sigma}\left(\alpha^{1/2}\mathbf{G}'^{-1}\right)\right)^2 = \frac{\alpha}{2}\frac{1}{\underline{\sigma}\left(\mathbf{G}'\right)^2} \quad (2.40)$$

where the constant $\alpha = \bar{\sigma}(\mathbf{J}_{uu})$ is independent of the choice of the controlled variable and $\underline{\sigma}(\mathbf{G}')$ denotes the minimum singular value of $\mathbf{G}'$. The second equality follows since $\bar{\sigma}$ is the induced 2-norm of a matrix. The third equality holds provided $\mathbf{J}_{uu}$ is unitary. The last equality holds since $\bar{\sigma}(\mathbf{G}'^{-1}) = 1/\underline{\sigma}(\mathbf{G}')$. Thus, we see from eq. (2.40) that in order to minimize the loss, we should select controlled variables in which the scaled steady-state gain matrix has a large minimum singular value.

This method may predict erroneously when we have multiple inputs, since the assumption that $\|\mathbf{e}_c'\|_2 \leq 1$ implicitly assumes that the variations $c_i - c_i^{opt}$ may occur. Thus the variables c are assumed independent which may hold for the implementation error, but certainly does not generally hold for the disturbances. This rule may therefore predict a structure to be poor, whereas in reality it is acceptable because of interaction between the controlled variables. For a more detailed discussion of the minimum singular value and for illustrating examples, see Halvorsen et al. (2003). The singular value method has been applied to many case studies, see e.g. Govatsmark (2003); Skogestad (2000) and the references therein.

Exact local method

The exact local method of Halvorsen et al. (2003) utilizes a Taylor series expansion of the loss function as given by eq. (2.38). The loss is

$$L = \frac{1}{2}\|\mathbf{z}\|_2^2 \quad (2.41)$$

and upon substitution of eq. (2.33) into eq. (2.39) yields

$$\mathbf{z} = \mathbf{J}_{uu}^{1/2}\left[\left(\mathbf{J}_{uu}^{-1}\mathbf{J}_{ud} - \mathbf{G}^{-1}\mathbf{G}_d\right)(\mathbf{d} - \mathbf{d}^*) + \mathbf{G}^{-1}\mathbf{n}\right] \quad (2.42)$$

Now, let $\mathbf{W}_d$ be a scaling matrix with the expected magnitudes of the disturbances on the diagonal. Further let $\mathbf{W}_n^y$ be a scaling matrix with the expected implementation errors for each measurement on the diagonal. Note that in general, $\mathbf{c} = \mathbf{Hy}$ and let the scaled disturbances and implementation errors be

$$\mathbf{d} - \mathbf{d}^* = \mathbf{W}_s\mathbf{d}' \quad (2.43)$$

and

$$\mathbf{n} = \mathbf{H}\mathbf{W}_n^y\mathbf{n}^{y\prime} = \mathbf{W}_n\mathbf{n}^{\mathbf{y}\prime} \quad (2.44)$$

where $\mathbf{d}'$ and $\mathbf{n}^{y\prime}$ have magnitudes less than 1. Assume that the combined measurement and implementation error vector are 2-norm bounded

$$\left\| \begin{bmatrix} \mathbf{d}' \\ \mathbf{n}^{y\prime} \end{bmatrix} \right\|_2 \leq 1 \quad (2.45)$$

With these assumptions the corresponding worst case loss is

$$\max_{\|[\mathbf{d}' \ \ \mathbf{n}^{y'}]^T\|_2 \leq 1} L = \bar{\sigma}(\mathbf{M})^2/2 \tag{2.46}$$

where $\mathbf{M} = \begin{bmatrix}\mathbf{M}_d & \mathbf{M}_n\end{bmatrix}$ and

$$\mathbf{M}_d = \mathbf{J}_{uu}^{1/2}\left(\mathbf{J}_{uu}^{-1}\mathbf{J}_{ud} - \mathbf{G}^{-1}\mathbf{G}_d\right)\mathbf{W}_d \tag{2.47}$$

and

$$\mathbf{M}_n = \mathbf{J}_{uu}^{1/2}\mathbf{G}^{-1}\mathbf{W}_n \tag{2.48}$$

and the identity in eq. (2.46) follows from the definition of induced (worst-case) 2-norm of a matrix. For each candidate, an estimate of the worst case loss is available from eq. (2.46) above and we can rank candidate controlled variables based on these estimates.

Optimal linear combination of variables

Halvorsen et al. (2003) propose to use brute force optimization and find the optimal linear combination of measurements to control. They restrict the controlled variables to be linear combinations of variables ($\mathbf{c} = \mathbf{H}\mathbf{y}$) and minimize the worst-case loss as given by eq. (2.46), that is:

$$\mathbf{H} = arg \min_{\mathbf{H}} L(\mathbf{H}, \mathbf{d}, \mathbf{n}_{\mathbf{y}}) \tag{2.49}$$

This method requires that the Hessian matrices are available.

Gradient function

Halvorsen (2001) (also later Cao (2003)) proposes to find the gradient function analytically from eq. (2.7) and to use this as controlled variables (since the gradient of the augmented cost function is zero). The augmented cost function (the Lagrangian) is

$$J_A = J_0 + \lambda^T \mathbf{f}'(\mathbf{x}, \mathbf{u}, \mathbf{d}) \tag{2.50}$$

where $\mathbf{f}'$ is given by eq. (2.8) and λ^T is the Lagrangian multiplier. Using the Karush-Kuhn-Tucker (KKT) optimality condition the gradient function is

$$\mathbf{G}(\mathbf{x}, \mathbf{u}, \mathbf{d}) \stackrel{\text{def}}{=} \mathbf{J}_{0,u} - \mathbf{f}'_u \mathbf{f}'^{-1}_x \mathbf{J}_{0,x} = 0 \tag{2.51}$$

where $\mathbf{J}_{0,u} = (\frac{\partial J_0}{\partial \mathbf{u}})$, $\mathbf{J}_{0,x} = (\frac{\partial J_0}{\partial \mathbf{x}})$, $\mathbf{f}'_x = (\frac{\partial \mathbf{f}'}{\partial \mathbf{x}^T})$ and $\mathbf{f}'_u = (\frac{\partial \mathbf{f}'}{\partial \mathbf{u}^T})$ and all matrices depend on $\mathbf{x}$, $\mathbf{u}$ and $\mathbf{d}$. It is assumed that $\mathbf{f}'^{-1}_x$ exists. For large systems, finding analytical derivatives may prove difficult and the resulting controlled variables are non-linear functions of the states, disturbances and the inputs. This is a major drawback, since information on the states and disturbances may not be available (here we assume that the disturbances are unmeasured). Thus controlling the gradient function directly may be feasible for simple systems, but the complexity of finding analytic derivatives and the need for direct state and disturbance information makes the method complex.

Input sensitivity

Cao (2004) proposes to use input sensitivity method for selecting self-optimizing controlled variables. This is the same as using eq. (2.33) although his derivation is somewhat different. It is already covered in the exact method above.

Other methods:

Mahajanam et al. (2001) propose a "short-cut" controllability measure to eliminate poor choices and to generate rank alternatives without solving the optimization problem. The method is based on scaling all candidate controlled variables so that they have similar effects on the steady-state profit. The method is similar to the singular value method above.

2.4 Conclusions

Here, the selection of controlled variables has been discussed with focus on self-optimizing control. Several other control objectives and other measures used for generating the control structure can be defined which is not discussed here, see e.g. Skogestad and Postlethwaite (1996) and van de Wal and de Jager (2001) for more information.

Almost all of the above methods suffer from the fact the form of the function $\mathbf{h} = \mathbf{h}(\mathbf{y})$ must be found by other means, thus the interconnection of measurements to produce the controlled variables must be based on physical insight and engineering experience. The gradient method is an exception, but requires state and disturbance information and analytical derivatives, and is not suited for typical chemical processes where information on the states and disturbances are not easily accessible. The optimal linear combination of measurements is also an exception, and is attractive as long as the second order information is available. In Chapter 3 we present a new and simpler method for finding the optimal linear combination of the measurements for control.

Bibliography

Ariyur, K. and Krstic, M. (2003). *Real-time optimization by extremum-seeking control*. Wiley-Interscience.

Arkun, Y. and Stephanopoulos, G. (1980). Studies in the synthesis of control structures for chemical processes: Part IV. Design of steady-state optimizing control structyres for chemical process units. *AIChE Journal*, 26(6):975–991.

Box, G. (1957). Evolutionary operation: A method for increasing industrial productivity. *Applied Statistics*, 81-1-1.

Camacho, E. and Bordons, C. (1998). *Model Predictive Control*. Springer.

Cao, Y. (2003). Self-optimizing control structure selection via differentiation. *in European Control Conference (ECC 2003)*, pages 445–453. In CDROM.

Cao, Y. (2004). Controlled variable selection for static self-optimising control. *in the IFAC Symposium on Advanced Control of Chemical Processes (ADCHEM) 2003, (Hong Kong)*, pages 63–71. In CDROM.

El-Farra, N. and Christofides, P. (2001). Integrating robustness, optimality and constraints in control of nonlinear processes. *Chem. Eng. Sci.*, 56:1841–1868.

Foss, C. (1973). Critique of chemical process control theory. *AIChE Journal*, 19(2):209–214.

Glemmestad, B., Skogestad, S., and Gundersen, T. (1999). Optimal operation of heat exchanger networks. *Comput. Chem. Eng.*, 23:509–522.

Govatsmark, M. (2003). *Integrated optimization and control*. PhD thesis, Norwegian University of Science and Technology.

Govatsmark, M. S. and Skogestad, S. (2002). Selection of controlled variables and robust setpoints. In *Proc. of IFAC World Congress*. IFAC. Paper T-Mo-M-11-4.

Grancharova, A., Johansen, T., and Kocijan, J. (2004). Explicit model predictive control of gas-liquid separation plant via orthogonal search tree partitioning. *Comput. Chem. Eng.*, 28:2481–2491.

Guay, M. and Zhang, T. (2003). Adaptive extremum seeking control of nonlinear dynamic systems with parametric uncertainties. *Automatica*, 39:1283–1293.

Halvorsen, I. (2001). *Minimum energy requirements in complex destillation arrangements*. PhD thesis, Dep. of Chemical Engineering, Norwegian University of Science and Technology.

Halvorsen, I., Skogestad, S., Morud, J., and Alstad, V. (2003). Optimal selection of controlled variables. *Ind. Eng. Chem. Res.*, 42(14):3273–3284.

Horn, R. A. and Johnson, C. R. (1991). *Topics in matrix analysis*. Cambridge.

Kadam, J., Marquardt, W., Schlegel, M., Backx, T., Bosgra, O., Brouwer, P.-J., Dünnebier, G., Hessem, D., and Wolf, A. T. S. (2003). Towards integrated dynamic real-time optimization and control of industrial processes. *FOCAPO 2003. 4th Int. Conf. of Computer-Aided Process Operations, Proceedings of the Conference held at Coral Springs, Florida, January 12-15, 2003*, pages 593–596.

Krstic, M. and Wang, H. (2000). Stability of extremum seeking feedback for general nonlinear dynamic systems. *Automatica*, 36:595–601.

Larsson, T. and Skogestad, S. (2000). Plantwide control: A review and a new design procedure. *Model. Ident. Control*, 21:209–240.

Loeblein, C. and Perkins, J. (1998). Economic analysis of different structures of on-line process optimization systems. *Comput. Chem. Eng.*, 22(9):1257–1269.

Maarleveld, A. and Rijnsdorp, J. (1970). Constraint control on distillation columns. *Automatica*, 6(1):51–58. 1.

Mahajanam, R., Zheng, A., and Douglas, J. (2001). A shortcut method for controlled variable selection and its application to the butane alkylation process. *Ind. Eng. Chem. Res.*, 40(14):3208–3216.

Marlin, T. (2000). *Process control designing processes and control systems for dynamic performance*. The McGraw-Hill Book Co.

Marlin, T. and Hrymak, A. (1997). Real-time optimization of continous processes. *American Institute of Chemical Engineering Symposium Series - Fifth International Conference on Chemical Process Control*, 93:85–112.

Morari, M., Stephanopoulos, G., and Arkun, Y. (1980a). Studies in the synthesis of control structures for chemical processes. Part I: Formulation of the problem, process decomposition and the classification of the controller task. Analysis of the optimizing control structures. *AIChE Journal*, 26(2):220–232.

Morari, M., Stephanopoulos, G., and Arkun, Y. (1980b). Studies in the synthesis of control structures for chemical processes. Part II: Structural aspects and the synthesis of alternative feasible control schemes. *AIChE Journal*, pages 220–232.

Morari, M., Stephanopoulos, G., and Arkun, Y. (1980c). Studies in the synthesis of control structures for chemical processes. Part III. Optimal selection of secondary measurements within the framework of state estimation in the presence of persistent unknown disturbances. *AIChE Journal*, pages 247–259.

Pistikopoulos, E., Dua, V., Bozinis, N., Bemporad, A., and Morari, M. (2000). On-line optimization via off-line parametric optimization tools. *Comput. Chem. Eng.*, 24:175–185.

Qin, S. and Badgwell, T. (2003). A survey of industrial model predictive control. *Control Eng. Pract.*, 11:733–764.

Skogestad, S. (2000). Plantwide control: The search for the self-optimizing control structure. *J. Proc. Control*, 10:487–507.

Skogestad, S. and Hovd, M. (1995). Letter to the editor on the decentralized versus multivariable control. *J. Proc. Control*, 5(6):399–400. Paper commented on: Hovd:93-1.

Skogestad, S. and Postlethwaite, I. (1996). *Multivariable Feedback Control*. John Wiley & Sons.

Stengel, R. (1993). *Optimal control and estimation*. Dover Publications Inc.

van de Wal, M. and de Jager, B. (2001). A review of methods for input/output selection. *Automatica*, 37:487–510.

Zhang, Y., Monder, D., and Forbes, J. (2002). Real-time optimization under parametric uncertainty: A probability constrained approach. *J. Proc. Control*, 12(3):373–389.

Zhang, Y., Nader, D., and Forbes, J. (2001). Results analysis for trust constrained real-lime optimization. *J. Proc. Control*, 11:329–341.

Chapter 3

The null space method for selecting optimal measurement combinations as controlled variables

Based on work presented at
AIChE Annual Meeting 2002, November 3-8, Indianapolis, USA, paper 247f
and
International Symposium on Advanced Control of Chemical Processes (ADCHEM) 2003, January 11-14, 2004, Hong Kong

We present a new simple method for selecting measurement combinations as controlled variables. The objective is to obtain self-optimizing control, which is when we can achieve near-optimal steady-state operation with constant setpoints for the controlled variables, without the need to re-optimize when new disturbances perturb the plant (Morari et al., 1980; Skogestad, 2000).

The new method yields controlled variables $\mathbf{c}$ that are linear combinations of measurements $\mathbf{c} = \mathbf{H}\mathbf{y}$ and is optimal in terms of uncertain disturbances $\mathbf{d}$. The requirement is that we at least have as many measurements as there are unconstrained degrees of freedom and disturbances. The measurement and control error is neglected, so it is important that the measurements are properly selected. The goal of this paper is to introduce the basic idea of the null space method and to illustrate the method on a simple gasoline mixing example where we find controlled variables that have good self-optimizing properties.

3.1 Introduction

Although not widely acknowledged by control theorists, controlling the right variables is a key element in overcoming uncertainty in operation. This paper focus on the interaction between the local optimization layer and the feedback control layer, see Figure 3.1, and more specifically on the selection of controlled variables that link the layers. Two sub-problems are important here:

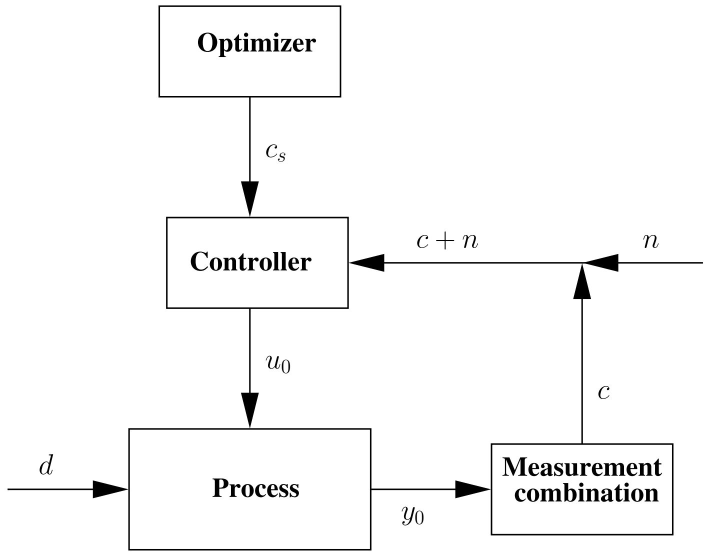

Figure 3.1: *Block diagram of a feedback control structure including an optimizer*

1. *Selection of the controlled variables* $\mathbf{c}$: This is a structural decision which is made before implementing the control strategy.
2. *Selection of setpoints* $\mathbf{c}_s$: This is a parametric decision which can be done both online and offline.

Here, we focus on the first, structural problem of finding the controlled variables and we will assume constant nominal setpoints. From Figure 3.1 we see that external disturbances ($\mathbf{d}$) and the manipulated inputs ($\mathbf{u}_0$) affect the plant, and information is available through the measurements $\mathbf{y}_0$. Single measurements or functions of the measurements are used as controlled variables ($\mathbf{c}$), and the setpoints $\mathbf{c}_s$ for the controlled variables are given by the optimization layer. As seen from Figure 3.1, two sources of uncertainty are present that will influence the operation:

1. **Disturbances d**: External unmeasured disturbances.
2. **Implementation error n**: This is the sum of the measurement error and the control error introduced by the feedback loop.

Here, we make the following assumptions:

A1 Steady-state: We consider only steady-state operation. The justification for this is that the cost of operation is primarily determined by the steady-state. Of course, this assumes that we have a control system in place that can quickly bring the plant to its new steady-state.

A2 No control error: We assume that the controllers have integral action, such that we have no steady-state control error in spite of external disturbances.

A3 Neglect measurement error: Here, we neglect the measurement error. This is a more serious assumption, so the method implicitly assumes that the measurements have been carefully selected. The effect of measurement error is the topic of Chapter 4.

A4 Disturbances: Only disturbances that have an effect on the steady-state and that affect the economics of the process is included. This is the topic of Chapter 5.

A5 Active constraints: We assume that all active constraints remain active for all values of the disturbances and that we control these constraints.

In typical chemical processes, the operational goal is to optimize an economic measure of the operation (often minimize the cost J), while satisfying equality and inequality constraints. Based on the online information in $\mathbf{y_0}$, the most obvious operational policy is probably to combine the "Optimizer" and the "Controller" in Figure 3.1 into an "optimizing controller", with frequent model update, re-optimization and subsequent implementation of the new optimal input $\mathbf{u}^{opt}$. However, this requires a rather complicated system for gathering information about the state of the process, fitting the model used for optimization to the data (system identification), re-optimization and implementation.

We assume here that we control all active constraints (assumption **A5**, see Section 2.3.1 for details on the reduced space problem). Thus, we split the original input vector $\mathbf{u}_0$ (degrees of freedom) into:

- $\mathbf{u}'$: vector of degrees of freedom used for controlling the active constraints.
- $\mathbf{u}$: vector of remaining degrees of freedom with dimension n_u not used for active constraints.

The issue in this paper is to find the controlled variables $\mathbf{c}$ to be associated with the "unconstrained" degrees of freedom $\mathbf{u}$.

Remark. It does not actually matter how the original degrees of freedom $\mathbf{u}_0$ are divided into the new subsets of manipulated variables selected for controlling the active constraints ($\mathbf{u}'$) and the "unconstrained" inputs $\mathbf{u}$, as long as the problem remains well posed. If all the inputs are used for controlling the active constraints, $\mathbf{u}' = \mathbf{u}_0$, then implementation is simple by the use of active constraint control (Maarleveld and Rijnsdorp, 1970; Arkun and Stephanopoulos, 1980).

With the active constraints controlled, we assume that the optimal operation of the process can be quantified in terms of a scalar cost function (performance index) J which is to be minimized with respect to the n_u remaining degrees of freedom (inputs) $\mathbf{u}$:

$$\min_{\mathbf{u}} J(\mathbf{u}, \mathbf{d}) \tag{3.1}$$

where J is generally not a simple function of $\mathbf{u}$ and $\mathbf{d}$.

In practice, the simpler scheme of Figure 3.1 is preferred if it yields acceptable operation. The idea is to select some "good" variables $\mathbf{c}$ such that near-optimal operation is obtained with constant setpoints $\mathbf{c}_s$:

Self-optimizing control (Skogestad, 2000) *is when an acceptable* ***loss*** *can be achieved using constant setpoints* $\mathbf{c_s}$ *for the controlled variables* $\mathbf{c}$ *(without the need to re-optimize when disturbances occur).*

The loss is defined as the difference between the objective value using the constant setpoint feedback structure and the true optimal objective value

$$L = J(\mathbf{c_s} + \mathbf{n}, \mathbf{d}) - J^{opt}(\mathbf{d}) \tag{3.2}$$

Here $\mathbf{n} = \mathbf{c} - \mathbf{c}_s$ is the sum of the measurement and control error. In this paper we assume $\mathbf{n} = 0$ (assumptions **A2** and **A3**).

We assume that online information about the system behavior is available from the measurements $\mathbf{y}_0$:

$$\mathbf{y_0} = \mathbf{f}_{y_0}(\mathbf{u}, \mathbf{d}) \tag{3.3}$$

The objective is to find a set of n_u controlled variables $\mathbf{c}$ as a function of the available measurements, $\mathbf{c} = \mathbf{h}(\mathbf{y}_0)$. In the measurement vector $\mathbf{y}_0$, we generally also include the original input vector $\mathbf{u}_0$. Note that the measurements of the active constraints are not included, because they are not helpful for the remaining control problem since we have zero gain from the remaining degrees of freedom to the active constraints.

We have in this chapter attempted to keep the mathematics as simple as possible. A more detailed comparison with previous results is presented in Chapter 4.

3.2 The null space method

We here consider the unconstrained optimization problem as given by eq. (3.1), and the goal is to find variables $\mathbf{c} = \mathbf{h}(\mathbf{y})$ to be kept at constant setpoints $\mathbf{c}_s$, where $\mathbf{y}$ is a subset of the available measurements $\mathbf{y}_0$. We consider linear measurement combinations

$$\mathbf{c} = \mathbf{H}\mathbf{y} \tag{3.4}$$

where $\mathbf{y} \in \mathbf{y_0}$ is a subset of the available measurements which we choose to make use of and $\mathbf{H}$ is a constant $n_u \times n_y$ coefficient matrix. Often, the controlled variables correspond to single measurements ($\mathbf{H}$ is a matrix with zeros and ones with as many ones as there are u's), e.g. a pressure or a temperature, so $c_i = y_i$. More generally, the matrix $\mathbf{H}$ is free to choose as long as the rank of $\mathbf{H}$ is equal to the number of remaining unconstrained degrees of freedom (u's). Here, we assume that the nominal point $(\mathbf{u}^*, \mathbf{d}^*) = (\mathbf{u}^{opt}, \mathbf{d}^*)$ is optimal such that $\mathbf{c} = \mathbf{c}^{opt}$ at the nominal point.

To find the optimal coefficient matrix $\mathbf{H}$ we make use of the following insight:

With no implementation error, the constant setpoint policy ($\mathbf{c} = \mathbf{c_s}$) *is optimal if* $\mathbf{c}^{\mathrm{opt}}(\mathbf{d})$ *is independent of* $\mathbf{d}$, *i.e.* $\Delta\mathbf{c}^{opt}(\mathbf{d}) = 0$.

Note that we do *not* require that the *change* in the controlled variables $\mathbf{c}$ is independent of the disturbances $\mathbf{d}$, but that the *optimal* values $\mathbf{c}^{opt}$ are independent of the disturbances. For small disturbances, the optimal sensitivity of the measurements to disturbances can be written

$$\Delta\mathbf{y}^{opt} = \mathbf{y}^{opt}(\mathbf{d}) - \mathbf{y}^{opt}(\mathbf{d}^*) = \mathbf{F}(\mathbf{d} - \mathbf{d}^*) = \mathbf{F}\Delta\mathbf{d} \tag{3.5}$$

where $\mathbf{F}$ is a constant sensitivity matrix

$$\mathbf{F} = \left(\frac{\mathrm{d}\mathbf{y}^{opt}}{\mathrm{d}\mathbf{d}^T}\right)^* = \begin{bmatrix} \frac{\partial y_1^{opt}}{\partial d_1} & \cdots & \frac{\partial y_1^{opt}}{\partial d_{n_d}} \\ & \ddots & \\ \frac{\partial y_{n_y}^{opt}}{\partial d_{n_1}} & \cdots & \frac{\partial y_{n_y}^{opt}}{\partial d_{n_d}} \end{bmatrix} \tag{3.6}$$

The $n_y \times n_d$ matrix $\mathbf{F}$ is evaluated at the nominal optimal point and $\mathbf{F}$ may be obtained numerically by perturbing the disturbances and re-solving the optimization problem in eq. (3.1).

Remark 1 Note that perturbing the disturbances and re-solving the optimization problem require that the set of active constraints remains constant. If not, the derivative is not well defined. Thus, for a perturbation of a disturbance $(d_i + \epsilon)$, we get by solving the optimization problem, $\mathbf{u}^{opt}(d_i + \epsilon)$ and thereby $\mathbf{y}^{opt}(d_i + \epsilon)$ and we can estimate the derivative numerically. Let n_d be the number of disturbances, then using a central difference formula, we must solve

$$n_{opt} = 2n_d + 1$$

optimizations in order to estimate $\mathbf{F}$. Ganesh and Biegler (1987) provide an efficient and rigorous strategy for finding the optimal sensitivity based on a reduced Hessian method.

Remark 2 Also, note that we do not necessarily need an explicit model of the plant as we can find the optimal sensitivity experimentally. In addition, many process simulators have built-in optimizers from which the optimal sensitivity $\mathbf{F}$ is easily available.

From eq. (3.4) the corresponding optimal change in the controlled variables are:

$$\Delta\mathbf{c}^{opt} = \mathbf{H}\Delta\mathbf{y}^{opt} \tag{3.7}$$

and by inserting eq. (3.5):

$$\Delta\mathbf{c}^{opt} = \mathbf{HF}\Delta\mathbf{d} \tag{3.8}$$

The optimal value of the controlled variables depends only on the disturbance and not on the particular inputs used. From the insight stated above, the constant setpoint policy is optimal if:

$$\Delta\mathbf{c}^{opt} = \mathbf{HF}\Delta\mathbf{d} = 0 \tag{3.9}$$

This needs to be satisfied for any $\Delta\mathbf{d}$ so we must require that

$$\mathbf{HF} = 0 \tag{3.10}$$

To fulfill this, $\mathbf{H}$ should be selected such that $\mathbf{H}$ is in the left null space of $\mathbf{F}$. The prerequisite for the null space to exist, is that the number of independent measurements is equal or larger than the number of unconstrained inputs plus disturbances:

$$n_y \geq n_u + n_d \tag{3.11}$$

Proof: Let the number of unconstrained degrees of freedom be n_u (the length of vectors $\mathbf{u}$ and $\mathbf{c}$ equals n_u), the number of independent measurements when forming $\mathbf{c}$ be n_y, and the number of disturbances be n_d. Then $\mathbf{F}$ is a $n_y \times n_d$ matrix and $\mathbf{H}$ a $n_u \times n_y$ matrix. We assume that $\mathbf{F}$ has full column rank, that is the disturbances are independent, so $r = rank(\mathbf{F}) = n_d$.

The fundamental theorem of linear algebra (Strang, 1988) gives that the left null space of $\mathbf{F}$ ($\mathcal{N}(\mathbf{F}^T)$) has rank $n_y - r$. Since $\mathbf{H} \in \mathcal{N}(\mathbf{F}^T)$ it follows that $rank(\mathbf{H}) = n_y - n_d$ and by assuming that the number of controlled variables must be equal to the number of inputs, $rank(\mathbf{H}) = n_u$, we get that

$$n_y - n_d = n_u \Leftrightarrow n_y = n_u + n_d \tag{3.12}$$

Thus, the *minimum number of measurements needed, is equal to the number of independent inputs plus disturbances.* □

The result can be summarized as follows:

Theorem 3.1 ***The null space method.*** *Assume that we have n_u independent unconstrained free variables $\mathbf{u}$, n_d independent disturbances $\mathbf{d}$, and n_y independent measurements $\mathbf{y}$. The measurements are combined linearly into $n_c = n_u$ controlled variables*

$$\mathbf{c} = \mathbf{H}\mathbf{y} \tag{3.13}$$

Let

$$\mathbf{F} = \left(\frac{\mathrm{d}\mathbf{y}^{\mathrm{opt}}}{\mathrm{d}\mathbf{d}^T}\right)^*$$

be the optimal sensitivity matrix. If $n_y \geq n_u + n_d$, it is possible to select the matrix $\mathbf{H}$ such that $\mathbf{HF} = 0$. With this choice for $\mathbf{H}$, keeping $\mathbf{c}$ constant at its nominal optimal value gives zero loss for small disturbance changes $\mathbf{\Delta d}$. The matrix $\mathbf{H}$ is generally not unique.

Selecting $\mathbf{H}$ according to Theorem 3.1 is *exact* for small disturbance perturbations.

For cases where we have more measurements

$$n_y > n_u + n_d \tag{3.14}$$

the null space of $\mathbf{F}^T$ is larger and we have additional freedom in selecting $\mathbf{H}$. We now illustrate the idea of the null space method with a simple example.

Example 3.1 *Consider a system with one unconstrained degree of freedom u and one disturbance d. Nominally $d^* = 0$. Let the cost function be defined by*

$$J(u, d) = (u - d)^2$$

and the measurements be

$$\begin{aligned} y_1 &= 0.9u + 0.1d \\ y_2 &= 0.5u - d \end{aligned}$$

Optimality is ensured when $\frac{\partial J}{\partial u} = 2(u^{opt} - d) = 0 \Rightarrow u^{opt} = d$ *and* $J^{opt} = 0 \; \forall d$. *The corresponding optimal outputs are*

$$\begin{aligned} y_1^{opt} &= d \\ y_2^{opt} &= -0.5d \end{aligned}$$

and we have that at $\mathbf{F}^T = [1 \;\; -0.5]$. *We require that* $\Delta c^{opt} = \mathbf{H}\Delta\mathbf{y}^{opt} = 0$ *and get*

$$h_1 + h_2(-0.5) = 0 \Rightarrow h_1 = 0.5h_2$$

that have an infinite number of solutions. For example, by selecting $h_2 = 1$ *we have.*

$$c = 0.5y_1 + y_2 \tag{3.15}$$

By varying u *to keep* c *at the nominal optimal setpoint* $c_s = 0.5y_1^{opt}(d^*) + y_2^{opt}(d^*) = 0$, *we remain optimal in spite of disturbances. To see this, note that* $c - c_s = 0$ *corresponds to*

$$c - c_s = 0 \Rightarrow 0.5(0.9u + 0.1d) + 1(0.5u - d) - 0 = 0.95u - 0.95d - 0 = 0$$

which has as solution $u = d$ *and, as expected, the loss for the null space candidate is zero,*

$$L_c = (u - d)^2 = (d - d)^2 = 0$$

To compare, the losses for keeping the individual measurements y_1 *or* y_2 *constant at the nominal value* $y_{1,s} = y_{2,s} = 0$ *are*

$$L_{y_1} = (-\frac{8}{9}d)^2 \quad \textit{and} \quad L_{y_2} = d^2$$

3.3 Discussion

Freedom in selecting H

The above null space method is not restricted to single controlled variables. The addition of one input, requires one additional measurement. The null space matrix $\mathbf{H}$ has the left null space basis vectors as rows. For systems with multiple unconstrained degrees of freedom ($n_u > 1$), the null vectors should span the null space, thus they cannot be linearly dependent. One possible solution is to select the null vectors such that they are orthogonal, thus

$$\mathbf{h}_i \perp \mathbf{h}_j \; \forall \; i \neq j \quad \text{where} \quad \mathbf{H} = \begin{bmatrix} h_1 \\ \vdots \\ h_{n_u} \end{bmatrix} \tag{3.16}$$

If we assume that the process model is given by

$$\Delta\mathbf{y} = \mathbf{G}^y \Delta\mathbf{u} + \mathbf{G}_d^y \Delta\mathbf{d} \tag{3.17}$$

we have that the controlled variables are:

$$\Delta \mathbf{c} = \mathbf{H}\Delta \mathbf{y} = \mathbf{H}\mathbf{G}^y \Delta \mathbf{u} + \mathbf{H}\mathbf{G}_d^y \Delta \mathbf{d} \tag{3.18}$$

so we must assume that $\mathbf{H}\mathbf{G}^y \neq 0$ and $\mathbf{H}\mathbf{G}_d^y \neq 0$ to avoid zero gain from the inputs (right-half plane zero at steady-state) or disturbances to the controlled variables.

There are an infinite number of matrices $\mathbf{H}$ that satisfy $\mathbf{HF} = 0$ which stems from the freedom of selecting basis vectors for the null space (Strang, 1988). Let $\mathbf{H}_0$ be one such matrix, i.e. $\mathbf{H}_0\mathbf{F} = 0$. For example, $\mathbf{H}_0$ may consist of the one set of basis vectors that span the null space of $\mathbf{F}^T$. Then $\mathbf{H} = \mathbf{C}\mathbf{H}_0$ also satisfies $\mathbf{HF} = 0$ provided the $n_c \times n_c$ matrix $\mathbf{C}$ is non-singular. The degrees of freedom in the matrix $\mathbf{C}$ may be used to affect $\mathbf{G} = \mathbf{H}\mathbf{G}^y$ and $\mathbf{G}_d = \mathbf{H}\mathbf{G}_d^y$. For example, it is possible to select $\mathbf{H}$ such that $\mathbf{G} = \mathbf{I}$, which may be desirable, because then we have a decoupled steady-state response from $\mathbf{u}$ to $\mathbf{c}$.

Numerically, $\mathbf{H}$ may be obtained from a singular value decomposition of $\mathbf{F}^T$. We have $\mathbf{F}^T\mathbf{H}^T = 0$. Thus, selecting $\mathbf{H}$ as the transpose of the input singular vectors of $\mathbf{F}$ corresponding to zero gain in $\mathbf{F}$ gives us an orthogonal basis.

Previous results

For the special case where a single measurement y_i is truly self-optimizing, then Δy_i^{opt} is zero or close to zero, and using a combination of measurements may be unnecessary. For such measurements, the corresponding row in the sensitivity matrix $\mathbf{F}$ would have small elements. Essentially, this is the idea of the singular value method of Skogestad and Postlethwaite (1996), where they select single measurements as controlled variables based on a scaled steady-state gain. The measurements are scaled with respect to the sum of the optimal change and the measurements error $(\Delta y_i^{opt} + n_y)$ and measurements with a large gain (small optimal change) should be selected.

The singular value method may fail when we have more than one degree of freedom, since the method assumes that any output deviation $\|\mathbf{c} - \mathbf{c}^{opt}\|_2 \leq 1$ is allowed. This holds for the measurement error, but certainly not for the disturbance error. The null space method provides a more systematic method for selecting controlled variables for the case of two or more degrees of freedom. For the case of measurements with zero optimal disturbance sensitivity, we could use those as controlled variables provided they fulfill the requirements on non-zero gain.

Physical interpretation

The proposed null space method yields controlled variables that are linear combinations of the available measurements. A disadvantage is that the physical interpretation of what we control is usually lost. This is by no means a fundamental limitation, since in principle we can control any signal from the process as long as they are independent. Thus, if all measurements are regarded as signals, the concept of controlling a combination of signals may be easier to grasp. If possible, one can choose to combine measurements of one type, for instance only temperatures (e.g. in a distillation column) or only mass flows. In any case, we can scale variables such that the resulting measurements are dimensionless, which is common in practice.

Active constraints

The assumption of the active constraints being constant, may limit the applicability of the method for some processes. For a process with a small operating window, where the active constraints shift with the disturbances, other methods may be better suited for optimizing control, e.g. real-time optimization (RTO)/ Model predictive control (MPC). Alternatively, we could use the ideas of Arkun and Stephanopoulos (1980) on how to handle varying active constraints.

Disturbances and observability

Self-optimizing control is based on using feedback to detect disturbances and optimally adjust the inputs so as to achieve near-optimal operation. Thus, one must require that the disturbances are observable in the measurements $\mathbf{y}$. One example of disturbances that are not visible in the measurements is prices. Prices enter only in the objective function, and are not visible in the measurements. Typically, the cost function is a sum of contributions from different utilities weighted with the utility cost (or a price), i.e. $J = \sum_i p_i x_i$.

Price changes can be handled in two ways:

1. Make the setpoints a function of the prices. Thus for a price change $\Delta\mathbf{p}$ we have that
$$\mathbf{c}_s = \mathbf{c}_s(p^*) + \mathbf{H}\mathbf{F}_p\Delta\mathbf{p} \tag{3.19}$$
where $\mathbf{F}_p = \left(\frac{\mathrm{d}\mathbf{y}^{opt}}{\mathrm{d}\mathbf{p}^T}\right)$ is the optimal sensitivity from the prices to the measurements.
2. Include the prices as "measured disturbances" and use the regular procedure of selecting self-optimizing control variables as above.

The first approach is probably the simplest. Note that prices are "measured disturbances" and add a feedforward term to to self-optimizing control structure. Other measured disturbances (regardless of whether they are observable in the measurements or not) can be handled similarly to prices. We illustrate this with a simple example:

Example 3.2 *Consider a process with one disturbance d and one "unconstrained" degree of freedom u. Assume that we have one measurement y_1 such that*

$$\Delta\mathbf{y}^{opt} = \begin{bmatrix} \Delta d \\ \Delta y_1^{opt} \end{bmatrix} = \begin{bmatrix} 1 \\ f_1 \end{bmatrix} d \tag{3.20}$$

Now, we require that $\mathbf{HF} = 0$ *which yields*

$$h_1 + h_2 f_1 = 0 \Rightarrow h_2 = -h_1/f_1 \tag{3.21}$$

One possible solution is $h_1 = 1$*, such that*

$$c = d - \frac{1}{f_1} y_1 \tag{3.22}$$

Let the nominal disturbance be $d^* = 0$ *which yields* $c_s = -\frac{1}{f_1} y_1^*$*. Then we have*

$$c = c_s \Rightarrow d - \frac{1}{f_1} y_1 = -\frac{1}{f_1} y_1^* \Rightarrow y_1 = f_1 d + y_1^* \tag{3.23}$$

which gives a feedforward term. Thus we can control y_1 *and have automatic adjustment of the setpoint* $y_s = f_1 d + y_1^*$ *by measuring* d*.*

All derivations here are based on steady-state models, and we must later check that the candidate structure has acceptable controllability. If not, we may go back and look for other measurements to use in the combination. Next we illustrate the null space method on a gasoline blending example.

3.4 Example: Gasoline blending

This simple gasoline blending example is included to illustrate the null space method. In practice, such a system is characterized by frequent price changes and thereby changes in the active constraints, and better suited for an online-optimization approach. Nevertheless, we want to use a constant setpoint policy and compare the control structure synthesized using the null space method with other candidate controlled variables. The system is illustrated in Figure 3.2 and consists of four gasoline feed streams with varying octane number and benzene concentration. The nominal data is given in Table 3.1.

The operational objective is to minimize the operational cost

$$\min_{\mathbf{u}_0} J = \sum_{i=1}^{i=4} p_i \dot{m}_i \tag{3.24}$$

where p_i and m_i are the price and mass flowrate for stream i respectively, while satisfying the following constraints

- Produce $\dot{m}_p = 1$ kg/s of gasoline.
- Minimum octane number of 98% ($C_p^o \geq 98$).
- The product stream should not contain more that 1 $wt\%$ benzene ($C_p^b \leq 1\ wt\%$).
- The maximum weight fraction of stream 4 in the product is 0.4, $\frac{\dot{m}_1}{\dot{m}_p} \leq 0.4$.

For the octane number we assume "linear mixing" on weight basis. The full set of manipulated variables are:

$$\mathbf{u}_0^T = [\dot{m}_1\ \dot{m}_2\ \dot{m}_3\ \dot{m}_4]$$

and the unmeasured disturbance is assumed to be the octane number of stream 3 ($d = C_3^o$) which is in the range $C_3^o \in [95\ 97]$. We assume that the available measurements are:

$$\mathbf{y}_0^T = [\dot{m}_1\ \dot{m}_2\ \dot{m}_3\ \dot{m}_4\ \dot{m}_p\ C_p^o\ C_p^b]$$

where C_i^o and C_i^b denote the octane and benzene concentration for stream i respectively. The feed streams have different prices (p_i) as shown in the last column of Table 3.1.

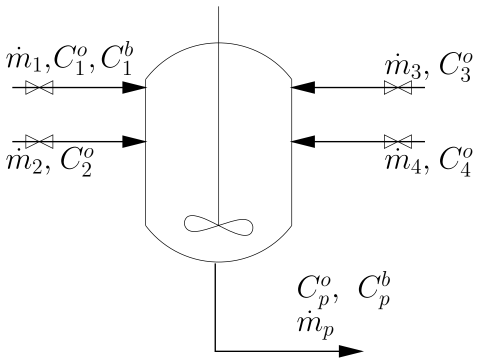

Figure 3.2: *Illustration of the gasoline blending process, where four gasoline feeds are blended to produce the product.*

Table 3.1: *Nominal data for the gasoline blending example*

Stream i	Octane (C_i^o) [wt %]	Benzene (C_i^b) [wt %]	Price Units/kg
1	99	2	1.85
2	105	0	2
3	95	0	1.20
4	99	0	$(1 + \dot{m}_4)$

For streams $(1 - 3)$ the prices are independent of the flow rate, while for stream 4 the price depends on the flow rate. The optimization problem may be formulated as QP-problem

$$\min_{\mathbf{u}_0} \frac{1}{2}\mathbf{u}_0^T \mathbf{Q}\mathbf{u}_0 + \mathbf{f}^T \mathbf{u}_0$$

subject to

$$\mathbf{A}\mathbf{u}_0 \leq \mathbf{b}$$

where:

$$\mathbf{Q} = \begin{pmatrix} 0 & 0 & 0 & 0 \\ 0 & 0 & 0 & 0 \\ 0 & 0 & 0 & 0 \\ 0 & 0 & 0 & 2 \end{pmatrix} \quad \mathbf{f} = \begin{pmatrix} 1.85 \\ 2.00 \\ 1.20 \\ 1 \end{pmatrix} \quad \mathbf{A} = \begin{pmatrix} -99 & -105 & -95 & -99 \\ 2 & 0 & 0 & 0 \\ -1 & 0 & 0 & 0 \\ 0 & -1 & 0 & 0 \\ 0 & 0 & -1 & 0 \\ 0 & 0 & 0 & -1 \\ 0 & 0 & 0 & 1 \end{pmatrix} \quad \mathbf{b} = \begin{pmatrix} -98 \\ 1 \\ 0 \\ 0 \\ 0 \\ 0 \\ 0.4 \end{pmatrix} \tag{3.25}$$

and $\mathbf{A}_{eq}\mathbf{u}_0 = \mathbf{b}_{eq}$ where

$$\mathbf{A}_{eq} = \begin{pmatrix} 1 & 1 & 1 & 1 \end{pmatrix} \quad \mathbf{b}_{eq} = 1 \tag{3.26}$$

The optimal solution to the above problem for the nominal disturbance is:

$$\mathbf{u}_0^{optT}(C_3^o = 95) = \begin{bmatrix} 0.000 & 0.196 & 0.544 & 0.260 \end{bmatrix} \tag{3.27}$$

The minimum cost is $J^{opt}(C_3^o = 95) = 1.3724$. For a disturbance $C_3^o = 97$ the optimal inputs are

$$\mathbf{u}_0^{optT}(C_3^o = 97) = \begin{bmatrix} 0 & 0.075 & 0.725 & 0.20 \end{bmatrix} \tag{3.28}$$

with a cost of $J^{opt}(C_3^o = 97) = 1.2600$. We note that the following constraints are active for all disturbances

$$\dot{m}_1 = 0 \quad C_p^o = 98 \quad \dot{m}_p = 1 \tag{3.29}$$

and we are left with one unconstrained degree of freedom which is not used to control the active constraints. We consider the four candidate control structures listed in Table 3.2. The last candidate is found using the null space method with $\dot{m}_2$ and $\dot{m}_4$

Table 3.2: *Candidate controlled variables including setpoints for the self-optimizing controlled variable*

CS #	c_1	c_2	c_3	c_4	Setpoint ($c_{4,s}$)
1	$\dot{m}_1$	C_p^o	$\dot{m}_p$	$\dot{m}_2$	0.1960
2	$\dot{m}_1$	C_p^o	$\dot{m}_p$	$\dot{m}_3$	0.5440
3	$\dot{m}_1$	C_p^o	$\dot{m}_p$	$\dot{m}_4$	0.2600
4	$\dot{m}_1$	C_p^o	$\dot{m}_p$	$c_{ns} = -0.53\dot{m}_2 + \dot{m}_4$	0.1550

as measurements. Note that $n_y = n_u + n_d = 2$, so it is possible to find an optimal combination with zero loss. The optimal sensitivity matrix at the nominal point is:

$$\begin{bmatrix} \Delta\dot{m}_2^{opt} \\ \Delta\dot{m}_4^{opt} \end{bmatrix} = \begin{bmatrix} -0.0448 \\ -0.0240 \end{bmatrix} \Delta C_3^o \tag{3.30}$$

and from the null space method

$$\mathbf{h} = \mathcal{N}(\mathbf{F}^T) = [-0.53 \ 1] \tag{3.31}$$

which gives

$$c_{ns} = -0.53\dot{m}_2 + \dot{m}_4 \tag{3.32}$$

The losses for the candidates for a disturbance $C_{3,0}^o = 95\% \rightarrow 97\%$ are shown in Table 3.3. The loss for the null space candidate (c_{ns}) is negligible and shows perfect self-

Table 3.3: *Loss for the different control structures for a disturbance* C_3^o : $95 \rightarrow 97wt\%$

Rank	c_4	L	$L[\%]$
1	$-0.53\dot{m}_2 + \dot{m}_4$	1.8×10^{-5}	0.0014
2	$\dot{m}_4$	0.0036	0.2857
3	$\dot{m}_3$	0.0582	4.6224
4	$\dot{m}_2$	inf	inf

optimizing properties. Candidate $\dot{m}_4$ also has small loss, and is also a good candidate

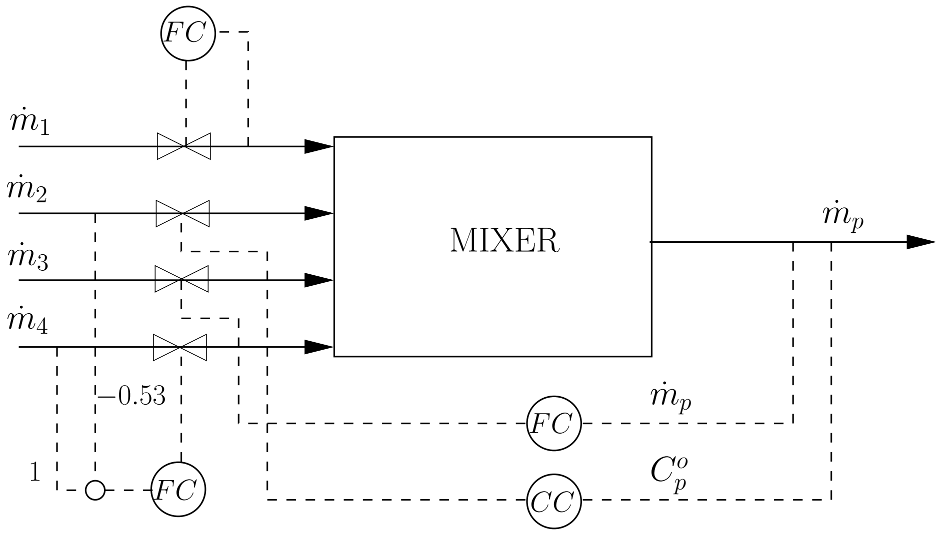

Figure 3.3: *Possible implementation with $c_{ns} = -0.53m_2 + m_4$ as the self-optimizing controlled variable.*

for self-optimizing control. Candidate $\dot{m}_3$ shows a loss of approximately 5% while $\dot{m}_2$ gives infeasible operation. Thus, the best candidate for self-optimizing control is c_{ns}.

One possible implementation of the control structure is shown in Figure 3.3. This is shown for illustration as the pairing of variables does not influence the steady-state.

Note that the self-optimizing controlled variable is a combined measurements of two inputs. The correction in the input when the disturbance enters, is done implicitly through the control of the active constraints, i.e. when the octane number of stream 3 (C_3^o) increases, this is measured in the product stream (the octane number of the product stream increases) which in turn leads to a reduction in the flowrate for stream 2. When reducing the flow of stream 2, the flow of stream 3 needs to be increased, since the total flowrate is now less than 1. At the same time, the flow rate of stream 4 is adjusted so that c_{ns} is kept at the nominal setpoint.

3.5 Conclusions

This paper has introduced the null space method for selecting controlled variables $\mathbf{c}$. We consider a constant setpoint policy, where the controlled variables are kept at constant setpoints $\mathbf{c}_s$. We propose to select self-optimizing controlled variables as linear combinations $\mathbf{c} = \mathbf{H}\mathbf{y}$ of a subset of the available measurements $\mathbf{y}$. With no implementation error, it is optimal to select $\mathbf{H}$ such that $\mathbf{HF} = 0$, where $\mathbf{F} = (\mathrm{d}\mathbf{y}^{opt}/\mathrm{d}\mathbf{d}^T)$ is the optimal sensitivity with respect to disturbance $\mathbf{d}$. The method has been illustrated on a simple gasoline blending example where we find that the null space method yields a controlled variable that has zero loss.

Bibliography

Arkun, Y. and Stephanopoulos, G. (1980). Studies in the synthesis of control structures for chemical processes: Part IV. Design of steady-state optimizing control structyres for chemical process units. *AIChE Journal*, 26(6):975–991.

Ganesh, N. and Biegler, L. T. (1987). A reduced Hessian strategy for sensitivity analysis of optimal flowsheets. *AIChE Journal*, pages 282–296.

Maarleveld, A. and Rijnsdorp, J. (1970). Constraint control on distillation columns. *Automatica*, 6(1):51–58. 1.

Morari, M., Stephanopoulos, G., and Arkun, Y. (1980). Studies in the synthesis of control structures for chemical processes. Part I: Formulation of the problem, process decomposition and the classification of the controller task. Analysis of the optimizing control structures. *AIChE Journal*, 26(2):220–232.

Skogestad, S. (2000). Plantwide control: The search for the self-optimizing control structure. *J. Proc. Control*, 10:487–507.

Skogestad, S. and Postlethwaite, I. (1996). *Multivariable Feedback Control*. John Wiley & Sons.

Strang, G. (1988). *Linear algebra and its applications*. Harcourt Brace & Company, 3 edition.

Chapter 4

Measurement selection in the null space method

Based on work presented at
AIChE Annual Meeting 2004, November 7-12, Austin, Texas, USA, poster 403e

Chapter 3 introduced the null space method for selecting self-optimizing controlled variables as linear combinations $\mathbf{c} = \mathbf{Hy}$ of a subset of the available measurements $\mathbf{y}$. With no implementation error, it is optimal to select $\mathbf{H}$ such that $\mathbf{HF} = 0$, where $\mathbf{F} = (\mathrm{d}\mathbf{y}^{opt}/\mathrm{d}\mathbf{d}^T)$ is the optimal sensitivity with respect to disturbance $\mathbf{d}$. Here we show how to deal with measurement and implementation errors and how to select measurements when using the null space method.

4.1 Introduction and motivation

Self-optimizing control is when a constant set-point policy yields near optimal operation with respect to external disturbances and *implementation errors*. Since optimal operation is in practice implemented in a feedback fashion, as shown in Figure 4.1, we have two sources of uncertainty.

1. The external disturbances $\mathbf{d}$
2. The implementation error $\mathbf{n} = \mathbf{c}_s - \mathbf{c}$.

The external disturbances can be suppressed by the feedback loop, provided the controlled variables are appropriately selected. One approach is the null space method (Alstad and Skogestad, 2004). However, the feedback introduces implementation error, which was previously neglected.

We here consider steady-state operation only, since the economics are mainly decided by the steady-state. The implementation error has two sources, (1) the steady-state control error, and (2) the measurement error. Here, we assume that all controllers have integral action, so we can neglect the steady-state control error. Thus, the term implementation error and measurements error have the same interpretation in this work.

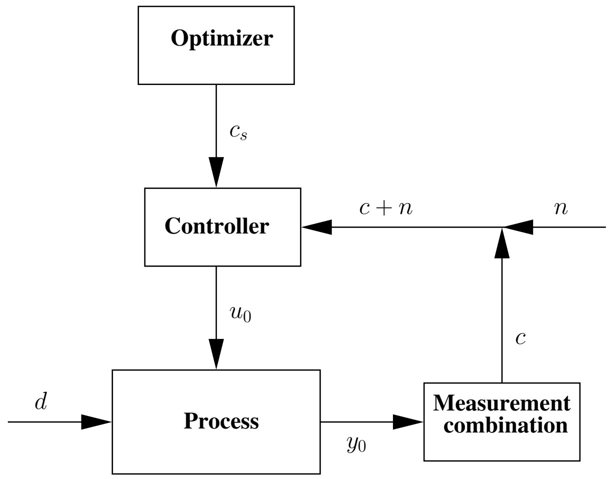

Figure 4.1: *Feedback implementation of optimal operation*

Measurement error is present in all control configurations, regardless of the policy for ensuring optimal operation. However, the implementation error is often neglected in the analysis and the focus is on disturbances. In many cases, the implementation error can be a more important contribution to the non-optimality of the operation than the disturbances. Thus, implementation error must be considered, regardless of what policy for ensuring optimal operation is chosen (real-time optimization, MPC, optimal control, etc.).

Implementation error has previously been discussed in the setting of self-optimizing control for systems where we control single measurements ($c = y_i$) (Skogestad and Postlethwaite, 1996; Halvorsen et al., 2003). The ideas presented therein are generally valid and not only restricted to self-optimizing control.

To motivate and illustrate, consider a case with two possible controlled variables c_1 and c_2, as shown in Figure 4.2. The figure shows the objective function value (upper) and the value of the controlled variable (lower) as a function of the input for a given disturbance. On the ordinate axis, the implementation error (n) in both c_1 and c_2 are given. We assume that the magnitude of the implementation error is equal for both controlled variables. The implementation error gives rise to an input deviation ($u - u^{opt}$) which in turn gives a loss. The figure shows that the deviation in the objective (as measured by ΔJ) from the optimal value, is larger for candidate c_1 than for candidate c_2, implying that c_2 has better robustness with respect to implementation error. This can be explained by noting that the gain from the input u to candidate c_2 is larger than to c_1, i.e. $|G_2| > |G_1|$.

This suggests that one should select controlled variables with a high gain from the input to the output. This is in line with the “minimum singular value rule” of Skogestad and Postlethwaite (1996), which states that “*select controlled variables that maximize the minimum singular value of the (scaled) steady-state gain matrix from inputs to selected controlled variables*”.

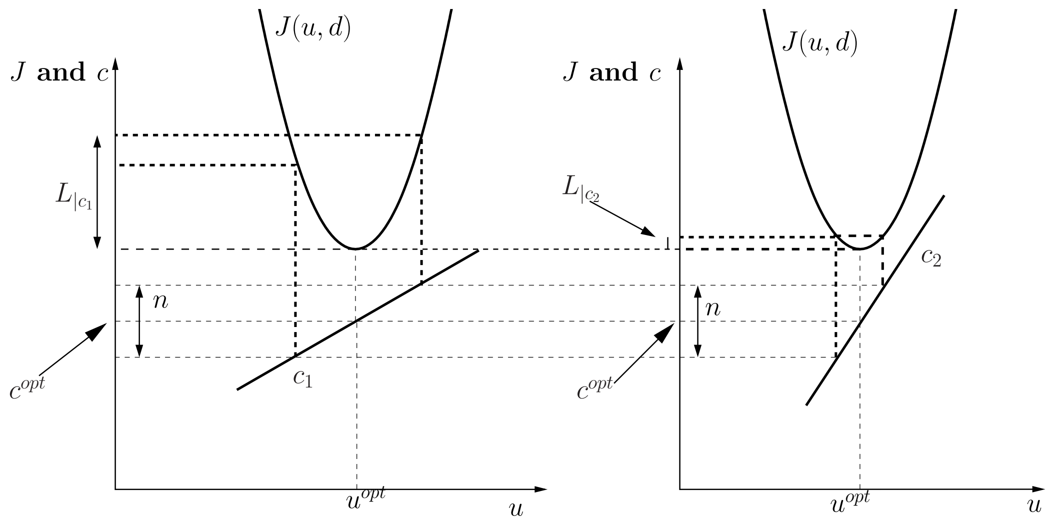

Figure 4.2: *Illustration of the effect of the implementation error on the loss for two different controlled variables, marked by c_1 and c_2 where $|G_2| > |G_1|$ and $\Delta c_i = G_i \Delta u$. The same implementation error is assumed for both candidates, as indicated by n*

In Chapter 3 we found that in order for the null space to exist, we need at least as many independent measurements (n_y) as there are unconstrained inputs (degrees of freedom) (n_u) and disturbances (n_d) in the process. Thus,

$$n_y \geq n_u + n_d \tag{4.1}$$

and we derived the null space method for the case where we have just enough measurements, i.e. $n_y = n_u + n_d$. Besides, we neglected implementation error and we assumed that it was possible to get zero disturbance loss. Now, we include the implementation error and we extend the null space method to the following cases:

1. Just enough measurements
2. Use of all available measurements
3. Use selected minimum number of measurements
4. Too few measurements

In summary, the effect of implementation error is important when selecting controlled variables. The objective of this paper is to discuss how implementation error should be handled when using the null space method to select controlled variables.

4.2 The null space method

In this section, we provide some background material and generalize the null space method. First, we introduce the governing equations. Second, we generalize the null space method and show how to use the null space method when considering both disturbances and implementation errors.

4.2.1 Notation and background

We use the following notation as listed in Table 4.1. We assume that any "active

Table 4.1: *Notation*

$\mathbf{u}$	-	vector of inputs (degrees of freedom) of dimension n_u
$\mathbf{d}$	-	vector of disturbances of dimension n_d
$\mathbf{y}_0$	-	vector of all measurements with dimension n_{y_0}
$\mathbf{y}$	-	vector of selected measurements with dimension n_y used in forming $\mathbf{c}$
$\mathbf{c}$	-	vector of selected controlled variables (to be found) with dimension n_c
$\mathbf{n}^y$	-	measurement error associated with $\mathbf{y}$
$\mathbf{n}$	-	implementation error associated with $\mathbf{c}$

constraints" have been implemented, and we consider the reduced problem in the unconstrained degrees of freedom. We assume that $n_c = n_u$, that is, the number of controlled variables is equal to the number of inputs.

The magnitudes of $\mathbf{d}$ and $\mathbf{n}^y$ are quantified by the diagonal scaling matrices $\mathbf{W}_d$ and $\mathbf{W}_n^y$, respectively. More precisely, we assume

$$\Delta\mathbf{d} = \mathbf{W}_d\mathbf{d}' \tag{4.2}$$

$$\mathbf{n}^y = \mathbf{W}_n^y\mathbf{n}^{y'} \tag{4.3}$$

where we assume that $\mathbf{d}'$ and $\mathbf{n}^{y'}$ are any vectors satisfying

$$\| \begin{bmatrix} \mathbf{d}' \\ \mathbf{n}^{y'} \end{bmatrix} \|_2 \leq 1 \tag{4.4}$$

We have the following linearized (local) relationships in terms of deviation variables[1]

$$\Delta\mathbf{c} = \mathbf{G}\Delta\mathbf{u} + \mathbf{G}_d\Delta\mathbf{d} \tag{4.5}$$

$$\Delta\mathbf{y}_0 = \mathbf{G}^{y_0}\Delta\mathbf{u} + \mathbf{G}_d^{y_0}\Delta\mathbf{d} \tag{4.6}$$

$$\Delta\mathbf{y} = \mathbf{G}^y\Delta\mathbf{u} + \mathbf{G}_d^y\Delta\mathbf{d} = \tilde{\mathbf{G}}^y \begin{bmatrix} \Delta\mathbf{u} \\ \Delta\mathbf{d} \end{bmatrix} \tag{4.7}$$

where $\tilde{\mathbf{G}}^y = \begin{bmatrix} \mathbf{G}^y & \mathbf{G}_d^y \end{bmatrix}$ is the augmented plant. The controlled variables are assumed to be linear combinations of the selected measurements

$$\mathbf{c} = \mathbf{H}\mathbf{y} \tag{4.8}$$

From eqs. (4.5), (4.7) and (4.8) we have

$$\mathbf{G} = \mathbf{H}\mathbf{G}^y \quad \text{and} \quad \mathbf{G}_d = \mathbf{H}\mathbf{G}_d^y \tag{4.9}$$

[1] We use Δ to denote deviation variables. Sometimes the Δ is omitted, for example, for the measurement noise n

We assume that the selected controlled variables $\mathbf{c}$ are independent such that $\mathbf{G}$ is non-singular and invertible. Further, we assume that we have integral action in the control of $\mathbf{c}$. The steady-state implementation error $\mathbf{n}$ for the control of $\mathbf{c}$, is then given by the measurement error in $\mathbf{y}$, and from eq. (4.8) we have

$$\mathbf{n} = \mathbf{H}\mathbf{n}^y \tag{4.10}$$

The reduced space optimization problem in the unconstrained degrees of freedom is for a given disturbance

$$\min_{\mathbf{u}} J(\mathbf{u}, \mathbf{d}) \tag{4.11}$$

This gives $J^{opt}(\mathbf{d})$, $\mathbf{u}^{opt}(\mathbf{d})$ and $\mathbf{y}^{opt}(\mathbf{d})$. The loss is defined as the difference between the objective value J, with a constant setpoint policy for $\mathbf{c}$ (with $\mathbf{c} = \mathbf{c}_s + \mathbf{n}$) and $J^{opt}(\mathbf{d})$ (Skogestad and Postlethwaite, 1996):

$$L = J^{opt}(\mathbf{c}_s + \mathbf{n}, \mathbf{d}) - J^{opt}(\mathbf{d}) \tag{4.12}$$

A second order Taylor series expansion of the cost function around the nominal point $(\mathbf{u}^*, \mathbf{d}^*)$ yields

$$J(\mathbf{u}, \mathbf{d}) = J(\mathbf{u}^*, \mathbf{d}^*) + \begin{bmatrix} \mathbf{J}_u & \mathbf{J}_d \end{bmatrix}^T \begin{bmatrix} \Delta\mathbf{u} \\ \Delta\mathbf{d} \end{bmatrix} + \frac{1}{2} \begin{bmatrix} \Delta\mathbf{u} \\ \Delta\mathbf{d} \end{bmatrix}^T \begin{bmatrix} \mathbf{J}_{uu} & \mathbf{J}_{ud} \\ \mathbf{J}_{ud}^T & \mathbf{J}_{dd} \end{bmatrix} \begin{bmatrix} \Delta\mathbf{u} \\ \Delta\mathbf{d} \end{bmatrix} \tag{4.13}$$

where $\Delta\mathbf{u} = (\mathbf{u} - \mathbf{u}^*)$ and $\Delta\mathbf{d} = (\mathbf{d} - \mathbf{d}^*)$. The non-linear functions $\mathbf{u}^{opt}(\mathbf{d})$ and $\mathbf{y}^{opt}(\mathbf{d})$ can be linearized, and we have that (Halvorsen et al., 2003)

$$\Delta\mathbf{u}^{opt} = -\mathbf{J}_{uu}^{-1}\mathbf{J}_{ud}\Delta\mathbf{d} \tag{4.14}$$
$$\Delta\mathbf{y}^{opt} = \mathbf{F}\Delta\mathbf{d} = -(\mathbf{G}^y\mathbf{J}_{uu}^{-1}\mathbf{J}_{ud} - \mathbf{G}_d^y)\Delta\mathbf{d} \tag{4.15}$$

An second-order accurate expansion of the loss function (see Appendix B) yields

$$L = \frac{1}{2}(\mathbf{u} - \mathbf{u}^{opt})^T\mathbf{J}_{uu}(\mathbf{u} - \mathbf{u}^{opt}) \tag{4.16}$$

Since $\mathbf{J}_{uu}$ is positive semidefinite and we have (Horn and Johnson, 1991):

Theorem 4.1 *Let* $\mathbf{A}$ *be a positive semidefinite matrix, then there exists a unique positive semi-definite square root* B *such that*

$$\mathbf{B}^2 = \mathbf{A} \tag{4.17}$$

Consequently, we can write

$$L = \frac{1}{2}\mathbf{z}^T\mathbf{z} \tag{4.18}$$

where

$$\mathbf{z} = \mathbf{J}_{uu}^{1/2}(\mathbf{u} - \mathbf{u}^{opt}) \tag{4.19}$$

4.2.2 Generalized null space method

The original derivation of the null space method in Chapter 3, neglects the implementation error. It also assumes that we have a sufficient number of measurements ($n_y = n_u + n_d$), such that it is possible to get zero disturbance loss. The conclusion is then to select $\mathbf{H}$ such that $\mathbf{HF} = 0$, where $\mathbf{F}$ is defined by eq. (4.15).

The overall objective is to find a matrix $\mathbf{H}$ such that controlling $\mathbf{c} = \mathbf{Hy}$ at constant setpoints, minimizes the loss L. The loss is generally non-zero due to disturbances $\mathbf{d}$ and implementation errors $\mathbf{n}$ associated with controlling $\mathbf{c}$. We assume, as mentioned earlier, that $\mathbf{n} = \mathbf{Hn}^y$, where $\mathbf{n}^y$ is the measurement error associated with $\mathbf{y}$. We now want to express the "local" loss $L = \frac{1}{2}\mathbf{z}^T\mathbf{z}$, where $\mathbf{z}$ is given by eq. (4.19) in terms of $\mathbf{d}$ and $\mathbf{n}^y$, where we assume that $\mathbf{u}$ is used to control $\mathbf{c}$ at constant setpoint ($\mathbf{c} = \mathbf{c}_s$)

We then have

$$(\mathbf{u} - \mathbf{u}^{opt}) = \mathbf{G}^{-1}(\mathbf{c} - \mathbf{c}^{opt}) = \mathbf{G}^{-1}(\Delta\mathbf{c} - \Delta\mathbf{c}^{opt}) \tag{4.20}$$

$$\Delta\mathbf{c} = \Delta\mathbf{c}_s + \mathbf{n} = \mathbf{n} \tag{4.21}$$

$$\Delta\mathbf{c}^{opt} = \mathbf{H}\Delta\mathbf{y}^{opt} = \mathbf{HF}\Delta\mathbf{d} \tag{4.22}$$

which gives

$$\mathbf{z} = \mathbf{J}_{uu}^{1/2}\mathbf{G}^{-1}(-\mathbf{HF}\Delta\mathbf{d} + \mathbf{n}) \tag{4.23}$$

Introducing the magnitudes of $\Delta\mathbf{d}$ and $\mathbf{n}$ from eqs. (4.2) and (4.3) and using that $\mathbf{G} = \mathbf{HG}^y$ then gives

$$\mathbf{z} = \mathbf{J}_{uu}^{1/2}(\mathbf{HG}^y)^{-1}\mathbf{H}\begin{bmatrix}-\mathbf{FW}_d & \mathbf{W}_n^y\end{bmatrix}\begin{bmatrix}\mathbf{d}' \\ \mathbf{n}^{y\prime}\end{bmatrix} \tag{4.24}$$

The worst case loss for all disturbances and measurement noise is then

$$\max_{\left\|\begin{smallmatrix}\mathbf{d}' \\ \mathbf{n}^{y\prime}\end{smallmatrix}\right\|\leq 1} L = \frac{1}{2}\bar{\sigma}\left(\mathbf{M}\right)^2 \tag{4.25}$$

where

$$\mathbf{M} = \mathbf{J}_{uu}^{1/2}(\mathbf{HG}^y)^{-1}\mathbf{H}\begin{bmatrix}-\mathbf{FW}_d & \mathbf{W}_n^y\end{bmatrix} \tag{4.26}$$

or

$$\mathbf{M} = \begin{bmatrix}\mathbf{M}_d & \mathbf{M}_n^y\end{bmatrix} \tag{4.27}$$

where

$$\mathbf{M}_d = -\mathbf{J}_{uu}^{1/2}(\mathbf{HG}^y)^{-1}\mathbf{HFW}_d \tag{4.28}$$

$$\mathbf{M}_n^y = \underbrace{\mathbf{J}_{uu}^{1/2}(\mathbf{HG}^y)^{-1}}_{\mathbf{M}_n}\mathbf{HW}_n^y \tag{4.29}$$

This is identical to the "exact local method" in Halvorsen et al. (2003), but expressed in terms of the easily available optimal sensitivity matrix $\mathbf{F}$. To minimize the worst case loss, we thus need to minimize $\bar{\sigma}(\mathbf{M})$ with respect to $\mathbf{H}$. $\mathbf{H}$ does not enter in eq. (4.26) in a simple manner, so generally $\mathbf{H}$ needs to be obtained numerically[2]. Optimally, we should minimize $\mathbf{M}$ with respect to $\mathbf{H}$. Instead, we use a simpler (two-step) approach, where we

1. minimize $\mathbf{M}_d$ (require $\mathbf{M}_d = 0$).
2. Then (with the above constraint), we minimize $\mathbf{M}_n^y$.

4.2.3 Re-derivation of the original null space method

With no measurement error, we have $\mathbf{W}_n^y = 0$ such that $\mathbf{M}_n^y = 0$ and the loss is zero if $\mathbf{M}_d = 0$. From eq. (4.28) we see that $\mathbf{M}_d = 0$ is achieved if we can find a non-trivial solution ($\mathbf{H} \neq 0$) such that

$$\mathbf{HF} = 0 \tag{4.30}$$

Thus, $\mathbf{H}$ should lie in the left null space of $\mathbf{F}$ and we have re-derived the null space method. As shown in Chapter 3, it is always possible to find $\mathbf{H}$ satisfying $\mathbf{HF} = 0$ provided the number of independent measurements (n_y) is greater than the number of independent inputs (n_u) plus disturbances (n_d), i.e. $n_y \geq n_u + n_d$.

This follows since the null space of $\mathbf{F}$ is of dimension $n_y - n_d$, and this must be larger than the number of rows in $\mathbf{H}$, which is $n_c = n_u$. Thus, we must require $n_y - n_d \geq n_u$ or $n_y \geq n_u + n_d$.

The more general treatment given above, will now be used to discuss and generalize the null space method.

4.2.4 Degrees of freedom in using the null space method

In general, there are an infinite number of matrices $\mathbf{H}$ which satisfy $\mathbf{HF} = 0$. First, consider the case with $n_y = n_u + n_d$ ("just enough measurements"). Let $\mathbf{H}_0$ be a solution to $\mathbf{H}_0\mathbf{F} = 0$. Then $\mathbf{CH}_0$ is also a solution, where $\mathbf{C}$ is any non-singular $n_u \times n_u$ matrix. Since the rows of $\mathbf{H}_0$ correspond to the left null space basis vectors of $\mathbf{F}$, multiplying with $\mathbf{C}$ rotates the basis vectors. Thus, if the rows of $\mathbf{H}_0$ span the left null space, multiplying with a non-singular matrix $\mathbf{C}$ yields a new set of basis vectors which is independent (Strang, 1988). Second, when $n_y > n_u + n_d$ we have even more degrees of freedom, because the null space of $\mathbf{F}$ has "excess" dimensions.

The question is now how to utilize these degrees of freedom? First, they can be used to affect the matrix $\mathbf{G} = \mathbf{HG}^y$ and $\mathbf{G}_d = \mathbf{HG}_d^y$. For example, it may be desirable to have $\mathbf{G} = \mathbf{I}$, because then we have a decoupled steady-state response from the inputs to the controlled variables $\mathbf{c}$. Second, and more importantly within the context of this paper, they can in some cases be used to affect the effect of the measurement error ($\mathbf{n}^y$) on the loss, as expressed by the matrix $\mathbf{M}_n$ (or $\mathbf{M}_n^y$) in eq. (4.29). In order to study this in more detail, we will first derive a more explicit form.

Remark 1 If we minimize $\bar{\sigma}(\mathbf{M})$ with $\mathbf{M} = \begin{bmatrix}\mathbf{M}_d & \mathbf{M}_n\end{bmatrix}$, we can still select $\mathbf{G}$ or $\mathbf{M}_n$ without affecting the loss. Consider $\mathbf{H} = \mathbf{CH}_0$, where $\mathbf{H}_0$ minimize $\mathbf{M}$ in eq. (4.26) and we assume

[2]We have used *fminunc.m* in Matlab for this, with overall good results.

that $\mathbf{C}$ is invertible. Then,

$$\begin{aligned}
\mathbf{M} &= \mathbf{J}_{uu}^{1/2}(\mathbf{C}\mathbf{H}_0\mathbf{G}^y)^{-1}\mathbf{C}\mathbf{H}_0\begin{bmatrix}-\mathbf{F}\mathbf{W}_d & \mathbf{W}_n^y\end{bmatrix} && (4.31)\\
&= \mathbf{J}_{uu}^{1/2}(\mathbf{H}_0\mathbf{G}^y)^{-1}\mathbf{C}^{-1}\mathbf{C}\mathbf{H}_0\begin{bmatrix}-\mathbf{F}\mathbf{W}_d & \mathbf{W}_n^y\end{bmatrix} && (4.32)\\
&= \mathbf{M}_0 && (4.33)
\end{aligned}$$

the loss is the same.

Remark 2 This freedom in selecting $\mathbf{G}$ or $\mathbf{M}_n$ is not new, it is very similar to decoupling used in multivariable control (Skogestad and Postlethwaite, 1996), see Chapter 7 for more on this.

Remark 3 Shaping $\mathbf{M}_n$ is possible. However, the effect of $\mathbf{n}$ on $\mathbf{z}$ has no direct physical interpretation here. Conversely, in Appendix C we show that for indirect control (a subproblem of self-optimizing control), $\mathbf{M}_n$ has a physical interpretation, where we show that it is the gain from the setpoints to the controlled variables in indirect control.

4.2.5 Noise sensitivity with the null space method

The effect of disturbances and measurement noise on the loss $L = \frac{1}{2}\mathbf{z}^T\mathbf{z}$, can generally be expressed as

$$\mathbf{z} = \mathbf{M}_n\mathbf{H}\mathbf{n}^y + \mathbf{M}_d\Delta\mathbf{d} \tag{4.34}$$

In the null space method we select $\mathbf{H}$ in the left null space of $\mathbf{F}$ ($\mathbf{HF} = 0$) such that $\mathbf{M}_d = 0$. We now want to derive what this implies in terms of $\mathbf{M}_n^y = \mathbf{M}_n\mathbf{H}$, which represents the effect of measurement noise $\mathbf{n}^y$ on the loss.

From the expansion of the loss function we have, see eqs. (4.14) and (4.20)

$$\mathbf{z} = \overbrace{\begin{bmatrix}\mathbf{J}_{uu}^{1/2} & \mathbf{J}_{uu}^{1/2}\mathbf{J}_{uu}^{-1}\mathbf{J}_{ud}\end{bmatrix}}^{\tilde{\mathbf{J}}}\begin{bmatrix}\Delta\mathbf{u}\\ \Delta\mathbf{d}\end{bmatrix} \tag{4.35}$$

Furthermore, with zero disturbance loss, we have from eqs. (4.34) and (4.35)

$$\mathbf{z} = \mathbf{M}_n\Delta\mathbf{c} = \mathbf{M}_n\mathbf{H}\Delta\mathbf{y} = \mathbf{M}_n\mathbf{H}\tilde{\mathbf{G}}^y\begin{bmatrix}\Delta\mathbf{u}\\ \Delta\mathbf{d}\end{bmatrix} \tag{4.36}$$

where $\tilde{\mathbf{G}}^y = \begin{bmatrix}\mathbf{G}^y & \mathbf{G}_d^y\end{bmatrix}$ is the augmented plant. Comparing eqs. (4.35) and (4.36) yields

$$\mathbf{M}_n\mathbf{H}\tilde{\mathbf{G}}^y = \tilde{\mathbf{J}} \tag{4.37}$$

This expression gives the noise sensitivity ($\mathbf{M}_n\mathbf{H}$) for a case with zero disturbance sensitivity ($\mathbf{M}_d = 0$).

Remark. It is clear from eq. (4.18) and (4.36) that it would be optimal to control $\mathbf{z}$ directly. However, since we cannot measure $\mathbf{z}$, we need to use "indirect control" to control $\mathbf{z}$ (see Appendix C).

4.3 Reducing the effect of measurement noise with the null space method

To minimize the combined effect of disturbances and measurement noise on the loss, we should ideally use all measurements and select $\mathbf{H}$ such that $\bar{\sigma}(\mathbf{M})$ in eq. (4.26) is minimized. However, whereas the disturbances are usually given, we usually have some freedom in selecting the measurements. Therefore, the "null space method" where we first minimize the disturbance effect (by selecting $\mathbf{HF} = 0$ to get $\mathbf{M}_d = 0$) may be a good approach in practice.

The basis for the null space method is to minimize the effect of the disturbance. In this section, we consider how we can, in addition, reduce the effect of measurement noise. The results in this section are based on the expression in eq. (4.37) for $\mathbf{M}_n^y$ which applies when $\mathbf{M}_d = 0$.

We will consider the following four cases:

1. Just enough measurements ($n_y = n_u + n_d$).
2. Use all measurements ($\mathbf{y} = \mathbf{y}_0$, $n_{y_0} > n_u + n_d$)
3. Use selected measurements ($\mathbf{y} \in \mathbf{y}_0$, $n_y = n_u + n_d$)
4. Too few measurements ($n_y < n_u + n_d$)

4.3.1 Original null space method (Just enough measurements)

In this case $n_y = n_u + n_d$ and $\tilde{\mathbf{G}}^y$ is invertible. Eq. (4.37) then gives

$$\mathbf{M}_n\mathbf{H} = \tilde{\mathbf{J}}[\tilde{\mathbf{G}}^y]^{-1} \tag{4.38}$$

This means that $\mathbf{M}_n^y = \mathbf{M}_n\mathbf{H}$ is given, so the extra degrees of freedom in the null space method have *no effect* on the sensitivity to measurement noise. From eq. (4.38) we see that the original null space method may give strong sensitivity to measurement noise if $\tilde{\mathbf{G}}^y$ is close to singular, because then the elements in $[\tilde{\mathbf{G}}^y]^{-1}$ are large. Note that $\tilde{\mathbf{G}}^y$ represents the effect of the independent variables on the measurements

$$\Delta\mathbf{y} = \tilde{\mathbf{G}}^y \begin{bmatrix}\Delta\mathbf{u}\\ \Delta\mathbf{d}\end{bmatrix} \tag{4.39}$$

Thus, $\tilde{\mathbf{G}}^y$ close to singular means that the measurements are closely correlated in the sense that they do not contain independent information about $\mathbf{u}$ and $\mathbf{d}$.

4.3.2 Null space method using all measurements

In this case we have extra measurements, $n_{y_0} > n_u + n_d$, and we select to use all available measurements when forming the controlled variables, i.e. $\mathbf{y} = \mathbf{y}_0$ and $\mathbf{c} = \mathbf{Hy} = \mathbf{Hy}_0$. From eq. (4.37) we have

$$\mathbf{M}_n\mathbf{H}\tilde{\mathbf{G}}^{y_0} = \tilde{\mathbf{J}} \tag{4.40}$$

where $\tilde{\mathbf{G}}^{y_0} = \begin{bmatrix}\mathbf{G}^{y_0} & \mathbf{G}_d^{y_0}\end{bmatrix}$ is the augmented plant model using all measurements. Since we have extra measurements ($\tilde{\mathbf{G}}^{y_0}$ is non-square) eq. (4.40) has an infinite number of solutions in terms of $\mathbf{M}_n\mathbf{H}$. We would like to find the solution $\mathbf{H}$, that minimize the effect of the measurement noise. More precisely, note that

$$\mathbf{z} = \mathbf{M}_n\mathbf{H}\mathbf{n}^{y_0} = \overbrace{\mathbf{M}_n\mathbf{H}\mathbf{W}_n^{y_0}}^{\mathbf{M}_n^{y_0\prime}}\mathbf{n}^{y_0\prime} \tag{4.41}$$

where $\mathbf{W}_n^{y_0}$ is a diagonal scaling matrix with the expected measurement error for each measurement in $\mathbf{y}_0$ along the diagonal. Rewriting eq. (4.40) as

$$\mathbf{M}_n\mathbf{H}\mathbf{W}_n^{y_0}(\mathbf{W}_n^{y_0})^{-1}\tilde{\mathbf{G}}^{y_0} = \tilde{\mathbf{J}} \tag{4.42}$$

we find that the solution to eq. (4.40) that minimizes $\|\mathbf{M}_n^{y_0\prime}\|_2$ is given by

$$\mathbf{H} = \mathbf{M}_n^{-1}\tilde{\mathbf{J}}(\mathbf{W}_n^{y_0 -1}\tilde{\mathbf{G}}^{y_0})^{\dagger}(\mathbf{W}_n^{y_0})^{-1} \tag{4.43}$$

where $(\mathbf{W}_n^{y_0 -1}\tilde{\mathbf{G}}^{y_0})^{\dagger}$ is the pseudo-inverse. Note that we also here have degrees of freedom left in choosing $\mathbf{G}$, since $\mathbf{M}_n$ may be specified by the designer.

Note again that this solution does not minimize the loss in eq. (4.25), but rather gives the best solution subject to having $\mathbf{M}_d = 0$.

Remark. It is appropriate at this point to make a comment about the pseudo-inverse $\mathbf{A}^{\dagger}$ of a matrix. Above we are looking for the best solution for $\mathbf{H}$ that satisfies the equation set $\mathbf{H}\tilde{\mathbf{G}}^{y} = \mathbf{M}_n^{-1}\tilde{\mathbf{J}}$. In general, we can write the solution of $\mathbf{HA} = \mathbf{B}$ as $\mathbf{H} = \mathbf{B}\mathbf{A}^{\dagger}$ where the following points are true.

1. $\mathbf{A}^{\dagger} = (\mathbf{A}^T\mathbf{A})^{-1}\mathbf{A}^T$ is the left inverse for the case when $\mathbf{A}$ has full column rank (we have extra measurements). In this case, there are an infinite number of solutions and we seek the solution that minimizes $\mathbf{H}$
2. $\mathbf{A}^{\dagger} = \mathbf{A}^T(\mathbf{A}\mathbf{A}^T)^{-1}$ is the right inverse for the case when $\mathbf{A}$ has row column rank (we have too few measurements). In this case there is no solution and we seek the solution that minimizes the two-norm of $\mathbf{E} = \mathbf{B} - \mathbf{HA}$ (regular least squares).
3. In the general case with extra measurements, but where some are correlated, $\mathbf{A}$ has neither full column or row rank, and the singular value decomposition may be used to compute the pseudo-inverse $\mathbf{A}^{\dagger}$.

Scaled variables

To simplify notation, we will in the following assume that the measurements ($\mathbf{y}$ and $\mathbf{y}_0$) are scaled with respect to the measurement noise, that is, the span for each measurement is its expected measurement noise. We then have that $\mathbf{W}_n^{y_0} = \mathbf{I}$, and eq. (4.43) simplifies to

$$\mathbf{H} = \mathbf{M}_n^{-1}\tilde{\mathbf{J}}(\tilde{\mathbf{G}}^{y_0})^{\dagger} \tag{4.44}$$

4.3.3 Null space method using selected measurements

In practice, we often want to use as few measurements as possible, and eq. (4.43) then gives invaluable insights.

Assume that $n_{y_0} > n_u + n_d$ and we want to select a subset $\mathbf{y}$ of the measurements $\mathbf{y}_0$, such that $n_y = n_u + n_d$. We assume that the measurements have been scaled such that $\mathbf{W}_n^y = \mathbf{I}$. The solution to eq. (4.43) that minimize the noise sensitivity $\|\mathbf{M}_n\mathbf{H}\|_2$ is then given by

$$\mathbf{M}_n\mathbf{H} = \tilde{\mathbf{J}}(\tilde{\mathbf{G}}^y)^{-1} \tag{4.45}$$

where we can take the inverse since $\tilde{\mathbf{G}}^y$ is invertible.

Now, the issue is to select the best minimum set of measurements y_i where $i \in \{1,..,n_y\}$ from the full set of measurements $y_{0,j}$ for $j = \{1,..,n_{y_0}\}$. First, note that the choice of $\mathbf{M}_n$ does not influence the effect of the measurement noise since the right hand side of eq. (4.45) is a constant matrix. Thus, for a given minimum set of measurements, we cannot affect the implementation error by manipulating $\mathbf{M}_n$.

Second, the selection of measurements does not affect the matrix $\tilde{\mathbf{J}}$, since it depends only on the Hessian matrices $\mathbf{J}_{uu}$ and $\mathbf{J}_{ud}$. However, the selection of measurements affects the matrix $\tilde{\mathbf{G}}^y$, and we should select measurements so that $\|\mathbf{M}_n\mathbf{H}\|_2 = \|\tilde{\mathbf{J}}(\tilde{\mathbf{G}}^y)^{-1}\|_2$ is minimized. Since the induced 2-norm or maximum singular value of a matrix ($\bar{\sigma}$) provides the worst case amplification in terms of the 2-norm, we have from eq. (4.45) that

$$\begin{aligned}\max_{\|\mathbf{n}^y\|_2\leq 1} \tfrac{1}{2}\mathbf{z}^T\mathbf{z} &= \max_{\|\mathbf{n}^y\|_2\leq 1} \tfrac{1}{2}\|\mathbf{z}\|_2^2 \\ &= \tfrac{1}{2}\bar{\sigma}(\tilde{\mathbf{J}}(\tilde{\mathbf{G}}^y)^{-1})^2 \leq \tfrac{1}{2}\left(\bar{\sigma}(\tilde{\mathbf{J}})\bar{\sigma}((\tilde{\mathbf{G}}^y)^{-1})\right)^2 = \tfrac{1}{2}\left(\bar{\sigma}(\tilde{\mathbf{J}})\underline{\sigma}(\tilde{\mathbf{G}}^y)\right)^2\end{aligned} \tag{4.46}$$

Thus, in order to minimize the effect of the implementation error, we propose the following two rules:

1. **Optimal**: In order to minimize the worst case value of $\|\mathbf{M}_n\mathbf{H}\|_2$ for all $\|\mathbf{n}^y\|_2 \leq 1$, select measurements such that $\bar{\sigma}\left(\tilde{\mathbf{J}}[\tilde{\mathbf{G}}^y]^{-1}\right)$ is minimized.

2. **Sub-optimal**: Remember that the measurement selection does not affect the matrix $\tilde{\mathbf{J}}$. From the inequality in eq. (4.46), it then follows that the effect of the measurement error $\mathbf{n}^y$ will be small when $\underline{\sigma}(\tilde{\mathbf{G}}^y)$ (the minimum singular value of $\underline{\sigma}(\tilde{\mathbf{G}}^y)$) is large. Thus, it is therefore reasonable to select measurements $\mathbf{y}$ such that $\underline{\sigma}(\tilde{\mathbf{G}}^y)$ is maximized.

Since the optimal rule needs information on the Hessian matrix of the cost function J, the sub-optimal selection rule above is preferred in practice. In Section 4.4 we propose a procedure for the null space method, where we first select measurements with a small measurement error, and then select $\mathbf{H}$ such that $\mathbf{M}_d = 0$.

4.3.4 Null space method with fewer measurements

In this case $n_y < n_u + n_d$, so it is not possible to get zero disturbance loss with $\mathbf{M}_d = 0$. Nevertheless, it turns out that selecting $\mathbf{H}$ such that

$$\mathbf{M}_n\mathbf{H} = \tilde{\mathbf{J}}(\tilde{\mathbf{G}}^y)^{\dagger} \tag{4.47}$$

may be reasonable. Note that $(\tilde{\mathbf{G}}^y)^\dagger$ no longer represents the left inverse, but rather the right inverse (see remark above). Actually, $\tilde{\mathbf{G}}^y$ might have neither full row or column rank, and in this case the pseudo-inverse should be obtained from the singular value decomposition (see e.g. Skogestad and Postlethwaite (1996)).

Mathematically, this choice of $\mathbf{H}$ gives the solution which minimize $\|\mathbf{E}\|_2$ where $\mathbf{E}$ is defined as

$$\mathbf{E} = \mathbf{M}_n\mathbf{H}\tilde{\mathbf{G}}^y - \tilde{\mathbf{J}} \tag{4.48}$$

The overall goal is to minimize $\mathbf{M}$ in eq. (4.26), and to see why it may be reasonable to minimize $\mathbf{E}$, note that we can express $\mathbf{M}_d$ as

$$\mathbf{M}_d = \mathbf{E}\begin{bmatrix}\mathbf{J}_{uu}^{-1}\mathbf{J}_{ud}\\ -\mathbf{I}\end{bmatrix} \tag{4.49}$$

Proof: Note that

$$\mathbf{M}_d = \mathbf{J}_{uu}^{1/2}(\mathbf{J}_{uu}^{-1}\mathbf{J}_{ud} - \mathbf{G}^{-1}\mathbf{G}_d) = \mathbf{M}_n\mathbf{H}\tilde{\mathbf{G}}^y\begin{bmatrix}\mathbf{J}_{uu}^{-1}\mathbf{J}_{ud}\\ -\mathbf{I}\end{bmatrix} \tag{4.50}$$

and since

$$\mathbf{E} = \mathbf{M}_n\mathbf{H}\tilde{\mathbf{G}}^y - \tilde{\mathbf{J}} \tag{4.51}$$

we see immediately that

$$\mathbf{M}_d = \mathbf{E}\begin{bmatrix}\mathbf{J}_{uu}^{-1}\mathbf{J}_{ud}\\ -\mathbf{I}\end{bmatrix} \tag{4.52}$$

□

Remark 1 In general we can write the solution of $\mathbf{HA} = \mathbf{B}$ as $\mathbf{H} = \mathbf{BA}^\dagger$. Further, as noted in Hori et al. (2005), we here use the right general inverse where $\mathbf{A}^\dagger = \mathbf{A}^T(\mathbf{A}^T\mathbf{A})^{-1}$ since $\mathbf{A}$ has full row rank (we have to few measurements). In this case there is no solution and we find the solution that minimize the 2-norm of

$$\mathbf{E} = \mathbf{B} - \mathbf{HA} \tag{4.53}$$

i.e. the regular least square solution and with the corresponding minimal $\|\mathbf{H}\|_2$.

Remark 2 The null space method focused on minimizing the effect of the disturbances on loss. In eq. (4.49) we try to minimize the effect of the measurement error and $\mathbf{M}_d = 0$. If we focus only on the disturbance effect on the loss, we should minimize $\mathbf{M}_d$ and we have from eq. (4.23) (assuming $\mathbf{n} = 0$) that

$$\mathbf{z} = \mathbf{M}_d\Delta\mathbf{d} = \mathbf{J}_{uu}^{1/2}(\mathbf{HG}^y)^{-1}\mathbf{HF}\Delta\mathbf{d} = \mathbf{M}_n\mathbf{HF}\Delta\mathbf{d} \tag{4.54}$$

and in order to minimize $\mathbf{M}_d$ we must select $\mathbf{M}_n\mathbf{H}$ that corresponds to the smallest singular value directions of $\mathbf{F} = \mathbf{U}_F\mathbf{\Sigma}_F\mathbf{V}_F^T$, i.e. select $\mathbf{M}_n\mathbf{H} = \begin{bmatrix}\mathbf{u}_{F,n_y-n_u} & \mathbf{u}_{F,n_y}\end{bmatrix}^T$ where $\mathbf{u}_{F,i}$ is the i'th output vector corresponding to the i'th singular value. Note, we can still select $\mathbf{M}_n$ or $\mathbf{G}$ as appropriate.

4.3.5 General discussion

The above derivations are local, since we assume a linear process and a second-order objective function in the inputs and the disturbances. Thus, we cannot guarantee that the proposed controlled variables are globally optimal. However, using the above expressions should give an indication on how sensitive the candidates are to measurement error. For a final validation, we should always check the loss for the proposed structures using the non-linear models of the process.

We see that the null space method generalizes to the case where we want to use all available measurements. In general, using all measurements should give a better estimate on the uncertain disturbances. However, in many cases many of the measurements are closely correlated or are prone with measurement error. In such cases the advantages of using additional measurements and the increased complexity of the control structure may not be justified.

A logic extension of the null space method, would be to use eq. (4.24) and to select $\mathbf{M}_n\mathbf{H}$ as the output singular vectors corresponding to the smallest singular values of $\tilde{\mathbf{F}} = \begin{bmatrix} -\mathbf{F}\mathbf{W}_d & \mathbf{W}_n^y \end{bmatrix}$. However, we then find the optimal solution when requiring $\|\mathbf{M}_n\mathbf{H}\|_2 = 1$ which is *not* necessarily the optimal solution.

Relationship to indirect control

Indirect control is when we want to control a set of primary variables $\mathbf{y}_1$, at constant setpoints. This is a special case of the results in this paper if we select

$$L = \frac{1}{2}\|\mathbf{y}_1 - \mathbf{y}_1^s\|_2 = \frac{1}{2}[\mathbf{y}_1 - \mathbf{y}_1^s]^T[\mathbf{y}_1 - \mathbf{y}_1^s] \tag{4.55}$$

with

$$\Delta\mathbf{y}_1 = \mathbf{G}_1\Delta\mathbf{u} + \mathbf{G}_{d1}\Delta\mathbf{d} = \tilde{\mathbf{G}}_1 \begin{bmatrix} \Delta\mathbf{u} \\ \Delta\mathbf{d} \end{bmatrix} \tag{4.56}$$

we find that

$$\mathbf{J}_{uu} = \mathbf{G}_1^T\mathbf{G}_1 \tag{4.57}$$

$$\mathbf{J}_{ud} = \mathbf{G}_1^T\mathbf{G}_{d1} \tag{4.58}$$

The case of indirect control is discussed in more detail by Hori et al. (2005) (see Appendix C). Note that the results in Hori et al. (2005) follows directly from this chapter with

$$\mathbf{M}_d = \mathbf{P}_d = (\mathbf{G}_{d1} - \mathbf{G}_1\mathbf{G}^{-1}\mathbf{G}_d) \tag{4.59}$$

$$\mathbf{M}_n = \mathbf{P}_c = \mathbf{G}_1^{-1}\mathbf{G} \tag{4.60}$$

where $\Delta\mathbf{c} = \mathbf{G}\Delta\mathbf{u} + \mathbf{G}_d\Delta\mathbf{d}$ is the variables we select to control (in order to indirectly control $\mathbf{y}_1$).

Next, we propose a procedure for using the null space method where we also include measurement error. The procedure is composed of two steps: First, we select a subset of the measurements that minimize the effect of the measurement error. Second, we use the null space method and require zero disturbance loss.

4.4 Procedure: Null space method and extra measurements

We propose a procedure for the null space method using the sub-optimal measurement selection rule of above. Assume that $n_{y_0} \geq n_u + n_d$, i.e. the number of available measurements is larger than the number of (unconstrained) inputs and disturbances

1. **Nominal Optimum**:
   Solve the reduced space optimization problem as defined by eq. (4.11) for the nominal disturbance $\mathbf{d}^*$. The solution is $(\mathbf{x}^*, \mathbf{y}^*) = (\mathbf{x}^{\mathbf{opt}}(\mathbf{d}^*), \mathbf{y}^{\mathbf{opt}}(\mathbf{d}^*))$.

2. **Linearization**:
   Linearize the process model around the nominal optimal point, which yields

$$\Delta \mathbf{y}_0 = \mathbf{G}^{y_0} \Delta \mathbf{u} + \mathbf{G}_d^{y_0} \Delta \mathbf{d} \tag{4.61}$$

   for all measurements $y_{0,i}$

3. **Scaling of variables**:
   Use the following variable scaling:

   - Scale each measurement $y_{0,i}$ with its corresponding implementation error ($|n_{y_{0,i}}|$).
   - Scale each input u_j with its corresponding allowable range ($|\Delta u_{j,max}|$). If we have direct information on the Hessian matrix $\mathbf{J}_{uu}$, scale u_j so that $\mathbf{J}_{uu}$ is close to unitary.
   - Scale each disturbance d_k by its corresponding expected disturbance ($|\Delta d_{k,max}|$).

   which yields the scaling matrices

$$\mathbf{W}_n^{y_0} = \begin{bmatrix} |n_{y_0,1}| & & \\ & \ddots & \\ & & |n_{y_0,n_{y_0}}| \end{bmatrix} \quad \mathbf{W}_u = \begin{bmatrix} |\Delta u_{1,max}| & & \\ & \ddots & \\ & & |\Delta u_{n_u,max}| \end{bmatrix} \tag{4.62}$$
$$\mathbf{W}_d = \begin{bmatrix} |\Delta d_{1,max}| & & \\ & \ddots & \\ & & |\Delta d_{n_d,max}| \end{bmatrix}$$

4. **Selection of measurements**.

   (a) **Augmented process model**. Calculate the scaled augmented process model

$$\Delta \mathbf{y}_0' = \mathbf{G}^{y_0\prime} \Delta \mathbf{u}' + \mathbf{G}_d^{y_0\prime} \Delta \mathbf{d}' = (\mathbf{W}_n^{y_0})^{-1} \mathbf{G}^{y_0} \mathbf{W}_u \Delta \mathbf{u}' + (\mathbf{W}_n^{y_0})^{-1} \mathbf{G}_d^{y_0} \mathbf{W}_d \Delta \mathbf{d}' \tag{4.63}$$

   and obtain the scaled augmented process matrix

$$\Delta \mathbf{y_0}' = \tilde{\mathbf{G}}^{y_0\prime} \Delta \tilde{\mathbf{u}}' = [\mathbf{G}^{y_0\prime} \; \mathbf{G}_d^{y_0\prime}] \begin{bmatrix} \Delta \mathbf{u}' \\ \Delta \mathbf{d}' \end{bmatrix} \tag{4.64}$$

(b) **Best subset of measurements**

- **Sequential method:** Two methods for selecting the best subset of measurements are proposed: (1) the *sequential method*, in which measurements are selected one-by-one, (2) the *direct method*, in which all measurements are selected simultaneously. The computational burden is the major difference between the two alternatives.
  i. **Selection of the first measurement**. Calculate the row 2-norm $\|\tilde{\mathbf{G}}_i^{y_0\prime}\|_2$ for all measurements $y_{0,i}$ and sort by decreasing row norm. Select the measurement with highest norm and add the measurement to a selection vector $\mathbf{y}_s$.
  ii. **Selection of the additional measurements**. For all remaining measurements, add measurements one-by-one to the selection vector $\mathbf{y}_s$ until $n_{y_s} = n_u + n_d$ and calculate the minimum singular value of the corresponding augmented process matrix

$$\begin{bmatrix} \tilde{\mathbf{G}}_i^{y_s\prime} \\ \tilde{\mathbf{G}}_{i-1}^{y_s\prime} \end{bmatrix}$$

  Select the new measurement which has the highest minimum singular value and add to the selection vector.
- **Direct selection (all combinations)**
  i. Let $\mathcal{I}$ be the set of all n_c possible combinations of n_y measurements from n_{y_0} measurements, i.e. $\mathcal{I} = \{\{1,2,3,\ldots\},\{1,2,4,\ldots\},\ldots\}$ where $\mathcal{I}_1$ is the first set. The number of possible combinations is $n_{ac} = \frac{n_{y_0}!}{n_y!(n_{y_0}-n_y)!}$
  ii. For all n_{ac} combinations, calculate the minimum singular value for the augmented matrix

$$\underline{\sigma}\left(\tilde{\mathbf{G}}_{\mathcal{I}_i}^{y\prime}\right) = \underline{\sigma}\left(\left[\mathbf{G}_{\mathcal{I}_i}^{y\prime}\ \mathbf{G}_{d,\mathcal{I}_i}^{y\prime}\right]\right)$$

  and sort in descending order. Select the subset $\mathcal{I}_i$ that maximize the minimum singular value.

$$\mathcal{I}^{opt} = arg\left[\max_{\mathcal{I}_i \in \mathcal{I}} \underline{\sigma}\left(\tilde{\mathbf{G}}_{\mathcal{I}_i}^{y\prime}\right)\right]$$

5. **Null space of F and selection of controlled variables**.

(a) Obtain the optimal sensitivity matrix **F**, for example numerically from the non-linear optimization problem,

$$\mathbf{F} = \left(\frac{d\mathbf{y}^{opt}}{d\,\mathbf{d}^T}\right)^*$$

or from eq. (4.15).

(b) Calculate the orthogonal basis $\mathbf{h}_1^T \ldots \mathbf{h}_{n_c}^T$ for the null space of $\mathbf{F}^T$, $\mathcal{N}(\mathbf{F}^T)$.

(c) Select the rows of $\mathbf{H} = \begin{bmatrix} \mathbf{h}_1 \\ \vdots \\ \mathbf{h}_{n_c} \end{bmatrix}$ such that $\mathbf{H} \in \mathcal{N}(\mathbf{F}^T)$ and the rows of $\mathbf{H}$ form a orthonormal basis. This ensures that $\mathbf{HF} = 0$.

6. **Shaping G or M$_n$**
Select the matrix $\mathbf{C}$ with dimension $n_u \times n_u$, where $\mathbf{H}' = \mathbf{CH}$, to get $\mathbf{G} = \mathbf{I}$ or as appropriate.

7. **Loss calculations & feasibility**
The above procedure does not ensure feasibility for all disturbances using nominal setpoints, so this needs to be verified. Usually it is sufficient to check the end points of the disturbance and implementation error space. In addition, calculate the loss for the different candidates using the non-linear model.

Remark. The sequential method needs fewer calculations, but it does not guarantee the subset that maximizes the minimum singular value of the augmented plant. The number of singular value calculations in the sequential method is

$$n_{sc} = \frac{1}{2} n_y (2n_{y_0} - n_y + 1)$$

For example, for a case with $n_{y_0} = 48$ and $n_y = 6$, $n_{ac} = 12,271,512$ calculations is needed for the direct selection rule, while only $n_{sc} = 273$ for the sequential method[3].

In the next two sections, we illustrate the above procedure on examples.

4.5 Example 1: Toy example

This example is an extension of the example found in Halvorsen et al. (2003). Assume that we have a SISO system with one disturbance and the following objective function

$$J = (u - d)^2 \tag{4.65}$$

with the nominal disturbance $d^* = 0$. From eq. (4.65) it is clear that $J_{opt} = 0 \ \forall \ d$ and the optimal input is $u^{opt}(d) = d$. Assume that the following measurements are available:

$$y_1 = 0.1(u - d) \qquad y_2 = 20u \qquad y_3 = 10u - 5d \qquad y_4 = u$$

We further assume that the system is scaled such that $|d| \leq 1$ and $|n_i| \leq 1$. In matrix notation, we have the following scaled model $\Delta \mathbf{y} = \mathbf{G}^{y_0} \Delta u + \mathbf{G}_d^{y_0} \Delta d$ where;

$$\mathbf{G}^{y_0 T} = \begin{bmatrix} 0.1 & 20 & 10 & 1 \end{bmatrix} \quad \text{and} \quad \mathbf{G}_d^{y_0 T} = \begin{bmatrix} -0.1 & 0 & -5 & 0 \end{bmatrix} \tag{4.66}$$

[3] On a Pentium 4 class processor with 1 GB RAM running GNU/Linux and Matlab, an estimated 30 minutes is needed for the direct method, while an estimated 0.0434 seconds for the sequential method

Since the optimal input is given as $u^{opt} = d$ we have that the optimal sensitivity matrix is $\mathbf{F}$

$$\Delta \mathbf{y}_0^{opt} = \mathbf{F}\Delta d = \mathbf{G}^{y_0}\Delta u^{opt}(d) + \mathbf{G}_d^{y_0}\Delta d = \begin{bmatrix} 0.1 \\ 20 \\ 10 \\ 1 \end{bmatrix} \Delta d + \begin{bmatrix} -0.1 \\ 0 \\ -5 \\ 0 \end{bmatrix} \Delta d = \begin{bmatrix} 0 \\ 20 \\ 5 \\ 1 \end{bmatrix} \Delta d \quad (4.67)$$

As seen from eq. (4.67), measurement y_1 have $\Delta y_1^{opt} = 0$ so the disturbance contribution to the loss is zero. However, it turns out that the low gain from the input to y_1 yields a high sensitivity to noise, which in turn results in large loss.

For the single measurement candidates ($c_i = y_i$) the losses are

$$L_1 = 100 \qquad L_2 = 1.0025 \qquad L_3 = 0.26 \qquad L_4 = 2$$

Candidate y_1 is the candidate with the largest loss and illustrates the importance of taking measurement error into account. y_3 is the best candidate.

Since $n_y = n_u + n_d = 1 + 1$, six sets of measurements are possible. Table 4.5 shows the results from the optimal and sub-optimal rule (as given by eq. (4.46)). From Table 4.5 we see that the candidates involving measurement y_1, all are sensitive to noise. From the sub-optimal rule, we see that the same internal rank applies. c_{23} is the best candidate followed by c_{34}, while c_{12}, c_{14} and c_{13} are predicted to have approximately the same sensitivity to noise. Note that using measurements y_2 and y_4 yields infinite

Table 4.2: *The sub-optimal and optimal rules for the toy example.*

$c_{y_i y_j}$	$y_\#$	$y_\#$	Sub-optimal $\underline{\sigma}(\tilde{\mathbf{G}}^y)$	Optimal $\bar{\sigma}(\tilde{\mathbf{J}}(\mathbf{G}^y)^{-1})$
c_{23}	2	3	4.4490	0.2915
c_{34}	3	4	0.4458	1.4422
c_{12}	1	2	0.1	14.1421
c_{14}	1	4	0.0995	14.1421
c_{13}	1	3	0.0447	14.1421
c_{24}	2	4	0	inf

sensitivity to noise, due to $\tilde{\mathbf{G}}^y$ being singular. The optimal combination ($\mathbf{H}$) is for the best candidate (c_{23}) is found as the null space of $\mathbf{F}$ were $F_{2,3} = [20\ 5]^T$. The null space vector is:

$$\mathcal{N}([20\ 5]) = [-0.2425\ 0.9701]^T \quad (4.68)$$

such that the controlled variable is $c_{23} = -0.2425y_2 + 0.9701y_3$. Note that for the candidates using measurement y_1, since ,

$$\mathcal{N}([F_1\ F_i]) = [1 \quad 0] \quad \text{for} \quad i \in \{2,3,4\} \quad (4.69)$$

so the candidates involving measurement y_1 would be equivalent to controlling y_1 alone (no contribution from the other measurement). Table 4.3 show the worst case loss for the candidate controlled variables. From Table 4.3 we see that the candidate with the

Table 4.3: *Worst-case loss for the different candidates*

Rank	c_i	$L = 1/2\bar{\sigma}(\mathbf{M})$
1	c_{23}	0.0425
2	y_3	0.26
3	y_2	1.0025
4	c_{34}	1.04
5	y_4	2
6	y_1,c_{21},c_{13},c_{14}	100
7	c_{24}	inf

lowest loss is c_{23} and it reduces the loss by a factor of 6 compared to the second best candidate variable which is using the single measurement y_3.

Note that controlling c_{34} has a higher loss than controlling y_2 or y_3, due to the noise contribution of y_4. This implies that when using the minimum number of measurements in the null space method, there may be single measurement candidates with a lower loss. Since we have a quadratic cost function and a linear process model, all candidates using the null space method has zero disturbance loss.

Halvorsen et al. (2003) show, by formulating the selection problem as an optimization problem, that by using all measurements and minimizing the loss, using eq. (4.25), with respect to h_i, $\mathbf{H} = [h_1 \dots h_4]$ this results in a controlled variable with a slightly lower loss of $L = 0.0405$. The contribution from the disturbance and the noise is

$$M_d = -0.0606 \qquad \mathbf{M}_n = \begin{bmatrix}0.0057 & -0.0645 & 0.2706 & -0.0032\end{bmatrix} \tag{4.70}$$

and

$$\mathbf{H}^{opt} = \begin{bmatrix}-0.2170 & -0.2213 & 0.9273 & -0.2100\end{bmatrix} \tag{4.71}$$

As seen it is not optimal to require $M_d = 0$, since we can lower the effect of the measurement error by allowing a small contribution from the disturbance. The reduction in loss ($L_{opt} = 0.0405$) is small compared to c_{23} ($L_{c_{23}} = 0.0425$) and using a two step approach (select measurements first, and thereafter require $\mathbf{M}_d = 0$) is acceptable here. Using only measurements y_2 and y_3, the optimal combination that minimize $\mathbf{M}$ is $\mathbf{H}_{23}^{opt} = [-0.2323\ 0.9727]$ with a loss of $L_{23}^{opt} = 0.0406$.

4.6 Example 2: CSTR with chemical reaction

In this section, we illustrate the null space method on a real example, namely a continuous stirred reactor (CSTR) with a reversible reaction (Economou et al., 1986). The process consists of an ideal continuous stirred tank reactor, see Figure 4.3, where the reversible exothermic reaction

$$A \rightleftharpoons B \tag{4.72}$$

takes place, with the reaction rate expressions on the form:

$$r = k_1 C_A - k_2 C_B \qquad \text{where} \quad k_1 = C_1 e^{\frac{-E_1}{RT}} \quad \text{and} \quad k_2 = C_2 e^{\frac{-E_2}{RT}} \tag{4.73}$$

The process model for the system is:
Mass balances

$$\frac{dC_A}{dt} = \frac{1}{\tau}(C_{A,i} - C_A) - r \quad \text{where} \quad \tau = \frac{M}{F} \tag{4.74}$$

$$\frac{dC_B}{dt} = \frac{1}{\tau}(C_{B,i} - C_B) + r \tag{4.75}$$

Energy balance

$$\frac{dT}{dt} = \frac{1}{\tau}(T_i - T) + \frac{-\Delta H_{rx}}{\rho C_p} r \tag{4.76}$$

where $C_{j,i}$ is the concentration of component j in the inflow, C_j is the concentration in the reactor for component j, T_i is the inlet temperature while T is the temperature in the reactor. Nominal data for the example is given in Table 4.4.

Table 4.4: *Nominal data for the CSTR case*

Parameter	Value	Units
F^*	1	$holdup\ min^{-1}$
C_1	5000	s^{-1}
C_2	10^6	s^{-1}
C_p	1000	$cal\ kg^{-1} K^{-1}$
E_1	10^4	$cal\ mole^{-1}$
E_2	15000	$cal\ mole^{-1}$
R	1.987	$cal\ mole^{-1}\ K^{-1}$
T_i^*	input	K
$C_{A,i}^*$	1	$mole\ L^{-1}$
$C_{B,i}^*$	0	$mole\ L^{-1}$
$-\Delta H_{rx}$	5000	$cal\ mole^{-1}$
ρ	1	$kg\ L^{-1}$
τ	1	min

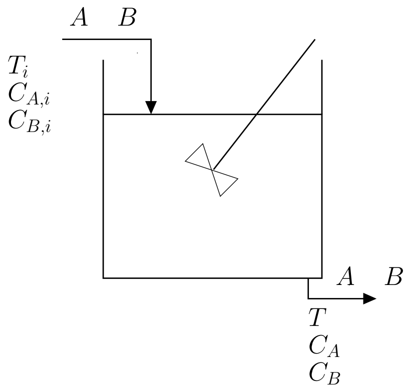

Figure 4.3: *CSTR*

4.6.1 Objective, inputs, outputs and disturbances

We assume that the economic operating objective is to maximize the profit ($\max -J = \min J$) where:

$$J = -\left[p_{C_B} C_B - (p_{T_i} T_i)^2\right] \tag{4.77}$$

where $p_{C_B} = 2.009$ is the price of product C_B and $p_{T_i} = 1.657 \times 10^{-3}$ is the utility cost of heating the input stream.

The input is $u = T_i$, the temperature in the inlet stream, the states are $\mathbf{x}^T = [C_A\ C_B\ T]$, and the disturbances are assumed to be $\mathbf{d}^T = [C_{A,i}\ C_{B,i}]$. The available measurements are $\mathbf{y}_0^T = [C_A\ C_B\ T\ T_i]$.

We assume that the disturbances are in the range $C_{A,i} \in C_{A,i}^* \pm 0.3$, $C_{B,i} \in C_{B,i}^* + 0.3$ where $C_{j,i}^*$ denotes the nominal disturbance, and that the measurement errors are $n_{C_A} = n_{C_B} = 0.01 mol/L$ and $n_T = n_{T_i} = 0.5\ K$ for the concentrations and the temperatures respectively. We assume that only one disturbance or implementation error is present at any time.

Table 4.5: *Optimal values for different disturbances for the CSTR-example*

Variable	$C_{A,i} = 1.3$	$C_{A,i} = 0.7$	$C_{B,i} = 0.3$	nominal
C_A	0.644	0.352	0.585	0.498
C_B	0.656	0.348	0.715	0.502
T	429.170	422.601	415.883	426.761
T_i	425.889	420.863	413.810	424.249
$-J$	0.821	0.212	0.966	0.515

4.6.2 Optimal operation

Table 4.5 summarizes the optimal values for different disturbance realizations. Figure 4.4 shows the absolute value of the objective for three disturbances with respect to the input. The nominal optimal input $T_i^{opt}(d^*)$ is indicated by the vertical line. The

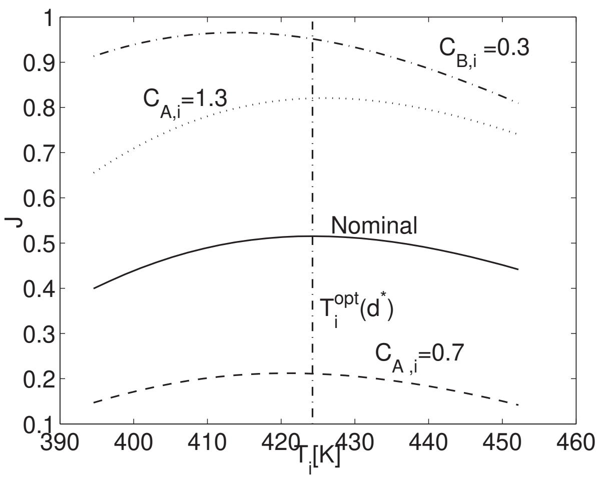

Figure 4.4: *Plot of objective with respect to the input for four different disturbances $C_{A,i} = 0.7$, $C_{A,i} = 1.3$, $C_{B,i} = 0.3$ and the nominal point. The vertical line indicates the nominal optimal input.*

optimal input lies in the range $T_i \in [413\ 426]$, while the optimal objective value lies in the range $J = 0.21$ to $J = 0.97$. With the given input and disturbances, we need $n_y = n_u + n_d = 1+2 = 3$ measurements to form the controlled variable based on the null space method. This results in $\frac{4!}{3!1!} = 4$ possible candidate measurements combinations. In addition to the four candidates synthesized using the null space method, we include all candidates controlling a single measurement, in total eight different candidates, see Table 4.6.

We use the sub-optimal rule of Section 4.3.3 to find the best subset of measurements, see Table 4.7. Candidates c_{123} and c_{124} have the highest minimum singular value $(\tilde{\mathbf{G}})$ and should therefore have the lowest sensitivity to noise, while c_{134} and c_{234} should be more sensitive to noise.

Table 4.6: *Candidate control structures*

#	Controlled variable	Measurements
1	C_A	C_A
2	C_B	C_B
3	T	T
4	T_i	T_i
5	c_{123}	C_A, C_B, T
6	c_{124}	C_A, C_B, T_i
7	c_{134}	C_A, T, T_i
8	c_{234}	C_B, T, T_i

Table 4.7: *Lower singular value for the four null space candidates*

Variable	$\underline{\sigma}(\tilde{\mathbf{G}})$
c_{123}	6.44
c_{124}	6.31
c_{134}	1.03
c_{234}	1.21

4.6.3 Loss calculation using non-linear model

The loss is calculated using the non-linear model and is shown in Table 4.8. For all null space candidates, the corresponding coefficient vector ($\mathbf{H}$) was calculated based on the null space of the sensitivity matrix found by numerical differentiation (not shown). As seen from Table 4.8, all four linear combination candidates show small losses with respect to the disturbances, with only minor differences between them. The largest difference is for the measurement errors, where candidates c_{134} and c_{234} have larger losses than candidates c_{123} and c_{124}. If we compare the loss due to measurement error in Table 4.8, with the singular values in Table 4.7, we see that the sub-optimal rule based on the minimum singular value, correctly predicts the sensitivity to measurement error. Both c_{123} and c_{124} are insensitive to measurement error while c_{134} and c_{234} are sensitive to measurement error. We see that the loss is marginally larger for c_{123} than for c_{124} which contradict the results from Table 4.7 and can be caused by using the sub-optimal rule.

Table 4.8: *Loss (in %) for all candidate structures with respect to disturbances and measurement errors. For the measurement error, the worst-case and the average loss are given in the last two columns.*

#	candidate	$C^*_{A,i}+0.3C^*_{A,i}$	$C^*_{A,i}-0.3C^*_{A,i}$	$C^*_{B,i}+0.3C^*_{B,i}$	$n^{i,max}$	$n^{i,avg}$
1	C_A	inf	89.668	inf	1.254	1.127
2	C_B	27.689	inf	32.781	inf	inf
3	T	0.102	0.698	1.566	0.006	0.006
4	T_i	0.048	0.469	1.4532	0.006	0.006
5	c_{123}	0.006	0.036	0.082	0.034	0.014
6	c_{124}	0.006	0.036	0.073	0.030	0.013
7	c_{134}	0.009	0.056	0.001	1.756	0.695
8	c_{234}	0.008	0.049	0.006	0.6735	0.2943

For the single measurement candidates, controlling the temperatures (either T_i or T) show good self-optimizing properties, both with respect to disturbances and measurement errors. The losses are largest for a disturbance in C_B (approximately 1.5%) for both candidates. Note that keeping the input (T_i) at the nominal optimal point, has better self-optimizing properties than controlling the reactor temperature. Controlling C_A or C_B lead to infeasible operation or a very large loss and are not suitable for self-optimizing control. In addition, both candidates show multiple steady-states and is not considered for further analysis.

Figure 4.5 shows the loss profiles for the feasible candidates with respect to the disturbances.

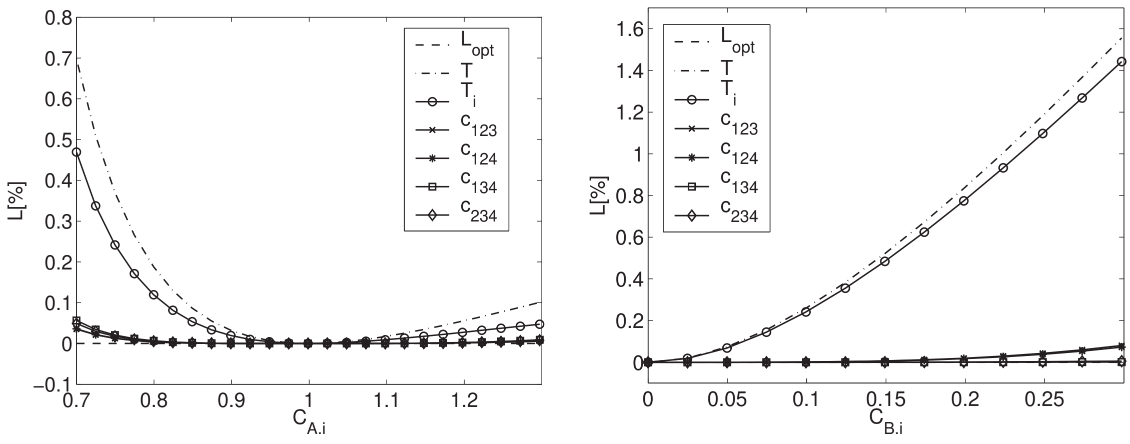

(a) Loss profiles with respect to disturbance $C_{A,i}$ for the feasible candidates.

(b) Loss profiles with respect to disturbance $C_{B,i}$ for the feasible candidates.

Figure 4.5: *Loss profiles for the feasible structures*

In conclusion, based on the loss calculations, the candidates c_{123} and c_{124} show the best self-optimizing properties, followed by the candidates T and T_i.

4.6.4 Controllability for the most promising candidates

Finally, we compare the controllability of the most promising candidates. The motivation is two-fold: First we want to find the candidate that is simplest to control. Second, we want to show that controlling a linear combination of measurements is possible in practice.

We expect no limitations for keeping the input constant (system is stable), so this candidate has not been considered in the dynamic simulations. The three candidates considered here, are T, c_{123} and c_{124}. We make the following assumptions for the dynamic simulations:

1. A time delay of 2 s is assumed for all measurements.
2. The disturbances are modeled as steps, filtered using a first order filter $f_i = \frac{1}{5s+1}$.
3. PI-controller is to be used, tuned with Skogestads IMC (Skogestad, 2003) tuning rules. See Table 4.9 for tuning parameters.

We include only the simulation for a disturbance in $C_{B,i}$. The responses for a disturbance in $C_{A,i}$ are similar for all candidates. Figure 4.6 shows the responses for a step in the feed composition of B. Figure 4.6(a) shows the response for C_A, C_B, T and the input T_i. The horizontal solid line represents the new optimal value (for

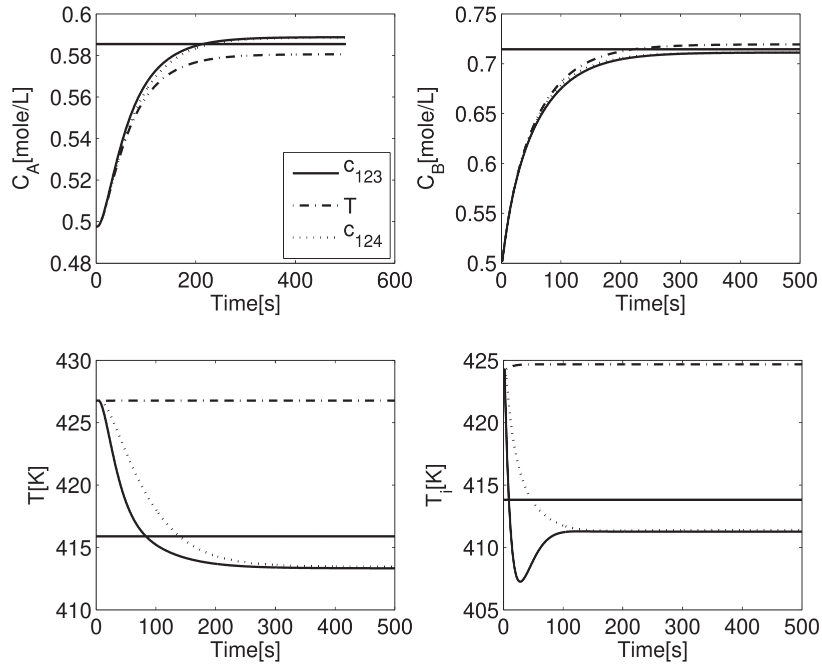

(a) Plot of concentration of A, concentration of B and temperature in the CSTR together with the input usage for a positive step in the concentration of B in the feed.

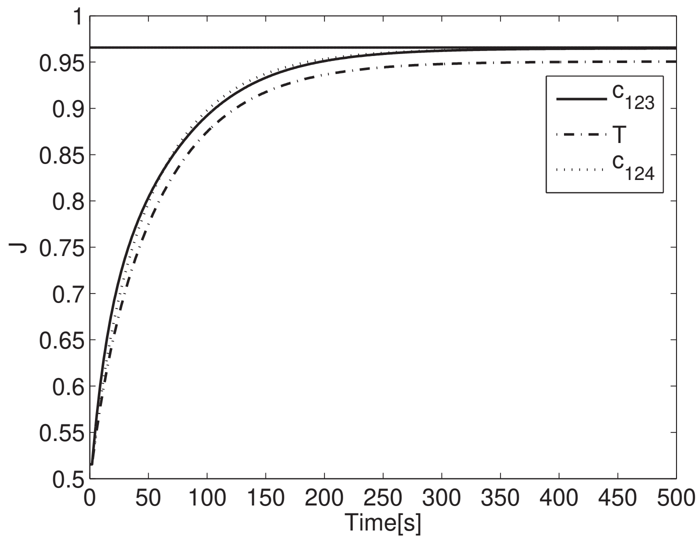

(b) Plot of the objective function value for a positive step in the concentration of B in the feed.

Figure 4.6: *Responses for a positive step in the concentration of B in the feed.*

Table 4.9: *PI-controller parameters using SIMC-tuning rules*

Variable	K_c	τ_I	τ_C
c_{123}	2.89	60	20
c_{124}	0.27^a	–	2
T	15.0	16	2

[a] Pure integral controller $K(s) = \frac{K_I}{s}$ where $K_I = \frac{1}{k}\frac{1}{(\theta+\tau_C)}$

$C_{B,I} = 0.3$). From the temperature responses, we see that candidates c_{123} and c_{124} settle reasonably close to the new optimal value (a steady-state offset of approximately 3 K), while candidate $c = T$ has a large steady-state offset. This is also confirmed by the response of the objective function, shown in Figure 4.6(b). Candidates c_{123} and c_{124} track the optimal value of the objective. Candidate c_{123} exhibits an overshoot in the controlled variable (not shown), which is reflected by the undershoot in the input. Based on the combined self-optimizing and dynamic performance, candidate c_{124} is the best controlled variable.

4.7 Conclusions

In this paper we have extended the null space method, where we select controlled variables as linear combinations of the measurements ($\mathbf{c} = \mathbf{Hy}$), to include measurement error. Explicit expressions have been derived to calculate the null space matrix $\mathbf{H}$ under the assumption that we want zero disturbance loss ($\mathbf{M}_d = 0$). A procedure for using the null space method has been proposed. The procedure is separated into two steps: First, we select the measurements that are insensitive to noise. Second, we find the coefficient matrix $\mathbf{H}$ that yields zero disturbance loss by requiring $\mathbf{HF} = 0$ where $\mathbf{F}$ is the optimal sensitivity matrix.

In addition, we have shown how to use the null space method for cases where we use all or have too few measurements. Finally, the ideas presented here have been illustrated on two examples. In both examples we are able to find candidates for self-optimizing control that are insensitive to *both* disturbances and measurements errors.

Bibliography

Alstad, V. and Skogestad, S. (2004). Self-optimizing contro: Optimal measurement selection. *AIChE Annual meeting, 2004*. Poster 403e.

Economou, C., Morari, M., and Palsson, B. (1986). Internal model control 5. Extension to nonlinear systems. *Ind. Eng. Chem. Process. Des. Dev.*, 22(2):403–411.

Halvorsen, I., Skogestad, S., Morud, J., and Alstad, V. (2003). Optimal selection of controlled variables. *Ind. Eng. Chem. Res.*, 42(14):3273–3284.

Hori, E., Skogestad, S., and Alstad, V. (2005). Perfect steady state indirect control. *Ind. Chem. Res.* In press.

Horn, R. A. and Johnson, C. R. (1991). *Topics in matrix analysis*. Cambridge.

Skogestad, S. (2003). Simple analytic rules for model reduction and PID controller tuning. *J. Proc. Control*, 13:291–309.

Skogestad, S. and Postlethwaite, I. (1996). *Multivariable Feedback Control*. John Wiley & Sons.

Strang, G. (1988). *Linear algebra and its applications*. Harcourt Brace & Company, 3 edition.

Chapter 5

Disturbance discrimination in self-optimizing control

Manuscript in preparation

In most chemical plants, a large number of disturbances are present. However, not all disturbances are equally important for the optimal operation of the plant. Below, we present new rules for selecting important disturbances, with emphasis on selecting important disturbances for self-optimizing control. Ideally, we would prefer to remove disturbances that are not economically important before we design and analyze the control structure. The main conclusion here, is that one cannot separate the selection of economically important disturbances from the selection of control structure. The rules presented here reflect this observation.

5.1 Introduction

Self-optimizing control is when, by keeping controlled variables at their nominal setpoints by the use of feedback, the process is indirectly kept at the optimal state in spite of external disturbances and implementation errors (Skogestad, 2000). The plant operational performance is measured using a scalar cost function (e.g. the economic cost) and depends on the manipulation of the degrees of freedom available to counteract external disturbances entering the plant.

Consider the steady-state where, for a given disturbance, an optimal value for the degrees of freedom (the manipulated inputs) can be found and implemented (either directly or indirectly by the use of feedback). However, for a disturbance change, the existing state of the process is not longer the optimal and new setpoints need to be found by repeating the optimization with subsequent implementation in the process.

To avoid the need of re-optimization and for a direct measurement or an estimate of the disturbances, we use feedback to correct for the new disturbances so that the plant is kept at (or near) the optimal state. The key to achieve this, is to select the correct feedback controlled variables.

One method for finding self-optimizing controlled variables $\mathbf{c}$, is the null space method of Alstad and Skogestad (2004). It gives controlled variables that are linear combinations of a subset of the available measurements, i.e. $\mathbf{c} = \mathbf{H}\mathbf{y}$ where $\mathbf{y}$ is a vector of a subset of the measurements. One important requirement, is that the number of measurements (the dimension of $\mathbf{y}$) must at least be equal to the number of unconstrained inputs (u's) and disturbances (d's), that is

$$n_y \geq n_u + n_d \tag{5.1}$$

In typical chemical plants, the number n_d of disturbances may be large and the required number of measurements as given by eq. (5.1), may not be available. Fortunately, not all disturbances are equally important for the optimal operation of the plant, and we then have the possibility of eliminating some of them. Thus, reducing the number of disturbances has two advantages: (1) we need fewer measurements in the null space method (design) and (2) less effort is needed in evaluating the self-optimizing properties of the candidate control structures (analysis).

The issue of reducing the number of disturbances has received limited attention in the literature on self-optimizing control. Previous methods for selecting self-optimizing controlled variables have focused on using single measurement candidates, i.e. $c_i = y_i$. Thus, the design of the self-optimizing control structures are unaffected by a large number of disturbances, and the only incentive for reducing the number of disturbances is to reduce the computational effort in analyzing the self-optimizing properties of the candidates. Often, the important disturbances are assumed given, by physical experience or by means of other methods. One exception is the early work of Morari et al. (1980) where several rules on how to select important disturbances were presented.

Related to this is the work on parameter estimation. For example, Krishnan et al. (1992) discussed selecting which parameters to estimate based on a given set of disturbances.

Below we present some background and previous work on the selection and evaluation of self-optimizing control structures. Thereafter, we present rules on how to discriminate disturbances, including illustrative examples.

5.2 Background and theory

Assume that we have the reduced space optimization problem, in the unconstrained variables $\mathbf{u}$

$$\min_{\mathbf{x},\mathbf{u}} J(\mathbf{x}, \mathbf{u}, \mathbf{d}_0) \tag{5.2}$$

$$\mathbf{f}'(\mathbf{x}, \mathbf{u}, \mathbf{d}_0) = 0 \tag{5.3}$$

where $\mathbf{f}'$ is the model equations, J the cost function, $\mathbf{d}_0$ the vector of disturbances, $\mathbf{x}$ the states and dim($\mathbf{f}'$)=dim($\mathbf{x}$), that is the problem has only equality constraints (see Section 2.3.1 for a motivation). The problem is to find the controlled variables $\mathbf{c}$ and setpoints $\mathbf{c}_s$ such that with $\mathbf{c} = \mathbf{c}_s$ the loss

$$L(\mathbf{d}_0) = J(\mathbf{c}, \mathbf{d}_0) - J^{opt}(\mathbf{d}_0) \tag{5.4}$$

is acceptable. Here, $J(\mathbf{c}, \mathbf{d}_0)$ is the objective value by enforcing $\mathbf{c} = \mathbf{c}^s$ and $J^{opt}(\mathbf{d}_0)$ is the true optimal objective value. Here, the focus is on steady-state economic performance which is motivated by the fact that the economics are mainly decided by steady-state effects (Skogestad, 2000).

Let $\mathbf{y}_0$ denote the measurements and $\mathbf{c} = \mathbf{H}\mathbf{y}_0$ denote the controlled variables (where $\mathbf{H}$ can be a full matrix). At the nominal optimal point we have

$$\Delta\mathbf{y}_0 = \mathbf{G}^{y_0}\Delta\mathbf{u} + \mathbf{G}^{y_0}_{d_0}\Delta\mathbf{d}_0 = \begin{bmatrix}\mathbf{G}^{y_0} & \mathbf{G}^{y_0}_{d_0}\end{bmatrix}\begin{bmatrix}\Delta\mathbf{u}\\ \Delta\mathbf{d}_0\end{bmatrix} = \tilde{\mathbf{G}}^{y_0}\begin{bmatrix}\Delta\mathbf{u}\\ \Delta\mathbf{d_0}\end{bmatrix} \tag{5.5}$$

$$\Delta\mathbf{c} = \mathbf{G}\Delta\mathbf{u} + \mathbf{G}_{d_0}\Delta\mathbf{d}_0 \tag{5.6}$$

where $\Delta\mathbf{y}_0 = (\mathbf{y}_0 - \mathbf{y}_0^*)$ is the vector of all measurements, $\Delta\mathbf{u} = (\mathbf{u} - \mathbf{u}^*)$ is the inputs and $\Delta\mathbf{d}_0 = (\mathbf{d}_0 - \mathbf{d}_0^*)$ is the vector of all disturbances in deviation variables.

A second order accurate expression for the loss is (Halvorsen et al., 2003):

$$L(\mathbf{c}, \mathbf{d}_0) = \tfrac{1}{2}(\mathbf{u} - \mathbf{u}^{opt})^T\mathbf{J}_{uu}(\mathbf{u} - \mathbf{u}^{opt}) = \tfrac{1}{2}\mathbf{z}^T\mathbf{z} \tag{5.7}$$

where $\mathbf{J}_{uu}$ is the Hessian matrix with respect to the inputs and $\mathbf{z} = \mathbf{J}_{uu}^{1/2}(\mathbf{u} - \mathbf{u}^{opt})$. If we neglect measurement error we have for a constant $\mathbf{c}$ (Halvorsen et al., 2003):

$$(\mathbf{u} - \mathbf{u}^{opt}(\mathbf{d}_0)) = (\mathbf{J}_{uu}^{-1}\mathbf{J}_{ud_0} - \mathbf{G}^{-1}\mathbf{G}_{d_0})\Delta\mathbf{d}_0 \tag{5.8}$$

where $\mathbf{J}_{ud_0}$ is the Hessian in $\mathbf{ud}_0$[1]. If we include measurement error $\mathbf{n} = \mathbf{c} - \mathbf{c}_s$ we have

$$\mathbf{z} = \overbrace{\mathbf{J}_{uu}^{1/2}(\mathbf{J}_{uu}^{-1}\mathbf{J}_{ud_0} - \mathbf{G}^{-1}\mathbf{G}_{d_0})}^{\mathbf{M}_{d_0}}(\mathbf{d}_0 - \mathbf{d}_0^*) + \overbrace{\mathbf{J}_{uu}^{1/2}\mathbf{G}^{-1}}^{\mathbf{M}_n}\mathbf{n} \tag{5.9}$$

From eq. (5.9) it is clear that the effect of a disturbance on the loss depends on both the controlled variables (through $\mathbf{G}$ and $\mathbf{G}_{d_0}$) and the cost function (trough $\mathbf{J}_{uu}$ and $\mathbf{J}_{ud_0}$). We neglect the measurement error, and we split the contributions from the disturbances into $\mathbf{M}^1_{d_0} = \mathbf{J}_{uu}^{1/2}\mathbf{J}_{uu}^{-1}\mathbf{J}_{ud_0}$ and $\mathbf{M}^2_{d_0} = -\mathbf{J}_{uu}^{1/2}\mathbf{G}^{-1}\mathbf{G}_{d_0}$ where

$$\mathbf{M}_{d_0} = \mathbf{M}^1_{d_0} + \mathbf{M}^2_{d_0} \tag{5.10}$$

where $\mathbf{M}^1_{d_0}$ is the contribution to the loss from the cost function and $\mathbf{M}^2_{d_0}$ the contribution to the loss function from feedback.

From eq. (5.9) we see that for disturbances where the rows of $\mathbf{M}_{d_0}$ have small elements (assuming $\mathbf{d}_0$ is scaled) have a negligible effect on the loss. Since $\mathbf{z}$ is independent of scaling, it seems to be an ideal metric for discriminating between disturbances. However, since $\mathbf{z}$ depends on the selection of controlled variables it is obvious of limited value.

In the next section we discuss the importance of disturbances for self-optimizing control, and propose a set of rules that can guide the discrimination of disturbances.

[1] If we assume that the disturbance vector is 2-norm bounded $\|\Delta\mathbf{d}_0\|_2 \leq 1$ and we neglect implementation error the worst case loss is given by

$$L = \frac{1}{2}\bar{\sigma}(\mathbf{M}_{d_0})^2$$

where $\mathbf{M}_{d_0} = \mathbf{J}_{uu}^{1/2}(\mathbf{u} - \mathbf{u}^{opt}) = \mathbf{J}_{uu}^{1/2}(\mathbf{J}_{uu}^{-1}\mathbf{J}_{ud} - \mathbf{G}^{-1}\mathbf{G}_d)$.

5.3 Rules for disturbance discrimination

Here, we present rules for discriminating between disturbances in self-optimizing control.

Rule 1: Steady-state effect: Include only disturbances that have a steady-state effect (on the cost or on the measurements $\mathbf{y}_0$)

The rule is obvious, since we have made "the pseudo steady-state assumption" where the plant economics (cost J) are determined by the steady-state behavior. In practice, this assumes that we have an effective control system in place such that the plant moves immediately from one steady-state to another, and that dynamic disturbances are immediately rejected.

Even though the rule may seem obvious, some additional remarks are in order.

1. A disturbance with no steady-state effect on the optimal cost should still be included if it has steady-state effect on the measurements. The reason is that the disturbance may result in non-optimal operation because the measurements are used in forming the controlled variable $\mathbf{c}$.

Example 5.1 *Let $J = (u - d_1)^2$ and*

$$\mathbf{y}_0 = \begin{bmatrix} y_1 \\ y_2 \\ y_3 \end{bmatrix} = \begin{bmatrix} u \\ 5u + d_1 + d_2 \\ 7u - d1 \end{bmatrix} \tag{5.11}$$

We then need to include disturbance d_2 if the measurement y_2 is included in the set of measurements y used in forming $\mathbf{c} = \mathbf{Hy}$, but not otherwise.

2. On the other hand, it is not necessary to include disturbances with no steady-state effect on the measurements $\mathbf{y}_0$, in the selection of controlled variables $\mathbf{c}$ (even if they do affect the cost J). The reason is that the loss with respect to this disturbance will be independent of the selected controlled variable $\mathbf{c}$. If the loss with respect to this disturbance is unacceptably large, then we need to obtain additional measurements that depend on the disturbance.

Example 5.2 *Let $J = d_2(u - d_1)^2 - u$ and*

$$\mathbf{y}_0 = \begin{bmatrix} y_1 \\ y_2 \\ y_3 \end{bmatrix} = \begin{bmatrix} u \\ 5u + d_1 \\ 7u - d_1 \end{bmatrix} \tag{5.12}$$

Note that d_2 has no effect in $\mathbf{y}_0$. For example, d_2 may be a price. There is then no need to include d_2 in the selection of the controlled variables $c = \mathbf{Hy}$. On the other hand, changes in d_2 do affect the optimal operation, but these can only be corrected for by introducing a measurement of d_2.

5.3.1 Initial screening rule (Rule 2)

It is difficult to eliminate disturbances because their effect depend on the selected controlled variables $\mathbf{c} = \mathbf{Hy}$, which is yet to be found. Therefore, disturbances cannot be eliminated without considering the measurements. Here, we propose a method for discriminating between disturbances based on controlling all available measurements $\mathbf{y}_0$ (minimize the overall measurement deviation). The idea is that if the disturbance is unimportant in terms of the loss when controlling all measurements, then it can be eliminated.

From eq. (5.5) we have

$$\Delta\mathbf{y}_0 = \mathbf{G}^{y_0}\Delta\mathbf{u} + \mathbf{G}^{y_0}_{d_0}\Delta\mathbf{d}_0 \tag{5.13}$$

For $n_{y_0} > n_u$ it is not possible to get $\Delta\mathbf{y}_0 = 0$, but the solution that minimizes $\|\mathbf{y}_0\|_2$ is

$$\Delta\mathbf{u} = -[\mathbf{G}^{y_0}]^{\dagger}\mathbf{G}^{y_0}_{d_0}\Delta\mathbf{d}_0 \tag{5.14}$$

where $[\mathbf{G}^{y_0}]^{\dagger}$ is the pseudo-inverse of $\mathbf{G}^{y_0}$. By recognizing that $\Delta\mathbf{u}^{opt} = -\mathbf{J}^{-1}_{uu}\mathbf{J}_{ud_0}\Delta\mathbf{d}_0$ (Halvorsen et al., 2003) we then have

$$\mathbf{z}_0 = \mathbf{J}^{1/2}_{uu}(\Delta\mathbf{u} - \Delta\mathbf{u}^{opt}) = \mathbf{J}^{1/2}_{uu}(\mathbf{J}^{-1}_{uu}\mathbf{J}_{ud_0} - [\mathbf{G}^{y_0}]^{\dagger}\mathbf{G}^{y_0}_{d_0})\Delta\mathbf{d}_0 = -\mathbf{J}^{1/2}_{uu}[\mathbf{G}^{y_0}]^{\dagger}\mathbf{F}\mathbf{W}_{d_0}\mathbf{d}'_0 \tag{5.15}$$

where the last equality follows since $\mathbf{F} = -(\mathbf{G}^{y_0}\mathbf{J}^{-1}_{uu}\mathbf{J}_{ud_0} - \mathbf{G}^{y_0}_{d_0})$.

We use the following scaling:

- We scale the disturbances with respect to the expected range, i.e. $(\mathbf{d}_0 - \mathbf{d}^*_0) = \mathbf{W}_{d_0}\mathbf{d}'_0$.
- We scale the measurements with respect to the measurement error $\mathbf{n}^y$.

Disturbance discrimination rule 2: *Include only disturbances that have a large effect on the loss when controlling all measurements (minimizes $\|\Delta\mathbf{y}_0|_2$). That is, eliminate disturbances that have a corresponding small effect on the elements of $\mathbf{z}_0$, which corresponds to small column vectors $[\mathbf{J}^{1/2}_{uu}[\mathbf{G}^{y_0}]^{\dagger}[-\mathbf{F}\mathbf{W}_{d_0}]_j$ $j \in 1..n_d$ as given by eq. (5.15).*

The above rule must be used with some caution, since a disturbance that yields a small loss when controlling all measurements, may be important for a small subset of measurements. Rule 2 has been applied to a Petlyuk distillation case, see Chapter 8.

Rules 1-2 are general methods for disturbance discrimination. We now discuss rules 3 and 4 that are specific to the null space method of Chapter 3. Typically, one would start with rules 1-2, and if the number of disturbances still exceeds the maximum for the null space method, we need methods for dealing with such situations.

5.3.2 Lumping similar disturbances (Rule 3)

Here we discuss disturbance discrimination based on the assumption that we want to use the null space method of Alstad and Skogestad (2004) to select controlled variables. We here assume that we have too few measurements, i.e. $n_{y_0} < n_u + n_{d_0}$.

In order to use the null space method with the given set of measurements, one possible solution is to lump similar disturbances and consider only significantly "different" disturbances. Thus, two disturbances that show the same effect on the measurements are assumed "equal". To achieve this we utilize a singular value decomposition (SVD) of $\mathbf{G}_{d_0}^{y_0}$ that has dimensions $n_{y_0} \times n_{d_0}$

$$\mathbf{G}_{d_0}^{y_0} = \mathbf{U}_{d_0}^{y_0}\mathbf{\Sigma}_{d_0}^{y_0}\mathbf{V}_{d_0}^{y_0 T} \tag{5.16}$$

where

$\mathbf{\Sigma}_{d_0}^{y_0}$ is a $n_{y_0} \times n_{d_0}$ matrix with $k = min(n_{y_0}, n_{d_0})$ non-negative singular values σ_i, arranged in descending order along its main diagonal; the other entries are zero.

$\mathbf{U}_{d_0}^{y_0}$ is a $n_{y_0} \times n_{y_0}$ unitary matrix of output singular vectors , $\mathbf{u}_{d_0,i}^{y_0}$.

$\mathbf{V}_{d_0}^{y_0}$ is a $n_{d_0} \times n_{d_0}$ unitary matrix of input singular vectors, $\mathbf{v}_{d_0,i}^{y_0}$.

The idea is to neglect disturbance directions that correspond to small singular values σ_j (as compared to σ_{j-1}) and form a set of pseudo-disturbances which is used in synthesizing the controlled variables using the null space method.

Assume that the singular values $\sigma_j,\ j = l, .., k$ are small as compared to σ_{l-1} and since $\mathbf{V}_{d_0}^{y_0}$ is unitary we have $[\mathbf{V}_{d_0}^{y_0 T}]^{-1} = \mathbf{V}_{d_0}^{y_0}$ and it follows that:

$$\mathbf{G}_{d_0}^{y_0}\mathbf{V}_{d_0}^{y_0} = \mathbf{U}_{d_0}^{y_0}\Sigma_{d_0} \tag{5.17}$$

and we select the columns of $\mathbf{V}_{d_0}^{y_0}$ corresponding to the "large" singular values of $\mathbf{\Sigma}_{d_0}^{y_0}$

$$\mathbf{G}_{d_0}^{y_0}[\mathbf{v}_{d_0,1}^{y_0}\ \mathbf{v}_{d_0,2}^{y_0}\ \cdots\ \mathbf{v}_{d_0,l-1}^{y_0}] = \mathbf{U}_{d_0}^{y_0}[\mathbf{\Sigma}_{d_0,1}^{y_0}\ \mathbf{\Sigma}_{d_0,1}^{y_0}\ \cdots\ \mathbf{\Sigma}_{d_0,l-1}^{y_0}] \tag{5.18}$$

and we have that

$$\Delta\mathbf{d}_0 \approx [\mathbf{v}_{d_0,1}^{y_0}\ \mathbf{v}_{d_0,2}^{y_0}\ \cdots\ \mathbf{v}_{d_0,l-1}^{y_0}]\Delta\tilde{\mathbf{d}} = \tilde{\mathbf{V}}_{d_0}^{y_0}\Delta\tilde{\mathbf{d}} \tag{5.19}$$

such that

$$\Delta\mathbf{y}_0 \approx \mathbf{G}^{y_0}\Delta\mathbf{u} + \mathbf{G}_{d_0}^{y_0}\tilde{\mathbf{V}}_{d_0}^{y_0}\Delta\tilde{\mathbf{d}} = \mathbf{G}^{y_0}\Delta\mathbf{u} + \tilde{\mathbf{G}}_{d_0}^{y_0}\Delta\tilde{\mathbf{d}} \tag{5.20}$$

Note that the pseudo-disturbances $\tilde{\mathbf{d}}$ are only used in the synthesis of the controlled variable (using the null space method). This method will not guarantee good self-optimizing controlled variables if the singular values $\sigma_i,\ i = 1, .., k$ are of equal magnitude. For such cases it is not possible to form pseudo-disturbances that properly represent the disturbances. In practice this will happen if the physical "source" of the disturbances differ.

Implication for the null space method

Assume that we form a new pseudo-disturbance as given by eq. (5.20) such that $n_{\tilde{d}} = n_{y_0} - n_u$, and $\Delta\mathbf{d}_0 \approx \Delta\tilde{\mathbf{V}}_{d_0}^{y_0}\tilde{\mathbf{d}}_0$. The the new optimal sensitivity matrix is

$$\tilde{\mathbf{F}} = \mathbf{F}\tilde{\mathbf{V}}_{d_0}^{y_0} \tag{5.21}$$

where $\tilde{\mathbf{V}}_{d_0}^{y_0}$ has dimensions $n_{y_0} \times (n_{y_0} - n_u)$ and it follows that:

$$\Delta\mathbf{y}_0^{opt} \approx \tilde{\mathbf{F}}\Delta\tilde{\mathbf{d}} \tag{5.22}$$

The coefficient matrix $\mathbf{H}$ is found by requiring $\mathbf{H}\tilde{\mathbf{F}} = 0$

Disturbance discrimination rule 3: Lump similar disturbances *Lump the n_{d_0} disturbances into $n_{\tilde{d}}$ pseudo-disturbances $\tilde{\mathbf{d}}$, based on a singular value decomposition of the steady-state gain matrix from disturbances to outputs ($\mathbf{G}_{d_0}^{y_0}$). The set of pseudo-disturbances is $\Delta\mathbf{d}_0 = \tilde{\mathbf{V}}_{d_0}^{y_0}\Delta\tilde{\mathbf{d}}_0$ where $\tilde{\mathbf{V}}_{d_0}^{y_0}$ is found from a singular value decomposition of the steady-state disturbance gain $\mathbf{G}_{d_0}^{y_0}$. Form the new optimal sensitivity matrix $\tilde{\mathbf{F}} = \mathbf{F}\tilde{\mathbf{V}}_{d_0}^{y_0}$ which is used in the null space method.*

Below we include a simple example to illustrate rule 3.

Example 5.3 ***Example*** *Consider the following objective function*

$$J(u, \mathbf{d}_0) = (u - d_1)^2 + 0.5(u - d_2)^2 + (u - d_3)^2 \tag{5.23}$$

with one input (u) and three disturbances (d_1, d_2 and d_3), where $|d_i| \leq 1$ and $d_1^* = d_2^* = d_3^* = 0$. The Hessian matrices are $J_{uu} = 5$ and $\mathbf{J}_{ud} = \begin{bmatrix}-2 - 1 - 2\end{bmatrix}$. In using the null space method, we need $n_{y_0} = n_u + n_{d_0} = 1 + 3 = 4$ measurements. Assume that we have only three measurements available:

$$\Delta\mathbf{y}_0 = \mathbf{G}^{y_0}\Delta u + \mathbf{G}_{d_0}^{y_0}\Delta\mathbf{d} = \begin{bmatrix}\Delta y_1 \\ \Delta y_2 \\ \Delta y_3\end{bmatrix} = \begin{bmatrix}0.1 \\ -1 \\ -0.5\end{bmatrix}\Delta u + \begin{bmatrix}1 & -1 & 0.42 \\ 5 & 2 & 5.8 \\ 3 & -2.5 & 2\end{bmatrix}\begin{bmatrix}\Delta d_1 \\ \Delta d_2 \\ \Delta d_3\end{bmatrix} \tag{5.24}$$

where $\mathbf{G}_{d_0}^{y_0}$ has full rank ($= 3$), and the singular value decomposition is

$$\mathbf{G}_{d_0}^{y_0} = \mathbf{U}_{d_0}^{y_0}\mathbf{\Sigma}_{d_0}^{y_0}\mathbf{V}_{d_0}^{y_0\,T} \tag{5.25}$$

where

$$\mathbf{U}_{d_0}^{y_0} = \begin{bmatrix}-0.106 & 0.340 & -0.934 \\ -0.917 & -0.398 & -0.041 \\ -0.385 & 0.852 & 0.354\end{bmatrix} \quad \mathbf{\Sigma}_{d_0}^{y_0} = \begin{bmatrix}8.506 & 0.000 & 0.000 \\ 0.000 & 3.421 & 0.000 \\ 0.000 & 0.000 & 0.114\end{bmatrix} \quad \mathbf{V}_{d_0}^{y_0} = \begin{bmatrix}-0.687 & 0.266 & -0.676 \\ -0.090 & -0.955 & -0.284 \\ -0.721 & -0.134 & 0.680\end{bmatrix}$$

From the singular values we see that $\frac{\sigma_2}{\sigma_3} \approx 30$ so we propose to lump the disturbances into two pseudo-disturbances. Recognizing that

$$\mathbf{F} = -\mathbf{G}^{y_0}\mathbf{J}_{uu}^{-1}\mathbf{J}_{ud} + \mathbf{G}_{d_0}^{y_0}$$

we have

$$\mathbf{F} = \begin{bmatrix}1.040 & -0.980 & 0.460 \\ 4.600 & 1.800 & 5.400 \\ 2.800 & -2.600 & 1.800\end{bmatrix}$$

and

$$\tilde{\mathbf{V}}_{d_0}^{y_0} = \begin{bmatrix}-0.687 & 0.266 \\ -0.090 & -0.955 \\ -0.721 & -0.134\end{bmatrix}$$

which give the new sensitivity matrix in terms of the pseudo-disturbances

$$\tilde{\mathbf{F}} = \begin{bmatrix}-0.958 & 1.150 \\ -7.216 & -1.222 \\ -2.988 & 2.984\end{bmatrix}$$

Calculating the null space we get

$$\mathbf{H} = \begin{bmatrix} -0.936 & -0.021 & 0.352 \end{bmatrix} \tag{5.26}$$

Let the controlled variable be $c_{ns} = \mathbf{H}\mathbf{y}_0$ *and compare the loss for this candidate with the single measurement candidates* ($c = y_i$)*. If we ignore the noise, the loss is given by* $L = \frac{1}{2}z^2$ *and is as in Table 5.1*[1]*. Compared to the candidates* $c = y_i$, $i = \{1, 2, 3\}$

Table 5.1: *Loss for different disturbances for candidate controlled variables. The loss in column 5 is for worst-case disturbance.*

c_i	$d_1 = 1$	$d_2 = 1$	$d_3 = 1$	$\|\mathbf{d}\| = 1$
c_{ns}	0.31	0.05	0.31	0.67
y_1	270.4	240.1	52.9	563.4
y_2	52.9	8.1	72.9	133.9
y_3	78.4	67.6	32.4	178.4

the candidate c_{ns} *has substantially lower loss and shows good self-optimizing properties, and lumping disturbances yields a candidate with acceptable loss.*

5.3.3 Extended null space method (Rule 4)

The above procedure where we lump disturbances, may not give candidate controlled variables with good self-optimizing properties if the disturbances are "different", so that we cannot form pseudo-disturbances. In Chapter 4 we generalized the null space method for the case of too few measurements. In Section 4.3.4 we found the locally exact expression

$$\mathbf{M}_n\mathbf{H}\tilde{\mathbf{G}}^{y_0} = \tilde{\mathbf{J}} \tag{5.27}$$

where $\tilde{\mathbf{G}}^{y_0} = [\mathbf{G}^{y_0} \quad \mathbf{G}^{y_0}_{d_0}]$ is the augmented plant and $\tilde{\mathbf{J}} = [\mathbf{J}^{1/2}_{uu} \quad \mathbf{J}^{1/2}_{uu}\mathbf{J}^{-1}_{uu}\mathbf{J}_{ud_0}]$.

Since the number of measurements $n_{y_0} < n_u + n_{d_0}$ the matrix $[\mathbf{G}^{y_0}\ \mathbf{G}^{y_0}_d]$ is non-square and not invertible. For this case, perfect disturbance rejection ($\mathbf{M}_d = 0$ in eq. 5.15) is not possible). We found in Section 4.3.4 that a reasonable approach was to use the pseudo-inverse (the Moore-Penrose generalized inverse, Horn and Johnson (1985)) and select $\mathbf{M}_n\mathbf{H}$ such that

$$\mathbf{M}_n\mathbf{H} = \tilde{\mathbf{J}}[\tilde{\mathbf{G}^{y_0}}]^\dagger \tag{5.28}$$

which is an explicit expression for the matrix $\mathbf{M}_n\mathbf{H}$. This is the best $\mathbf{M}_n\mathbf{H}$ with $\mathbf{M}_d \approx 0$. This motivates rule 4.

Disturbance discrimination rule 4: Extended null space method *Use the extended null space method and select* $\mathbf{M}_n\mathbf{H}$ *such that*

$$\mathbf{M}_n\mathbf{H} = \tilde{\mathbf{J}}[\mathbf{G}^{y_0}]^\dagger \tag{5.29}$$

$\mathbf{M}_n$ *can be selected freely.*

[1]Note that when calculating the loss in Table 5.1 the full disturbance vector is used. The reduced disturbance space is only used in the synthesis of the controlled variable.

Now, we illustrate the null space specific rules 3 and 4 on a simple example.

Example 5.4 ***Example*** *Here we consider a simple example with two inputs, u_1 and u_2, and three disturbances, d_1, d_2 and d_3. Assume that the objective function is*

$$J = (u_1 - d_1)^2 + 0.5(u_2 - d_2)^2 + 2(u_1 - d_3)^2 + u_1 u_2 \tag{5.30}$$

and assume that we have four measurements available, where $\mathbf{y}_0 = \mathbf{G}^{y_0}\mathbf{u} + \mathbf{G}^{y_0}_{d_0}\mathbf{d}$ and

$$\mathbf{G}^{y_0} = \begin{bmatrix} 16.492 & 0.2300 \\ -14.675 & 6.5730 \\ 1.4760 & 1.8520 \\ 2.7840 & -3.6420 \end{bmatrix} \quad \text{and} \quad \mathbf{G}^{y_0}_{d_0} = \begin{bmatrix} -19.044 & 14.801 & 11.385 \\ 1.9460 & -9.2150 & -6.6230 \\ 2.8300 & -2.1020 & -11.343 \\ 6.4410 & 1.9830 & 7.4590 \end{bmatrix}$$

and the nominal disturbances are $d_1 = d_2 = d_3 = 0$ Here, we consider the following candidates for self-optimizing control, see Table 5.2. The worst case loss for the case

Table 5.2: *Candidate controlled variables for the example.*

c_1	c_2	Comment
$c^1_{ns,1}$	$c^1_{ns,2}$	Linear combination all four measurements using the extended null space method (Rule 4)
$c^2_{ns,1}$	$c^2_{ns,2}$	Linear combination all four measurements using lumping of disturbances (Rule 3)
y_1	y_2	Measurements y_1 and y_2
y_1	y_3	Measurements y_1 and y_3
y_1	y_4	Measurements y_1 and y_4
y_2	y_3	Measurements y_2 and y_3
y_2	y_4	Measurements y_2 and y_4
y_3	y_4	Measurements y_3 and y_4

of no noise is $L^d = \frac{1}{2}\bar{\sigma}(\mathbf{M}_d)^2$ and if we include noise the loss is $L^{dn} = \frac{1}{2}\bar{\sigma}([\mathbf{M}_d\ \mathbf{M}^y_n])^2$ as given by eq. (5.9). Table 5.3 summaries the losses for all candidates, where we also include the true minimum loss. From the table we see that both Rule 3 and 4 yield

Table 5.3: *Worst case loss for all candidates with and without noise. L^d denotes the worst-case disturbance loss, while L^{nd} denotes the worst-case combined noise and disturbance loss*

c_1	c_2	L^d	L^{dn}
c^1_{opt}	c^2_{opt}	1.4651	1.6472
$c^1_{ns,1}$	$c^1_{ns,2}$	1.6602	1.7968
$c^2_{ns,1}$	$c^2_{ns,2}$	1.6588	1.8857
y_1	y_2	15.303	15.335
y_1	y_3	26.470	26.576
y_1	y_4	12.097	12.131
y_2	y_3	25.121	25.352
y_2	y_4	17.362	17.645
y_3	y_4	43.549	44.075

candidates with good self-optimizing properties. In fact, the lumping of disturbances yields a candidate with lower disturbance loss than using the extended null space method

(Rule 4). However, when we include noise, the candidate using the extended method has smaller loss. All single measurement candidates show large losses.

The above methods are not exact and must be used with some caution.

5.4 General discussion

Rule 1 above is generic in the sense that it does not depend on the resulting controlled variables. Rule 2 may yield inaccurate results, and must be used with caution. Rules 3 and 4 are specific for the null space method.

Morari et al. (1980) proposed several disturbance classification rules. Their "disturbance classification rule 2" proposed to include only disturbances that have a serious impact on the objective function. They suggest to measure the impact by the the Lagrange multiplier, $\lambda_i = (\partial J^{opt}/\partial d_i)_{\mathbf{f}'=0}$, which is a constrained derivative ($\mathbf{f}' = 0$) evaluated at the nominal disturbance $\mathbf{d}^*$. The value of the Lagrangian multiplier indicates the sensitivity of the optimal objective value for a perturbation of the disturbance. Intuitively, this rule makes sense since a disturbance that has a small impact on the optimal value of the objective function, could be neglected. However, the rule is not sound. First, it does not consider the measurements. Second, the idea of considering the effect on the Lagrangian multiplier may give wrong results, as illustrated by the two scenarios in Figure 5.1. In Figure 5.1(a) we see that for a given disturbance change the optimal change in the objective function is small; Nevertheless, the optimal change in the input is large, so the disturbance is important. Conversely, in Figure 5.1(b) we show that a large change in the optimal objective function may correspond to a small input change. For both scenarios, it is clear that selecting disturbances based on the Lagrangian multipliers may be inaccurate. Thus, we do not recommend using "rule 2" of Morari et al. (1980).

The above rules have been illustrated on simple examples. In Chapter 8 we use rule 2 above on finding important disturbances for a Petlyuk distillation column. In Chapter 11 we use the lumping of disturbances (rule 3), on a Evaporator case.

5.5 Conclusions

In typical chemical processes, the number of disturbances can be large. Few methods for discriminating between disturbances exist in the literature. Here, we have focused on disturbance discrimination in the setting of self-optimizing control. We find that we cannot separate the disturbance discrimination from the selection of control structure. Nevertheless, we propose two generic rules for selecting disturbances. The first rule is to select disturbances that have a impact on the cost *or* the measurements. The second rule says that we should include measurements that have an impact on loss when minimizing the measurement deviation from the nominal point.

In addition, we propose two rules that are specific for the null space method of Chapter 3. The above rules must be used with some caution.

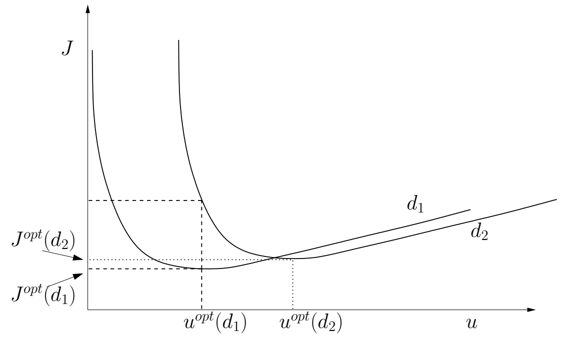

(a) Scenario 1: The optimal sensitivity is small, while the optimal change in input is large

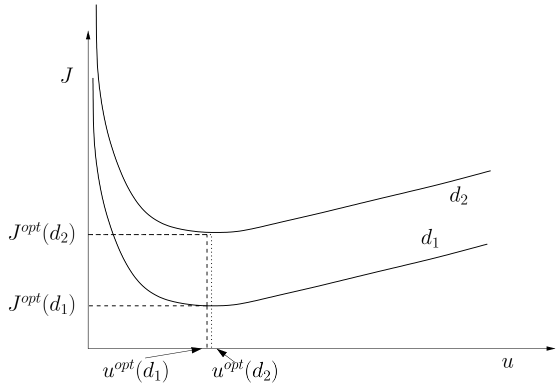

(b) Scenario 2: The optimal sensitivity is large, while the optimal change in the input is negligible

Figure 5.1: *Effect of disturbances on optimal objective function (J) and corresponding optimal change in input*

Bibliography

Alstad, V. and Skogestad, S. (2004). Combinations of measurements as controlled variables; Application to a petlyuk distillation column. *in the IFAC Symposium on Advanced Control of Chemical Processes (ADCHEM) 2003, (Hong Kong).*

Halvorsen, I., Skogestad, S., Morud, J., and Alstad, V. (2003). Optimal selection of controlled variables. *Ind. Eng. Chem. Res.*, 42(14):3273–3284.

Horn, R. and Johnson, C. (1985). *Matrix analysis.* Cambridge University Press, Cambridge.

Krishnan, S., Barton, G., and Perkins, J. (1992). Robust parameter estimation in online optimization - Part 1. Methodology and simulated case study. *Comput. Chem. Eng.*, 16(6):545–562.

Morari, M., Stephanopoulos, G., and Arkun, Y. (1980). Studies in the synthesis of control structures for chemical processes. Part I: Formulation of the problem, process decomposition and the classification of the controller task. Analysis of the optimizing control structures. *AIChE Journal*, 26(2):220–232.

Skogestad, S. (2000). Plantwide control: The search for the self-optimizing control structure. *J. Proc. Control*, 10:487–507.

Chapter 6

Effect of non-optimal nominal setpoints on self-optimizing control structures

Manuscript in preparation

The previous work on self-optimizing control has assumed that the nominal point is optimal. This paper shows that the average difference in loss between alternative choices of controlled variables is the same when the nominal point is non-optimal. Thus, the previous results hold also for non-optimal nominal setpoints.

6.1 Introduction

In this paper we consider the loss imposed by using a constant setpoint policy, $\mathbf{c} = \mathbf{c}_s$. We have previously shown that the expected loss may depend strongly on the selected controlled variables. However, in the previous work we assumed that the nominal point was optimal, but this is not likely to be the case in practice. The question then is: Does the ranking of candidate controlled variables depend on the nominal point? In this paper we show that the answer is "no". We show that the average difference in loss between alternative choices for the controlled variables $\mathbf{c}$ is the same, irrespective of the nominal point.

The selection of non-optimal nominal setpoints has been discussed for the constrained case, when all controlled variables lie on active constraints. We then need to "backoff" from the constraints for the solution to remain feasible in presence of measurement errors (Perkins et al., 1990; Narraway et al., 1991; Kookos and Perkins, 2002b,a). For the case of "unconstrained" degrees of freedom, which is the focus here, the effect of nominal setpoint error has not been discussed. Govatsmark and Skogestad (2005) discuss the selection of robust setpoints, by the use of robust optimization (Glemmestad et al., 1999), to remain feasible for all disturbances, but do not discuss the effect of using non-optimal setpoints on the candidate rank and the effect on the loss.

The goal of this paper is to answer questions such as:

1. How do non-optimal nominal setpoints affect the loss for each candidate controlled variable, i.e. how sensitive is each candidate to nominal setpoint error?
2. How is the rank (if at all) between the best candidates for self-optimizing control altered when uncertainties in the nominal point exist?

Let the true optimal point, corresponding to the nominal disturbance $\mathbf{d}^*$ be

$$(\mathbf{u}^*, \mathbf{d}^*) = (\mathbf{u}^{opt}(\mathbf{d}^*), \mathbf{d}^*) \tag{6.1}$$

where $\mathbf{u}$ is the input and $\mathbf{d}$ is the disturbance and let the actual nominal point be

$$(\mathbf{u}^0, \mathbf{d}^*) \tag{6.2}$$

where by assumption $\mathbf{u}^0 \neq \mathbf{u}^*$, so the nominal point is not optimal.

Below we illustrate the effect of non-optimal setpoints on a simple example. The observations made in this example are analyzed in the subsequent section.

Example 6.1 ***Introductory example***
Consider a simple toy example, with one unconstrained input (u) and one disturbance (d) with the following operational objective

$$J = (u - d)^2 \tag{6.3}$$

Let the nominal disturbance be $d^* = 0$. From eq. (6.3), we see that the optimal input is $u^{opt}(d) = d$ and the nominal optimal input is $u^{opt}(d^*) = 0$. Assume that the following measurements are available:

$$y_1 = 0.1(u - d) \qquad y_3 = 2u - 0.5d \tag{6.4}$$
$$y_2 = 2u - d \qquad y_4 = u - 3d \tag{6.5}$$
$$\tag{6.6}$$

Using the true nominal optimal setpoint ($u^{opt}(d^*)$), we have the following setpoints $y_i^s = 0 \;\forall\; i$ and the resulting corresponding inputs when requiring $y_i = y_i^s$

$$y_1 - y_1^s = 0 \rightarrow u = d \qquad y_3 - y_3^s = 0 \rightarrow u = 1/4d \tag{6.7}$$
$$y_2 - y_2^s = 0 \rightarrow u = 1/2d \qquad y_4 - y_4^s = 0 \rightarrow u = 3d \tag{6.8}$$

Since $J^{opt}(d) = 0 \;\forall\; d$ we have that the loss for the different candidates with respect to the disturbance is:

$$L_1 = (d - d)^2 = 0 \qquad L_3 = (1/4d - d)^2 = 9/16d^2 \tag{6.9}$$
$$L_2 = (1/2d - d)^2 = 1/4d^2 \qquad L_4 = (3d - d)^2 = 4d^2 \tag{6.10}$$

The losses using nominal optimal setpoints are plotted in Figure 6.1 for all candidate controlled variables. As seen, candidate y_1 has the lowest loss for all disturbances, followed by y_2, y_3 and y_4, in that order. At the nominal point, all candidates have zero

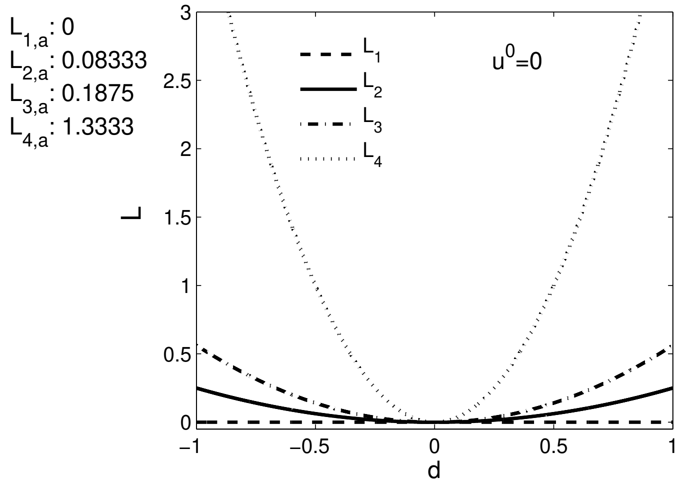

Figure 6.1: *Loss using nominal optimal setpoints u^*. The average loss for each candidate is shown to the left of the plot.*

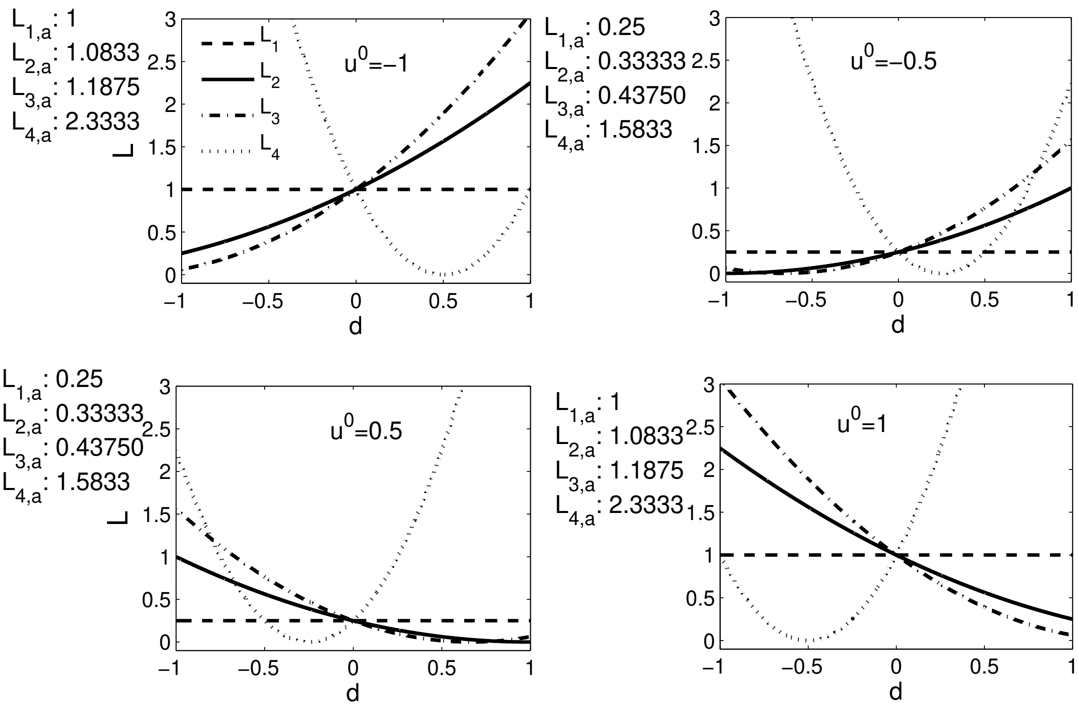

Figure 6.2: *Loss with non-optimal nominal operation ($u^0 \neq u^* = 0$). The average loss ($L_{i,a}$) is shown to the left of each plot. Note that the difference in loss (in going from u^* to u^0) is the same for all candidates, e.g. $(L_{i,a}^{(u^0=-1)} - L_{i,a}^{(u^0=0)}) = 1$ for all candidates going from $u^* = 0$ to $u^0 = -1$.*

Table 6.1: *Average loss for all candidates using nominal optimal setpoint.*

y_i	y_1	y_2	y_3	y_4
L_i	0	0.0833	0.1875	1.333

loss. The average loss for all candidates using nominal optimal setpoint is shown in Table 6.1.

Assume now that the actual nominal point is not optimal, but lies in the range $u^0 \in [-1,\ 1]$. In Figure 6.2 we plot the loss with respect to the disturbance for all candidates (with u^0 as a parameter).

With a nominal setpoint error we find, as expected, that the loss is reduced for some disturbances, but on the other hand it becomes even larger for other disturbances. Thus, if we consider a ***specific*** *value of the disturbance, then the ranking may vary. However, more importantly we find that the difference in the average loss (assuming that all values of d are equally likely) is not changed. That is, candidate y_1 has always the lowest average loss, followed by y_2, y_3 and y_4. This shows that, at least for this example, the effect of using non-optimal nominal setpoint does not change the rank between the candidates. In fact, it seems that the* difference *in the loss between the candidates is* unaffected *by the setpoint error. Note that the difference in worst case loss between the candidates increases.*

Example 6.1 shows that the internal rank of the candidate does not change for a setpoint error. Below, we show that this holds generally for the local loss for cases with one disturbance and one input.

6.2 Problem definition and governing equations

We assume that the operational objective can be described by

$$\min_{u} J(\mathbf{u}, \mathbf{d}) \tag{6.11}$$

where J is a scalar cost function and we assume that all active constraints have been implemented. Locally, let the controlled variables be given by

$$\mathbf{c} = \mathbf{G}\mathbf{u} + \mathbf{G}_{\mathbf{d}}\mathbf{d} \tag{6.12}$$

where $\mathbf{G}$ and $\mathbf{G}_d$ are the steady-state gain from the inputs and disturbances, respectively, to the controlled variables $\mathbf{c}$. Assume that the nominal point $(\mathbf{u}^0, \mathbf{d}^*)$ (with the nominal disturbance $\mathbf{d}^*$) is different from the true optimal nominal point $(\mathbf{u}^{opt}, \mathbf{d}^*)$. The nominal setpoints are:

$$\mathbf{c}_s = \mathbf{G}\mathbf{u}^0 + \mathbf{G}_d\mathbf{d}^* \tag{6.13}$$

Requiring $\mathbf{c} - \mathbf{c}_s = 0$ yields

$$\begin{aligned} \mathbf{c} - \mathbf{c}_s &= \mathbf{G}\mathbf{u} + \mathbf{G}_d\mathbf{d} - \left[\mathbf{G}\mathbf{u}^0 + \mathbf{G}_d\mathbf{d}^*\right] \\ &= \mathbf{G}(\mathbf{u} - \mathbf{u}^0) + \mathbf{G}_d(\mathbf{d} - \mathbf{d}^*) = 0 \end{aligned} \tag{6.14}$$

We assume that $\mathbf{G}$ is invertible such that

$$\mathbf{u} = \mathbf{u}^0 - \mathbf{G}^{-1}\mathbf{G}_d(\mathbf{d} - \mathbf{d}^*) \tag{6.15}$$

which is an expression for the actual implemented input, if we neglect control error (assuming integral action in the controllers). Halvorsen et al. (2003) show that the true optimal input vector is:

$$\mathbf{u}^{opt}(\mathbf{d}) = \mathbf{u}^{opt}(\mathbf{d}^*) - \mathbf{J}_{uu}^{-1}\mathbf{J}_{ud}(\mathbf{d} - \mathbf{d}^*) \tag{6.16}$$

where $\mathbf{J}_{uu}$ and $\mathbf{J}_{ud}$ are the Hessian matrices of the cost function J given in eq. (6.11). The input deviation (the deviation from the true optimal input) is from eqs. (6.15) and (6.16)

$$\begin{aligned}\mathbf{u} - \mathbf{u}^{opt} &= \left(\mathbf{u}^0 - \mathbf{G}^{-1}\mathbf{G}_d(\mathbf{d} - \mathbf{d}^*)\right) - \left(\mathbf{u}^{opt}(\mathbf{d}^*) - \mathbf{J}_{uu}^{-1}\mathbf{J}_{ud}(\mathbf{d} - \mathbf{d}^*)\right) \\ &= \left(\mathbf{u}^0 - \mathbf{u}^{opt}(\mathbf{d}^*)\right) + \left(\mathbf{J}_{uu}^{-1}\mathbf{J}_{ud} - \mathbf{G}^{-1}\mathbf{G}_d\right)(\mathbf{d} - \mathbf{d}^*)\end{aligned} \tag{6.17}$$

Let $\mathbf{e}_u = \mathbf{u} - \mathbf{u}^{opt}$ and $\mathbf{e}_u^0 = \mathbf{u}^0 - \mathbf{u}^{opt}(\mathbf{d}^*)$, and eq. (6.17) simplifies to:

$$\mathbf{e}_u = \mathbf{e}_u^0 + \mathbf{G}^{-1}\left(\mathbf{v}(\mathbf{d}) + \mathbf{n}\right) \tag{6.18}$$

where $\mathbf{v}(\mathbf{d}) = \mathbf{G}\mathbf{J}_{uu}^{-1}\mathbf{J}_{ud} - \mathbf{G}_d$ and $\mathbf{n}$ is the measurement error in $\mathbf{c}$. Thus, the input deviation for a given $\mathbf{d}$ is the sum of the nominal setpoint error $\mathbf{e}_u^0$ and the error from the disturbances ($\mathbf{v}(\mathbf{d})$) and the implementation error ($\mathbf{n}$). From eq. (6.18) we see that $\mathbf{e}_u$ may be zero for a disturbance $\mathbf{d} \neq \mathbf{d}^*$, if $\mathbf{e}_u^0 = -\mathbf{G}^{-1}\left(\mathbf{v}(\mathbf{d}) + \mathbf{n}\right)$.

Halvorsen et al. (2003) show that the loss,

$$L = J(\mathbf{c} + \mathbf{n}, \mathbf{d}) - J^{opt}(\mathbf{d}) \tag{6.19}$$

defined as the difference between the objective value for a given controlled variable and the true optimal objective value, is given by

$$L = \frac{1}{2}\mathbf{e}_u^T\mathbf{J}_{uu}\mathbf{e}_u = \frac{1}{2}\mathbf{z}^T\mathbf{z} \quad \text{where} \quad \mathbf{z} = \mathbf{J}_{uu}^{1/2}\mathbf{e}_u \tag{6.20}$$

where J_{uu} is positive semi-definite so $L \geq 0 \ \forall \ \mathbf{d}$ and L is quadratic in the input deviation.

Below, we study the scalar case with one degree of freedom (u) and one disturbance (d).

6.3 Effect of using non-optimal nominal points: Scalar case

We first study the effect of using non-optimal nominal setpoint for the simplest possible system with one disturbance (d) and one unconstrained input (u). We make the following assumptions:

1. The true loss function is given by eq. (6.20), i.e. we consider the local behavior.
2. The equations describing input-output behavior are linear as given by eq. (6.12).

For the moment, we disregard the effect of noise ($n = 0$). Eq. (6.17) yields

$$\begin{aligned} e_u &= \left(u^0 - u^{opt}(d^*)\right) + \left(J_{uu}^{-1} J_{ud} - G^{-1} G_d\right)(d - d^*) \\ &= e_u^0 + \left(J_{uu}^{-1} J_{ud} - G^{-1} G_d\right)(d - d^*) \end{aligned} \tag{6.21}$$

Since e_u is scalar, we have from eq. (6.20),

$$L = 1/2 z^2 \tag{6.22}$$

i.e. the loss is proportional to z^2 where z is given by

$$\begin{aligned} z = J_{uu}^{1/2} e_u &= J_{uu}^{1/2} e_u^0 + J_{uu}^{1/2}\left(J_{uu}^{-1} J_{ud} - G^{-1} G_d\right)(d - d^*) \\ &= J_{uu}^{1/2} e_u^0 + M_d (d - d^*) \end{aligned} \tag{6.23}$$

where $M_d = J_{uu}^{1/2}(J_{uu}^{-1} J_{ud} - G^{-1} G_d)$. For the case of optimal nominal point ($e_u^0 = 0$) (we indicate this by prime (" $'$ "):

$$z' = M_d (d - d^*) \tag{6.24}$$

For a given controlled variable (given M_d), the increase in loss for having non-optimal nominal setpoint is:

$$\begin{aligned} L(d) - L(d)' = 1/2(z(d)^2 - z(d)'^2) &= 1/2\left(\left[J_{uu}^{1/2} e_u^0 + M_d (d - d^*)\right]^2 - \left[M_d (d - d^*)\right]^2\right) \\ &= 1/2\left(J_{uu} {e_u^0}^2 + 2 {J_{uu}}^{1/2} e_u^0 M_d (d - d^*)\right) \end{aligned} \tag{6.25}$$

Since J_{uu} is positive definite (positive in the scalar case), we have that the first term on the last line in eq. (6.25) is always positive. Assume now that $d \in [d_1, d_2]$, and $\Delta d_{max} = (d_2 - d^*) = -(d_1 - d^*)$ such that the disturbance is symmetric around the nominal disturbance d^*. The maximum (worst-case) and minimum (best-case) change in loss are:

$$L - L'_{|max} = 1/2\left(J_{uu} {e_u^0}^2 + 2 J_{uu}^{1/2} |e_u^0 M_d| \Delta d_{max}\right) \tag{6.26}$$

$$L - L'_{|min} = 1/2\left(J_{uu} {e_u^0}^2 - 2 J_{uu}^{1/2} |e_u^0 M_d| \Delta d_{max}\right) \tag{6.27}$$

Depending on the relative magnitude of the first and second term, the loss may in fact decrease ($L \leq L'$) for some values of Δd_{max}. This was confirmed in Example 6.1, see for instance for candidate y_4 for $d = -0.25$, where the loss is higher for $u_0 = 0$ (the optimal nominal value) than for $u_0 = 0.5$.

However, let us consider the average loss over $d \in [d_1, d_2]$, which is defined as:

$$L_{avg} = \frac{1}{d_2 - d_1} \int_{d_1}^{d_2} L(d)\, \mathrm{d}d \tag{6.28}$$

The *change* in loss when introducing non-optimal nominal setpoint is given by:

$$\begin{aligned}
[L - L']_{avg} &= \frac{1}{d_2 - d_1} \int_{d_1}^{d_2} [L - L']\, \mathrm{d}d \\
&= \frac{1}{d_2 - d_1} \int_{d_1}^{d_2} 1/2 \left(J_{uu} {e_u^0}^2 + 2 J_{uu}^{1/2} e_u^0 M_d (d - d^*) \right) \mathrm{d}d \\
&= \frac{1}{2(d_2 - d_1)} \left[J_{uu} {e_0^0}^2 d + J_{uu}^{1/2} e_u^0 M_d (d - d^*)^2 \right]_{d_1}^{d_2} \\
&= \frac{1}{2(d_2 - d_1)} \left(J_{uu} {e_u^0}^2 (d_2 - d_1) + J_{uu}^{1/2} e_u^0 M_d \left((d_2 - d^*)^2 - (d_1 - d^*)^2 \right) \right) \\
&= \frac{1}{2\Delta d_{max}} \left(J_{uu} {e_u^0}^2 \Delta d_{max} + e_u^0 M_d \left(\Delta d_{max}^2 - (-\Delta d_{max})^2 \right) \right) \\
&= \frac{J_{uu}}{2} {e_u^0}^2
\end{aligned} \tag{6.29}$$

where we have assumed that $d_{max} = (d_2 - d^*) = -(d_1 - d^*)$. Thus, we have the very important result that for a nominal setpoint error, the increase in loss is independent of what we control (independent of c).

Remark. If the nominal disturbance is not in the center of the allowable range, the second term on line four in eq. (6.29) (quadratic in d) is not zero, and would bias the change in loss. Depending on what direction the nominal disturbance is biased, this could potentially result in a decrease in the average loss.

In summary, the increase in average loss is independent of what candidate we select to control. Thus, the difference in average loss between two candidates is equal to the difference with optimal nominal setpoints. In other words, the candidate rank remains the same, independent of the nominal setpoint error. If the average increase in loss is not acceptable, focus should be on finding better estimates of the nominal optimum, since we cannot affect the loss by selecting another controlled variable.

6.4 General derivation

The generalization to multiple inputs and multiple disturbances is straightforward. The loss is given by

$$L(\mathbf{d}) = 1/2 \mathbf{z}(\mathbf{d})^T \mathbf{z}(\mathbf{d}) \triangleq 1/2 \|\mathbf{z}(\mathbf{d})\|_2^2 \triangleq 1/2 \sum_{i=1}^{n_u} (z_i)^2 \tag{6.30}$$

where $\mathbf{z} = [z_1 \ \cdots z_{n_u}]$ and we assume that z_i is real. The loss is then given as the sum of squares of z_i. If we neglect the implementation error ($\mathbf{n} = 0$) we have that

$$\mathbf{z}^T = \mathbf{J}_{uu}^{1/2}\mathbf{e}_u^0 + \mathbf{M}_d(\mathbf{d} - \mathbf{d}^*) \tag{6.31}$$

where $\mathbf{M}_d = \mathbf{J}_{uu}^{1/2}(\mathbf{J}_{uu}^{-1}\mathbf{J}_{ud} - \mathbf{G}^{-1}\mathbf{G}_d)$. The loss is the sum of squares of z_i and

$$z_i = \mathbf{J}_{uu,i}^{1/2}\mathbf{e}_u + \mathbf{M}_{d,i}(\mathbf{d} - \mathbf{d}^*) \tag{6.32}$$

where $\mathbf{J}_{uu,i}$ and $\mathbf{M}_{d,i}$ is the i'th row of the matrices $\mathbf{J}_{uu}$ and $\mathbf{M}_d$, respectively. Let $\mathbf{d} \in \mathcal{D}$ where each d_i is in $[d_{1,i}, d_{2,i}]$, ($\mathcal{D}$ is a hyper-rectangle). Then the average loss is given by

$$L_{avg} = \frac{1}{V_{\mathcal{D}}} \underset{\mathcal{D}}{\int \cdots \int} \sum_i z_i^2 \mathrm{d}\mathcal{D} = \frac{1}{V_{\mathcal{D}}} \sum_i \underset{\mathcal{D}}{\int \cdots \int} z_i^2 \mathrm{d}\mathcal{D} \tag{6.33}$$

where $V_{\mathcal{D}}$ is the "volume" of the n_d-dimensional hyper-rectangle defined by $\mathcal{D}$ and the integral of the sums equals the sum of the integrals. Thus, the loss is the sum of the contributions from each element in the vector z_i^2. The effect of a nominal setpoint error on the loss for a given set of controlled variables is then

$$L_{avg} - L'_{avg} = \frac{1}{V_{\mathcal{D}}} \sum_i \underset{\mathcal{D}}{\int \cdots \int} (z_i^2 - z_i'^2)\ \mathrm{d}\mathcal{D} \tag{6.34}$$

and it can be shown that

$$\underset{\mathcal{D}}{\int \cdots \int} (z_i^2 - z_i'^2)\mathrm{d}\mathcal{D} = 2n_d \left(\mathbf{J}_{uu,i}^{1/2}\mathbf{e}_u^0\right)^2 \prod_{j=1}^{n_d} \Delta d_{j,max} \tag{6.35}$$

where n_d is the number of disturbances and it has been assumed that $d_i \in [d_{1,i}, d_{2,i}]$. Since the volume of a hyper-rectangle is given by

$$V_{\mathcal{D}} = 2n_d \prod_{j=1}^{n_d} \Delta d_{j,max} \tag{6.36}$$

we have eq. (6.34) that the total increase in loss is

$$\begin{aligned} L_{avg} - L'_{avg} &= 1/2 \frac{1}{2n_d \prod_{j=1}^{n_d} \Delta d_{j,max}} \sum_i 2n_d \left(\mathbf{J}_{uu,i}^{1/2}\mathbf{e}_u^0\right)^2 \prod_{j=1}^{n_d} \Delta d_{j,max} \\ &= 1/2 \sum_i \left(\mathbf{J}_{uu,i}^{1/2}\mathbf{e}_u^0\right)^2 \end{aligned} \tag{6.37}$$

which is always positive, and more importantly, independent of what we select to control. Thus, the ranking of the candidate controlled variables $\mathbf{c}$ does not depend on the nominal point being optimal in the multivariable case either.

Effect of non-optimal nominal point on candidate rank

For illustration, compare two candidates, where we have for each candidate that

$$z_i^1 = {\mathbf{J}_{uu,i}^1}^{1/2}\mathbf{e}_u + \mathbf{M}_{d,i}^1(\mathbf{d} - \mathbf{d}^*) \tag{6.38}$$

and

$$z_i^2 = {\mathbf{J}_{uu,i}^2}^{1/2}\mathbf{e}_u + \mathbf{M}_{d,i}^2(\mathbf{d} - \mathbf{d}^*) \tag{6.39}$$

As was the case for the single input-single disturbance case, the increase in the loss for a nominal setpoint error is independent of the controlled variable as given by eq. (6.37). Comparing two candidate control structures, $\mathbf{c}_1$ and $\mathbf{c}_2$, (these are vectors) we can easily show that the increase in loss due to a nominal setpoint error is given by:

$$\begin{aligned}[L_2 - L_1]_{avg} = 1/2\sum_i z_{2,i}^2 - z_{1,i}^2 = 1/6\sum_i \left(\sum_{j=1}^{n_d}\left(\left(M_{d,i}^{2,j}\right)^2 - \left(M_{d,i}^{1,j}\right)^2\right)[\Delta d_{max}^j]^2\right) \\ = [L_2' - L_1']_{avg} \end{aligned} \tag{6.40}$$

where $M_{d,i}^j$ is matrix element from row i and column j. If we assume that

$$\left(\left(M_{d,i}^{2,j}\right)^2 - \left(M_{d,i}^{1,j}\right)^2\right) \geq 0 \ \forall j$$

then the effect of implementation error does not influence the rank between the candidates, nor the difference in loss.

The implication of this assumption, is that for all disturbance directions the loss is higher for candidate $\mathbf{c}_2$ than for $\mathbf{c}_1$. This assumption is strong, since the difference in loss between two candidates is independent of the nominal setpoint error. Thus, we may have directions in which $\left(\left(M_{d,i}^{2,j}\right)^2 - \left(M_{d,i}^{1,j}\right)^2\right) \leq 0$, as long as the sum over all disturbances are positive (as long as $[L_2' - L_1'] \geq 0$).

While the nominal setpoint error does not influence the rank between the candidates, the absolute loss is higher, as given by eq. (6.37). If the increase in loss is not acceptable, one should improve the estimate on the nominal optimum, since the loss is unavoidable, regardless of which controlled variables are being used.

6.5 Conclusions

In this paper, the effect of non-optimal nominal setpoints on the self-optimizing control properties has been investigated. The nominal setpoint error yields a higher loss for all candidates structures, but the average effect on the loss is independent of the candidate controlled variable. This is fortunate, since then the best structure for self-optimizing control does not depend on the nominal setpoint error.

The assumptions on system behavior (linear models, quadratic objective), are restrictive but hold, at least, locally.

Bibliography

Glemmestad, B., Skogestad, S., and Gundersen, T. (1999). Optimal operation of heat exchanger networks. *Comput. Chem. Eng.*, 23:509–522.

Govatsmark, M. and Skogestad, S. (2005). Selection of controlled variables and robust setpoints. *Ind. Eng. Chem. Res.* In press.

Halvorsen, I., Skogestad, S., Morud, J., and Alstad, V. (2003). Optimal selection of controlled variables. *Ind. Eng. Chem. Res.*, 42(14):3273–3284.

Kookos, I. and Perkins, J. (2002a). An algorithmic method for the selection of multivariable process control structures. *J. Proc. Control*, pages 85–99.

Kookos, I. and Perkins, J. (2002b). Regulatory control structure selection of linear systems. *Comput. Chem. Eng.*, 26:875–887.

Narraway, L., Perkins, J., and Barton, G. (1991). Interaction between process design and process control: Economic analysis of process dynamics. *J. Proc. Control*, 1:243–250.

Perkins, J., Gannavarapu, C., and Barton, G. (1990). Choosing control structures based on economics. *IEE Colloquium*.

Chapter 7

Dynamics of controlling measurements combinations

Manuscript in preparation

In this paper, we discuss the dynamics of controlling measurement combinations. The basis for the discussion is the null space method of Chapter 3, where we proposed to form controlled variables $\mathbf{c} = \mathbf{Hy}$ as linear combination of measurements. The coefficient matrix $\mathbf{H}$ is selected as the null vectors of the optimal sensitivity matrix $\mathbf{F}$ from the disturbances to the measurements such that $\mathbf{HF} = 0$. For systems with multiple unconstrained degrees of freedom, we discuss the freedom of changing the null vector basis, and how this degree of freedom may be used in order to achieve improved dynamic properties.

The null space method is steady-state only, and selecting controlled variables as linear combinations of measurements may give rise to complex dynamic behavior. We show here, that the freedom of selecting basis vectors for the left null space of $\mathbf{F}$, translates into the use of static compensators. We compare this work with previous work on compensator design (Skogestad and Postlethwaite, 1996). More importantly, using a combination of measurements as controlled variables may give rise to right-half plane (RHP) zeros and we propose a method of using filters on the measurements to avoid the limitations imposed by RHP zeros.

7.1 Introduction

Self-optimizing control deals with how to select controlled variables based on stationary economic models (Skogestad, 2000) and is a sub-task of the plantwide control design procedure, see Larsson and Skogestad (2000) for a review on plantwide control design. In plantwide control design procedures the selection of controlled variables (outputs) is decoupled from the actual linking of the manipulated inputs and outputs. The selection of controlled variables in the supervisory control layer is often based on steady-state, and the controllability of the resulting control structure must be analyzed before the control structure can be accepted. If the controllability of the proposed structure is not acceptable, we need to go back and redo the design.

Here, we discuss controllability issues related to the use of the null space method of Chapter 3. The null space method is a systematic method for selecting self-optimizing controlled variables as linear combinations of measurements ($\mathbf{c} = \mathbf{Hy}$), where the coefficient matrix $\mathbf{H}$ is selected such that the rows $\mathbf{h}_i$ of $\mathbf{H}$ span the left null space of the optimal sensitivity matrix from the disturbances to the measurements $\mathbf{F}$. That is, $\mathbf{h}_i$ is the null vectors of the left null space of $\mathbf{F}$. The basis vectors can be selected freely (see Chapter 4), as long as they are linearly independent (they span the left null space), i.e. $\mathbf{HF} = 0$. Thus, the choice of basis vectors does not affect the steady-state self-optimizing properties of the resulting structure. Another set of basis vectors will certainly produce another set of controlled variables (the measurements are weighted differently), however the self-optimizing properties are retained. Especially, in the case of multiple unconstrained degrees of freedom, we can use this freedom in shaping the plant.

We extend the static coefficient matrix $\mathbf{H}$, and propose a new transfer function matrix

$$\mathbf{H}^c(s) = \mathbf{C}(s)\mathbf{H}\mathbf{C}^y(s) \tag{7.1}$$

where the $n_c \times n_y$ matrix $\mathbf{H}$ is selected such that $\mathbf{HF} = 0$, $\mathbf{C}(s)$ is a $n_c \times n_c$ transfer function compensator matrix and $\mathbf{C}^y(s)$ is a diagonal filter matrix. We require that $\mathbf{C}^y(0) = \mathbf{I}$ and $\mathbf{C}(0)$ is non-singular such that $\mathbf{H}^c(0)\mathbf{F} = 0$, i.e. the self-optimizing properties are retained. This configuration is illustrated in Figure 7.1.

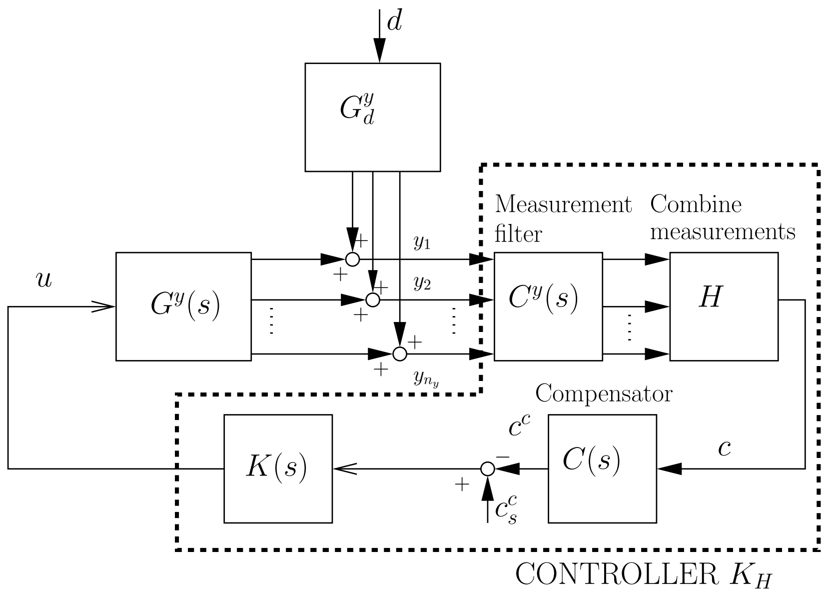

Figure 7.1: *Block diagram of the extended coefficient matrix* $\mathbf{H}^c(s)$ *for the null space method*

First, we recapitulate some results from the null space method of Chapter 3. Thereafter, we discuss the use of compensators ($\mathbf{C}(s)$ above) and finally, we discuss the use of measurement filters ($\mathbf{C}^y(s)$ above) for improving the controllability for controlled variables that are combinations of measurements.

7.2 Previous work: The null space method

The basic idea of the null space method for selection of self-optimizing control variables is to find a linear combination of measurements (the matrix $\mathbf{H}$) and by using constant nominal setpoints, operation is near-optimal in spite of disturbances and implementation errors.

In general, the controlled variables, synthesized using the null space method, are on the form:

$$\mathbf{c}(s) = \mathbf{H}\mathbf{y}(s) = \mathbf{H}\mathbf{G}^y(s)\mathbf{u}(s) = \mathbf{G}(s)\mathbf{u}(s) \tag{7.2}$$

where $\mathbf{G}(s)$ is a transfer function matrix and the real constant matrix $\mathbf{H}$ (the coefficient matrix) is selected such that the rows of $\mathbf{H}$ correspond to the null vectors of the left null space of the optimal sensitivity matrix

$$\Delta\mathbf{y}^{opt} = \mathbf{F}(0)\Delta\mathbf{d} \tag{7.3}$$

where $\mathbf{d}$ is the disturbance vector (inputs which we cannot affect) and $\mathbf{F}(0)$ is evaluated at steady-state. We want to select $\mathbf{H}$ such that $\Delta\mathbf{c}^{opt} = 0$ for all disturbances. This is obtained by selecting $\mathbf{H}$ in the left null space of $\mathbf{F}(0)$ such that $\mathbf{H}\mathbf{F}(0) = 0$. The optimal sensitivity matrix $\mathbf{F}$ depends on the objective function J which we want to minimize. In Chapter 4 we showed that selecting another set of basis vectors for the left null space of $\mathbf{F}$ yields

$$\mathbf{H}^c = \mathbf{C}\mathbf{H} \tag{7.4}$$

where $\mathbf{C}$ is a $n_c \times n_c$ non-singular matrix and $\mathbf{C}\mathbf{H}\mathbf{F}(0) = 0$, i.e. the matrix $\mathbf{C}$ rotates the basis vectors for the null space. In addition, we showed that changing the basis vectors do not affect the steady-state loss from disturbances ($\mathbf{M}_d$), nor affect the contribution from the implementation error ($\mathbf{M}_n$) on the loss for a given set of measurements $\mathbf{y}$. Thus we cannot improve the steady-state self-optimizing behavior by selecting another set of basis vectors (by manipulating matrix $\mathbf{C}$).

7.3 Dynamic compensators

Here we consider using the freedom of selecting $\mathbf{C}$ for systems with multiple unconstrained degrees of freedom ($\mathbf{u}$) and show that this is similar to the use of compensators (Skogestad and Postlethwaite, 1996) in multivariable control design.

Consider the block diagram representation in Figure 7.2. Inputs and disturbances enter through $\mathbf{G}^y(s)$ and $\mathbf{G}^y_d(s)$, respectively. The measurements from the plant enter the block H which takes all (or a subset of the) measurements and returns the controlled variables $\mathbf{c}$. Normally, the controlled variables $\mathbf{c}$ correspond to single measurements y_i, but in general it can be any function $\mathbf{f}_y(\mathbf{y})$ of the measurements, as long as the number of controlled variables equals the number of inputs. The block C represents a compensator, resulting from the freedom of selecting basis vectors for the null space method. Thus, the analogy to the use of compensators in multivariable control design is apparent. We assume that $\mathbf{C}$ is static (rotating the null vectors), but this is not a fundamental limitation, and we can use any transfer function matrix $\mathbf{C}(s)$ as long as $\mathbf{C}(0) \neq 0$ which would give zero steady-state gain.

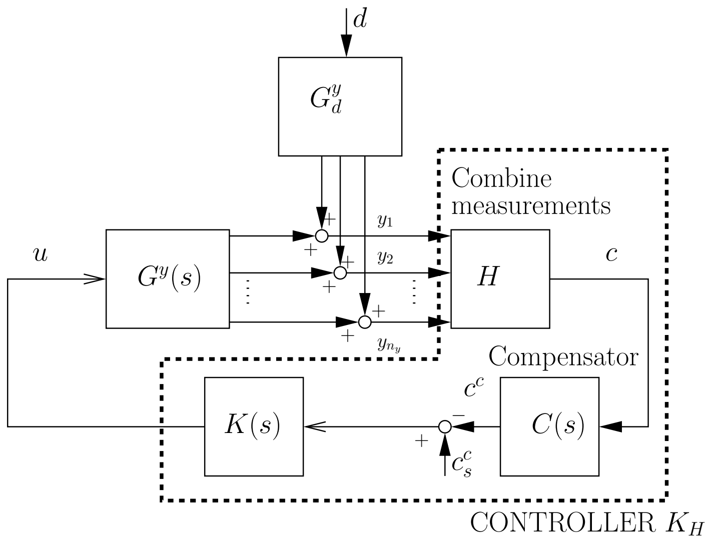

Figure 7.2: *Block diagram representation of the use of compensators* $\mathbf{C}$.

To illustrate, assume for the moment that $\mathbf{G}(s)$ is invertible. Introducing the compensator $\mathbf{C}(s)$ yields the new shaped plant

$$\mathbf{c}^c(s) = \mathbf{C}(s)\mathbf{H}\mathbf{y}(s) = \overbrace{\mathbf{C}(s)\underbrace{\mathbf{H}\mathbf{G}^y(s)}_{\mathbf{G}(s)}}^{\mathbf{G}^c(s)}\mathbf{u}(s) + \overbrace{\mathbf{C}(s)\underbrace{\mathbf{H}\mathbf{G}_d^y(s)}_{\mathbf{G}_d(s)}}^{\mathbf{G}_d^c(s)}\mathbf{d}(s) \tag{7.5}$$

Assume now that the preferred plant is diagonal, i.e. $\mathbf{G}^c(s) = \mathbf{C}(s)\mathbf{G}(s) = \mathbf{I}$. By selecting $\mathbf{C} = \mathbf{G}(s)^{-1}$ we have the shaped plant

$$\mathbf{c}^c(s) = \mathbf{G}(s)^{-1}\mathbf{G}(s)\mathbf{u}(s) + \mathbf{G}(s)^{-1}\mathbf{G}_d(s)\mathbf{d}(s) = \mathbf{I}\mathbf{u}(s) + \mathbf{G}_d^c(s)\mathbf{d}(s) \tag{7.6}$$

This approach is similar to the use of pre- and post-compensators ($\mathbf{W}_1$ and $\mathbf{W}_2$ respectively) in multivariable controller design, where the shaped plant is

$$\mathbf{G}^c = \mathbf{W}_2\mathbf{G}\mathbf{W}_1 \tag{7.7}$$

The compensator terms $\mathbf{W}_i(s)$ are used to counteract the interactions in the plant and to give a resulting desired plant (Skogestad and Postlethwaite, 1996). Both pre- and post-compensators are used, such as in SVD-controllers (Hovd et al., 1994; Hung and MacFarlane, 1982). Typically, a set of controlled variables with a corresponding control objective is given, and the compensators are added such that the controller design is simplified. The most important result from the use of compensators in multivariable controller design is the use of decoupling in decentralized control. Below we summarize the most important results.

7.3.1 Decoupling

A decoupled control is achieved when the compensator (or the null vector rotation) matrix $\mathbf{C}$ is such that $\mathbf{G}^c(s)$ in eq. (7.5) is diagonal at a selected frequency (or range of frequencies). Skogestad and Postlethwaite (1996) list several possible decoupled systems:

1. *Dynamic decoupling*: $\mathbf{G}^c(s)$ is diagonal at all frequencies. Then the compensator is $\mathbf{C}(s) = \mathbf{G}(s)^{-1}$ and the resulting plant is $\mathbf{G}^c(s) = \mathbf{I}$ for all frequencies. Since the system is diagonal for all frequencies, we can design a diagonal controller $\mathbf{K}(s) = \begin{bmatrix} k_1(s) & & \\ & \ddots & \\ & & k_{n_c} \end{bmatrix}$.
2. *Steady-state decoupling*: $\mathbf{G}^c(0)$ is diagonal. Thus we select the post-compensator as $\mathbf{C} = \mathbf{G}(0)^{-1}$.
3. *Approximate decoupling at frequency* ω_0: $\mathbf{G}^c(j\omega_0)$ is as diagonal as possible . This is achieved by selecting the post-compensator as a constant $\mathbf{C} = \mathbf{G}_0^{-1}$ where $\mathbf{G}_0$ is the real approximation of $\mathbf{G}(j\omega_0)$. A real approximation may be found using the align method of Edmuns and Kouvaritakis (1979) (see also Maciejowski (1989)). The bandwidth frequency is a good selection for ω_0, because the effect on performance of reducing interaction is normally greatest at this frequency.

In the setting of the null space method, the steady-state decoupling is of greatest interest since we consider slow varying disturbances (low frequency disturbances). Note that the above decoupling may simplify the controller design since we can design a diagonal controller. To summarize, the selection of $\mathbf{C}$ (basis vectors) is similar to the use of compensators in multivariable controlled design.

Next, we consider the effect of rotating the null vectors on the resulting poles and zeros of the plant.

7.4 Effect of null space basis on poles and zeros

Here we consider the effect of changing the null space basis vectors (selecting a static $\mathbf{C}$) for the poles and zeros of the resulting controlled plant. From eq. (7.5) we have

$$\mathbf{c}^c(s) = \mathbf{G}^c(s)\mathbf{u}(s) + \mathbf{G}_d^c(s)\mathbf{d}(s) \tag{7.8}$$

where $\mathbf{G}^c(s) = \mathbf{C}\mathbf{G}(s)$ and $\mathbf{G}_d^c(s) = \mathbf{C}\mathbf{G}_d(s)$.

Poles

For a multi-input multi-output (MIMO) system on transfer function form, the poles are defined as:

Theorem 7.1 *(MacFarlane and Karcanias, 1976) The pole polynomial $\phi(s)$ corresponding to a minimal realization of a system with transfer function matrix $G(s)$, and is the least common denominator of all non-identically zero minors of all orders of $G(s)$.*

As seen from eq. (7.8), $\mathbf{G}^c(s)$ has the same set of poles as the transfer function $\mathbf{G}(s)$ as long as the compensator $\mathbf{C}$ does not have any dynamic terms. For dynamic compensators, the situation is different in that the resulting plant contains the poles of the two subsystems (if no pole/zero cancellation is allowed). For the case of a dynamic decoupler, as discussed above, we intentionally cancel poles and zeros by using the inverse of the plant as a decoupler.

Zeros

In general, zeros are the values of s for which $\mathbf{G}(s)$ loses rank. More specific, following the definition of MacFarlane and Karcanias (1976), the zeros are defined as:

Theorem 7.2 *Zeros. z_i is a zero of $\mathbf{G}(s)$ if the rank of $\mathbf{G}(z_i)$ is less that the normal rank of $\mathbf{G}(s)$.*

From eq. (7.8) it is clear that if $\mathbf{C}$ is a static matrix, the rank of $\mathbf{G}^c$ equals the rank of $\mathbf{G}$, as long as $\mathbf{C}$ is non-singular (Skogestad and Postlethwaite, 1996). To conclude, the poles and zeros are unaffected by using another set of basis vectors (by changing the matrix $\mathbf{C}$) for the null space. Next, we show that the pole and zero directions depend on the basis vectors used.

Pole and zero directions

Let $\mathbf{G}(s)$ have a zero at $s = z$. Then $\mathbf{G}(s)$ loses rank at $s = z$, and we have non-zero vectors $\mathbf{u}_z$ and $\mathbf{c}_z$ such that

$$\mathbf{G}(z)\mathbf{u}_z = 0, \ \mathbf{c}_z^H\mathbf{G}(z) = 0 \tag{7.9}$$

Here $\mathbf{u}_z$ is defined as the input zero direction and $\mathbf{c}_z$ is defined as the output zero direction. The output directions yield the directions that may be difficult to control (zero gain).

Let $\mathbf{G}(s)$ have a pole at $s = p$, then $\mathbf{G}(p)$ is infinite, and we may write

$$\mathbf{G}(p)\mathbf{u}_p = \infty \quad \mathbf{c}_p^H\mathbf{G}(p) = \infty \tag{7.10}$$

where $\mathbf{u}_p$ is the input pole direction and $\mathbf{c}_p$ is the output pole direction. By using static compensators (no additional poles or zeros in the compensator $\mathbf{C}$) the output pole and zero directions are

$$\mathbf{c}_z^{cH}\mathbf{G}^c(z) = (\mathbf{c}_z^H\mathbf{C})\mathbf{G}(z) = 0 \quad \text{and} \quad \mathbf{c}_p^{cH}\mathbf{G}^c(p) = (\mathbf{c}_p^H\mathbf{C})\mathbf{G}(p) = \infty \tag{7.11}$$

and it is evident that we can move the effect of zeros and poles to one output. One example, is to move a RHP zero to one output (Skogestad and Postlethwaite, 1996).

If the zero is pinned to one output (e.g. $\mathbf{c}_z$ has only one element different from zero), we cannot move the effect to another output.

To summarize, the use of a static compensator does not affect the poles and zeros, however, we can affect the pole and zero output direction. On the other side, we can use a static compensator (freedom of selecting the basis vectors) to shape the plant at a desired frequency. Next, we illustrate, by means of an example, the use of static compensators in the null space method, and how it affects the economics of operation.

Example 7.1 *Here we study a system with three measurement, two inputs and one disturbance*[1]. *The input and disturbance gains are:*

$$\mathbf{G}^y(s) = f(s)\begin{bmatrix} 16.8(920s^2+32.4s+1) & 30.5(52.1s+1) \\ -16.7(75.5s+1) & 31.0(75.8s+1)(1.582s+1) \\ 1.27(-939s+1) & 54.1(57.3s+1) \end{bmatrix} \tag{7.12}$$

and

$$\mathbf{G}^y_d(s) = f(s)\begin{bmatrix} 4.30(7.28s+1) \\ -1.41(74.6s+1) \\ 5.40 \end{bmatrix} \quad \textit{where} \quad f(s) = \frac{e^{-2s}}{(18.8s+1)(78.8s+1)(5s+1)} \tag{7.13}$$

We assume that the operational objective is $J(u,d) = (y_2 - y_1)^2 + (y_1 - d)^2$ and we find that the optimal sensitivity matrix $\Delta \mathbf{y}^{opt} = \mathbf{F}\Delta d$ evaluated at steady-state ($s = 0$) is $\mathbf{F}^T = \begin{bmatrix} 1 & 1 & 4.4154 \end{bmatrix}$. The orthogonal basis for the null space is

$$\begin{bmatrix} \mathbf{h}_1 \\ \mathbf{h}_2 \end{bmatrix} = \begin{bmatrix} -0.2157 & 0.9617 & -0.1690 \\ -0.9523 & -0.1690 & 0.2540 \end{bmatrix} \tag{7.14}$$

Now, we consider three different static decouplers $\mathbf{C}$:

1. *Using the above basis vectors the resulting system is (labeled 'c$_0$' hereafter).*

$$\mathbf{G}_0(s) = f(s)\begin{bmatrix} -19.8991(1+3.126s)(1+53.59s) & 14.0942(1+2.542s)(1+99.66s) \\ -12.8551(1+47.31s+(33.84s)^2) & -20.5454(1+0.5602s)(1+54.51s) \end{bmatrix} \tag{7.15}$$

with the poles and zeros

$$\begin{aligned} p &= \{-0.2000, -0.0532, -0.0132, -0.2000, -0.0532, -0.0132\} \\ z &= \{-0.4054, -0.0533, -0.0379, -0.0132\} \end{aligned} \tag{7.16}$$

respectively.

2. *Steady state decoupling $\mathbf{C} = \mathbf{G}_0(0)^{-1} = \begin{bmatrix} -0.822 & -0.564 \\ 0.514 & -0.796 \end{bmatrix}$ (labeled 'c$_{ss}$' hereafter)*

$$\mathbf{G}_{ss}(s) = f(s)\begin{bmatrix} 23.6(10.9s+1)(42.9s+1) & -545.9s(4.72s+1) \\ -96.2s(-104s+1) & 23.7(1.45s+1)(68.1s+1) \end{bmatrix} \tag{7.17}$$

with the same poles and zeros as in eq. (7.16).

[1]This model is actually a very crude model of a Fluid Catalytic Cracking (FCC) reactor (Skogestad and Postlethwaite, 1996), where the inputs $[\mathbf{u}\ d]^T = [F_s\ F_a\ k_c]$ represent the circulation, airflow and feed composition, and $\mathbf{y}^T = [T_1\ T_{cy}\ T_{rg}]$ represent three temperature measurements in the reactor. It is assumed that the feed composition to the reactor is a disturbance to the system. Here we treat the model as a purely mathematical model, without any reference to the origin.

3. Decoupling at $\omega = 10^{-0.3}$ (labeled 'c$_{hf}$') where $\mathbf{C} = \mathbf{G}_0(\omega)^{-1} = \left[\begin{smallmatrix} 0.147 & 0.343 \\ -0.970 & 0.233 \end{smallmatrix}\right]$

$$\mathbf{G}_{hf}(s) = f(s)\begin{bmatrix} -7.3412(1+51.06s+(27.48s)^2) & -4.9792(1-1.678s)(1+37.11s) \\ 16.3121(1-0.2018s)(1+58.64s) & -18.4572(1+2.229s)(1+87.76s) \end{bmatrix} \tag{7.18}$$

with the same poles and zeros as in eq. (7.16).

As expected, we see that all three candidates have the same poles and zeros.

Assume that we want to use decentralized control, and we pair inputs and outputs based on the relative gain array (RGA). Figure 7.3 shows the frequency dependent RGA for all candidates (plotting element RGA$^{(1,1)}$)($j\omega$). Based on Figure 7.3 it follows that

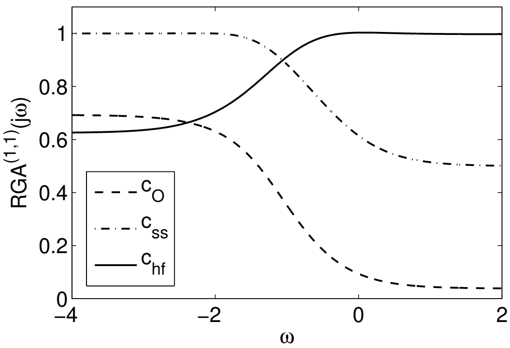

Figure 7.3: *RGA$^{(1,1)}$-element with respect to frequency for candidates c_{ss}, c_0 and c_{hf}*

Candidate	Loop	K_c	τ_I	τ_D
c_0	1	−0.3187	16	5
	2	−0.1692	21	–
c_{ss}	1	0.1614	5	–
	2	0.22	18.8	3.547
c_{hf}	1	−0.2572	18.8	5
	2	−0.2361	20.18	–

Table 7.1: *PID tunings for all candidates control structures using the Skogestad IMC tuning rules where we have assumed that the closed-loop time constant τ_c is equal to the dominating time constant of the process*

we should pair on the diagonal at low frequencies, while at high frequencies we should pair on the off-diagonal elements for c_0. We are mainly interested in tight control at low frequencies and select to pair on the diagonal elements. Using Skogestad IMC tuning rules (Skogestad, 2003) we get the PI(D)-parameters as given in Table 7.1.

The dynamic response for a ramped up disturbance $d = 1$ using 100 time units is shown in Figures 7.4-7.5. The measurement responses in Figure 7.4 show the same steady-state behavior for all candidates, however candidate c_{hf} exhibits an over-shoot due to large input usage for u_2 (see Figure 7.4(a)). Candidates c_{ss} and c_0 show similar dynamic behavior. From the plot of the dynamic cost in Figure 7.5, it is evident that candidate c_{ss} has the lowest cost, while candidate c_{hf} has the highest cost. The integrated cost for all candidates are

$$J_0^{int} = 11.3570 \quad J_{ss}^{int} = 8.6793 \quad J_{hf}^{int} = 13.2439 \tag{7.19}$$

and we see that candidate c_{hf} has a total cost that is 1.5 times higher as compared to the best candidate, while the steady-state is equal for all candidates. This can easily be explained from the RGA, where we see that the steady-state decoupler yields only small interactions at low frequencies as opposed to the other two candidates. This results in less interaction between the control loops and better dynamic performance.

This example has shown that the effect of rotating the null space basis will influence the dynamic performance of the closed loop system (at least for decentralized control),

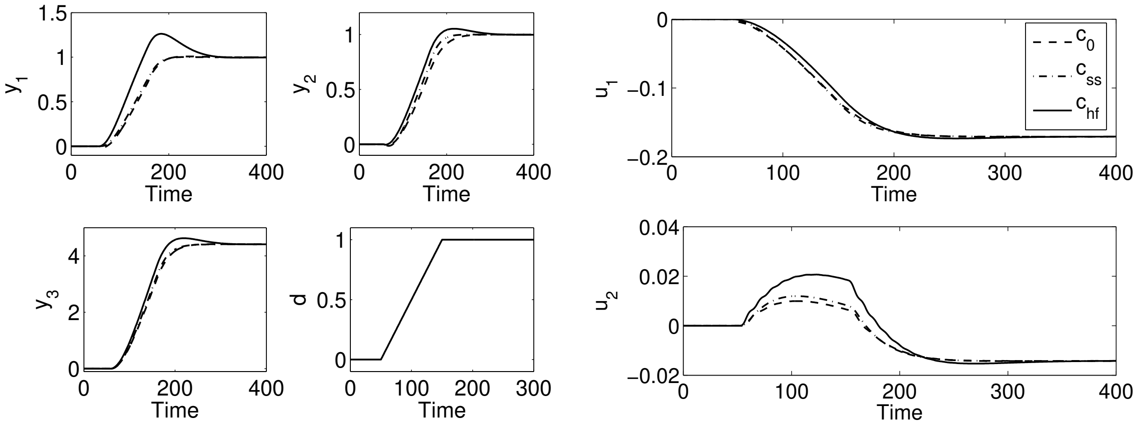

(a) Plot of output response y_i and the imposed disturbance d for all candidates

(b) Plot of input response u_i for all candidates

Figure 7.4: *Dynamic responses for a disturbance change*

while the steady-state performance is unaffected. As shown, the steady-state decoupler improves the performance compared to using the orthogonal basis vectors, due to the decoupled loops at low frequencies where there are strong interactions for the other two candidates.

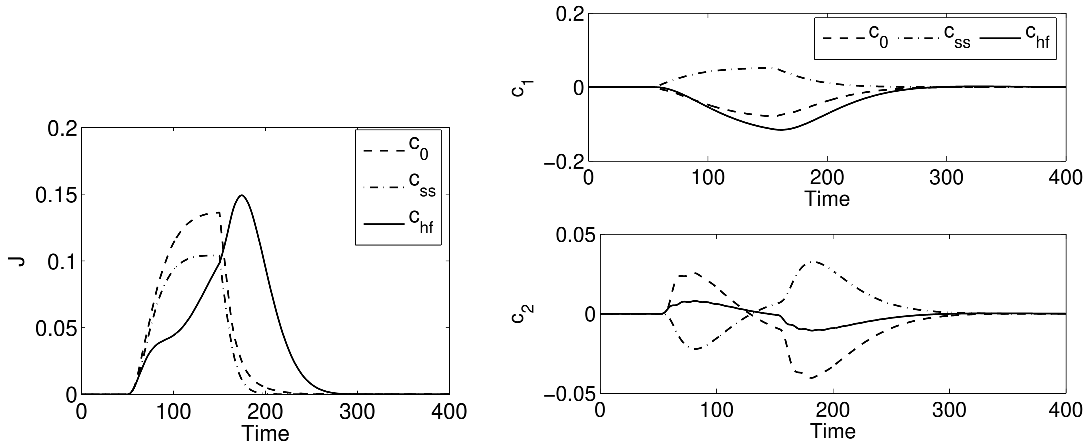

(a) Plot of objective function value J for all candidates

(b) Plot of controlled variables for all candidates

Figure 7.5: *Plot of objective function value J and controlled variables for all candidates*

In the rest of this paper, we discuss single-input single-ouput (SISO) systems and the use of measurement filters for improving the dynamic properties of a controlled variable that is a combination of measurements.

7.5 Improving dynamic performance using measurement filtering

In the previous section, compensator design was discussed based around the freedom of selecting basis vectors for the left null space of $\mathbf{F}(0)$. Here the approach is slightly different, in which we use compensators (or filters) on the measurements as illustrated by the block C^y in Figure 7.1. Let the filter block $\mathbf{C}^y(s)$ be diagonal, such that

$$\mathbf{C}^y(s) = \begin{bmatrix} c_1^y(s) & & \\ & \ddots & \\ & & c_{n_y}^y(s) \end{bmatrix} \tag{7.20}$$

The goal is to design $\mathbf{C}^y$ for SISO systems to improve the dynamic performance. Performance limitations for SISO systems can be summarized as the effect of

- Right-half plane (RHP) zeros
- Right-half plane poles
- Time delays
- Disturbances
- Input limitations
- Uncertainties

More specifically, we focus on how to avoid the limiting effects of right half plane zeros for controlled variables synthesized using the null space method. For SISO systems, the null space has a given direction ($\mathbf{H}$ is a vector) and all other null space vectors are in the same direction $\mathbf{H}_j = c\mathbf{H}$. The resulting plant is

$$c^c(s) = \mathbf{H}\mathbf{C}^y(s)\mathbf{y}(s) = \mathbf{H}\mathbf{C}^y(s)\mathbf{G}^y(s)\mathbf{u}(s) \tag{7.21}$$

The only requirement we impose is that at steady-state

$$\mathbf{C}^y(0) = \mathbf{I}$$

that is, the identity matrix, which is necessary since altering the steady-state gain will affect the direction of $\mathbf{H}^c$ such that $\mathbf{H}^c(0)\mathbf{F}(0) \neq 0$.

The motivation for considering right-half plane zeros, is that, when selecting controlled variables as a combination of measurements based on the steady-state, one may select measurements that are located at different positions in the plant. Thus, the disturbance and input propagation to the measurements may have different time scales, which in turn may lead to competing effects propagating to the measurement. The competing effects may give rise to right half plane zeros, which limits the close-loop performance for SISO systems. More specifically, a RHP zero will give inverse response and limit the bandwidth of the controller. We illustrate this with a simple example with two measurements and one input.

$$c(s) = G(s)u(s) = h_1 g_1(s)u(s) + h_2 g_2(s)u(s) \tag{7.22}$$

The process $G(s)$ consists of two sub-systems interconnected in parallel with a weighting vector $\mathbf{H} = [h_1 \ h_2]$, as illustrated in Figure 7.6. Assume that each sub-system $g_i(s)$ is

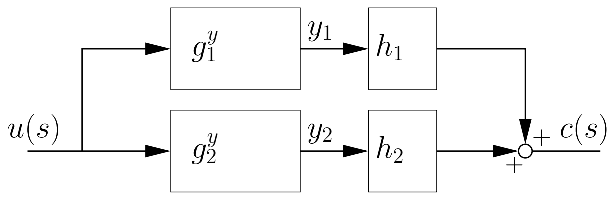

Figure 7.6: *Parallel interconnection of two sub-systems*

modeled as a rational transfer function on the form $g_i(s) = \frac{n_{g_i}(s)}{d_{g_i}(s)}$, thus the resulting plant is:

$$\begin{aligned} c(s) &= (h_1 g_1(s) + h_2 g_2(s))\, u(s) = \left(h_1 \frac{n_{g_1}(s)}{d_{g_1}(s)} + h_2 \frac{n_{g_2}(s)}{d_{g_2}(s)} \right) u(s) \\ &= \left(\frac{h_1 n_{g_1}(s) d_{g_2}(s) + h_2 n_{g_2}(s) d_{g_1}(s)}{d_{g_1}(s) d_{g_2}(s)} \right) u(s) \end{aligned} \tag{7.23}$$

From eq. (7.23) it is clear that the poles of the resulting plant, are the poles of the two sub-systems g_1 and g_2 while the zeros are changed. For systems where $h_1 g_1^y$ and $h_2 g_2^y$ have opposing effects, this may lead to right-half plane zeros, which limit the control performance. Note that even for sub-systems g_i with no zeros ($n_{g_i} = k_i$), the resulting plant $G = \sum h_i g_i$ may have zeros arising from competing effects of the poles.

The idea here is to utilize dynamic compensators in series with the individual measurements in order to reduce the competing effects, and to smooth out the resulting controlled variable signal c. The following example illustrates the idea:

Example 7.2 *Let two sub-systems be of first order*

$$y(s) = \begin{bmatrix} \frac{1.4}{s+1} \\ \frac{-2}{0.2s+1} \end{bmatrix} u(s) \tag{7.24}$$

Both sub-systems are stable and have no right-half plane zeros. The system has one input and we assume that the null space of the optimal sensitivity matrix is $\mathbf{H} = [h_1 \ h_2] = [0.6 \ 0.3]$. *The process* G *consists of two systems in parallel, weighted with* $\mathbf{H}$ *as seen in Figure 7.6. The resulting plant is*

$$c(s) = [0.6 \ 0.3] \begin{bmatrix} \frac{1.4}{s+1} \\ \frac{-2}{0.2s+1} \end{bmatrix} u(s) = \frac{0.24(-1.8s+1)}{(s+1)(0.2s+1)} u(s) \tag{7.25}$$

and we have a right-half plane zero at $z = 1/1.8 = 0.5556$ *and the poles are the poles of the two sub-systems. The RHP-zero results in an inverse response for a step in the inputs as illustrated in Figure 7.7(a) and it is clear that the competing effects in the*

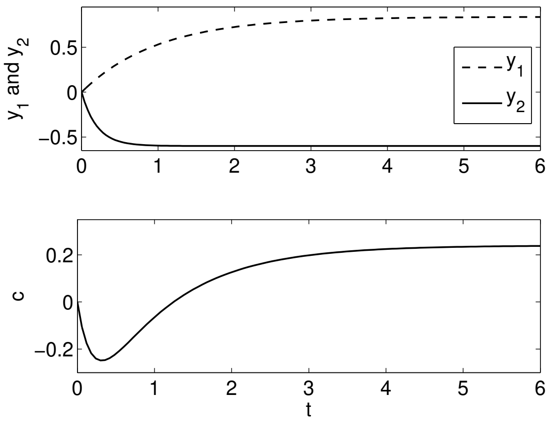

(a) Unfiltered response for y_1, y_2 and c

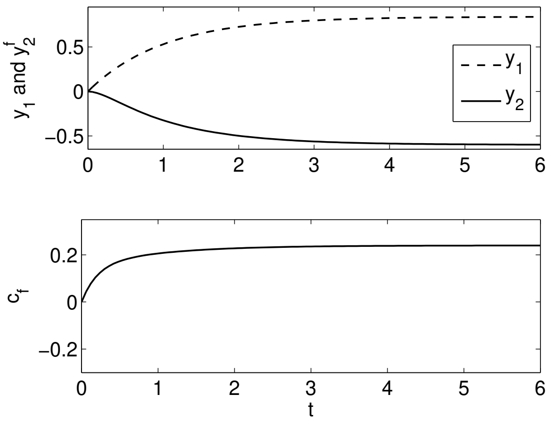

(b) Filtered response for y_1, y_2^f and c^c

Figure 7.7: *Unfiltered and filtered responses*

two measurements, give rise to the inverse response. Assume now that we filter y_2 with the low-pass filter $c_2^y(s)$ where

$$c_2^y(s) = \frac{1}{s+1} \tag{7.26}$$

which results in the following plant $c^c(s) = G^c u(s)$ where

$$G^c = 0.24\frac{0.7s+1}{(s+1)(0.2s+1)} \tag{7.27}$$

We see that the zero of the filtered plant is in the left-half plane ($z = -1/0.7 = -1.4286$) and does not impose any limitation on the controllability of the plant. The resulting dynamic response for a step in the input is shown in Figure 7.7(b). We see that the filtered plant has a smooth response and that the rise time is faster than for the unfiltered plant, even when the response for y_2 is slower than in the unfiltered case. Note, that the steady-state is unchanged.

Comparing different filter time-constants, see Figure 7.8, we see that it is important to select the time-constant of the filter appropriately. As seen from the figure, a filter time constant of $\tau_{C^y} = 1$ yields a smooth response. Note that irrespectively of the filter time constant, the steady-state performance is unchanged.

The above example illustrates a method for using measurement filters for removing the bandwidth limiting effect of RHP zeros, without changing the steady-state. For n_y number of measurements we have in general that

$$c^c(s) = \mathbf{H}\mathbf{C}^y(s)\mathbf{y}(s) = \mathbf{H}\mathbf{C}^y(s)\mathbf{G}^y(s)u(s) \tag{7.28}$$

where $\mathbf{C}^y$ is a diagonal filter matrix. For the case of multiple measurements which exhibit complex dynamic behavior, it may prove difficult to find what measurements

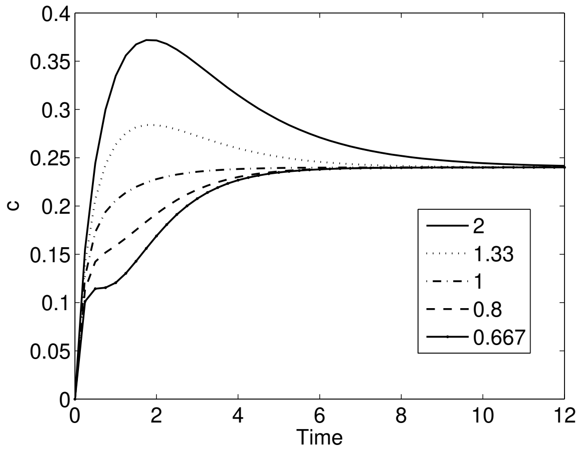

Figure 7.8: *Time response of $c^c = G^c(\tau_{c^y})u$ for a step in the input with respect to the time constant of the filter τ_{c^y}.*

to filter and the form and parameters of the time-constants. If we restrict the filter design to 1-order transfer functions, a reasonable approach to the design of the filter is:

Proposition: Given the sub-plants $g_i = \frac{n_i(s)}{d_i(s)}$ with dominating time constants $\tau_{i,1}$ and the static vector $\mathbf{H}$ such that the resulting plant is $c(s) = \sum_i h_i g_i(s) u(s)$ add a filter $c_i^y(s) = \frac{1}{\tau_i s+1}$ to measurements that have fast poles (small τ's) such that all measurements have the same dominating pole (largest τ).

This is of course not a general rule, and for more complex plants, more advanced controller design methods (e.g. H_∞ design methods (Skogestad and Postlethwaite, 1996)) may be a better approach. Alternatively, if there is freedom in selecting a different set of measurements, selecting measurements that are physically close may improve the dynamics the system.

7.6 Conclusions

In this paper we have extended the null space method to improve the dynamics of the resulting plant. We have discussed the freedom of selecting basis vectors for the null space method, and have shown that this is similar to the use of compensators in the design of multivariable controllers. In addition, we discussed the use of measurement filters, where we focused on using filters to remove right-half plane zeros. We proposed a simple rule, to eliminate the performance limiting effects of right-half plane zeros.

Bibliography

Edmuns, J. and Kouvaritakis, B. (1979). Extensions of the frame alignment technique and their used in the characteristic locus design method. *Int. J. Control*, 5:787–796.

Hovd, M., Braatz, R., and Skogestad, S. (1994). SVD-controllers for H_2-, H_∞-, and μ-optimal control. *Proc. of American Control Conference 1994, Baltimore, MD, June 1994*, pages 1233–1237.

Hung, Y. and MacFarlane, A. (1982). *Multivariable feedback: A quasi-classical approach*. Springer Verlag, Berlin. Vol 40 of lecture notes in control and information sciences.

Larsson, T. and Skogestad, S. (2000). Plantwide control: A review and a new design procedure. *Model. Ident. Control*, 21:209–240.

MacFarlane, A. and Karcanias, N. (1976). Poles and zeros of linear multivariable systems: A survey of the algebraic, geometric and complex-variable theory. *Int. J. Control*, 24(1):33–74.

Maciejowski, J. (1989). *Multivariable feedback design*. Addison Wesley, UK.

Skogestad, S. (2000). Plantwide control: The search for the self-optimizing control structure. *J. Proc. Control*, 10:487–507.

Skogestad, S. (2003). Simple analytic rules for model reduction and PID controller tuning. *J. Proc. Control,*, 13:291–309.

Skogestad, S. and Postlethwaite, I. (1996). *Multivariable Feedback Control*. John Wiley & Sons.

Chapter 8

Selection of self-optimizing control structures for a Petlyuk distillation column

Based on work presented at
AIChE Annual Meeting 2002, November 3-8, Indianapolis, USA, paper 247f
and
International Symposium on Advanced Control of Chemical Processes (ADCHEM) 2003, January 11-14, 2004, Hong Kong

8.1 Introduction

The Petlyuk distillation column is an appealing alternative for the separation of ternary mixtures. Compared with the traditional configuration of two columns in series, Smith and Triantafyllou (1992) report typical savings in the order of 30% in *both* energy and capital cost. Several authors have studied the potential energy savings in using the Petlyuk column, see for example Fidkowski and Krolikowski (1986); Carlberg and Westerberg (1989b,a), and minimum energy expressions have been derived both for sharp splits and for non-sharp splits (Fidkowski and Krolikowski, 1986; Halvorsen and Skogestad, 2003). Distillation columns are often the unit operation with the highest energy cost in chemical plants. However, despite the relative large savings in both energy and capital cost, few implementations of the Petlyuk column exist in industry (Adrian et al. (2002, 2004) report approximately 40 industrial columns world-wide).

One explanation for its limited usage can be difficulties with the design of and operational issues with (uncertainty) the Petlyuk column (Smith and Triantafyllou, 1992). The Petlyuk column, being more coupled both in mass and energy, imposes operational challenges that are more difficult to understand than the alternative and simpler configuration of two columns in series. In fact, non-optimal operation of the Petlyuk column may easily yield worse performance in terms of energy usage as compared with the direct or indirect columns in series. Thus, the advantage of being more energy efficient, comes at a price of more complex operation.

The goal here is to suggest simple operating policies that ensure near-optimal operation. We are looking for a self-optimizing control structure which, despite of external disturbances and measurements errors, gives near-optimal operation with constant setpoints. The null space method of Chapter 3 is used for synthesizing the controlled variables, and the proposed control structures are compared with previously proposed structures and structures synthesized using alternative methods.

8.1.1 The Petlyuk column structure

The Petlyuk column, illustrated in Figure 8.1, consists of six column sections. Here, the sections are arranged in the same column shell (often named a "divided wall column"). The ternary feed consists of components A, B and C with mole fractions $\mathbf{z}^T = [z_A \; z_B \; z_C]$, component A being the most volatile and component C the least volatile. The feed point is located between sections 1 and 2 in the pre-fractionator. Ideally, components A and B (rich in A) go over the top of the pre-fractionator, while a mixture of B and C (rich in C) leaves the bottom. In the main column (sections $3-6$), three product streams are drawn off. The light component A dominates the distillate stream (D), component B dominates in the side-stream (S) while the heavy component C dominates the bottom stream (B). The boilup and reflux streams are split over the "dividing wall" with split fractions R_V and R_L respectively, where

$$R_L = \frac{L_1}{L_3} \quad \text{and} \quad R_V = \frac{V_2}{V_6}$$

where L_i and V_i denote the molar liquid and vapor flows in section i respectively.

With a given feed and pressure, the Petlyuk column has five steady-state degrees of freedom. For example, these may be selected as

$$\mathbf{u}^T = \begin{bmatrix} L & V & S & R_L & R_V \end{bmatrix} \tag{8.1}$$

corresponding to the reflux, boilup, side-stream flow, liquid split and vapor split, respectively. Dynamically, the level in the condenser and reboiler must be stabilized, and we choose to use D and B, respectively (resulting in the "LV"-configuration).

For the Petlyuk column, three product specifications may be specified during operation (Halvorsen and Skogestad, 2003):

1. Distillate purity ($x_{A,D}$)
2. Bottom purity ($x_{C,B}$)
3. Side-stream purity ($x_{B,S}$)

where $x_{i,j}$ denotes the mole fraction of component i in stream j.

In the side-stream there are two impurities, and one may wish to specify these independently, resulting in four purity specifications. However, in practice, this leads to discontinuities in the feasible region (Wolff et al., 1994; Wolff and Skogestad, 1996) and is not recommended in operation. For a detailed analysis of the Petlyuk column and explicit expressions for the minimum energy required for a given separation, see Halvorsen and Skogestad (2003).

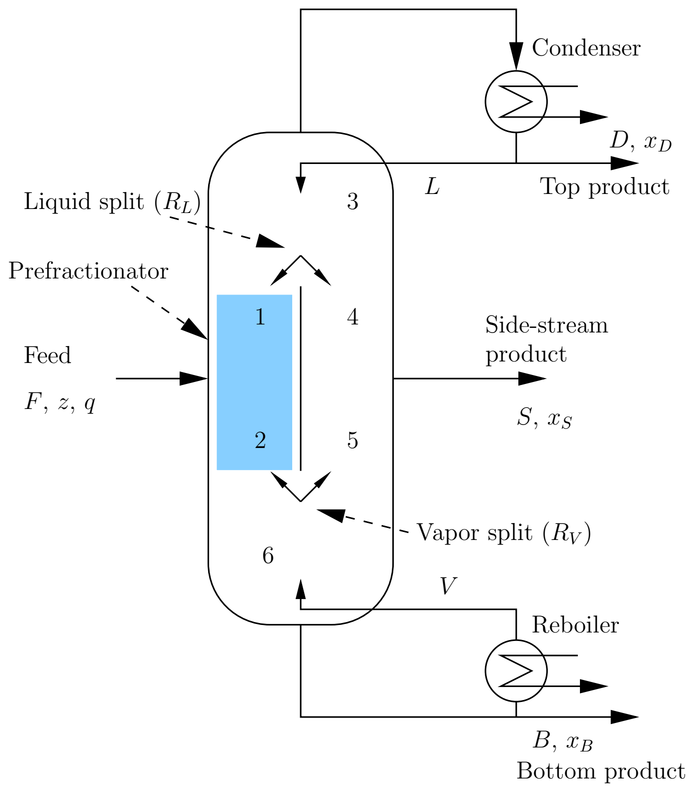

Figure 8.1: *The Petlyuk Distillation column implemented in a single column shell ("the divided wall column").*

Measurements

The following measurements are assumed available online:

- Temperatures (T_i) on each stage. Index i denotes the stage number in increasing order for sections 1-6, in total $6N_T$ temperatures, where N_T is the number of stages in each section.
- The main component composition in each product stream $x_{A,D}$, $x_{B,S}$ and $x_{C,B}$.
- All flows and flow ratios in **u** as given by eq. (8.1).
- Holdup in the distillate drum (M_D) and bottom sump (M_B).

resulting in the measurement vector:

$$\mathbf{y}_0^T = \begin{bmatrix} x_{A,D} & x_{B,S} & x_{C,B} & \mathbf{T}^T & \mathbf{u}^T & M_B & M_D \end{bmatrix} \tag{8.2}$$

Unmeasured external disturbances

The unmeasured external disturbances are assumed to be:

- The feed flow rate (F).
- The feed compositions $\mathbf{z}^T = [z_A \; z_B \; z_C]$.
- The liquid fraction of the feed (q_l).

In addition, we assume that all measurements have corresponding measurement error, while we assume that the control error is negligible (integral action in all control loops).

8.2 Operational objective and active constraints

We assume that the operational objective is to minimize the cost of energy while maintaining the product purity specifications. This translates into minimizing the boilup V, since all products are assumed to have equal economic value. Note that we are not over-fractionating any of the product streams in accordance with normal operational practice. However, as shown in Chapter 9, this is not necessarily optimal for the Petlyuk distillation column, where we in fact can *save energy* by over-fractionating one of the product streams. A preliminary optimization study of the Petlyuk distillation column, revealed that for certain column specifications, it is optimal to over-fractionate one of the products (Aaboen, 2003).

Nevertheless, we here consider "three-point" composition control, and we then have two degrees of freedom left for optimizing the operation, that is, to reduce the boilup. Since the objective is to minimize the boilup, which also is an input, one may mistakenly believe that one can use an open-loop approach, where the optimal value for the boilup is calculated and implemented in the column:

$$V = V^{opt} \tag{8.3}$$

where V^{opt} is the minimal boilup. Halvorsen and Skogestad (1999) point out that such an approach is impossible (or at least very difficult):

1. Operation is infeasible for $V < V^{opt}$, so we need to ensure that $V \geq V^{opt}$.
2. The optimal value of V varies with respect to disturbances and may be hard to find, requiring a detailed model and a direct measurement of the disturbances (or a very accurate estimate) in order to be viable. This is unrealistic in most cases.
3. Measurement or estimation of V may be difficult to achieve (measuring vapor flow), thus it may be sensitive to measurement error when trying to implement the optimal V.

Thus, the approach here is to use feedback control to ensure optimality, eliminating the need of estimating the disturbances and the problems of measuring and implementing V directly.

8.3 Previous work on control structure selection for the Petlyuk column

The Petlyuk column has been studied extensively in the literature, with the main focus on the potential energy savings as compared with the traditional two columns in series design. The methods and control structures for achieving the potential savings in energy have received much less attention in the literature. However, Halvorsen and Skogestad (2003); Halvorsen et al. (2000) discuss several candidate self-optimizing control structures based on the assumption of three-point composition control. In addition, Halvorsen and Skogestad (2003) studied the effect of keeping one additional degree of freedom constant (fixing the input R_V), and found that this yields acceptable self-optimizing control for most control structures. Thus, in order to operate (near) optimally, only one of the remaining degrees of freedom needs to be adjusted. A short summary of their findings is given below:

1. *Temperature profile symmetry*, DT_S: This candidate was proposed based on the visual observation that the optimal temperature profile across the dividing wall remained almost constant for different disturbances implying good self-optimizing properties. The controlled variable is defined as
$$DT_S = (\overline{\mathbf{T}}_1 - \overline{\mathbf{T}}_4) + (\overline{\mathbf{T}}_2 - \overline{\mathbf{T}}_5) \tag{8.4}$$
where $\overline{\mathbf{T}}_i$ denotes the average temperature in section i. In practice only one or two temperature measurements from each section need to be selected. The DT_S-variable showed the best self-optimizing properties of all proposed candidates and is attractive due to the availability of temperature measurements. Note that eq. (8.4) is actually a linear combination of measurements with a unit ($\pm$) weight for each measurement.
2. *Position of profile in the main column*, ΔN: The peak composition of the mid-component occurs at the location of the side-stream when the column operates optimally. A measurement of the stage number with the highest composition is proposed as a feedback controlled variable. This candidate is unlikely to be used in practice since online measurement of the compositions on each stage is rarely available. The candidate showed good self-optimizing performance for disturbances in the feed composition.
3. *Fractional recovery of intermediate component B leaving pre-fractionator*, β: Christiansen (1997) showed that the key to optimal operation is to operate the pre-fractionator at minimum reflux characteristics and proposed to control the impurity of the heavy component in the top and/or the impurity of the light component in the bottom of the pre-fractionator. This candidate behaves almost as good as the DT_s, and is robust against measurement error. Again, the need of a composition measurement makes it less attractive as a feedback variable.
4. *Pre-fractionator flow split*, D_1: The variable $D_1 = V_1 - L_1$ is the flow difference between vapor and liquid flow in the top of the pre-fractionator. This candidate may be difficult to measure, since we need to measure a vapor flow. In addition it was found that it yields very poor performance for disturbances in the feed composition.

Of the candidates proposed above, the temperature profile symmetry (DT_S) was evaluated as the best candidate for self-optimizing control, both based on the availability of temperature measurements and that it has good self-optimizing properties (Halvorsen and Skogestad, 2003).

Serra et al. (2003, 2001) studied the controllability of the divided wall column and compared it with the controllability of direct and indirect column configurations for several different feed compositions and relative volatilities. They fail to utilize the remaining degrees of freedom for control, as they fix both R_V and R_L. They conclude that the best controllability is achieved when a non-optimal nominal setpoint is used for R_L and R_V which implies that the nominal operation is non-optimal.

Adrian et al. (2002, 2004) claim that the Petlyuk column is difficult to control using decentralized control. They claim that in order to achieve good controllability and acceptable economic operation, a multivariable controller must be used (MPC). They compared the performance of the decentralized control structure with an model predictive controller. For the decentralized controller, the following three loops are closed.

1. They select to control a temperature in the top of the pre-fractionator with L/D in the main column (to prevent component C from going over the top of the pre-fractionator).
2. In addition, they propose to control a temperature in the top of the bottom section (section 6) with the side-stream (S) (indirect control of component C in the bottom stream).
3. And finally, they select to control a temperature in top of section 4 with the liquid split R_L (to control indirectly the composition in the side-stream).

Note that the boilup (V) is kept constant and that there is no control of the composition of the distillate. In practice, the bottom is over-fractionated by using excess energy (V). For the multivariable controller, they include the boilup (V) as an extra manipulated variable (more inputs than outputs) and conclude that the multivariable controller has better performance than the decentralized structure. The improved performance for the multivariable controller must partly be assigned the use of the extra manipulated variable. In addition they claim that the potential energy savings are not meet using the decentralized controller, which is obvious since V is kept constant. They do not justify the choice of which temperatures to control. Thus, they fail to discuss the possibly most important aspect of controllability, namely the selection of controlled variables. On the other side, they close two temperatures in the main column and one in the pre-fractionator, which is sufficient for stabilization of the temperature profile.

8.3.1 Modeling assumptions and data used

The following standard modeling assumptions are used for the simulations:

1. *Constant relative volatility* α: The relative volatility between components i and j is:
$$\alpha_{ij} = \frac{(y_i/x_i)}{y_j/x_j} = \frac{K_i}{K_j} \tag{8.5}$$
where x and y are the composition of the liquid and gas, respectively. In practice, $K_i = K_i(T, P)$ is a function of pressure and temperature. The relative volatility is less dependent on temperature, so in most cases it is a good approximation for simple calculations. See Halvorsen and Skogestad (2000) for more details.
2. *Constant molar flows*: That is $L_n = L_{n+1}$ and $V_{n-1} = V_n$ on a non-feed or non-product stream stage. No energy balance is then needed. The first two assumptions are reasonable for separation of similar components (similar heat of vaporization).
3. *Equilibrium on each stage.*
4. *Constant pressure* P.

5. *Estimation of temperatures based on composition.* The temperature estimates are based on the method of Halvorsen and Skogestad (2000)

$$T \approx \frac{B_r}{\log(p_r^0) - A_r} + C_r \quad \text{where} \quad p_r^0 = \frac{P}{\sum_i x_i \alpha_i} \tag{8.6}$$

   and where A_r, B_r and C_r are Antoine parameters.

6. The liquid flow dynamics are modeled as

$$L_i = L_{0,i} + \frac{M_i - M_{0,i}}{\tau_L} + (V_{i-1} - V_{0,i-1})\lambda \tag{8.7}$$

   where M_i is the holdup on stage i and $M_{0,i}$ is the nominal holdup. Thus, it takes some time for changes in the liquid flow to propagate through the column, e.g. see Skogestad (1997). The liquid holdup has no steady-state effect, and is only important for the dynamic simulations.

Data for the simulations are shown in Table 8.1 (x^* denotes the nominal value):

Table 8.1: *Data for the Petlyuk simulation case*

Column		
Physical data	Relative volatilities	$\alpha^T = \begin{bmatrix} 9 & 3 & 1 \end{bmatrix}$
	Liquid time constant	$\tau_L = 3.78$
	Holdup distillate drum and bottom	$M_B = M_D = 20M_i$
	Holdup stages	$M_i = 1$
	Number of stages for the 6 sections	$N_T = 8$
	Boiling point A, B and C	$\mathbf{T}_B^T = \begin{bmatrix} 299.3 & 342.15 & 399.3 \end{bmatrix}$
	Antoine's parameters	$[A_r\ B_r\ C_r] =$
		$\begin{bmatrix} 2.8594 & -1142.8 & -0.34965 \end{bmatrix}$
Feed	Flow	$F^* = 1$
	Composition	$\mathbf{z}^{*T} = [1/3\ 1/3\ 1/3]$
	Liquid fraction	$q_l^* = 0.477$
Product compositions	Distillate	$x_{A,D}^{0^*} = 0.97$
	Side-stream	$x_{B,S}^{0^*} = 0.97$
	Bottom	$x_{C,B}^{0^*} = 0.97$
Disturbances	Feed flow	$F = F^* \pm 0.1$
	Feed composition	$z_A = z_A^* \pm 0.1$
		$z_B = z_B^* \pm 0.1$
	Liquid fraction	$q_l = q_l^* \pm 0.1$
	Product specification	$x_{A,D}^0 = x_{A,D}^{0^*} \pm 0.01$
		$x_{C,B}^0 = x_{C,B}^{0^*} \pm 0.01$
		$x_{B,S}^0 = x_{B,S}^{0^*} \pm 0.01$
Measurement error		
	Temperatures	0.5 K (absolute)
	Flows	2.5% (relative)
	Flow splits	0.025 absolute

8.3.2 Nominal optimum

The nominal optimal flows that minimize the energy (V) are

$$\mathbf{u}^{opt}(\mathbf{d}^*)^T = [L^*\ V^*\ S^*\ R_L^*\ R_V^*] = \begin{bmatrix} 0.7618 & 0.5811 & 0.3227 & 0.3792 & 0.5123 \end{bmatrix} \tag{8.8}$$

The minimum boilup (V_{min}) using infinite number of stages is $V_{min}^{\infty} = 0.5438$ so the design gives a nominal optimal boilup that is approximately 6% higher than the theoretical minimum. The nominal concentration profile is shown in Figure 8.2. Note that no component C is present in the distillate and no component A is present in the bottom stream B. Interestingly, there is also no component A in the side-stream S. Thus, the side-stream consists of components B and C only. The corresponding

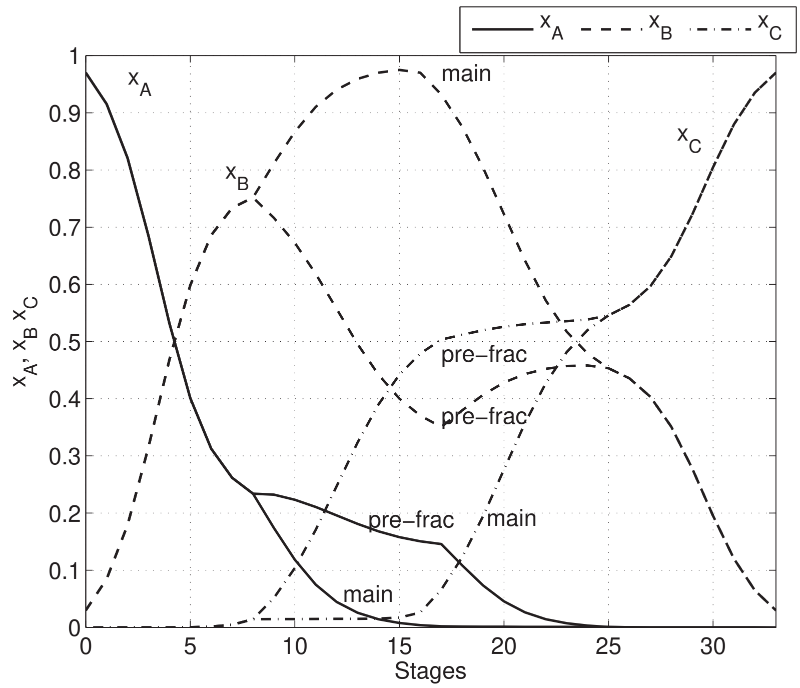

Figure 8.2: *Nominal composition profile, component A solid (−), component B dashed (−−) and component C dash-doted (−·).*

temperature profile is shown in Figure 8.3.

8.4 Selection of self-optimizing control structures

Below, we compare two different methods for selecting good self-optimizing controlled variables, namely the singular value method (Skogestad and Postlethwaite, 1996; Halvorsen et al., 2003) and the null space method of Chapter 3. Both methods assume that the active constraint loops (here, the product compositions) are closed and we analyze the reduced space problem. The best candidates found using these methods, are compared with the DT_S-candidate proposed by Halvorsen et al. (2000) and we also include the

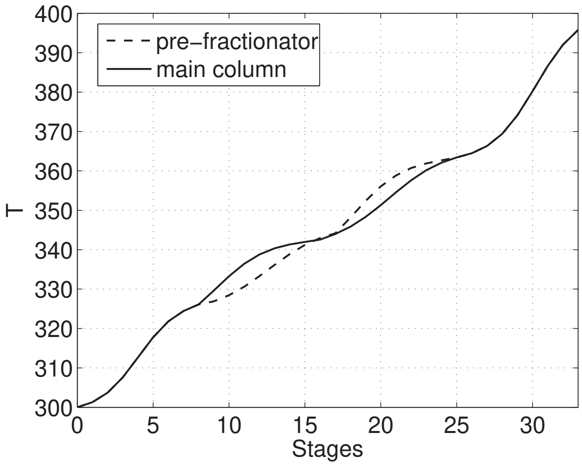

Figure 8.3: *Nominal temperature profile, sections* $(1-2)$ *dashed,* $(4-5)$ *solid line.*

structure proposed by Serra et al. (2003) where R_V and R_L are fixed. Thus, the goal of the following analysis is two-folded:

1. Compare the null space method and the singular value method for selecting controlled variables that are self-optimizing.
2. Find good candidate variables for self-optimizing control and compare the best candidate with previous proposed structures (DT_S).

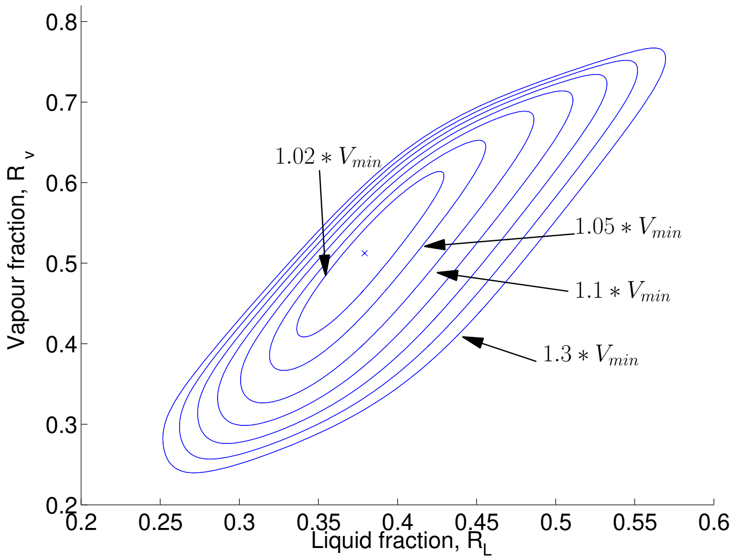

Figure 8.4: *Contour plot at the nominal disturbance* $V(R_L, R_V)$

Halvorsen et al. (2000) found that the vapor split (R_V) can be fixed and good self-optimizing control can be achieved by selecting the last controlled variable correctly.

The argument for keeping R_V constant is the observation that the solution surface when the active constraint loops are closed has shape as a "valley", see Figure 8.4. As seen from the figure this also holds for the nominal data used in this example (the solution surface is sensitive to the liquid fraction in the feed). If we are able to operate in the "valley", then fixing R_V may give acceptable economic performance. This argument holds, if the solution surface is similar for all disturbances.

8.4.1 Candidate control structures using the null space method

Using the null space method we propose to control combination of measurements, and base the selection on the optimal sensitivity matrix from the disturbances to the measurements. Two candidate structures are proposed based on the null space method of Chapter 3, denoted CS 1 and CS 2. Below we also include the DT_S (denoted CS 3) and the structure where we fix both remaining degrees of freedom (denoted CS 4).

1. CS 1 (*Control structure 1, controlling* $c_{tdf,1}$ *and* $c_{tdf,2}$):
   Here, both remaining degrees of freedom are used for self-optimizing control. The disturbance vector is

$$\mathbf{d}_{0,tdf}^T = \begin{bmatrix} F & z_A & z_B & q_l & n_{x_{A,D}} & n_{x_{B,S}} & n_{x_{C,B}} \end{bmatrix} \tag{8.9}$$

   resulting in a total of $n_{y_{0,tdf}} = n_u + n_{d_{0,tdf}} = 2 + 7 = 9$ measurements, where the sub-script "*tdf*" denotes "two degrees of freedom". To reduce the dimensionality of the problem by removing unimportant disturbances we apply Rule 2 of Section 5.3.1 and the resulting disturbance vector to include in the synthesizing of the controlled variables is:

$$\mathbf{d}_{tdf}^T = \begin{bmatrix} z_A & z_B & q_l & n_{x_{B,S}} \end{bmatrix} \tag{8.10}$$

   Note that the implementation error in controlling the product compositions in the distillate (D) and the bottom stream B is not important . The total number of measurements needed in the null space method is then

$$n_{y_{tdf}} = n_u + n_{d_{tdf}} = 2 + 4 = 6 \tag{8.11}$$

   The sequential method of Section 4.4 is used to select the best sub-set of measurements and gives:

$$\mathbf{y}_{tdf}^T = \begin{bmatrix} T_{37} & T_{11} & T_{43} & T_{25} & T_4 & T_9 \end{bmatrix} \tag{8.12}$$

   The physical location of the selected measurements is shown in Figure 8.5(a). The null space method gives the following measurement combinations

$$c_{tdf,1} = -0.472T_{37} + 0.312T_{11} + 0.113T_{43} - 0.457T_{25} + 0.561T_4 - 0.378T_9 \tag{8.13}$$
$$c_{tdf,2} = 0.185T_{37} + 0.376T_{11} - 0.667T_{43} - 0.524T_{25} - 0.154T_4 + 0.285T_9 \tag{8.14}$$

2. CS 2 (*Controlling* c_{odf} *and fixing* R_V):
   In practice it may be difficult to implement a vapor split, so if the resulting loss

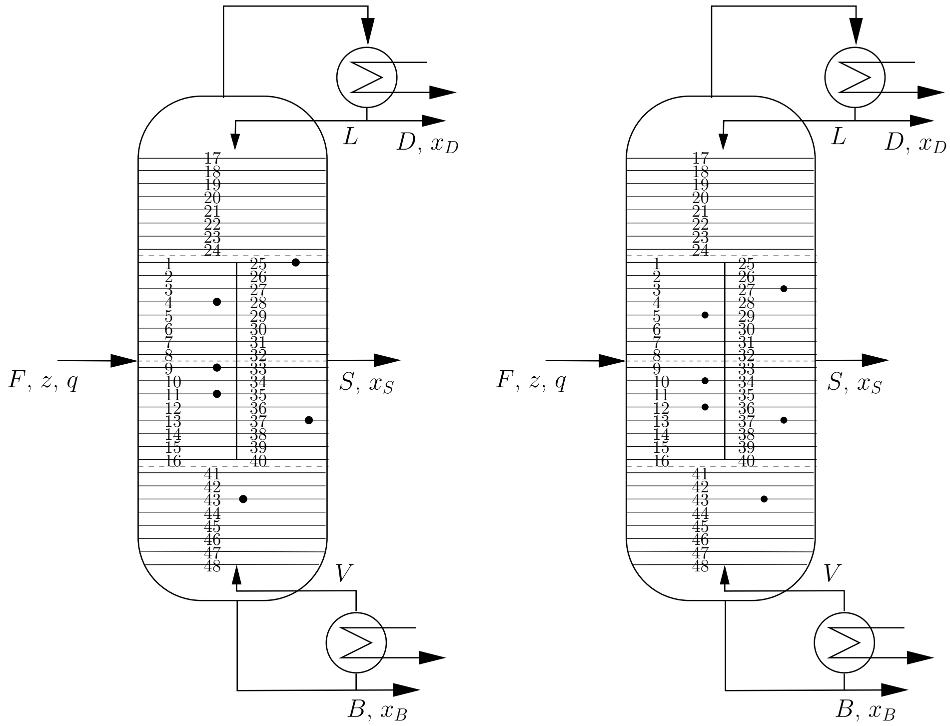

(a) Best subset of measurements when using both degrees of freedom for control.

(b) Best set of measurements when fixing R_V and using R_L for control.

Figure 8.5: *Physical location of the best subset of measurements*

using a fixed R_V is acceptable, this is the preferred structure. In fixing R_V, we add the implementation error of controlling R_V to the disturbance vector and we get

$$\mathbf{d}_{0,odf}^T = \begin{bmatrix} F & z_A & z_B & q_l & n_{x_{A,D}} & n_{x_{B,S}} & n_{x_{C,B}} & n_{R_V} \end{bmatrix} \tag{8.15}$$

and we use sub-script "*odf*" to denote the use of "one degree of freedom". Following the null space method of Chapter 3, the number of measurements required is $n_{y_{0,odf}} = n_u + n_{d_{0,odf}} = 1 + 8 = 9$ measurements. As above, the important disturbances are found from the method of Section 5.3.1 and correspond to

$$\mathbf{d}_{odf}^T = \begin{bmatrix} z_A & z_B & q_l & n_{x_{B,S}} & n_{R_V} \end{bmatrix} \tag{8.16}$$

Note, that in addition to the above selected disturbances, we must include the implementation error in controlling R_V as an important disturbance in synthesizing the controlled variable using the null space method. The corresponding minimum number of measurements needed is:

$$n_{y,odf} = n_u + n_{d_{odf}} = 1 + 5 = 6 \tag{8.17}$$

and using the sequential method of Section 4.4 to select the best subset of measurements (selected sequentially), the following subset of measurements is found:

$$\mathbf{y}_{odf}^T = \begin{bmatrix} T_{37} & T_{10} & T_{43} & T_{27} & T_5 & T_{12} \end{bmatrix} \tag{8.18}$$

and the corresponding physical location are illustrated in Figure 8.5(b). Note, the location of the measurements is similar to the ones found for CS 1. Note that the majority of measurements are located in the bottom part of the column, and only two measurements are located above the feed point. The optimal measurement combination is

$$c_{odf} = -0.388T_{37} - 0.658T_{10} + 0.192T_{43} - 0.0471T_{27} + 0.448T_5 + 0.421T_{12} \tag{8.19}$$

3. *CS 3 (controlling DT_S and fixing R_V)*:
   We select to use the middle temperature in each of the sections and select

$$c_{DT_S} = (T_4 - T_{28}) + (T_{12} - T_{36}) \tag{8.20}$$

   CS 3 is included since it has been proposed as a good self-optimizing variable in the literature (Halvorsen et al., 2000).
4. CS 4 (*Fixing both R_V and R_L*):
   In addition, we include the candidate where we fix the last degree of freedom (R_L) as this control structure is proposed in the literature (Serra et al., 2001, 2003).

8.4.2 The singular value method

The singular value method of Skogestad and Postlethwaite (1996) is used as an alternative method for finding good candidates for control. For this method, the user must define the candidate variables and the singular value method is used to rank the most promising candidates. In using the singular value method we select to fix R_V and seek in all candidate measurements as given by eq. (8.2) for a good self-optimizing controlled variable. The singular value method is based on ranking variables with a large scaled steady-state gain (minimum singular value in the multiple input case). The gain is found by linearizing with the active constraints closed (including R_V). Each candidate controlled variable is scaled with the sum of the optimal range and the measurement error. Table 8.2 gives the scaled steady-state gain for all candidates considered.

As seen, the most promising candidates are temperatures from section 5 and 1. The variable R_L is ranked number 16 and has better (predicted) self-optimizing properties than many of the temperature measurements. Temperatures from section 6 (the lower section) have the smallest gain indicating poor self-optimizing properties. The same is true for temperature measurements in the top of the column and for the inputs L, V and S. Note that all active constraints have zero gain. The eight most promising candidates are selected for further analysis and Table 8.3 summarizes the candidate control structures selected for further analysis.

Table 8.2: *Most promising candidates sorted by scaled steady-state gain ($|G(0)|$)*

Rank	c	$\lvert G(0)\rvert$	Rank	c	$\lvert G(0)\rvert$
1	T_{35}	89.408	29	T_{24}	2.5723
2	T_{36}	79.260	30	T_9	2.3445
3	T_{34}	73.433	31	T_{16}	2.2577
4	T_{37}	48.482	32	T_{32}	1.1068
5	T_{33}	47.022	33	T_{23}	0.86450
6	T_{38}	29.189	34	T_{29}	0.67638
7	T_4	22.455	35	T_{22}	0.30016
8	T_3	21.540	36	T_{41}	0.26000
9	T_5	19.753	37	T_{25}	0.21658
10	T_2	16.694	38	T_{21}	0.11830
11	T_{39}	16.116	39	T_{42}	0.096164
12	T_6	15.159	40	T_{20}	0.057791
13	T_{31}	11.199	41	T_{43}	0.041086
14	T_7	10.219	42	L	0.025043
15	T_1	9.7529	43	T_{19}	0.023880
16	R_L	8.0979	44	T_{44}	0.022758
17	T_{30}	6.8319	45	T_{45}	0.016549
18	T_{40}	6.6713	46	T_{46}	0.013955
19	T_{12}	6.5947	47	T_{47}	0.0078295
20	T_{13}	5.9587	48	T_{18}	0.0072547
21	T_8	5.8239	49	V	0.0053109
22	T_{11}	5.8082	50	T_{48}	0.0030346
23	T_{14}	4.6642	51	T_{17}	0.00068834
24	T_{10}	4.2749	52	S	1.0637×10^{-5}
25	T_{27}	3.9173	53	R_V	0
26	T_{15}	3.4791	54	$x_{B,S}$	0
27	T_{28}	3.0981	55	$x_{A,D}$	0
28	T_{26}	2.6186	56	$x_{C,B}$	0

Table 8.3: *Most promising control structures*

CS #	c_1	c_2	c_3	c_4	c_5	
1	$x_{A,D}$	$x_{B,S}$	$x_{C,B}$	c^1_{tdf}	c^2_{tdf}	Null space method, use R_V and R_L
2	$x_{A,D}$	$x_{B,S}$	$x_{C,B}$	R_V	c_{odf}	Null space method, fix R_V
3	$x_{A,D}$	$x_{B,S}$	$x_{C,B}$	R_V	DT_S	Fix DT_S and R_V
4	$x_{A,D}$	$x_{B,S}$	$x_{C,B}$	R_V	R_L	Constant splits R_V and R_L
5	$x_{A,D}$	$x_{B,S}$	$x_{C,B}$	R_V	T_{35}	Single temperature, fix R_V
6	$x_{A,D}$	$x_{B,S}$	$x_{C,B}$	R_V	T_{36}	Single temperature, fix R_V
7	$x_{A,D}$	$x_{B,S}$	$x_{C,B}$	R_V	T_{34}	Single temperature, fix R_V
8	$x_{A,D}$	$x_{B,S}$	$x_{C,B}$	R_V	T_{37}	Single temperature, fix R_V
9	$x_{A,D}$	$x_{B,S}$	$x_{C,B}$	R_V	T_{33}	Single temperature, fix R_V
10	$x_{A,D}$	$x_{B,S}$	$x_{C,B}$	R_V	T_{38}	Single temperature, fix R_V
11	$x_{A,D}$	$x_{B,S}$	$x_{C,B}$	R_V	T_4	Single temperature, fix R_V
12	$x_{A,D}$	$x_{B,S}$	$x_{C,B}$	R_V	T_3	Single temperature, fix R_V

8.5 Loss evaluation using the non-linear model

Using constant nominal setpoints for the controlled variables, the loss for all candidates is shown in Table 8.4. Note that we allow only one disturbance or implementation error at a time.

Table 8.4: *Percentage loss (L) for all disturbances using nominal setpoints . ("−" denotes negative perturbation, "+" denotes positive perturbation from the nominal value). The last two columns give maximum loss and average loss for the measurement errors. "inf" means infeasible operation.*

	Loss [%]							
CS #	F_-	F_+	z_{A-}	z_{A+}	z_{B-}	z_{B+}	q_{l-}	q_{l+}
1	0.0	0.0	0.0171	0.0207	0.0166	0.0111	0.0001	0.0000
2	0.0	0.0	0.0037	0.1340	0.2247	0.1666	0.1876	0.1084
3	0.0	0.0	5.0840	11.8810	0.3469	0.8295	1.0441	1.1740
4	0.0	0.0	46.7037	6.3019	95.1660	9.8256	32.4629	6.0578
5	0.0	0.0	0.22826	2.6973	0.30078	0.40385	0.18903	0.12882
6	0.0	0.0	0.43234	inf	0.56891	1.7347	0.20494	0.17341
7	0.0	0.0	0.12667	1.3807	0.22211	0.18703	0.18794	0.11290
8	0.0	0.0	0.82264	inf	1.1556	inf	0.25233	0.31315
9	0.0	0.0	0.11772	1.7075	0.31570	0.16848	0.21236	0.10722
10	0.0	0.0	1.6053	inf	2.3873	inf	0.38058	1.0685
11	0.0	0.0	9.3786	42.029	0.22507	0.28417	0.66607	1.0851
12	0.0	0.0	inf	33.300	0.52408	0.28762	0.77086	1.0070

	Loss [%]							
CS #	$n_{x^0_{A,D}+}$	$n_{x^0_{A,D}-}$	$n_{x^0_{C,B}+}$	$n_{x^0_{C,B}-}$	$n_{x^0_{B,S}+}$	$n_{x^0_{B,S}-}$	L_n^{max}	L_n^{avg}
1	0.0025	0.0095	0.0639	0.2082	0.0002	0.0007	0.0213	0.0117
2	0.0040	0.0110	0.0060	0.0174	0.0004	0.0004	0.0847	0.0206
3	0.0074	0.0207	0.0033	0.0034	0.0025	0.0075	0.2108	0.0475
4	0.0262	0.0253	0.0245	0.0311	0.2579	1.0198	9.3142	3.6254
5	0.0040	0.0110	0.0029	0.0035	0.3334	2.5693	0.0861	0.0673
6	0.0040	0.0110	0.0041	0.0063	0.3088	2.7112	0.0857	0.0587
7	0.0040	0.0112	0.0028	0.0026	0.4040	2.8982	0.1215	0.1034
8	0.0040	0.0110	0.0069	0.0126	0.3037	3.6569	0.0864	0.0586
9	0.0044	0.0128	0.0055	0.0042	0.7108	4.9155	0.7517	0.3805
10	0.0040	0.0110	0.0132	0.0289	0.3148	inf	0.0881	0.0667
11	0.0036	0.0108	0.0072	0.0106	0.3439	1.9349	0.1046	0.0589
12	0.0034	0.0131	0.0087	0.0130	0.3318	1.7321	0.1097	0.0963

8.5.1 Discussion loss evaluation

All candidate structures consist of intensive variables and since the column efficiency is assumed independent of load, they show perfect self-optimizing control for changes in the feed flow rate.

For a negative perturbation in the composition of component A in the feed, the loss for CS 4 (keeping R_L and R_V constant) and CS 11 is high (46% and 9% respectively).

Candidate CS 3 (DT_s) has a loss of approximately 5%, while candidate CS 12 yields infeasible operation. All other candidates have a loss below 1.6%, with candidates CS 1 and CS 2 having the smallest losses.

For a positive perturbation in the composition of component A, CS 3 (DT_S) has a higher loss than keeping the inputs constant (CS 4), while CS 6, CS 8 and CS 10 give infeasible operation. Again, candidates CS 1 and CS 2 have the smallest losses.

For a disturbance in the feed concentration of component B, CS 4 shows the highest loss. The same is true for changes in the feed liquid ratio (q_l). Thus, keeping both R_V and R_L constant leads to non-acceptable operation from a steady-state point of view. Note, that the best single measurement candidate (CS 7) has smaller losses than DT_S.

CS 7 has small losses for all perturbations, except for a measurement error in $x_{B,S}$ where the loss is approximately 3%.

Note that all candidates selected using the singular value method, are sensitive to noise in the composition of the side-stream, while the losses for CS 1-CS 3 are small.

For all perturbations, the candidates CS 1 and CS 2 show small losses. Keeping R_V constant (CS 2) gives a somewhat larger loss compared to CS 1, however the loss remains lower than 0.22%. Taking the additional complexity of using R_V as a degree of freedom (CS 1) into account, CS 2 is the best candidate structure with respect to the steady-state loss. The second best candidate is CS 7 using a single measurement on stage 34, which shows remarkably good self-optimizing properties.

The last two columns of Table 8.4 list the maximum and average loss for the measurement errors. The effect of measurement error on the loss shows that CS 4 (fix R_V and R_L) gives high loss, while the other candidates show negligible losses. This can be seen from Figure 8.4, where the contours are close (large losses) in the positive vertical direction (R_V) direction. Thus, failing to realize the importance of using the additional degrees of freedom for optimization, may give operation that has a higher energy cost than the corresponding direct or indirect split. One of the benefits in using the Petlyuk column is then lost.

8.5.2 Summary loss calculation

To summarize, the candidates with acceptable loss are CS $1, 2, 5, 7$ and CS 9. We select candidates CS 2, CS 3 (DT_S), CS 7 and CS 11 for further analysis. We include CS 11 since this is the best candidate using a single temperature and that utilize information from the pre-fractionator. Candidate CS 3 is also included, since it is a linear combination of the measurements. Fixing both R_L and R_V (CS 4) is eliminated due to high losses (up to 95%).

Figure 8.6 shows the losses with respect to disturbances in F, z_A and z_B for the four candidate structures selected for further analysis. As seen, the losses are not symmetrical around the nominal disturbance. Figure 8.6(a) confirms that the feed rate does not have any steady-state effect on the loss. Figure 8.7 plots the losses with respect to disturbances in the feed liquid fraction (q_l) and the control errors in the purities ($n_{x_{A,D}}$, $n_{x_{B,S}}$ and $n_{x_{C,B}}$). CS 11 and CS 7 are sensitive ($2-3\%$ loss) to a control error in $x^0_{B,S}$.

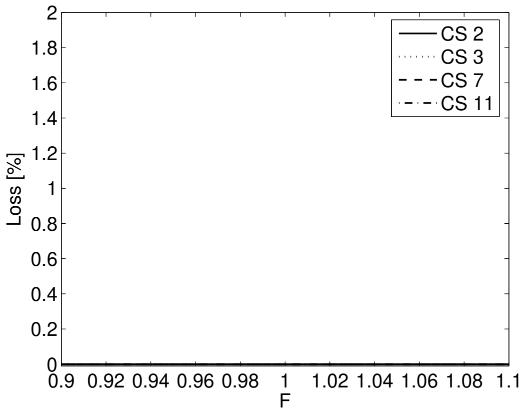

(a) Loss with respect to F for all candidate structures

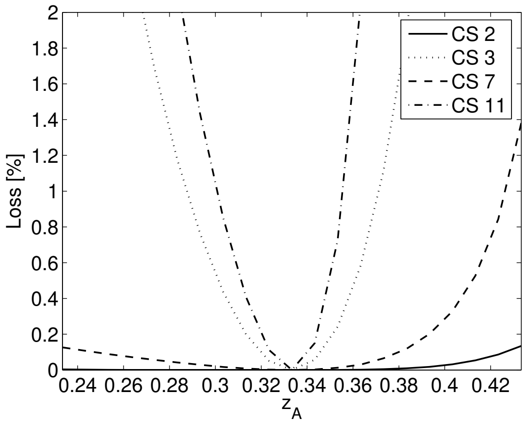

(b) Loss with respect to z_A for all candidate structures

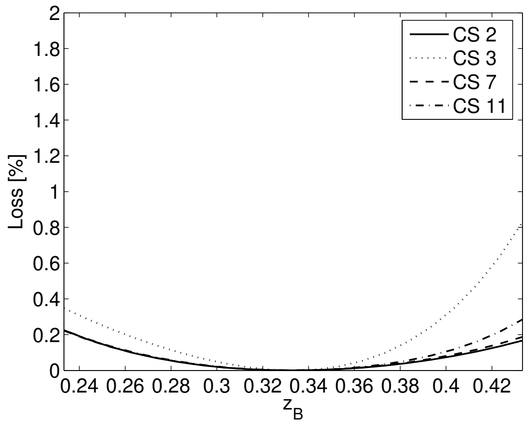

(c) Loss with respect to z_B for all candidate structures

Figure 8.6: *Loss with respect to disturbance F, z_A and z_B for all candidate structures*

8.6 Controllability analysis

Up until now, only the steady-state operation has been considered in discriminating between the candidate control structures. For the final validation, a controllability analysis was performed on the four above mentioned control structures, namely CS 2, CS 3, CS 7 and CS 11. The dynamic degrees of freedom are

$$\mathbf{u}_d^T = \begin{bmatrix} L & V & S & R_L & R_V & D & B \end{bmatrix} \tag{8.21}$$

In addition, the internal accumulator for the liquid split and the side-stream accumulator are assumed perfectly controlled. The reboiler and condenser levels (holdups) need

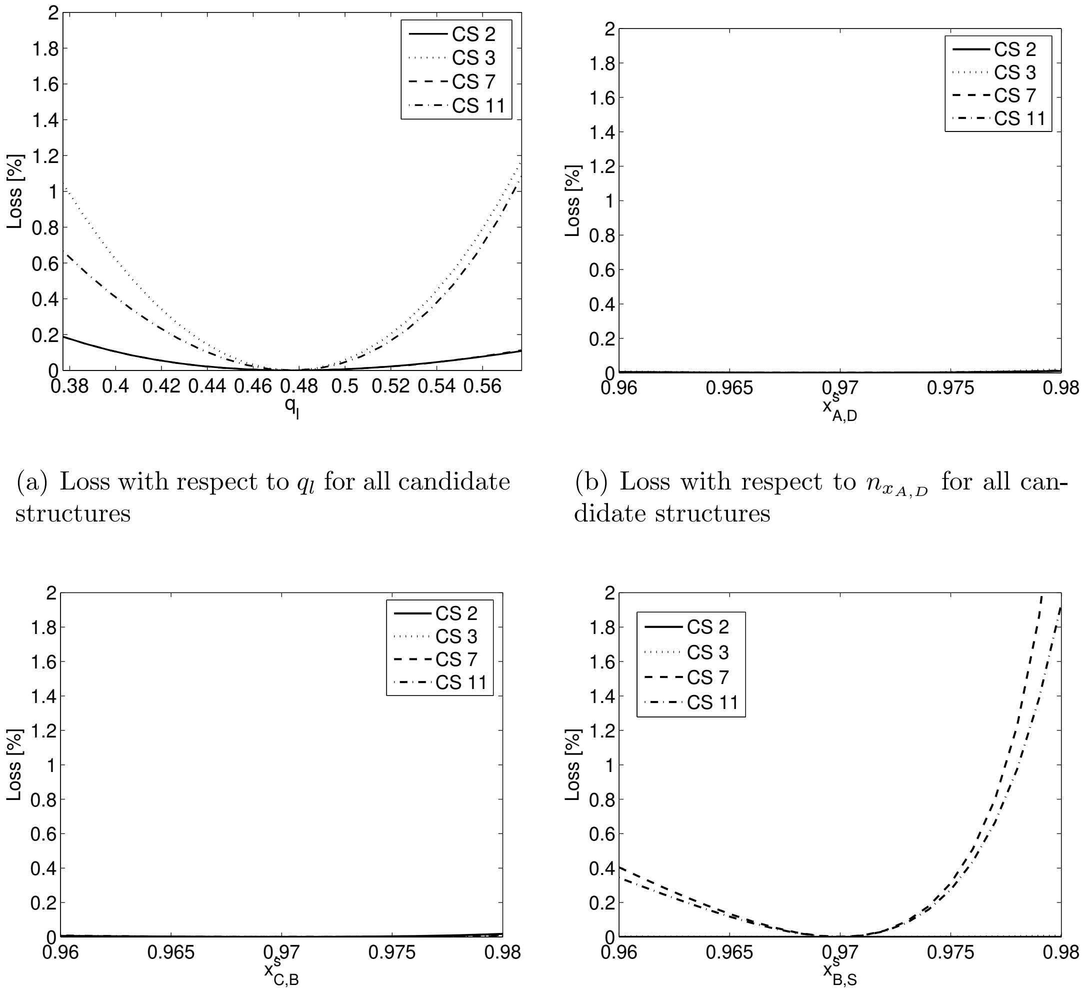

(a) Loss with respect to q_l for all candidate structures

(b) Loss with respect to $n_{x_{A,D}}$ for all candidate structures

(c) Loss with respect to $n_{x_{C,B}}$ for all candidate structures

(d) Loss with respect to $n_{x_{B,S}}$ for all candidate structures

Figure 8.7: *Loss with respect to disturbances q_l, $n_{x_{A,D}}$, $n_{x_{B,S}}$ and $n_{x_{C,B}}$ for all candidate structures*

to be stabilized, and we select B and D as manipulated variables, respectively, leaving five degrees of freedom. In addition, for all candidates we fix R_V at the nominal optimal value, leaving 4 inputs for control. We choose to use a decentralized control structure for all candidates and we pair the inputs and outputs based on the steady-state relative gain array (RGA) (Skogestad and Postlethwaite, 1996). Using the RGA we should:

1. Avoid pairing on negative RGA-elements
2. Preferably pair on RGA-elements close to one.

For candidates where more than one possible pairing exist, we select to make use of the RGA-number to discriminate between the candidate pairings. The RGA-number is defined as

$$\text{RGA-number}(\omega) = \|\Lambda(\omega) - \mathbf{I}\|_{sum} \tag{8.22}$$

and is a measure of the diagonal dominance (Skogestad and Postlethwaite, 1996). It is preferable to select structures that have a small RGA-number at the crossover frequency.

The linear model used in tuning the controllers and in calculating the RGA is found with the level loops closed. All systems are open-loop stable, but have right-half plane zeros which may limit the bandwidth of the resulting controller.

8.6.1 Pairing

CS 2

For candidate CS 2 we have the following inputs and outputs:

$$\mathbf{u}_{cl}^T = \begin{bmatrix} L & V & S & R_L \end{bmatrix} \quad \text{and} \quad \mathbf{c}_{CS\ 2}^T = \begin{bmatrix} x_{A,D} & x_{C,B} & x_{B,S} & c_{odf} \end{bmatrix}$$

and the steady-state RGA is:

$$\Lambda_{CS\ 2}(0) = \begin{bmatrix} 1.0697 & -0.0672 & -0.0015 & -0.0009 \\ -1.6937 & 2.0186 & 0.6748 & 0.0003 \\ 1.6228 & -0.9513 & 0.3268 & 0.0018 \\ 0.0012 & -0.0001 & -0.0000 & 0.9989 \end{bmatrix} \tag{8.23}$$

From pairing rule 1, the only possible choice is to pair on the diagonal elements. Alternatively, one could pair on elements close to zero for input V, and some alternative pairings are shown in Table 8.5. The first pairing is the one as given by the steady-state RGA, as discussed above. For the other candidate pairings, we must pair on elements close to zero. Using the RGA-number, we see from Figure 8.8. that at frequencies below $\omega = 10^0$, pairing 1, as proposed by the steady-state RGA, is preferred.

Table 8.5: *Alternative pairings for CS* 2

Pairing #	L	V	S	R_L
1	$x_{A,D}$	$x_{C,B}$	$x_{B,S}$	c_{odf}
2	$x_{A,D}$	c_{odf}	$x_{C,B}$	$x_{B,S}$
3	$x_{B,S}$	c_{odf}	$x_{C,B}$	$x_{A,D}$
4	c_{odf}	$x_{B,S}$	$x_{C,B}$	$x_{A,D}$

It turns out that the RGA for the other control structures are very similar. For example for CS 3 (DT_S) we have

$$\mathbf{c}_{CS\ 4}^T = \begin{bmatrix} x_{A,D} & x_{C,B} & x_{B,S} & c_{DT_S} \end{bmatrix}$$

and the steady state RGA matrix is:

$$\Lambda_{CS\ 4}(0) = \begin{bmatrix} 1.0691 & -0.0671 & -0.0015 & -0.0005 \\ -1.6939 & 2.0187 & 0.6748 & 0.0005 \\ 1.6226 & -0.9513 & 0.3268 & 0.0019 \\ 0.0022 & -0.0003 & -0.0000 & 0.9981 \end{bmatrix} \tag{8.24}$$

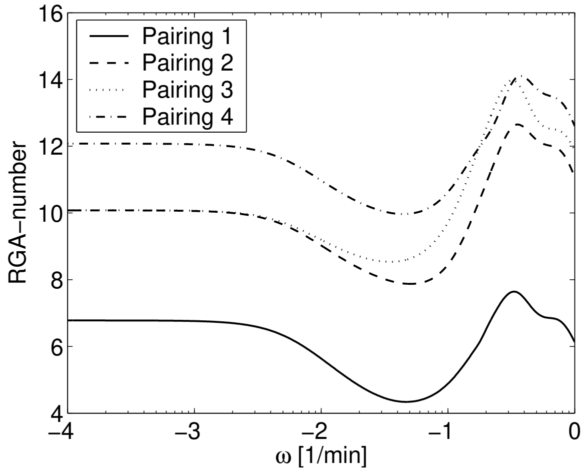

Figure 8.8: *Frequency dependent RGA-number, $\Lambda(\omega)$ for candidate CS 2*

which is almost identical to eq. (8.23). Thus, for the candidates CS 3, CS 7 and CS 11 we select to pair in the same manner with R_L used for temperature control.

8.6.2 PI-controller parameters

Here, we use PI-controllers tuned with Skogestad's IMC tuning rules (Skogestad, 2003). A schematic diagram of the the control structures are shown in Figure 8.9. Each composition measurement is assumed to have a measurement delay of $\theta_x = 5\ min$ and each temperature measurement a delay of $\theta_T = 1\ min$. The PI-controller parameters are shown in Table 8.6. The interaction between the control loops makes it necessary to

Table 8.6: *PI-controller parameters for all control structures using Skogestad's IMC tuning rules. τ_C is the specified first-order closed loop response time.*

CS 2	u_i	c_i	K_c	τ_I	τ_C	CS 7	u_i	c_i	K_c	τ_I	τ_C
	L	$x_{A,D}$	2.6568	80	15		L	$x_{A,D}$	2.6568	80	15
	V	$x_{C,B}$	2.1916	110	22.5		V	$x_{C,B}$	2.1916	110	22.5
	S	$x_{B,S}$	−2.8197	81.7	25.5		S	$x_{B,S}$	−2.8197	81.7	22.5
	R_L	c_{odf}	−0.0175	21	10		R_L	T_{34}	0.0327	44	10
CS 3	u_i	c_i	K_c	τ_I	τ_C	CS 11	u_i	c_i	K_c	τ_I	τ_C
	L	$x_{A,D}$	2.6568	80	15		L	$x_{A,D}$	2.6568	80	15
	V	$x_{C,B}$	2.1916	110	22.5		V	$x_{C,B}$	2.4599	98	22.5
	S	$x_{B,S}$	−2.8197	81.7	22.5		S	$x_{B,S}$	−2.8197	81.7	22.5
	R_L	c_{DTS}	−0.061	33.5	10		R_L	T_4	−0.0337	33.3	20

have a rather large desired closed loop time constant (τ_C). For CS 7, the proposed structure and PI-parameters gave oscillatory response, with resulting unstable operation for a disturbance in feed composition z_A. Re-tuning of the controllers was not successful. Since this structure does not use measurements from the pre-fractionator

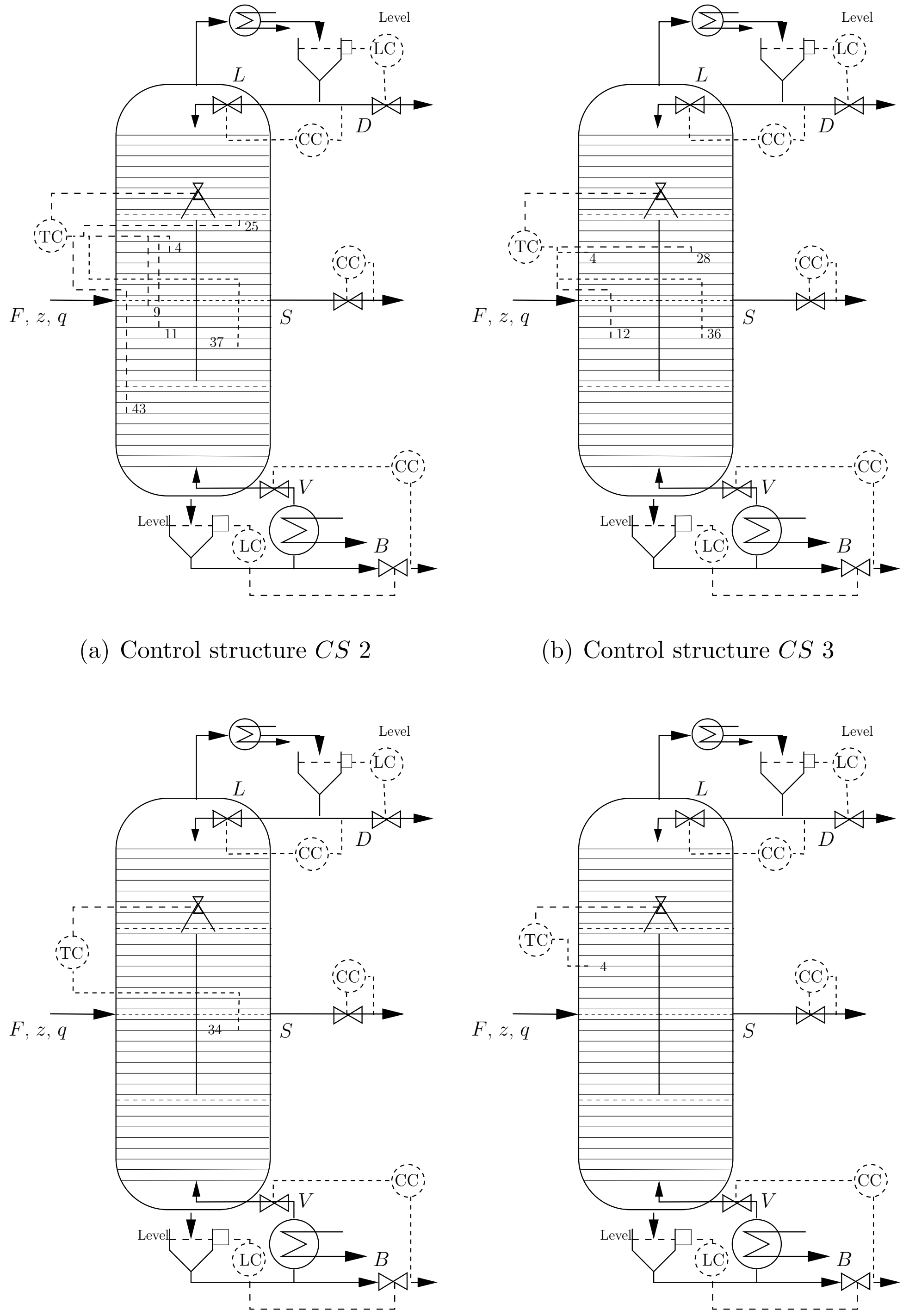

(a) Control structure *CS* 2

(b) Control structure *CS* 3

(c) Control structure *CS* 7

(d) Control structure *CS* 11

Figure 8.9: *Control structures CS 2, CS 3, CS 7 and CS 11*

(sections 1 and 2), the pre-fractionator may drift and component C can go over the top without being measured. Thus, in order to get stable operation using T_{34} as a self-optimizing controlled variable, the pre-fractionator must be stabilized. In order to avoid that component C breaks through in the top of the pre-fractionator, we select to control temperature T_4 (which is the self-optimizing controlled variable in CS 11) and use the setpoint of this loop as the new input for the self-optimizing control loop.

For candidates CS 2 and CS 3 this stabilization is implicit, since information on the state of the pre-fractionator is included in the self-optimizing controlled variable (c_{odf} and DT_S respectively). Thus, the self-optimizing controlled variable for these two loops serves two purposes:

1. Stabilize the pre-fractionator to avoid component C distributing over the top of the pre-fractionator.

2. Self-optimizing control to keep the system near the true optimal point when disturbances enter.

In practical implementations, this dual control objective may not be acceptable. Typically, the pre-fractionator is stabilized, say, controlling a temperature in section 1, and thereafter, the setpoint for this loop would be used as an input for the self-optimizing control loop. In this simulation study, we neglect this for structures CS 2 and CS 3, while for candidate CS 7, we use the cascade structure of Figure 8.10. The tuning of the cascade controller was based on the tunings for the candidate CS 11 and the cascade loop was tuned based on a linear model where the four inner loops were closed. The PI-controller parameters for the cascade controller are:

$$K_C = -1.4420 \quad \tau_I = 50 \quad \tau_C = 40 \tag{8.25}$$

8.6.3 Non-linear closed-loop simulations

The main goal with the dynamic simulations, see Figures 8.11-8.13, is to compare the closed-loop performance for the disturbances z_A and control error in $x_{B,S}$, which were found to be the worst disturbances. The disturbances z_A and $x_{B,S}$ are ramped up or down over a time period of 200 min, starting at t = 100 min, respectively. The dynamic response for the disturbances F, z_B, q_l, $x^s_{A,D}$ and $x^s_{C,B}$ are similar for all control structures, and is not shown.

Disturbance z_A

The input and output responses for a negative change in the feed composition of component A ($\Delta z_A = -0.1$) are shown in Figure 8.11. Note that:

- CS 2 tracks the steady-state optimal values for both a negative and a positive perturbation of z_A. The composition loops show smooth responses.
- CS 3 yields a steady-state loss for both a negative and a positive disturbance in z_A. For a positive disturbance, the responses are oscillatory with a large control error in the bottom purity in Figure 8.12.

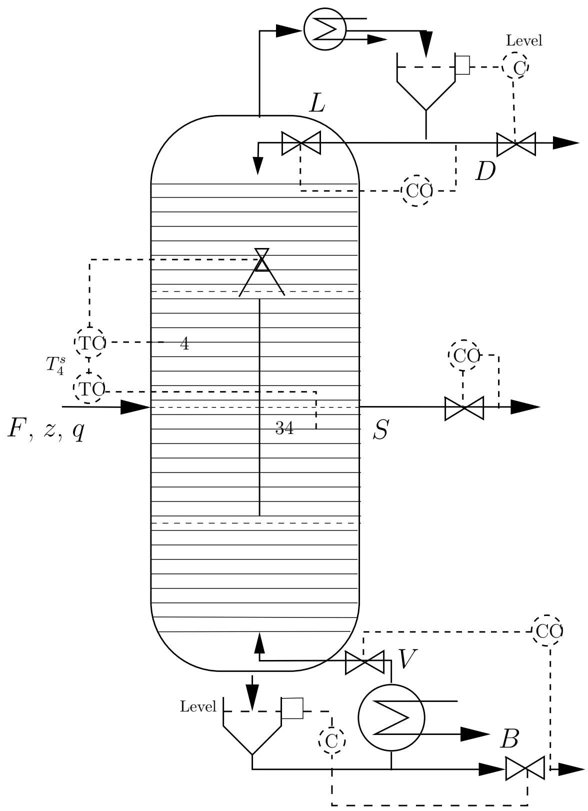

Figure 8.10: *Cascade structure for CS 7.*

- CS 7 is very similar to CS 2 with respect to a disturbance in z_A. For a positive disturbance, see Figure 8.12, the boilup is higher than for CS 2 (in accordance with the steady-state results of Table 8.4.
- CS 11 shows the worst performance with the highest boilup. A positive disturbance in z_A results in a large control error in $x_{C,B}$ (0.92) before it returns to the setpoint.

For all candidates, the side-stream purity is least affected by a disturbance in z_A, while both the bottom and top composition show large deviations for CS 7 and CS 11 (the single temperature candidates).

Measurement error $x_{B,S}$

Figure 8.13 shows the responses for a negative control error in $x_{B,S}$.

- CS 2 tracks the steady-state optimal value. The composition loops show smooth responses.
- CS 3 is similar to CS 2.
- CS 7 gives the highest boilup. The purity responses are slower as compared to CS 2 and CS 3.
- CS 11 gives a higher boilup than CS 2 and CS 3. The purity responses are similar to CS 7.

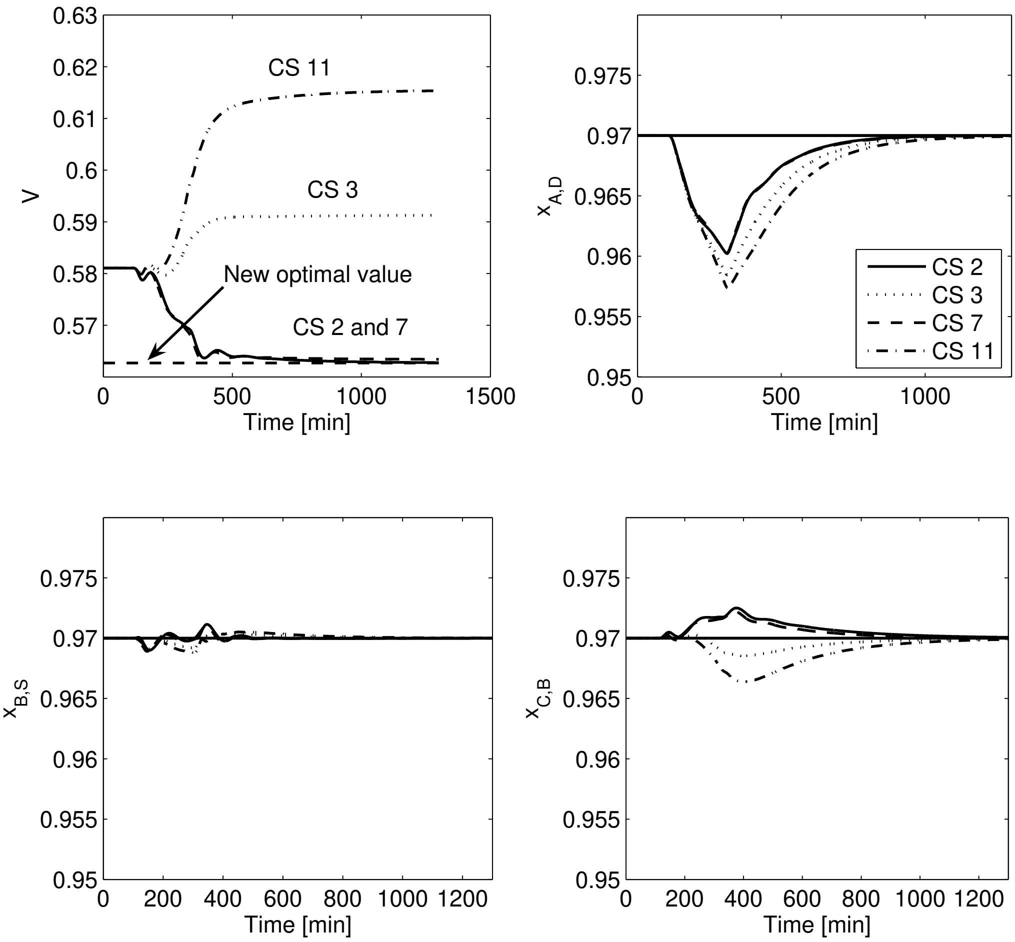

Figure 8.11: *Plot of boilup (V) and purities ($x_{A,D}$, $x_{B,S}$ and $x_{C,B}$) for a change* $z_A : 0.33 \rightarrow 0.23$

Conclusions dynamic simulations

From the dynamic simulations it is clear that CS 2 and CS 7 show the best dynamic performance, while CS 11 and CS 3 yield oscillatory and poor performance for a positive disturbance in z_A. Taking into account the higher boilup for CS 7 for with a control error in the side-stream purity, CS 2 shows the best combined steady-state and dynamic performance.

8.7 Conclusions

In this chapter, different self-optimizing control structures for a Petlyuk distillation column have been compared for both dynamic and steady-state performance. New

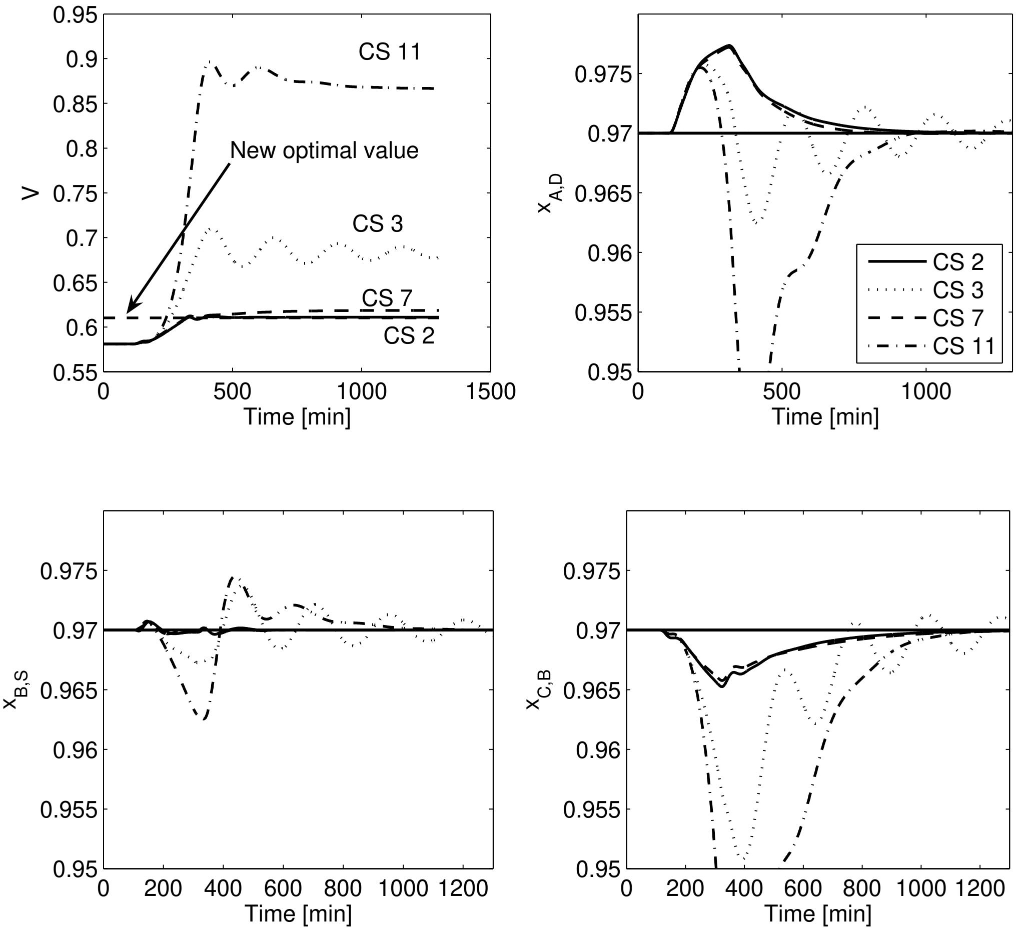

Figure 8.12: *Plot of boilup (V) and purities ($x_{A,D}$, $x_{B,S}$ and $x_{C,B}$) for a change $z_A : 0.33 \rightarrow 0.43$*

control structures have been proposed which have improved steady-state and dynamic properties as compared to previously proposed structures in the literature. Failing to utilize the degrees of freedom in the Petlyuk column may yield non-optimal operation for disturbances entering the column. In order to achieve near optimal operation, it is acceptable to fix the vapor split R_V, while we need to manipulate the liquid split R_L to remain optimal. A new structure based on the null space method has been compared to candidate variables found with the singular value method. Both methods provide candidate variables with good self-optimizing properties. Based on both steady-state and dynamic performance, the best self-optimizing control structure is CS 2 which is a combination of six temperature measurements.

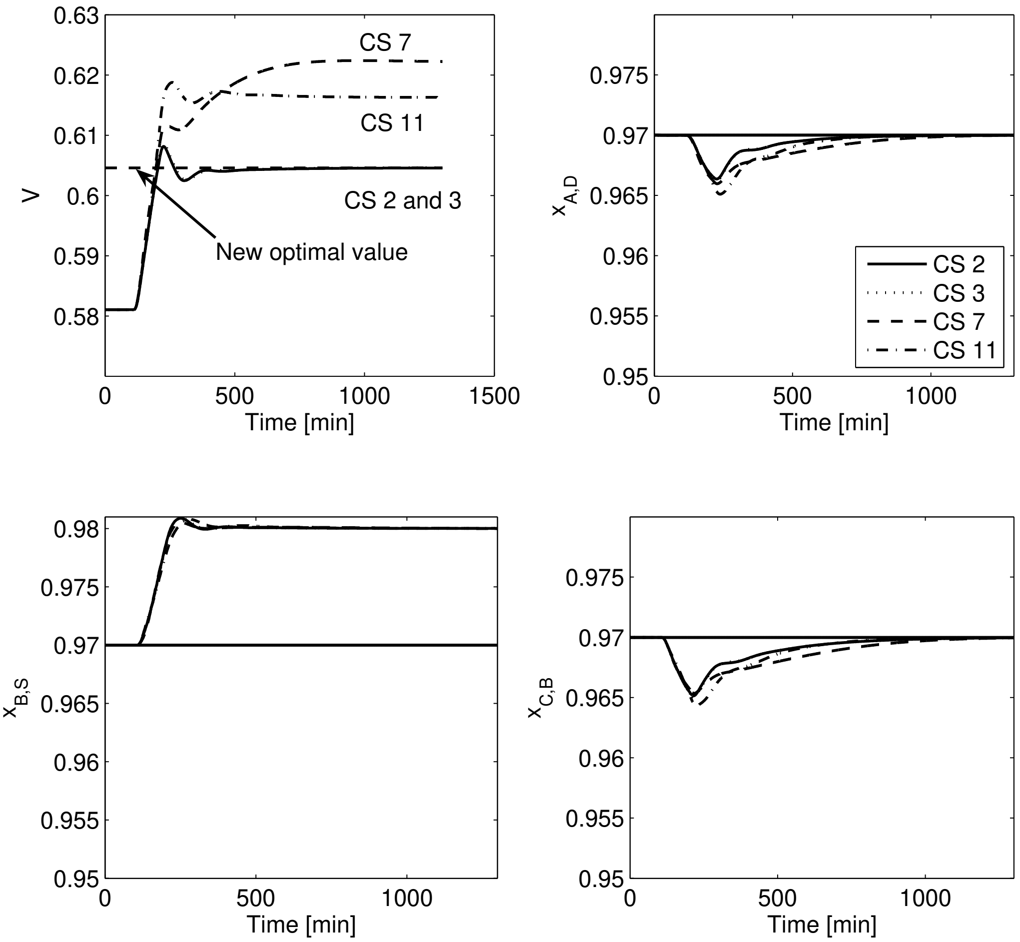

Figure 8.13: *Plot of boilup (V) and purities ($x_{A,D}$, $x_{B,S}$ and $x_{C,B}$) for a control error in purity of side-stream, $n_{x_{B,S}} = -0.01$)*

Bibliography

Aaboen, G. (2003). MPC and self-optimizing control with application to the Petlyuk distillation column. Master's thesis, Norwegian University of Science and Technology. In Norwegian.

Adrian, T., Schoenmakers, H., and Boll, M. (2002). Model predictive control of integrated unit operations control of a divided wall column. *Distillation & Absorption 2002, Baden-Baden, October 2002*.

Adrian, T., Schoenmakers, H., and Boll, M. (2004). Model predictive control of integrated unit operations: Control of a divided wall column. *Chem. Eng. Process*, 43:347–355.

Carlberg, N. and Westerberg, A. (1989a). Temperature-heat diagrams for complex columns. 2: Underwood's method for the side-strippers and enrichers. *Ind. Eng. Chem. Res*, 28:1379–1386.

Carlberg, N. and Westerberg, A. (1989b). Temperature-heat diagrams for complex columns. 3: Underwood's method for the Petlyuk configuration. *Ind. Eng. Chem. Res*, 28:1374–1379.

Christiansen, A. C. (1997). *Studies on optimal design and operation of integrated distillation arrangements*. PhD thesis, Norwegian University of Science and Technology.

Fidkowski, Z. and Krolikowski, L. (1986). Thermally coupled system of distillation columns: Optimization procedure. *AIChE Journal*, 32(4):537–546.

Halvorsen, I., Serra, M., and Skogestad, S. (2000). Evaluation of self-optimizing control structures for an integrated petlyuk distillation column. *Hung. J. of Ind.Chem.*, 28:11–15.

Halvorsen, I. and Skogestad, S. (1999). Optimal operation of petlyuk distillation: Steady-state behavior. *J. Proc. Control*, pages 407–424.

Halvorsen, I. and Skogestad, S. (2000). Theory of distillation. *Int. Encylopedia of Separation Science*, II.

Halvorsen, I. and Skogestad, S. (2003). Minimum energy consumption in multicomponent distillation. Part 2. Three-product Petlyuk arrangements. *Ind. Eng. Chem. Res.*, 3(42):605–615.

Halvorsen, I., Skogestad, S., Morud, J., and Alstad, V. (2003). Optimal selection of controlled variables. *Ind. Eng. Chem. Res.*, 42(14):3273–3284.

Serra, M., na, A. E., and Puigjaner, L. (2003). Controllability of different distillation arrangements. *Ind. Eng. Chem. Res.*, 42:1773–1782.

Serra, M., Perrier, M., na, A. E., and Puigjaner, L. (2001). Analysis of different control possibilities for the Divided wall column: Feedback diagonal and dynamic matrix control. *Comput. Chem. Eng.*, 25:859–866.

Skogestad, S. (1997). Dynamics and control of distillation columns - A tutorial introduction. *Trans IChemE, Part A*, 75:539–562.

Skogestad, S. (2003). Simple analytic rules for model reduction and PID controller tuning. *J. Proc. Control*, 13:291–309.

Skogestad, S. and Postlethwaite, I. (1996). *Multivariable Feedback Control*. John Wiley & Sons.

Smith, R. and Triantafyllou, C. (1992). The design and operation of fully thermally coupled distillaton columns. *Trans. IChemE.*, pages 118–132.

Wolff, E. and Skogestad, S. (1996). Operation of integrated three-product (Petlyuk) distillation columns. *Ind. Eng. Chem. Res*, 34:2094–2103.

Wolff, E., Skogestad, S., and Havre, K. (1994). Dynamics and control of integrated three product (Petlyuk) distillation columns. *ESCAPE'4 Dublin.* Published in IChemE Symp. Ser. No. 107, 111-118.

Chapter 9

Optimal operation of a Petlyuk distillation column: Energy savings by over-fractionation

Based on work presented at
the 14th European Symposium on Computer-Aided Process Engineering (ESCAPE 14), 16-19 May 2004, Lisbon, Portugal

This paper shows the unexpected result that over-fractionating one of the product streams in a Petlyuk distillation column may be optimal from an energy point of view. Based on the Underwood equations, we derive analytic expressions for the potential energy savings. The potential energy savings by over-fractionation may be further increased by bypassing some of the feed and mixing it with the over-fractionated product to meet product specifications. For normal operating conditions the energy savings are small, so the main significance of our results is to point out that over-fractionation is energetically optimal in some cases.

9.1 Introduction

The Petlyuk distillation column, see Figure 9.1, with a pre-fractionator (C_1) and a main column (consisting of sections C_{21} and C_{22}), is an interesting alternative to the conventional cascade of binary columns for separation of ternary mixtures. The potential savings are reported to be of approximately 30% in both energy and capital cost (Smith and Triantafyllou, 1992). The savings in energy are possible since the pre-fractionator and the main column are thermally coupled. The saving in capital cost as compared with two columns in series is possible since the column can be implemented in a single colum shell with one reboiler and one condenser.

The feed (F) consists of components A, B and C and enters the pre-fractionator with composition $\mathbf{z}^T = \begin{bmatrix} z_A & z_B & z_C \end{bmatrix}$, liquid fraction q_l and relative volatility $\alpha^T = \begin{bmatrix} \alpha_A & \alpha_B & \alpha_C \end{bmatrix}$ where component A is the light and C the heavy component. The column has three product streams, the bottom stream (B), the side stream (S) and the distillate (D). $x_{i,j}$ is the mole fraction of component i in stream j. The internal vapor and reflux flows are split (with split fraction R_V and R_L respectively) to the pre-fractionator and the main column.

9.1.1 Problem Formulation

In this work it is assumed that the operational objective is to minimize the energy conversion, which translates into minimizing the boilup V, while satisfying constraints on the composition of the main component in the three product streams. With this formulation, we implicitly assume that all product streams have the same economic value. In mathematical terms, the operational objective is

$$\min_{\mathbf{u}} V \tag{9.1}$$

s.t.

$$x_{A,D} \geq x^0_{A,D},\; x_{B,S} \geq x^0_{B,S},\; x_{C,B} \geq x^0_{C,B} \tag{9.2}$$

where $\mathbf{u}^T = [L\ V\ S\ R_L\ R_V]$ is the vector of steady-state degrees of freedom (manipulated inputs), and $x^0_{i,j}$ denotes the minimum mole fraction for the main component $i \in \{A, B, C\}$ in each product stream $j \in \{D, S, B\}$. In addition we must require that all flows are positive.

It is well known that when the products have different economic value, it may be economically optimal to over-fractionate the least valuable product in order to maximize the amount of the most valuable product. Here, we intend to show that there may be cases where it is optimal to over-fractionate one of the products to save energy even when they are equally valuable. Bagajewich and Manousiouthakis (1992) showed that for a conventional binary distillation column, bypassing a portion of the feed and mixing it with the products does not affect the energy consumption to produce a specified product.

9.1.2 Motivation

The motivation for this work was a preliminary study on the optimal operation of the Petlyuk column, see Chapter 8. We found that one of the constraints on the composition in eq. (9.2), was not active. To illustrate, consider a column with data as given in Table 9.1. When treating the inequality constraints in eq. (9.2) as equality constraints

$$x_{A,D} = x^0_{A,D},\; x_{B,S} = x^0_{B,S},\; x_{C,B} = x^0_{C,B} \tag{9.3}$$

in the optimization, the Lagrangian multipliers for the composition constraints $x_{A,D}$, $x_{C,B}$ and $x_{B,S}$ are:

$$[\lambda_{x_{A,D}}\ \lambda_{x_{C,B}}\ \lambda_{x_{B,S}}] = [-0.0342 \quad 0.5896 \quad 1.0445] \tag{9.4}$$

and the optimal inputs are

$$\begin{bmatrix} L & V & S & R_L & R_V \end{bmatrix}^T = \begin{bmatrix} 0.603 & 0.946 & 0.323 & 0.215 & 0.610 \end{bmatrix} \tag{9.5}$$

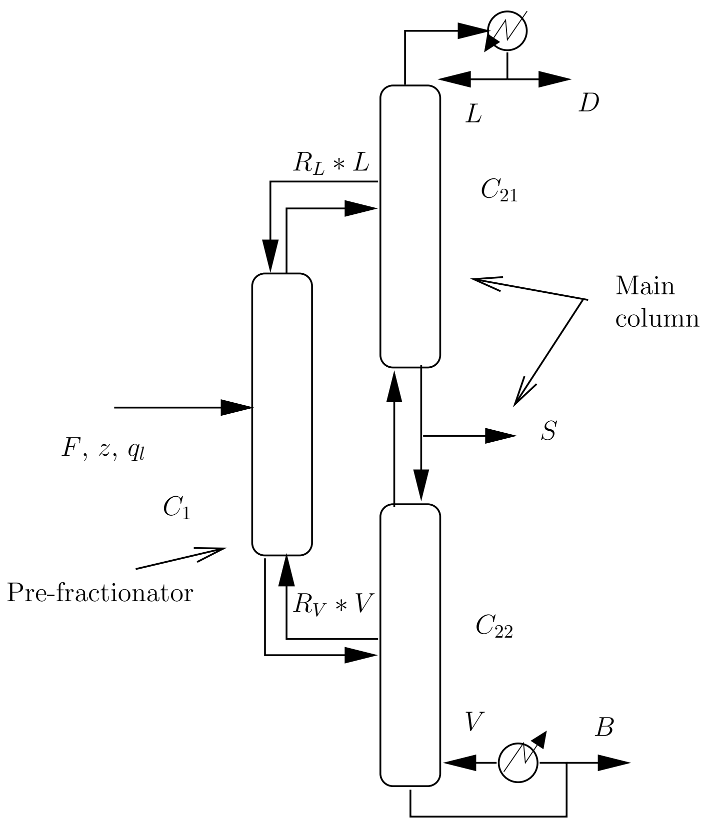

Figure 9.1: *Illustrative sketch of the Petlyuk column, for separation of ternary mixtures with one reboiler and one condenser.*

Table 9.1: *Data for the Petlyuk simulation case.*

Feed	Flow	$F = 1$
	Composition	$\mathbf{z}^T = [1/3\ 1/3\ 1/3]$
	Liquid fraction	$q_l = 1$
Product compositions	Distillate	$x^0_{A,D} = 0.97$
	Side-stream	$x^0_{B,S} = 0.97$
	Bottom	$x^0_{C,B} = 0.97$
Physical data	Relative volatilities	$\alpha^T = \begin{bmatrix} 9 & 3 & 1 \end{bmatrix}$
	Number of stages each section	$N_T = 16^a$

[a] The column is divided into 6 sections with two sections in the pre-fractionator, one section below the split of V one above the split of L and two sections above and below the side-stream outlet S

The Lagrangian multiplier is a measure of how a small perturbation of the value of the constraint affects the optimal objective value (Nocedal and Wright, 1999). From eq. (9.4), we see that by increasing the purity constraint on the distillate stream, the boilup is reduced (negative change in the boilup), i.e. a 0.01 increase in the purity of the distillate, yields a reduction of $\Delta V = 0.946 - 0.0342 * 0.01 = 0.0003$, a 0.03% decrease in the boilup. Thus by increasing the purity to pure component A a 0.1% reduction of the boilup is possible. Similar behavior was observed for other feed compositions and relative volatilities, and motivated the derivations in this paper.

9.2 V_{min}-diagram and Underwood equations for the Petlyuk distillation column

The V_{min}-diagram is a graphical representation of the energy requirements in distillation columns and provides an effective tool for analyzing the minimum energy requirements for different mixtures and feed properties (Halvorsen and Skogestad, 2003). Here, we construct the V_{min}-diagram from the Underwood equations (Underwood, 1945) based on the assumption of constant molar flows, constant relative volatility and we assume an infinite number of stages.

An example is shown in Figure 9.2 for a given ternary feed mixture (A, B, C) in a two-product column, where the vapor flow V_T (above the feed stage) and net product split D/F are the degrees of freedom. The peaks in the diagram represent the minimum energy required for a sharp split between A/BC (P_{AB}) or AB/C (P_{BC}). A sharp split between A/C requires operation above the V-shaped P_{AB}-P_{AC}-P_{BC}. In the triangular region below the V-shaped region, a set of components AB, ABC or BC may be distributed to both products.

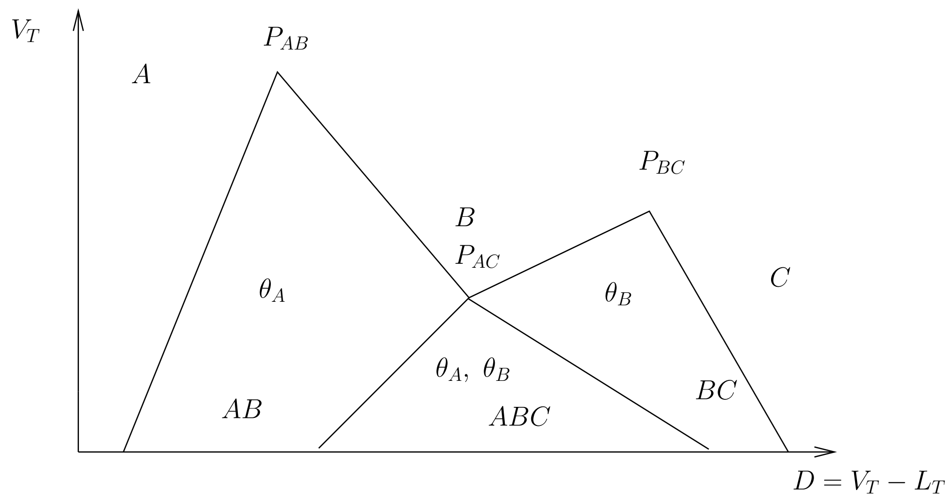

Figure 9.2: *V_{min}-diagram for a binary column (the pre-fractionator) with sharp splits when where the separation A/AB is limiting.*

For a three-product column with sharp splits, it can be shown that the minimum energy diagram maps the V_{min}-diagram for the pre-fractionator C_1 operated at the preferred split (Halvorsen and Skogestad, 2003). Thus, Figure 9.2 also illustrates the V_{min} diagram for the Petlyuk column with sharp splits. The peak P_{AB} corresponds to the split A/BC, while the peak P_{BC} corresponds to the split AB/C. The minimum energy is given by the highest peak, which corresponds to the most difficult separation.

For non-sharp splits the same diagrams apply, but now with the vapor flows related to the non-sharp splits D/SB and DS/B, so the minimum energy for non-sharp splits is (Halvorsen and Skogestad, 2003):

$$V_{T,min}^{Petl} = \max(V_{T,min}^{D/SB}, V_{T,min}^{DS/B}) = \max(V_{T,min}^{C_{21}}, V_{B,min}^{C_{22}} + (1-q_l)F) \tag{9.6}$$

where D, S and B here represent the three products with their defined compositions. For the case of non-sharp splits there will be no component C in the distillate ($x_{C,D} = 0$) and no component A in the bottom stream ($x_{A,B} = 0$) in normal operation regions. However, in the side-stream (S) all components may be present, and we select $x_{A,S}$ as a free variable, since we only specify one of the product compositions in each product stream. Halvorsen and Skogestad (2003) show that three different regimes of operation are possible, with accompanying optimal values for $x_{A,S}$:

- **Case 1: C_{22} is limiting:**
  This is the case when the separation B/C is the most difficult separation, so peak P_{BC} is above peak P_{AB}, thus: $V_{T,min}^{Petl} = V_{B,min}^{C_{22}}(0) + (1-q_l)F > V_{T,min}^{C_{21}}(1-x_{B,S})$ for $x_{A,S} = 0$ and $x_{C,S} = 1 - x_{B,S}$. This case is illustrated in the V_{min}-diagram of Figure 9.3.
- **Case 3: C_{21} is limiting:**
  This is the case when the separation A/B is the most difficult separation and: $V_{T,min}^{Petl} = V_{T,min}^{C_{21}}(0) > V_{B,min}^{C_{22}}(1-x_{B,S}) + (1-q_l)F$ where $x_{A,S} = 1 - x_{B,S}$ and $x_{C,S} = 0$. This case is illustrated in Figure 9.4
- **Case 2: Balanced main column:**
  This is when the required vapor loads are equal: $V_{T,min}^{Petl} = V_{B,min}^{C_{22}}(x_{A,S}) + (1-q_l)F = V_{T,min}^{C_{21}}(x_{A,S})$ for $0 < x_{A,S} < 1 - x_{B,S}$ and $x_{C,S} = 1 - x_{B,S} - x_{A,S}$.

Based on the Underwood equations, Halvorsen and Skogestad (2003) found that the vapor flows are given by

$$V_{T,min}^{C_{21}} = \frac{\alpha_A w_{A,T}^{C_{21}}}{\alpha_A - \theta_A} + \frac{\alpha_B w_{B,T}^{C_{21}}}{\alpha_B - \theta_A} = D\left[\frac{\alpha_A x_{A,D}}{\alpha_A - \theta_A} + \frac{\alpha_B(1-x_{A,D})}{\alpha_B - \theta_A}\right] \tag{9.7}$$

and

$$V_{B,min}^{C_{22}} = \frac{\alpha_B w_{B,B}^{C_{22}}}{\alpha_B - \theta_B} + \frac{\alpha_C w_{C,B}^{C_{22}}}{\alpha_C - \theta_B} = -B\left[\frac{\alpha_A(1-x_{C,B})}{\alpha_A - \theta_B} + \frac{\alpha_B(x_{C,B})}{\alpha_B - \theta_B}\right] \tag{9.8}$$

where $\theta_A = \theta_A(\mathbf{z}, q_l, \alpha)$ and $\theta_B = \theta_B(\mathbf{z}, q_l, \alpha)$ are the Underwood roots carried over from C_1 to C_{21} and C_{22}, respectively.

$$w_{A,T}^{C_{21}} = x_{A,D}D \quad \text{and} \quad w_{B,T} = x_{B,D}D = (1-x_{A,D})D$$

are the net component flow of A and B in C_{21} respectively and

$$w_{B,B}^{C_{22}} = -(1-x_{C,B})B \quad \text{and} \quad w_{C,B}^{C_{22}} = -x_{C,B}B$$

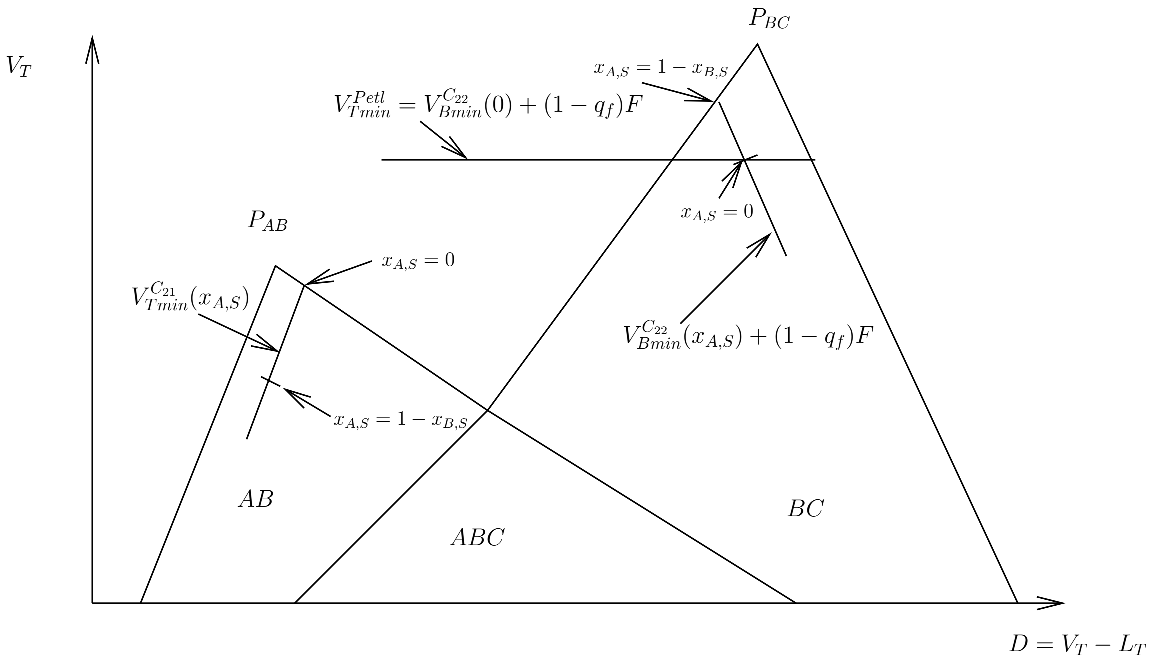

Figure 9.3: *V_{min}-diagram for Case 1 where C_{22} is limiting. No component A is present in the side-stream ($x_{A,S} = 0$). The most difficult separation corresponds to peak P_{BC} corresponding to the split AB/C. The line parallel with the right-most line, corresponds to the minimum energy with respect to the parameter $x_{A,S}$, and we see that the energy is minimized for $x_{A,S} = 0$ as indicated by the horizontal line.*

are the net component flow of B and C in C_{22}. The Underwood roots θ_A and θ_B are functions of the feed properties only and independent of the product specifications.

The key observations from eqs. (9.7) and (9.8) are:

- When C_{21} is the limiting section, keeping $x_{C,B}$ constant, $V_{T,min}^{C_{21}}/D$ is constant.
- When C_{22} is the limiting section, keeping $x_{A,D}$ constant, $V_{B,min}^{C_{22}}/B$ is constant.

The only restriction is that C_{21} and C_{22} remain the limiting column section, respectively. Based on the above eqs. (9.7) and (9.8) we now use the material balance of the column and express B and D with respect to the feed properties and product specifications. Based on these expressions, we develop explicit expressions for the energy savings from over-fractionating one of the product streams.

9.3 Energy savings by over-fractionation

Inside the main column, the same amount of vapor flows in both sections C_{21} and C_{22}. This implies that when the column operates in either Case 1 or Case 3 modus, the non-limiting section has a higher vapor flow than necessary for the separation to

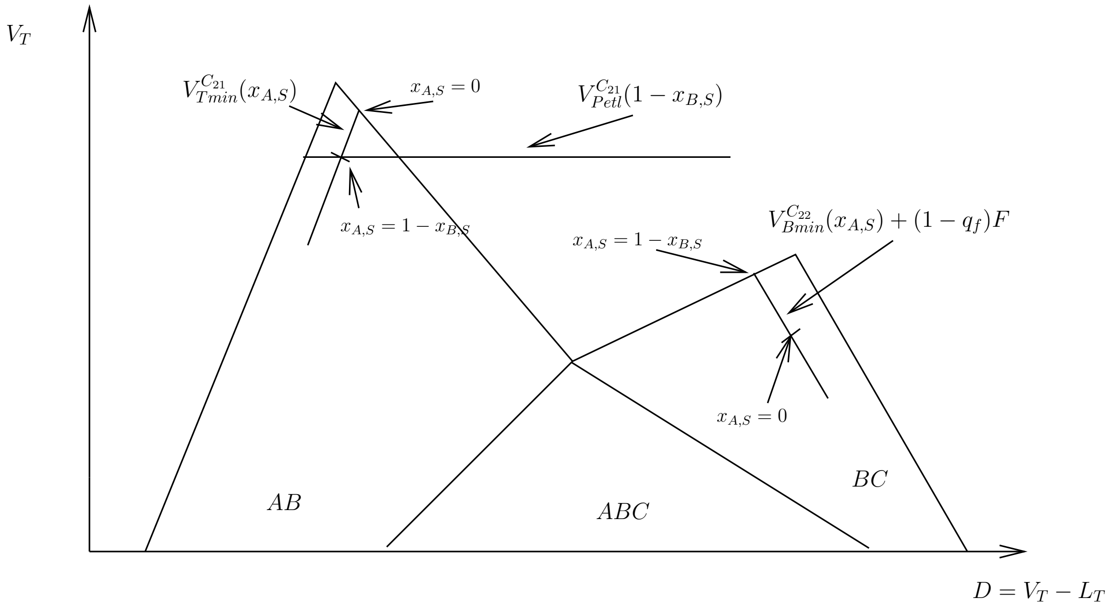

Figure 9.4: *V_{min}-diagram for Case 3 where C_{21} is limiting. No component C is present in the side-stream ($x_{C,S} = 0$). The most difficult separation is A/BC which is indicated by the horizontal line.*

take place. Thus, it is possible to over-fractionate in the non-limiting section without increasing the boil-up.

Actually we can go even further and decrease the overall boilup. This is less obvious, so consider Case 1 where AB/C is the most difficult separation (C_{22} is limiting). For this case we have excess vapor in the top of the main column (C_{21}) so the top product can be over-fractionated, for example, we can get pure A in the distillate product. The intermediate component B, that used to go into the top product, now goes into the side-stream product, thus increasing the purity of the side-stream with respect to component B. The purity of the side-stream product can then be maintained at its specified value $x^0_{B,S}$ by moving some (small) amount of component C from the bottom to the side-stream product. This results in a smaller bottom flow B and we can reduce the boilup V accordingly, while keeping V/B constant as seen from eq. (9.8). Thus, in conclusion, we can reduce the boilup to the limiting bottom section by over-fractionating in the top.

The same argument applies for operation in Case 3, when the top section C_{21} limits the separation, but now we over-fractionate the bottom product B.

Below we derive expressions for the potential reduction in boilup for the two cases when

1. The bottom section C_{22} is limiting, and we can over-fractionate the distillate in order to reduce the boilup.
2. The top section C_{21} is limiting and we can over-fractionate the bottom stream in order to reduce the boilup

9.3.1 Energy savings by over-fractionation, Case 1: C_{22} is limiting

The material balance of the column is as given by eq. (9.9)

$$\begin{bmatrix} z_A \\ z_B \\ z_C \end{bmatrix} F = \begin{bmatrix} x_{A,D} & x_{A,S} & 0 \\ (1-x_{A,D}) & x_{B,S} & (1-x_{C,B}) \\ 0 & (1-x_{B,S}-x_{A,S}) & x_{C,B} \end{bmatrix} \begin{bmatrix} D \\ S \\ B \end{bmatrix} \tag{9.9}$$

where it is assumed that there is no heavy product in the top ($x_{C,D}=0$) and no light component in the bottom stream ($x_{A,B}=0$). The assumption for this work is that only the main component in each product stream is specified, so in order to solve eq. (9.6), it has to be minimized with respect to $x_{A,S}$, as is evident from eq. (9.9). For Case 1, the optimal value is $x_{A,S}=0$. The cause for this is that it is optimal to introduce as much B into the side-stream as possible in order to reduce the boilup in the limiting section, thus moving A to the top. Therefore, when operating in Case 1 mode, the constraints in (9.2) are given by

$$\begin{aligned} x_{B,S} &= x^0_{B,S} \\ x_{C,B} &= x^0_{C,B} \\ x_{A,D} &\geq x^0_{A,D} \end{aligned}$$

From eq. (9.9) we find that the bottom stream is given by

$$B = -F\frac{\left(1-\frac{z_A}{x_{A,D}}\right)x_{C,S}-z_C}{x_{C,B}-x_{C,S}} \tag{9.10}$$

which is found by setting $x_{A,S}=0$ and inverting. From the mass balance equations it follows that when the fraction of component B is reduced in the distillate, we can transfer an amount

$$\Delta L_{C_{21}} = Fz_A\frac{(1-x^0_{A,D})}{x^0_{A,D}}$$

to the side-stream S, see also Figure 9.5. To fulfill the side stream purity constraint, we can transfer an amount

$$\Delta V_{C_{22}} = \Delta L_{C_{21}}\frac{x^0_{C,S}}{x^0_{C,B}-x^0_{C,S}}$$

from the bottom stream to the side-stream. Further, it follows that the relative energy savings, when the purity is increased from the constraint value $x^0_{A,D}$ to $x_{A,D}$, is

$$\begin{aligned} E_S^{C_{22}} = \frac{V^{C_{22},0}_{B,min}-V^{C_{22}}_{B,min}}{V^{C_{22},0}_{B,min}} &= \frac{x^0_{C,S}z_A\left(x_{A,D}-x^0_{A,D}\right)}{\left(z_Ax^0_{C,S}+z_Cx^0_{A,D}-x^0_{A,D}x^0_{C,S}\right)x_{A,D}} \\ &= \frac{\frac{1}{x^0_{A,D}}-\frac{1}{x_{A,D}}}{\frac{z_C}{z_A}\frac{1}{x^0_{C,S}}+\frac{1}{x^0_{A,D}}-\frac{1}{z_A}} \end{aligned} \tag{9.11}$$

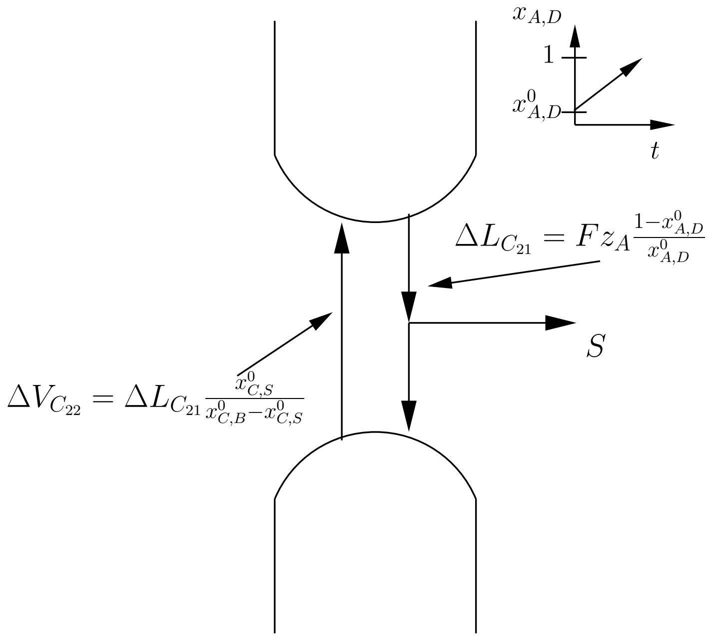

Figure 9.5: *Illustration of the change in the internal streams when increasing the purity of the distillate from $x^0_{A,D}$ to $x_{A,D} = 1$ for operation in Case 1.*

which is positive as long as

$$z_A x^0_{C,S} + z_C x^0_{A,D} - x^0_{A,D} x^0_{C,S} = x_A x^0_{C,S} + x^0_{A,D}(z_C - x^0_{C,S}) \geq 0$$

which is usually the case, since in practice $z_C > x^0_{C,S}$.

From eq. (9.11) we note that:

- Lowering the purity requirement ($x^0_{A,D}$) will increase the potential energy savings.
- Normally
$$\frac{z_C}{x^0_{C,S}} \gg 1$$
so increasing z_A will also increase the energy savings.
- Increasing the amount of C in the side-stream S will reduce the energy savings.
- Normally $x_{A,D} = 1$ and $z_A x^0_{C,S} + z_C x^0_{A,D} - x^0_{A,D} x^0_{C,S} \approx 1$ (let $z_A = z_C = z$ and $x^0_{B,D} = x^0_{C,S} = x$), then
$$E_S^{C_{22}} \approx x^2$$
the energy savings is proportional to the impurity specifications in the side-stream and the distillate. Thus, for high purity distillation, the savings are modest.

Note that the relative energy savings, as given by eq. (9.11), do not depend on the Underwood roots nor the product specifications of the bottom stream, as long as the same column section is limiting the separation.

To illustrate the potential energy savings, several cases are shown in Figure 9.6 for different feed compositions and product specifications. As seen from Figure 9.6, if some impurity is allowed in the side-stream, energy savings up to 3.5% are achievable

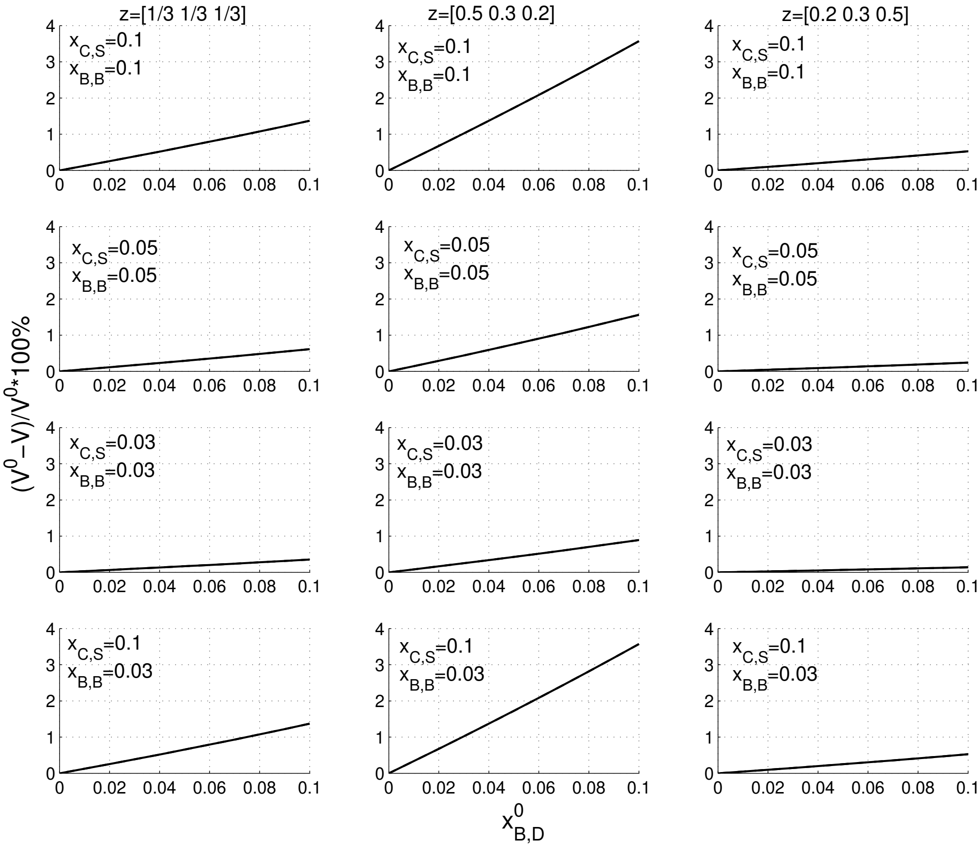

Figure 9.6: *Energy savings by over-fractionation for different feed compositions and purity requirements. The impurity specification is shown on the ordinate for the different sub-figures, while the feed specifications are shown on the abscissa.* $\frac{V^0-V}{V^0} * 100\%$ *yields the savings in percent by increasing the purity from* $x_{A,D} = x^0_{A,D}$ *to* $x_{A,D} = 1$.

for the data shown. For the case of equimolar feed, see column 1 of the sub-plots, we see that the potential energy saving is in the order of 1%. Also, note that the impurity requirements of the bottom stream do not influence the energy savings, as was noted above.

9.3.2 Energy savings by over-fractionating, Case 3: C_{21} is limiting

We here summarize the results for Case 3 for completeness. For Case 3 we have that

$$V^{C_{21}}_{T,min} = \frac{\alpha_A w^{C_{21}}_{A,T}}{\alpha_A - \theta_A} + \frac{\alpha_B w^{C_{21}}_{B,T}}{\alpha_B - \theta_A} = \left[\frac{\alpha_A x_{A,D}}{\alpha_A - \theta_A} + \frac{\alpha_B(1 - x_{A,D})}{\alpha_B - \theta_A}\right] D \tag{9.12}$$

where $w_{A,T}^{C_{21}} = x_{A,D}D$ and $w_{B,T} = x_{B,D}D = (1-x_{A,D})D$, and it is assumed that there is no C in the distillate. We see that for a given purity in the distillate, in order to reduce the boilup we must reduce the distillate stream. From the component mass balance in eq. (9.9) and using that $z_B = 1 - z_A - z_C$ we get

$$D = F\frac{x_{A,S}\left(\frac{z_C}{x_{C,B}} - 1\right) + z_A}{x_{A,D} - x_{A,S}} \tag{9.13}$$

where $x_{C,S} = 0$, as seen from Figure 9.4. Assume that $x_{B,S}$ and $x_{A,D}$ are fixed at the constraint, as given by (9.1), then

$$\begin{aligned} x_{B,S} &= x_{B,S}^0 \\ x_{A,B} &= x_{A,B}^0 \\ x_{C,B} &\geq x_{C,B}^0 \end{aligned}$$

and the change in boilup in over-fractionating the bottom stream (going from $x_{C,B}^0$ to $x_{C,B}$) is given by

$$\begin{aligned} E_S^{C_{21}} = \frac{V_{T,min}^{C_{21},0} - V_{T,min}^{C_{21}}}{V_{T,min}^{C_{21},0}} &= \frac{x_{A,S}^0\, z_C\, \left(x_{C,B} - x_{C,B}^0\right)}{\left(z_A\, x_{C,B}^0 - x_{C,B}^0\, x_{A,S}^0 + x_{A,S}^0\, z_C\right) x_{C,B}} \\ &= \frac{\frac{1}{x_{C,B}^0} - \frac{1}{x_{C,B}}}{\frac{z_A}{z_C}\frac{1}{x_{A,S}^0} + \frac{1}{x_{C,B}^0} - \frac{1}{z_C}} \end{aligned} \tag{9.14}$$

which is positive as long as

$$\left(z_A\, x_{C,B}^0 - x_{C,B}^0\, x_{A,S}^0 + x_{A,S}^0\, z_C\right) > 1$$

We see that eq. (9.14) is structurally similar to eq. (9.11) and if we assume equimolar feed ($z_A = z_C$) and that the allowable impurity in the product streams is $(1 - x_{C,B}^0) = x_{A,S} = x$, the energy savings in over-fractionating the bottom stream to pure C ($x_{C,B} = 1$) is given by $E_S^{C_{21}} \approx x^2$, the same as for Case 1. From the above discussions it is clear that there is a potential for saving energy when increasing the purity of one of the product streams. Explicit expressions for the savings have been derived, together with a physical explanation of the behavior. Below, we discuss the possibility of increasing the savings by allowing bypass of a fraction of the feed and mix it with the over-fractionated product.

9.3.3 Energy savings for a finite number of trays

The discussion so far has assumed a column with an infinite number of stages. In practice, for a finite number of stages the achievable purity in each product stream depends on the the number of stages in each section. For the case of an infinite number of stages, it was optimal to produce pure product in the section that was not limiting the column. For a real column, the optimum degree of over-fractionation will move away from pure product, as the number of stages in the non-limiting section is reduced. Here, we illustrate the effect of changing the number of stages in each section and how this affects the degree of over-fractionation.

To illustrate, consider a feed with composition $\mathbf{z}^T = \begin{bmatrix}0.45 & 0.3 & 0.25\end{bmatrix}$, relative volatility $\alpha^T = \begin{bmatrix}9 & 3 & 1\end{bmatrix}$ and the product specifications $x^0_{B,S} = 0.9$ and $x^0_{C,B} = 0.97$. A plot of the boilup with respect to the purity of the distillate is shown in Figure 9.7. When the number of stages is reduced, the optimum with respect to the purity in the distillate moves away from pure product and it is optimal to produce a distillate with some component B. Depending on the design of the column and on the product

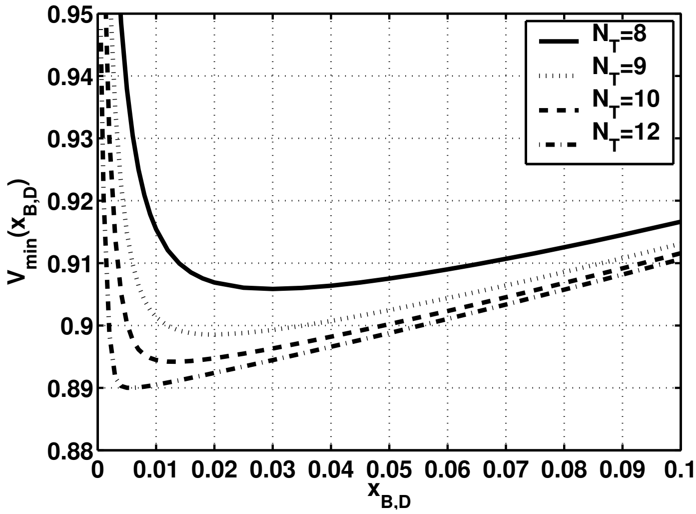

Figure 9.7: *Plot of the boilup with respect to the amount of impurity of component B in the distillate for different number of stages ($N_T = 8, 9, 10, 12$) in each section.*

specifications, the optimum may or may not be on the constraint. Thus, for the case of a non-balanced column (either Case 1 or Case 3) we may use the available separation work in the non-limiting sections in two ways:

1. To over-fractionate the non-limiting section of the column to produce a product with higher purity than the required, and mix a fraction of the feed into the product to achieve the product specification. This would have the effect of reducing the boilup for a given feed *and* increase the throughput of the process which would reduce the operational cost of the column.
2. We can reduce the number of stages in the non-limiting section, and by that save capital cost.

These results have also been confirmed using the process simulator HYSYS®, with a mixture of n-pentane (A), n-hexane (B) and n-heptane (C) with feed $z = [1/3\ 1/3\ 1/3]$, liquid fraction $q_l = 1$ and $x_{B,S} = 0.9$ and $x_{C,B} = 0.97$ and where we assume 28 theoretical stages in the pre-fractionator, and 40 in the main column. The Peng-Robinson equation of state was used for the thermodynamic calculations. A plot of the boilup with respect to the purity of the distillate is shown in Figure 9.8, where increasing the purity from $x_{A,D} = 0.9$ to $x_{A,D} = 0.997$ yields a 1.2% decrease in the heat input to the column, which is approximately the same energy savings as predicted by Figure 9.6. Taking into account that distillation often is the main energy consumer in a plant, a 1% reduction can yield large cost savings.

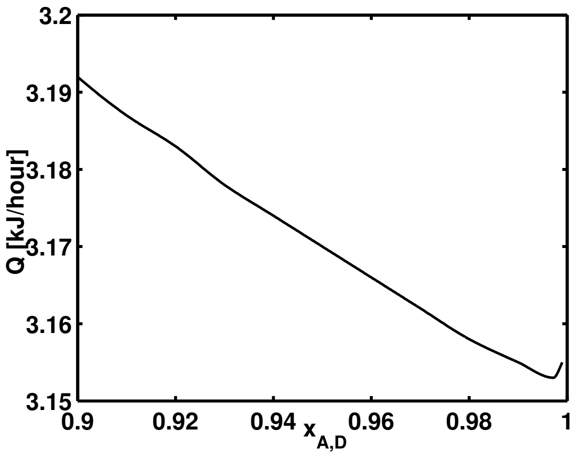

Figure 9.8: *Plot of heat input to boiler (Q) with respect to the product specification in the distillate ($x_{A,D}$) for the HYSYS® model*

9.4 Additional energy savings by introducing bypass

Over-fractionating one of the product streams makes it possible to bypass some of the feed and mix it with the product while retaining the constraints on the composition of the products as given by (9.2). Two scenarios are possible:

- *Case 1*: This results in a distillate containing pure A, while the side-stream contain B and C (rich in B), and the bottom stream contains C and B (rich in C).
- *Case 3*: We have pure C in the bottom stream, the side-stream contains B and A (rich in B) and the distillate contains A and B (rich in A).

For both cases, one of the streams contains a purer product than necessary (as given by the product specifications in eq. (9.2) and in order to fulfill the constraint, we can mix some of the feed into the over-fractionated product. Thus, we can further increase the energy savings, since for a given feed we can bypass a fraction of the feed and mix it with the product. However, we must allow component C (A) in the distillate (bottom stream), a component that normally is not present in that stream.

For Case 1 (see Figure 9.9), we assume that the distillate is over-fractionated to pure A ($x_{A,D} = 1$). The resulting distillate flow is then $D = z_A F$ (remember $x_{A,S} = 0$). The amount of feed to bypass (F_B) is then given by (9.15)

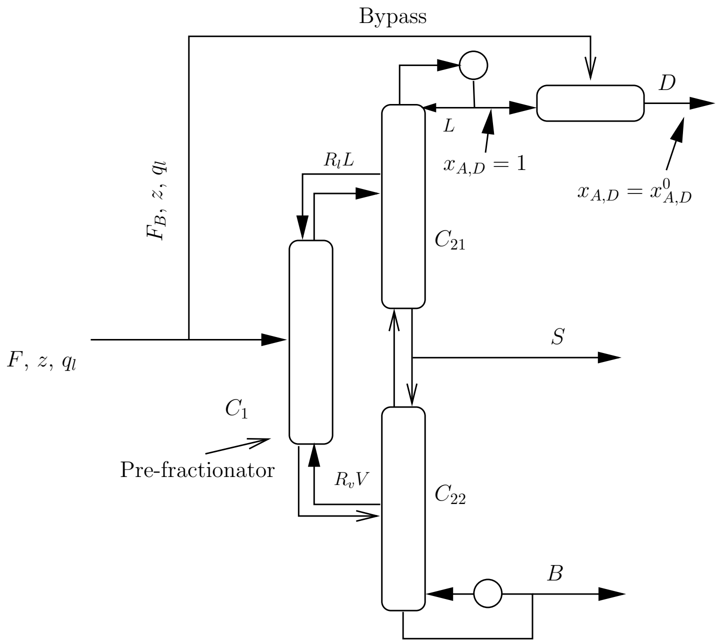

Figure 9.9: *Illustration of bypass for Case 1 where a fraction of the feed is bypassed the main Petlyuk column and mixed with the over-fractionated product (the distillate for Case 1) while retaining the composition constraint on the distillate*

$$F_B^{C22} = D(x_{B,D} = 0) \frac{x^0_{B,D}}{1 - x^0_{B,D} - z_A} \tag{9.15}$$

where $D(x_{B,D} = 0)$ is the distillate flow for pure product, which can be calculated by eq. (9.13). To illustrate, consider Figure 9.10 which shows the relative energy savings calculated as the reduction in boilup per feed unit with respect to $x^0_{B,D}$ for different feed compositions and purity specifications when increasing the purity from $x^0_{A,D}$ to $x_{A,D} = 1$ in the distillate.

A potential saving of maximum 3.5% is possible without bypass, while including bypass the potential saving is approximately 14%. Since the amount of bypass depends on the composition of the distillate and the feed stream only, the total energy savings are not sensitive to the product specifications of the other streams. Bypassing some of the feed has two effects:

1. First, the energy savings would increase, since we for a given feed can reduce the boilup.
2. Second, for a column that is a bottleneck in the process, we can increase the throughput of the plant by bypassing some of the feed.

For Case 3, when C_{21} is limiting, we have that $x_{C,S} = 0$ optimally. Assume that the bottom stream is over-fractionated to pure component C, then $B = z_C F$ and the

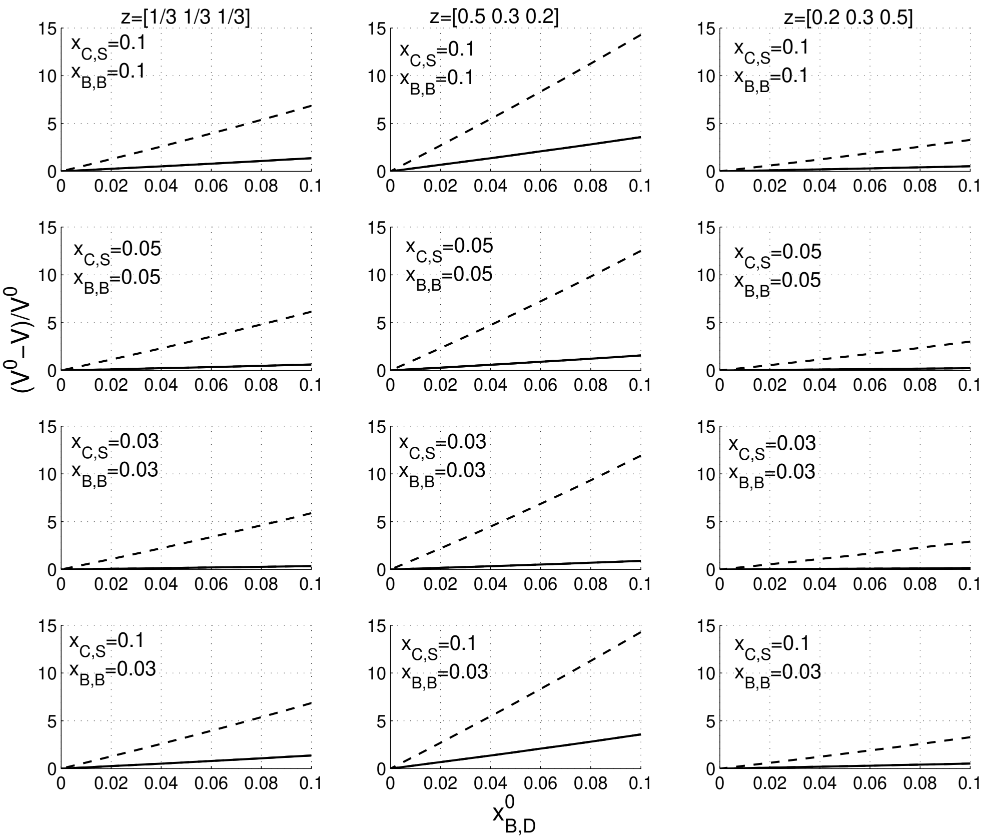

Figure 9.10: *Energy savings per feed unit by over-fractionation with bypass (dashed) and without (solid) for different feed compositions and purity requirements. The impurity specification is shown on the ordinate for the different sub-figures, while the feed specifications are shown on the abscissa.* $\frac{V^0-V}{V^0} * 100\%$ *yields the savings in percent by increasing the purity from* $x_{A,D} = x^0_{A,D}$ *to* $x_{A,D} = 1$

bypass is given by

$$F_B^{C_{21}} = B(x_{B,B} = 0)\frac{x^0_{B,B}}{1 - x^0_{B,B} - z_C} \tag{9.16}$$

The same savings can be achieved for the bottom stream as was shown for Case 1 above.

9.5 Discussion

9.5.1 Alternative configurations

Above we assumed that we can tolerate all three components in the product that is over-fractionated. If we require that the products should have the following product specifications:

$$\begin{aligned} x_{A,D} &= x^0_{A,D} \\ x_{B,S} &= x^0_{B,S} \\ x_{C,B} &= x^0_{C,B} \end{aligned} \tag{9.17}$$

and we can not tolerate any component C in the distillate or any component A in the bottom stream, several alternative column structures could be proposed where we assume that we over-fractionate the distillate (or bottom stream) and add component B by

1. Separating the bypass stream in a binary column, where we split AB/C and add the distillate from that column to the over-fractionated distillate stream from the Petlyuk column.
2. Taking the side-stream product from the Petlyuk column (which contains B and C) and separating in a binary column a fraction of the side-stream to get the required amount of B and mix it with the distillate from the Petlyuk column
3. and several other possible column structures.

The calculations showed that we could not lower the energy input (the boilup) by using alternative structures. The alternative structures had the same or higher energy demand as running the Petlyuk column without over-fractionation. The entropy production for the different configurations were also compared, with the same conclusion. For the product specification in eq. (9.17) running the Petlyuk column without over-fractionation was the optimal configuration.

9.5.2 Implications on control

From Figure 9.7 it is evident that the boilup increases rapidly if we operate to the left of the optimal impurity. This has important implications for control, since a small measurement error would yield large penalties in the boilup. Thus, controlling the composition at the optimum is a poor self-optimizing controlled variable, that is very sensitive to measurement error. Thus it may be preferable to back-off from the optimal value (since the gradient is much smaller to the right of the optimum) where a measurement error would have a much smaller effect on the boilup.

9.6 Conclusions

In this paper it is has been shown that for Petlyuk distillation columns, it may be optimal from an energy point of view, to over-fractionate one of the product streams.

Additional energy savings may also be possible when bypassing some of the feed and mixing it with the over-fractionated product stream. However, it should be noted that the resulting product will contain a component that normally is not present. These results have been confirmed numerically for the case of finite number of stages, where it is optimal to over-fractionate the non-limiting section as expected.

Acknowledgment

We are grateful to Dr.Ing. Ivar J. Halvorsen at SINTEF for useful discussions.

Bibliography

Bagajewich, M. and Manousiouthakis, V. (1992). Mass heat-exchange network representation of distillation networks. *AIChE Journal*, 38(11):1769–1800.

Halvorsen, I. and Skogestad, S. (2003). Minimum energy consumption in multicomponent distillation. Part 2. Three-product Petlyuk arrangements. *Ind. Eng. Chem. Res.*, 3(42):605–615.

Nocedal, J. and Wright, S. (1999). *Numerical Optimization.* Springer.

Smith, R. and Triantafyllou, C. (1992). The design and operation of fully thermally coupled distillaton columns. *Trans. IChemE.*, pages 118–132.

Underwood, A. (1945). Fractional distillation of ternary mixtures. Part i. *J. Inst. Petroleum*, 31:111–118.

Chapter 10

Control structure selection for oil and gas production networks

Based on work presented at
the 13th European Symposium on Computer-Aided Process Engineering (ESCAPE 13), June 1-4, 2003, Lappeenranta, Finland (Case 1)
and
Petronics Workshop - 2004: "Joining Petroleum, Multiphase Flow, Chemical and Control Engineering", June 15-16, 2004, Trondheim, Norway (Case 2)

In this paper, we study two cases related to the production of oil and gas from typical offshore facilities. Offshore production networks are prone with uncertainty due to the low degree of observability, with few and unreliable measurements. The focus here is on how to deal with uncertainty in such systems by selecting self-optimizing control structures. The first case deals with the optimal allocation of lift gas, which is a technology for increasing the production by injecting gas in the wells. The main conclusion is that we are able to find a control structure with acceptable loss using the null space method. The second case considers a special type of horizontal wells where free gas from the reservoir is drawn directly into the well. We find that by using practically available measurements and by using the null space method to find the control structure, the loss is acceptable. In both cases we neglect measurement and control error.

10.1 Introduction

Typical offshore production networks for oil and gas consist of multiple wells that are connected to nodes (manifolds). From each node, the hydrocarbons flow through transportation lines to new nodes or to a processing facility. From the reservoirs the fluid flows due to the pressure gradient into the well. The total flowrate in each well can be controlled using valves situated at the top of the well, see Figure 10.1. The reservoir fluid is a mixture of hydrocarbons and water, and, depending on the pressure and temperature in the reservoir, a free gas phase may be present. Due to the pressure drop the fraction of free gas increases downstream. The reservoir fluid consists of the three phases oil, water and gas which flow concurrently in the wells and transportation lines to the separation unit where water, light and heavy hydrocarbons are separated by reducing the pressure in a three-phase separator (or separators). Thereafter, the gas and oil are transported to the market, while water is re-injected into the reservoir or released to sea after cleaning. Gas can also be re-compressed and re-injected in the reservoirs or used as process fuel.

Typical constraints are:

- Processing capacity topside. Gas production may be limited by the compressor capacity, while water processing capacity may be limited by size of the separators.
- Flow constraints in the wells and transportation lines, because of friction.
- Reservoir constraints, for example to avoid sand in the production system.

The above constraints are not a complete list, see e.g. Golan and Whitson (1996) for more details. Below we consider two case-studies. In both cases we aim at (indirectly) achieving near optimal production by feedback control of the "right" variables utilizing the ideas of self-optimizing control (Skogestad, 2000).

1. The first study deals with the optimal distribution of lift gas in gas-lifted wells. A simple system, consisting of two wells with a common transportation line, is considered. The relative amount of gas to oil in the reservoir is unknown and is considered as a disturbance. We assume that the wells produce from different reservoirs such that the disturbances are not correlated. To increase production, a portion of the produced gas is recycled back into the wells. The operational objective is to maximize profit, where we add a penalty for re-compressing the lift gas. Gas-lift technology is typically used in systems where the pressure gradient is not sufficient to produce the reservoir fluids to the surface.

2. The second case study deals with a special type of reservoir, where free gas is present (as a gas phase) and is drawn directly into the well. The effect on production is that the relative amount of gas and oil from the reservoir depends on the rate of production from the well. In this case, the rate of change of free gas to the production rate is considered a disturbance. The system under study consists of five wells, of which three wells have uncertain inflow characteristics. The topside processing capacity for gas is limited, and we study how to find a self-optimizing control structure that yields acceptable economic operation.

10.2 Case 1: Optimal operation of gas-lifted wells

10.2.1 Introduction

In many offshore hydrocarbon production networks, the production of oil, gas and water is constrained by the processing capacity and other process constraints, such as available flow-line transportation capacity. Wang et al. (2002) point out that the available literature does not provide robust procedures on how to formulate and solve typical optimization problems for such systems. Often, the "optimization" considers the constraints sequentially, or only sub-problems are considered (e.g. by not including the transportation line to the processing facility). Many heuristic rules on how to operate "optimally" exist, see e.g. Golan and Whitson (1996), and often an open-loop approach is used where the setpoints for the inputs are calculated off-line without considering uncertainty.

Dutta-Roy and Kattapuram (1997) studied the effect of including process constraints for a two-well case that share a common transportation line to the process. They found that failing to include the process constraints (in this case the transportation line) gave a sub-optimal solution to the the problem.

Here, we focus on how to *implement* optimal operation in the presence of low frequency disturbances. In typical hydrocarbon producing systems, there are many uncertainties (e.g. reservoir properties, models, etc.) and few measurements. Thus, methods that can improve the operation such that the process is operated near-optimally in presence of disturbances, are of great value. Here, we propose to use the ideas of self-optimizing control (Skogestad, 2000) as a method for achieving near-optimal operation.

10.2.2 Case description

We consider the gas-lift structure shown in Figure 10.1, with two vertical wells and one vertical transportation line. The data for the case are shown in Table 10.1. We use a distributed pseudo one-phase flow model (Taitel, 2001), where we assume black oil compositional PVT behavior (Golan and Whitson, 1996). The valves are modeled as one-phase valves, with a linear valve characteristic. The flow-model represents a two-point boundary value problem and the partial differential equations are discretized using orthogonal collocation (Villadsen and Stewart, 1967) and solved as a set of algebraic equations.

Problem formulation

The two wells (W_1 and W_2) produce from separate reservoirs and are connected to the same manifold. Thus, both wells share a common transport line (T) to the processing facility. We assume that the system is dynamically stable. Gas is injected into the wells through valves CV_6 and CV_7 to increase the production from the reservoir.

The operating objective is to maximize the profit,

$$J = p_o \dot{m}_0 + p_g \dot{m}_g - p_{gi} \dot{m}_{gi} \tag{10.1}$$

where indices o, g, gi are oil, gas and injected gas respectively, p_i is the price and m_i is the mass rate for phase i. We have neglected water in this work. The seven degrees of freedom are

$$\mathbf{u}^T = [V_1\ V_2\ V_3\ V_4\ V_5\ \dot{m}_{gi,1}\ \dot{m}_{gi,2}] \tag{10.2}$$

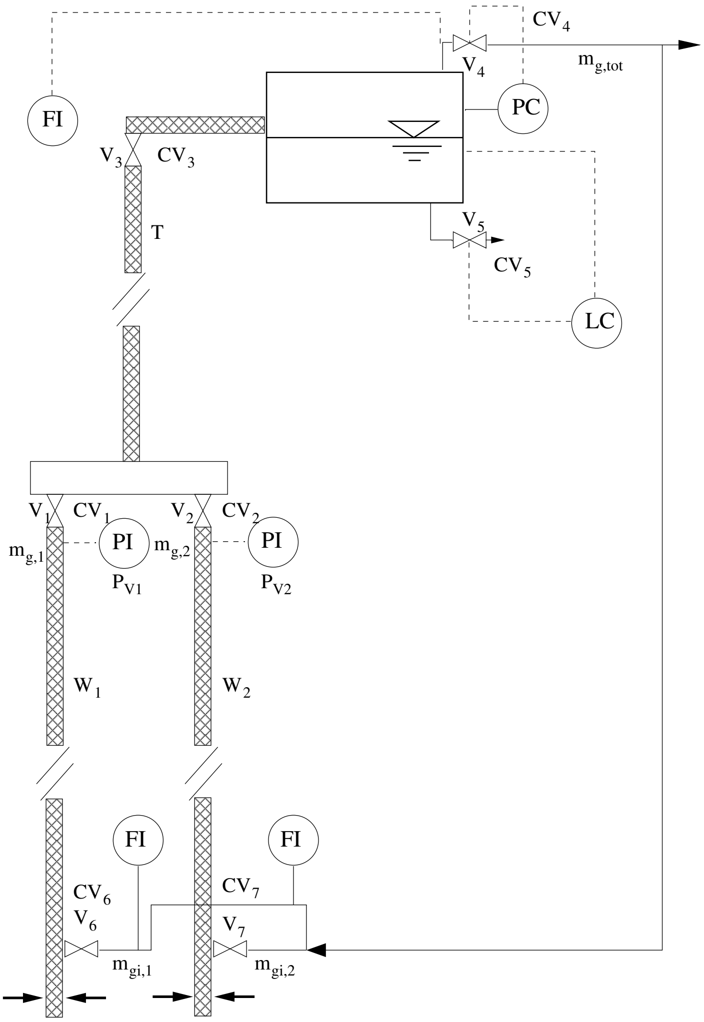

Figure 10.1: *Illustration of the gas-lift allocation network*

where V_i is the valve position for valve i and $\dot{m}_{gi,j}$ is the mass rate of injected gas in well j. We assume that the pressure and level in the separator are controlled using V_4 and V_5, respectively. The level has no steady-state effect and we assume that the pressure of the separator is given, thus removing two degrees of freedom.

In some reservoirs, the ratio of oil and gas (GOR, the ratio of stock-tank gas mass rate to stock-tank oil mass rate) is not exactly known, and we assume that the disturbances (uncertain parameters) are the ratio of gas and oil in reservoir 1 and 2.

$$\mathbf{d}^T = [GOR_1 \; GOR_2] = \begin{bmatrix} 0.1 \pm 0.03 & 0.05 \pm 0.02 \end{bmatrix}$$

The available measurements are the pressures upstream of the valve in each well, the mass rate of lift gas, the flow of gas in each well and the total mass rate of gas (i.e. the sum from both wells).

$$\mathbf{y}_0^T = \begin{bmatrix} P_{V_1} & P_{V_2} & \dot{m}_{gi,1} & \dot{m}_{gi,2} & \dot{m}_{g,1} & \dot{m}_{g,2} \; \dot{m}_{g,tot} \end{bmatrix} \tag{10.3}$$

Table 10.1: *Data for the gas-lift allocation case*

Parameter	Value	Unit	Comment
$L_{W1,W2}$	1500	m	Length well 1 and 2
$D_{W1,W2}$	0.12	m	Diameter well 1 and 2
L_T	300	m	Length transportation line
D_T	0.2	m	Diameter transportation line
$P_{res,1}$	150	bar	Pressure reservoir 1
$P_{res,2}$	155	bar	Pressure reservoir 2
$PI_{res,1}$	1×10^{-7}	$\frac{m^3}{s\ Pa}$	Production index well 1
$PI_{res,2}$	0.98×10^{-7}	$\frac{m^3}{s\ Pa}$	Production index well 2
P_{sep}	50	bar	Pressure separator
ρ_1	750	$\frac{kg}{m^3}$	Black oil density reservoir 1
ρ_2	800	$\frac{kg}{m^3}$	Black oil density reservoir 2
M_g	20	$\frac{kg}{kmol}$	Molecular weight gas
GOR_1^0	0.1	$\frac{kg}{kg}$	Nominal gas oil ratio [a]
GOR_2^0	0.05	$\frac{kg}{kg}$	Nominal gas oil ratio
$\dot{m}_{g,tot}$	14	$\frac{kg}{s}$	Maximum gas processing capacity

[a] GOR is defined as $\frac{\dot{m}_g}{\dot{m}_o}$ at standard conditions

It is assumed that there is an upper limit in the gas processing capacity ($\dot{m}_{g,tot}^{max}$) of the process, due to compressor capacity limitations. The optimally active constraints (for all disturbances) are found to be $[\dot{m}_{g,tot}^{max}\ V_1^{max}\ V_2^{max}\ V_3^{max}]$ corresponding to the total mass flow of gas, the valve positions for well 1 and well 2, and the transportation line. This is reasonable, since decreasing the valve position restricts the flow from the reservoir. Here, we assume that we control these constraints, removing four degrees of freedom. The remaining degrees of freedom are one, see Table 10.2.

Table 10.2: *Degrees of freedom analysis*

	Manipulated variables	7
	Valve positions $V_{1,2}$ (2)	
	Valve trans.line V_3	
	Gas injection $\dot{m}_{gi,12}$ (2)	
	Pressure P	
	Level L	
-	Control L and P	2
-	Active constraints	4
	Total mass flow gas $\dot{m}_{g,tot}^{max}$	
	Valves $V_{1,2,3}$	
=	Steady-state degrees of freedom	1

Thus, we have only one unconstrained DOF. Since it is optimal to control the total mass flow of gas at the constraint, we have

$$J' = p_o\dot{m}_o + p_g\dot{m}_g^{max} - p_{gi}\dot{m}_{gi} = p_o\dot{m}_o - p_{gi}\dot{m}_{gi} + \overbrace{p_g\dot{m}_g^{max}}^{constant} \tag{10.4}$$

and we can reformulate the objective and only consider the cost of injecting the gas into the wells

$$J = p_o\dot{m}_0 - p_{gi}\dot{m}_{gi} \tag{10.5}$$

Here we have assumed that $p_o = 0.17[\$/kg]$, corresponding to an oil price of \$ 20 per barrel. The cost of re-compressing gas for gas-lift is assumed to be $p_{gi} = 0.05[\$/kg]$, where we assume the cost to be half the market price of gas (assumed to be $0.1\$/Sm^3$).

10.2.3 Nominal optimal values

The nominal optimal values are summarized in Table 10.3.

Table 10.3: *Nominal optimal values for the gas lift allocation case*

Variable	Value	Units
$\dot{m}_{g,1}$	7.6661	kg/s
$\dot{m}_{g,2}$	6.3339	kg/s
$\dot{m}_{o,1}$	37.8880	kg/s
$\dot{m}_{o,2}$	42.2843	kg/s
$\dot{m}_{gi,1}$	3.8773	kg/s
$\dot{m}_{gi,2}$	4.2197	kg/s
P_{V_1}	60.982	bar
P_{V_2}	61.022	bar
J	13.2244	\$/s

10.2.4 Candidate control structures for self-optimizing control

With only one degree of freedom left for optimization, we need to select one controlled variable c. We select the controlled variable c as a linear combination of the measurements

$$c = \mathbf{H}\mathbf{y} \tag{10.6}$$

where $\mathbf{H}$ is a vector. If $\mathbf{H}$ consists of only one non-zero element, then a single measurement is used. We consider the measurements in eq. (10.3), except for the total mass flow of gas (since we already have assumed that we control that variable at its constraint value). We are looking for a controlled variable that, when kept at the nominal optimal value, yields optimal operation in the presence of uncertainty. We compare the use of a single measurement, $c = y_i$, with the candidate c_{ns} synthesized using the null space method of Chapter 3. In this case we have neglected the implementation and measurement error and we assume for all candidates that the active constraints are controlled.

Null space method

Following Section 3.2, we have that the minimum required number of measurements is

$$n_y = n_u + n_d = 1 + 2 = 3$$

where n_y is the number of measurements, n_u the number of unconstrained degrees of freedom and n_d the number of disturbances. Thus, we need three measurements for the null space method. We select to make use of measurements $\dot{m}_{gi,1}$, $\dot{m}_{gi,2}$ (the inputs) and $\dot{m}_{g,1}$ because the gas lift flowrates are easily available since they can be measured topside. In addition, we assume that we can measure the flowrate of gas from well 1 (we could have used another measurement here). Following Chapter 3, we obtain the optimal sensitivity function $\Delta \mathbf{y}^{opt} = \mathbf{F}\Delta \mathbf{d}$ where

$$\begin{bmatrix} \Delta \dot{m}_{gi,1}^{opt} \\ \Delta \dot{m}_{gi,2}^{opt} \\ \Delta \dot{m}_{g,1}^{opt} \end{bmatrix} = \begin{bmatrix} -20.253 & -16.026 \\ -12.332 & -22.473 \\ 12.819 & -17.356 \end{bmatrix} \begin{bmatrix} \Delta GOR_1 \\ \Delta GOR_2 \end{bmatrix}$$

$\mathbf{F}$ is calculated by imposing the above active constraints. Upon requiring $\mathbf{HF} = 0$, the resulting controlled variable is

$$\begin{aligned} c_{ns} = \mathbf{Hy} &= \begin{bmatrix} 0.633 & -0.703 & 0.325 \end{bmatrix} \begin{bmatrix} \dot{m}_{gi,1} & \dot{m}_{gi,2} & \dot{m}_{g,1} \end{bmatrix}^T \\ &= 0.633\dot{m}_{gi,1} - 0.703\dot{m}_{gi,2} + 0.325\dot{m}_{g,1} \end{aligned} \tag{10.7}$$

with nominal setpoint $c_{ns}^s = 1.9811$.

10.2.5 Loss evaluation for all candidates

The loss

$$L = J(c, d) - J^{opt}(d)$$

is the difference between the objective function value using controlled variable c and the true optimal objective value. The results from the loss calculation for nine different disturbance combinations are shown in Table 10.4.

From Table 10.4 it is evident that controlling c_{ns} at the nominal optimum yields perfect self-optimizing control for all disturbance combinations.

Controlling either P_{V_1} or P_{V_2} yield infeasible operation for cases where the amount of gas in the reservoir increases (the pressure at the wellhead decreases due to less liquid in the well).

Controlling either $\dot{m}_{gi,1}$ or $\dot{m}_{gi,2}$ at constant nominal setpoint, yield feasible operation for all disturbances with a worst-case loss of 0.92% and 0.59%, respectively. Controlling the mass rate of gas in either well 1 or well 2 at constant nominal setpoint, yields a worst-case loss of 0.42%. The percentage losses are small, which indicates that the optimum is flat in these variables. Keeping the mass rate of well 1 or well 2 constant yields similar loss, since we also control the total gas rate (the active constraint). Thus, as long as the gas processing capacity of the process are utilized (by actively controlling the total rate of gas), near-optimal operation is achieved.

Table 10.4: *Loss for the candidate control variables for the gas-lift allocation case. The disturbance values are indicated in the two left-most columns. Loss for each candidate is given in % ($L_{\%}$) and in 10^6\$/year ($L_{\$}$). "inf" denotes infeasable operation*

Disturbance		P_{V_1}		P_{V_2}		$\dot{m}_{gi,1}$		$\dot{m}_{gi,2}$		$\dot{m}_{g,1}$		$\dot{m}_{g,2}$		c_{ns}	
GOR_1	GOR_2	$L_{\%}$	$L_{\$}$	$L_{\%}$	$L_{\$}$	$L_{\%}$	$L_{\$}$	$L_{\%}$	$L_{\$}$	$L_{\%}$	$L_{\$}$	$L_{\%}$	$L_{\$}$	$L_{\%}$	$L_{\$}$
0.07	0.03	0.41	1.75	0.34	1.48	0.65	2.80	0.52	2.21	0.00	0.01	0.00	0.01	0.00	0.00
0.07	0.05	0.27	1.15	0.22	0.93	0.30	1.28	0.12	0.51	0.12	0.51	0.12	0.51	0.00	0.00
0.07	0.07	0.08	0.34	0.25	1.04	0.08	0.33	0.00	0.01	0.42	1.76	0.42	1.76	0.00	0.00
0.10	0.03	0.17	0.74	0.17	0.72	0.09	0.39	0.16	0.69	0.09	0.38	0.09	0.38	0.00	0.00
0.10	0.05	0	0	0	0	0	0	0	0	0	0	0	0	0	0
0.10	0.07	inf	inf	inf	inf	0.09	0.39	0.18	0.73	0.09	0.38	0.09	0.38	0.00	0.00
0.13	0.03	inf	inf	inf	inf	0.07	0.29	0.01	0.04	0.40	1.67	0.40	1.67	0.00	0.00
0.13	0.05	inf	inf	inf	inf	0.38	1.54	0.11	0.44	0.11	0.44	0.11	0.44	0.00	0.00
0.13	0.07	inf	inf	inf	inf	0.92	3.69	0.59	2.37	0.00	0.00	0.00	0.00	0.00	0.00

On the other side, because of the very large flowrates in an oil and gas production networks, the losses when measured in profit are large. In fact, the worst-case losses are in the range $1.76 - 3.69$ million \$/year and this could possibly be saved by controlling another variable, such as c_{ns}.

10.2.6 Conclusions Case 1

Here, selection of controlled variables has been illustrated on a gas lift allocation example. The results show that the control structures as synthesized using the null space method yields increased profit as compared to the alternative structures.

10.3 Case 2: Optimal operation of horizontal wells in high-permeable reservoirs by selecting the right control structure

10.3.1 Introduction

In this section we study a special type of reservoir, where the gas-oil ratio (GOR) depends on the flowrate in each well. This may occur in high-permeability reservoirs, where a gas cap (also called "free gas") exists or where the injected gas accumulates and forms a gas cap over the oil layer over time, see Figure 10.2. In many cases the gas

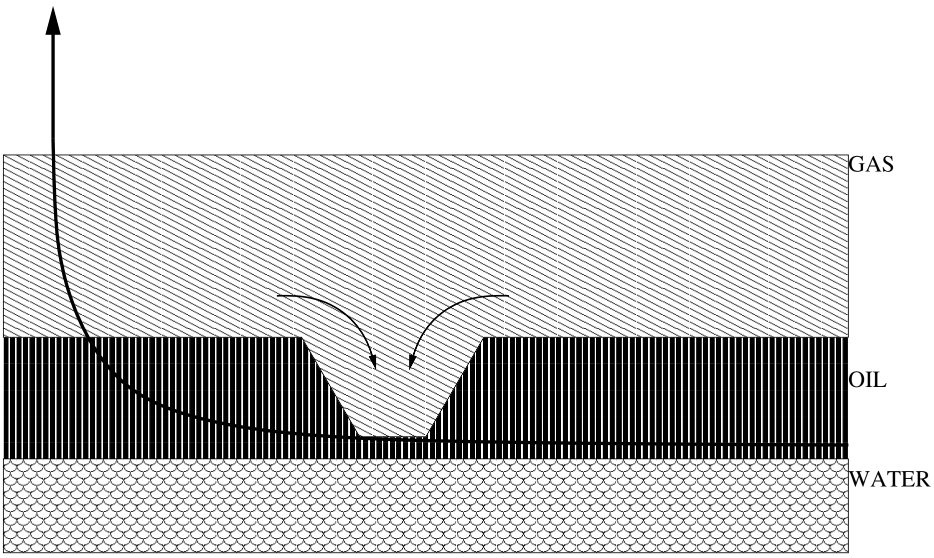

Figure 10.2: *Schematic illustration of a well with separate zones producing "free gas". When the production from the well is increased, the area*

production is unwanted, so the production from each well is limited by a critical rate (q_c) in which gas penetrates into the well. When the reservoir matures, production of free gas is unavoidable. How to operate such reservoirs optimally is of great importance for the economics of a production field.

Giger (1989) develops a model for when the gas-oil contact reaches the well (called cresting), focusing on the time before cresting. Papatzacos et al. (1989) further developed the methods of Giger (1989) to estimate the time before breakthrough of gas. Konieczek (1990) developed a model for the production of oil from a thin oil layer with an overlaying gas cap by using a semi-analytic two dimensional model of the contact layer between the oil and gas. The model assumes a horizontal well and predicts the GOR reasonably well. Tiefenthal (1992) extended the model of Konieczek (1990), allowing for non-homogeneous permeability in the reservoir.

While complex models and simulation tools exist for predicting the variable gas oil ratio (e.g. reservoir simulators), simple semi-analytical models are more commonly used based on fitting experimental data. Depending on the quality of the experimental data, the models may have large uncertainty with respect to the prediction of the rate dependencies of the GOR.

The inherent uncertainty in predicting the inflow behavior to the wells makes the planning and implementation of the optimal operation difficult. Two approaches for the implementation of optimal operation are

- Real-time optimization (RTO). At each optimization step, measurements are used to estimate the uncertain parameters in the model. Based on the updated model, new optimal inputs are implemented. For a brief discussion of RTO, see Chapter 2.

- Self optimizing control (Skogestad, 2000) based on simple feedback. Self-optimizing control is when constant setpoints indirectly give near-optimal operation.

Note that, feedback is necessary in order to achieve more optimal operation, either through the model update step of the RTO or with the direct feedback in self-optimizing control.

10.3.2 Case description

The system under study is illustrated in Figure 10.3. The system consists of five wells, W_1-W_5. All wells are connected to the same manifold and fluid is transported to the processing unit through a common transportation line (T). The processing unit operates at a constant pressure (P) and constant level (L).

The operational objective is to maximize the oil production ($\dot{m}_{o,tot}$) while keeping the gas production below the processing capacity ($\dot{m}_{g,tot} \leq \dot{m}_{g,tot}^{max}$). Since the wells share the same transportation line, the flow in the wells are constrained by the common downstream pressure in the manifold. Each well has a production choke valve at the inlet to the manifold with a valve opening V_i. The choke valve for the transportation line is situated at the inlet to the separation unit with valve opening V_T. The manipulated variables are listed in Table 10.5 and the available measurements are

Table 10.5: *Manipulated variables*

Variable	Unit	Comment
V_i	m^2	Valve opening[a] well i, $i = 1, \cdots, 5$
V_T	m^2	Valve opening transportation line
P	bar	Pressure separation unit
L	m	Level separation unit

[a]We model the valves as compressible flow of ideal gas through an area A_i and we manipulate directly on the allowable flow area of the valve.

listed in Table 10.6. The data and the models used are given in Appendix D.

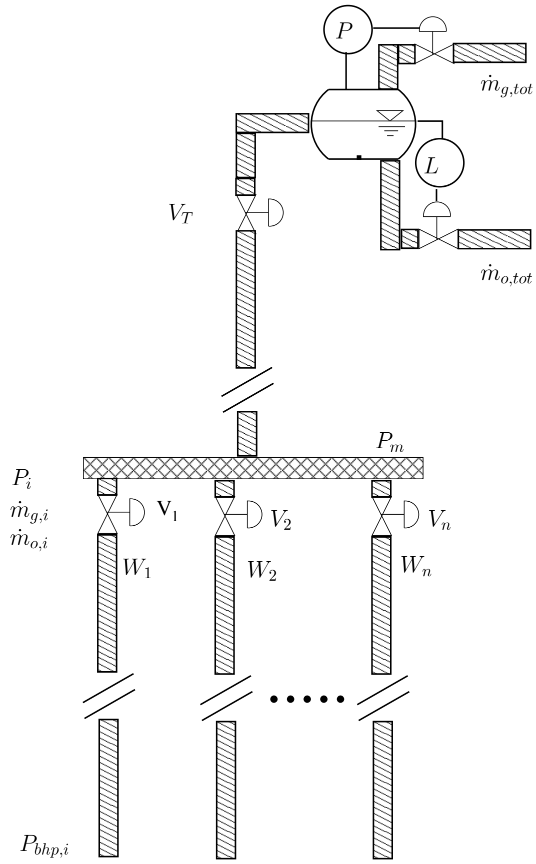

Figure 10.3: *Network of wells to be optimized (the horizontal part of the well is not included).*

Table 10.6: *Available measurements*

Variable	Unit	Comment
P_i	bar	Pressure upstream choke valve well i
$P_{bhp,i}$	bar	Bottom hole pressure well i
P_m	bar	Pressure manifold
V_i	m^2	Choke valve opening well i
V_T	m^2	Choke valve opening transportation line
$\dot{m}_g$	kg/s	Total mass rate of gas
$\dot{m}_o$	kg/s	Total mass rate of oil
$\dot{m}_{g,i}$	kg/s	Mass flowrate gas well i
$\dot{m}_{o,i}$	kg/s	Mass flowrate oil well i

Gas oil ratio (GOR) model

The GOR is defined as the ratio of gas and oil (measured at standard conditions)

$$GOR_i = \frac{\dot{m}_{g,i}}{\dot{m}_{o,i}}$$

where we here use mass basis. A typical dependency of GOR on the flowrate is shown in Figure 10.4. At low oil rates, the GOR is constant and equal to the fraction of gas

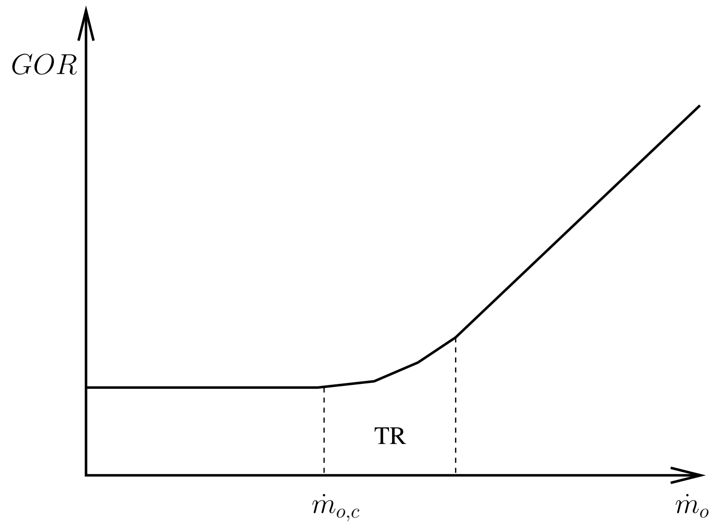

Figure 10.4: *Sketch of the dependency of GOR with respect to flowrate of oil for a typical horizontal well with free gas.*

dissolved in the oil. In a small transition region, the GOR increases non-linearly (TR in Figure 10.4) with oil rate. At higher rates, the change in GOR is close to linear with respect to the oil rate. Thus, if we assume that the operation of each well should be above the transition region, then a change in GOR with respect to oil rate is close to linear.

Fitting the data to the GOR model is not trivial and the resulting model has uncertain parameters. This can be seen from Figure 10.5, where two different realizations that fit the experimental data are shown for wells W_1, W_4 and W_5. As can be seen, the transition region is rather small such that a piecewise linear model of the data gives a reasonable description. This results in a model on the form

$$GOR_i = \max\left(GOR_{i,sol}, GOR_{i,0} + d_i(\dot{m}_{o,i} - \dot{m}^0_{o,i})\right) \tag{10.8}$$

where the parameter d_i can be seen as an uncertain parameter (disturbance) and $GOR_{i,sol}$ is the GOR without breakthrough of gas. A piecewise linear approximation to the data is shown in Figure 10.6 and the parameters for the model are given in Table 10.7. We assume that only three of the wells have uncertain parameters.

We select to include only some disturbance combinations, see Table 10.8 to reduce the computation time. We assume that the nominal point (nominal disturbance) cor-

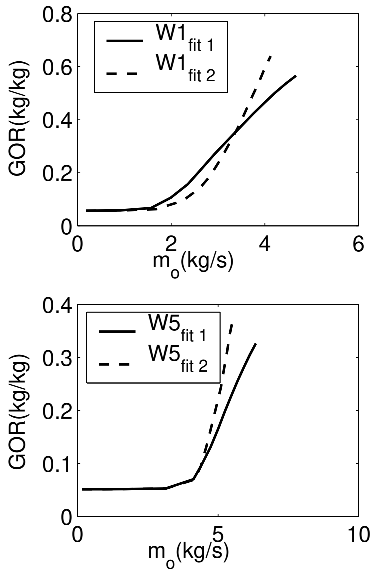

Figure 10.5: *Different model realizations for three different wells W_1, W_4 and W_5*

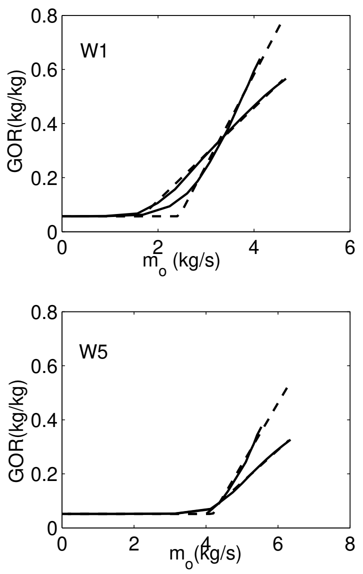

Figure 10.6: *A piecewise linear approximation of the data for the three wells*

Table 10.7: *Data for the GOR model*

	Well				
Parameter	W_1	W_2[a]	W_3[b]	W_4	W_5
$GOR_{i,0}$	0.331	0.053	0.053	0.392	0.096
$\dot{m}^0_{i,o}$	3.2534	3.8129	2.8129	2.1181	4.3885
d^1_i	0.1716	0.1522	0.1810	0.4745	0.1193
d^2_i	0.3370	0.1522	0.1810	0.648	0.223
$GOR_{i,sol}$	0.056	0.0530	0.0530	0.0578	0.0513

[a]No uncertainty
[b]No uncertainty

Table 10.8: *Disturbance combinations, where the sign ± indicates the low and high value of the disturbance, as given by Table 10.7*

#	d_1	d_4	d_5
0	-	-	-
1	+	-	-
2	-	+	-
3	-	-	+
4	+	+	+

responds to the disturbance scenario “0” in Table 10.8 since the amount of gas drawn into the well typically increases with time.

Optimal operation

We assume that the operational objective is to maximize the production of oil. For a given disturbance the optimization problem is:

$$\begin{aligned} &\max_{V_i} J = \dot{m}_{o,tot} \\ &\sum_i \dot{m}_{g,i} \leq \dot{m}^{max}_{g,tot} = 7.172\ [kg/s] \\ &0 \leq V_i \leq V_{i,max} \end{aligned} \tag{10.9}$$

Table 10.9 summaries the optimal flowrates for the disturbance combinations given in Table 10.8.

Degrees of freedom analysis

As seen from Table 10.9, it is optimal for all disturbance combinations to operate at the maximum gas processing capacity ($\dot{m}_{g,tot} = \dot{m}^{max}_{g,tot} = 7.172$). This removes one degree of freedom. In addition, it is optimal to have V_T, the transportation line valve, fully open (not shown), removing additionally one degree of freedom. Thus, there are four degrees of freedom at steady-state, see Table 10.10.

Table 10.9: *Optimal flowrates for different disturbances combinations.*

			Well					
#	Variable	Units	W_1	W_2	W_3	W_4	W_5	Sum
0	$\dot{m}_{g,i}$	kg/s	1.6666	1.5332	1.3812	0.4413	2.1497	7.172
0	$\dot{m}_{o,i}$	kg/s	3.7236	5.148	4.1422	1.7291	6.1812	20.92
0	GOR_i	kg/kg	0.44757	0.29782	0.33344	0.25521	0.34779	-
1	$\dot{m}_{g,i}$	kg/s	0.61139	1.8401	1.6392	0.53932	2.542	7.172
1	$\dot{m}_{o,i}$	kg/s	2.7701	5.4114	4.3637	1.8132	6.5178	20.88
1	GOR_i	kg/kg	0.22071	0.34004	0.37566	0.29744	0.39	-
2	$\dot{m}_{g,i}$	kg/s	1.7355	1.6112	1.4468	0.12902	2.2495	7.172
2	$\dot{m}_{o,i}$	kg/s	3.7844	5.2168	4.2001	1.5509	6.2691	21.0213
2	GOR_i	kg/kg	0.4586	0.30885	0.34447	0.083194	0.35882	-
3	$\dot{m}_{g,i}$	kg/s	2.0661	1.9853	1.7614	0.58571	0.77355	7.172
3	$\dot{m}_{o,i}$	kg/s	4.061	5.5298	4.4632	1.8511	4.4928	20.3978
3	GOR_i	kg/kg	0.50877	0.35902	0.39464	0.31642	0.17217	-
4	$\dot{m}_{g,i}$	kg/s	0.92433	2.5355	2.224	0.34541	1.1428	7.172
4	$\dot{m}_{o,i}$	kg/s	3.012	5.9489	4.8157	1.7223	4.7741	20.2729
4	GOR_i	kg/kg	0.30688	0.42621	0.46183	0.20056	0.23937	-

Table 10.10: *Degrees of freedom analysis*

	Manipulated variables	8
	Valve position wells V_i (5)	
	Valve trans.line V_T	
	Pressure P	
	Level L	
-	Control L and P	2
-	Active constraints	2
	Total mass flow gas $\dot{m}_{g,tot}^{max}$	
	Valve trans.line V_T	
=	Steady-state degrees of freedom	4

10.3.3 Loss for alternative control structures

Based on the degrees of freedom analysis, we need to find four variables to control. Again, we neglect the effect of implementation error. Since the number of possible candidate structures is very large, we consider only structures which would be plausible in practice and compare these structures with the structure using the null space method of Chapter 3. The alternative candidates are summarized in Table 10.11.

For all candidate structures we have assumed that V_3 is used for satisfying the total flowrate of gas (we can select any of the steady-state degrees of freedom). Candidates (4-6) utilize flowrate information from the wells. In practice, measuring the flowrate in multiphase flow is difficult, and in many cases these measurements are not available. Thus, if possible, a control structure with practically available measurements is preferred.

Table 10.11: *Candidate control structures*

CS #	$c_{ac,1}$	$c_{ac,2}$	c_1	c_2	c_3	c_4	Description
1	V_T	$\dot{m}_{g,tot}$	P_1	P_2	P_4	P_5	Well head pressures
2	V_T	$\dot{m}_{g,tot}$	$P_{bhp,1}$	$P_{bhp,2}$	$P_{bhp,4}$	$P_{bhp,5}$	Bottom hole pressures
3	V_T	$\dot{m}_{g,tot}$	V_1	V_2	V_4	V_5	Inputs constant
4	V_T	$\dot{m}_{g,tot}$	GOR_1	GOR_2	GOR_4	GOR_5	GOR
5	V_T	$\dot{m}_{g,tot}$	$\dot{m}_{g,1}$	$\dot{m}_{g,2}$	$\dot{m}_{g,4}$	$\dot{m}_{g,5}$	Mass flowrate gas
6	V_T	$\dot{m}_{g,tot}$	$\dot{m}_{o,1}$	$\dot{m}_{o,2}$	$\dot{m}_{o,4}$	$\dot{m}_{o,5}$	Mass flowrate oil
7	V_T	$\dot{m}_{g,tot}$	$c_{ns,1}$	$c_{ns,2}$	$c_{ns,3}$	$c_{ns,4}$	Null space method

Controlled variables for the null space method

We have $n_u = 4$ unconstrained degrees of freedom and $n_d = 3$ disturbances, so the number of measurements to include in the null space method is

$$n_y = n_u + n_d = 3 + 4 = 7 \tag{10.10}$$

To get a simple system, we choose not to include any flowrate measurements from the wells. The following seven measurements are used:

$$\mathbf{y}^T = \begin{bmatrix} \dot{m}_{o,tot} & P_m & V_1 & V_2 & V_3 & V_4 & V_5 \end{bmatrix} \tag{10.11}$$

As discussed in Chapter 3, the disturbances and inputs (if not measured) must be visible in the measurement space. With the measurements given by eq. (10.11), it may seem that we cannot distinguish between the disturbances since we utilize five input measurements and only two measurements from the process. However, note that there is feedback from the active constraint (by controlling $\dot{m}_{g,tot}$). Thus, the use of three measurements $m_{o,tot}$, P_m and one of the inputs is sufficient. Calculating the optimal sensitivity matrix

$$\Delta \mathbf{y}^{opt} = \mathbf{F} \Delta \mathbf{d} \tag{10.12}$$

and finding $\mathbf{H}$ in the left null space of $\mathbf{F}$ ($\mathbf{HF} = 0$) yields

$$\mathbf{H} = \begin{bmatrix} 0.006 & -0.007 & 0.135 & 0.991 & -0.011 & 0.003 & -0.020 \\ 0.009 & -0.011 & 0.159 & -0.011 & 0.987 & 0.003 & -0.024 \\ -0.013 & 0.019 & -0.054 & 0.005 & 0.006 & 0.998 & 0.010 \\ -0.036 & 0.045 & 0.242 & -0.013 & -0.014 & 0.003 & 0.968 \end{bmatrix}$$

with the corresponding setpoints $\mathbf{c}^s_{ns} = \begin{bmatrix} -0.146 & -0.258 & 0.539 & 1.147 \end{bmatrix}$.

Table 10.12 summarizes the loss results, for all seven control structures and we find that:

- Control structure 1, with wellhead pressure control, yields infeasible operation for all disturbance combinations. As can be seen from Figure 10.5, all disturbance combinations give a higher GOR ratio, implying that the static pressure drop over the well decreases. In order to keep the well head pressure constant, the rate must be increased, such that the effect of friction compensates for the loss in pressure drop due to the increased holdup of gas, or the rate must be decreased

Table 10.12: *Loss in kg/s (L) and in* 10^6 \$ *($L_\$$) for all control structures for different realizations of the uncertain parameters*

	$d_1^1 \rightarrow d_1^2$		$d_4^1 \rightarrow d_4^2$		$d_5^1 \rightarrow d_5^2$		$d_i^1 \rightarrow d_i^2, i \in \{1,4,5\}$	
CS #	L[kg/s]	L[\$ 10^6/year]	L[kg/s]	L[\$ 10^6/year]	L[kg/s]	L[\$ 10^6/year]	L[kg/s]	L[\$ 10^6/year]
1	*inf*	*inf*	*inf*	*inf*	*inf*	*inf*	*inf*	*inf*
2	0.3528	1.5723	0.0214	0.0956	*inf*	*inf*	*inf*	*inf*
3	0.5896	2.6279	5.0189	22.3695	6.2979	28.0702	4.5353	20.2142
4	0.1568	0.6991	0.0441	0.1964	0.1562	0.6960	0.1802	0.8033
5	0.1949	0.8689	0.0395	0.1759	0.2368	1.0554	0.2870	1.2790
6	0.3528	1.5723	0.0214	0.0956	*inf*	*inf*	*inf*	*inf*
7	0.0708	0.3156	0.0000	0.0000	0.0370	0.1647	0.0604	0.2691

in order for the GOR to be reduced with resulting increase in the pressure drop. As seen, this is not feasible.

- Control structure 2, with bottom hole pressure control, yields feasible operation for disturbance combinations 1 and 2 and infeasible operation for combinations 3 and 4. An additional important point is that the gain from the manipulated variables to the bottom hole pressure is small, making it sensitive to measurement noise (which is not included in this analysis).
- Control structure 3, with constant valve opening, is feasible for all disturbance scenarios. This structure is often used in practice. The loss is in the range $2.7\% - 29.5\%$, corresponding to a yearly loss in the range $2.6 - 28$ million \$.

All the above control structures utilize measurements that are found in most production systems. All proposed structures either give infeasible operation or a high economic loss. Next, we consider control structures 4-6 where we assume that flow measurements are available.

- Control structure 4, with constant GOR for each well (assumed measured) gives a loss of $0.2 - 0.8$ million \$/year, which is acceptable.
- Control structure 5, with constant mass flowrates for gas for each well (assumed measured), yields losses in the range $0.18\% - 1.38\%$ corresponding to $0.17 - 1.3$ million \$/year, which is acceptable.
- Control structure 6, with constant mass flowrate for oil for each well (assumed measured), yields infeasible operation for disturbance combinations 3 and 4. The physical explanations is that one tries to produce more oil than the well can deliver, while satisfying the maximum gas constraint.

Finally, let us consider control structure 7, which is based on using practically available measurements and the null space method.

- Control structure 7, with the optimal combination of measurements, yields the lowest losses of all candidates (in the range $0 - 0.3$ million \$/year). This is achieved, without any direct measurement of the flowrate from each well.

10.3.4 Conclusions Case 2

In summary, we have shown that using practically available measurements we can achieve almost perfect self-optimizing control, using the null space method. Keeping the valve positions (the inputs) constant, yield feasible but far from optimal operation, a loss which can be saved by using the correct variables to control.

10.4 Conclusions

This paper has focused on the selection of controlled variables for two cases related to offshore production of oil and gas. The goal has been to achieve self-optimizing control. For the first case, where we maximize the profit by distributing lift gas to the wells, we found that using the null space method for selecting controlled variables yield zero disturbance loss and true optimal operation. For the second case, where we maximize the amount of oil for a cluster of five wells with uncertain inflow characteristic, we found that using the null space method with practically available measurements, we are able to operate near-optimally, in the presence of disturbances. We neglected measurement error in this work.

Acknowledgment

We are grateful to Dr.Ing Are Mjåvatten at Norsk Hydro ASA for useful discussions.

Bibliography

Dutta-Roy, K. and Kattapuram, J. (1997). A new approach to gas-lift allocation optimization. In *paper SPE38333 presented at the 1997 SPE Western Regional Meeting, Long Beach, California*.

Giger, F. (1989). Analytic two-dimensional models of water cresting before breakthrough for horizontal wells. *SPE Reservoir Engineering*.

Golan, M. and Whitson, C. H. (1996). *Well perfomance*. Tapir, 2 edition.

Konieczek, J. (1990). The concept of critical rate in gas coning and its use in production forecasting. *SPE Journal*.

Papatzacos, P., Herring, T., Martinsen, R., and Skjaeveland, S. (1989). Cone breakthrough time for horizontal wells. *SPE Journal*.

Skogestad, S. (2000). Plantwide control: The search for the self-optimizing control structure. *J. Proc. Control*, 10:487–507.

Taitel, Y. (2001). *Multiphase flow modeling; Fundamentals and application to oil producing system*. Department of Fluid Mechanics and Heat Transfer, Tel Aviv University. Course held at Norwegian University of Science and Technology, September 2001.

Tiefenthal, S. (1992). Super-critical production from horizontal wells in oil rim reservoirs. *SPE Journal*.

Villadsen, J. and Stewart, W. (1967). Solution of boundart-value problems by orthogonal collocation. *Chem. Eng. Sci.*, pages 1483–1501.

Wang, P., Litvak, M., and Aziz, K. (2002). Optimization of production from mature fields. In *Proceedings of the 17th World Petroleum Congress*, Rio de Janeiro, Brazil.

Chapter 11

Control structure selection for an evaporator example

Based on work presented at
12th Nordic Process Control Workshop (NPCW), August 19-22, Göteborg, Sweden.

11.1 Introduction

The evaporator example of Newell and Lee (1989) has been studied by several authors in search for the best self-optimizing control structure (Govatsmark and Skogestad, 2001; Cao, 2003; Govatsmark, 2003). In the evaporator process, see Figure 11.1, the concentration of dilute liquor is increased by means of a heat exchanger with recirculated liquor. The feed enters with flow F_1, composition x_1 and temperature T_1 and is evaporated by the use of steam (F_{100}). The evaporated liquid is fed to a flash separator, where a fraction of the liquid is recycled back and mixed with the feed (F_3). The product stream (F_2), with temperature T_2 and composition x_2, is split off the recycled stream. The vapor from the separator is cooled using cooling water with flow F_{200} and temperature T_{200}. The model equations for the evaporator case are given in Appendix E.

11.1.1 Problem formulation

The objective of the operation is to minimize the operational cost J [$\$/h$] related to utility cost of steam, cooling water and pump work (Wang and Cameron, 1994),

$$J = 600F_{100} + 0.6F_{200} + 1.009(F_2 + F_3) \tag{11.1}$$

when satisfying the process constraints

$$\begin{array}{rcccl} 35\% & \leq & x_2 & & \\ 40\ kPa & \leq & P_2 & \leq & 80\ kPa \\ & & P_{100} & \leq & 400\ kPa \\ 0\ kg/min & \leq & F_{200} & \leq & 400\ kg/min \\ 0\ kg/min & \leq & F_3 & \leq & 100\ kg/min \end{array} \tag{11.2}$$

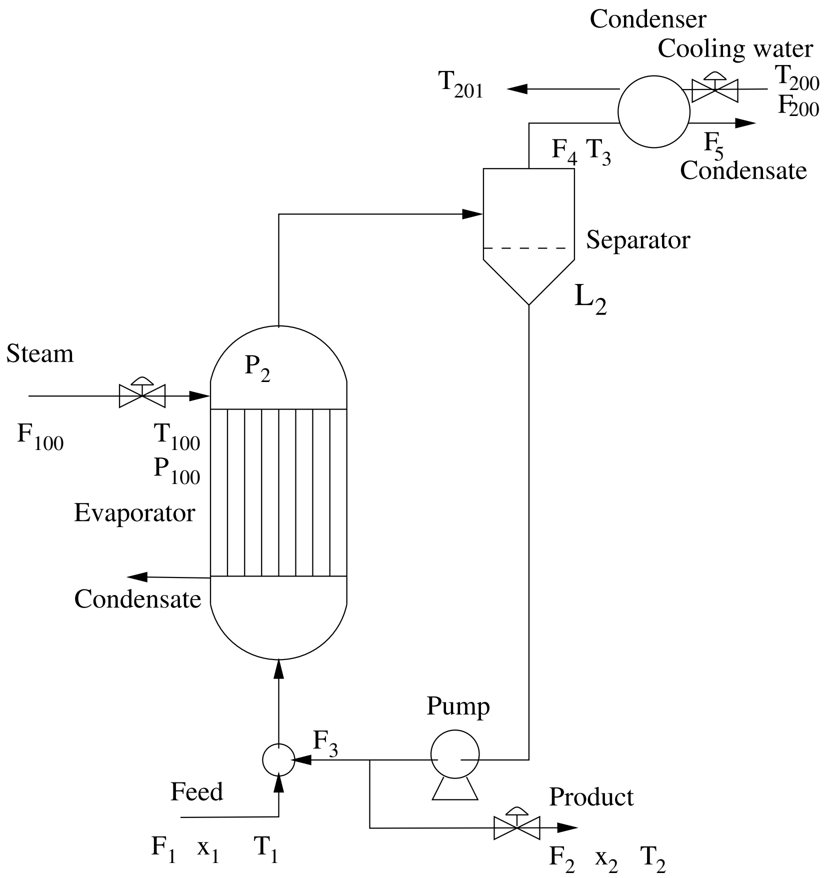

Figure 11.1: *Evaporation case*

using the four manipulated variables

$$\mathbf{u}_0^T = [F_{200}\ P_{100}\ F_3\ F_2] \tag{11.3}$$

which correspond to the flow of cooling water, steam pressure, recirculating flow rate and the product flow rate, respectively. The separator level must be controlled; however it has no steady state effect, resulting in three steady-state degrees of freedom. The major disturbances are assumed to be the feed flow rate, feed composition, feed temperature and cooling water temperature, each with a expected variation of $\pm 20\%$ from the nominal value:

$$\mathbf{d}^T = [F_1\ x_1\ T_1\ T_{200}] = [10 \pm 2 \text{ kg/min } 5 \pm 1\%\ 40 \pm 8°C\ 25 \pm 5°C] \tag{11.4}$$

Here we assume that the available measurements in the system are as given in eq. (11.5) (note that all inputs are assumed to be measurable) with

$$\mathbf{y}_0^T = [F_2\ F_3\ F_4\ F_5\ x_2\ T_2\ T_3\ L_2\ P_2\ F_{100}\ T_{100}\ P_{100}\ Q_{100}\ F_{200}\ T_{201}\ Q_{200}]; \tag{11.5}$$

with corresponding expected measurement error as shown in Table 11.1 (Govatsmark, 2003):

Table 11.1: *Measurement errors.*

Measurement type	Measurement error
Flow rates	± 10 %
Compositions	± 1 % (absolute)
Temperatures	± 1 $^\circ C$
Pressures	± 2.5 %
Flow ratios	± 22 %

11.1.2 Nominal optimal point

The steady-state optimal point is found by minimizing the cost function in in eq. (11.1) subject to the constraints in eq. (11.2), and the resulting optimal nominal data are shown in Table 11.2.

Table 11.2: *Nominal optimal values for the evaporator case*

Variable	Description	Value	Units
F_1	Feed flow rate	10	kg/min
F_2	Product flow rate	1.43	kg/min
F_3	Circulating flow rate	27.72	kg/min
F_4	Vapor flow rate	8.57	kg/min
F_5	Condensate flow rate	8.57	kg/min
x_1	Feed composition	5	%
x_2	Product composition	35	%
T_1	Feed temperature	40	°C
T_2	Product temperature	90.92	°C
T_3	Vapor temperature	83.49	°C
L_2	Separator level	1	m
P_2	Operating pressure	56.19	kPa
F_{100}	Steam flow rate	9.99	kg/min
T_{100}	Steam temperature	151.52	°C
P_{100}	Steam pressure	400	kPa
Q_{100}	Heat duty	365.65	kW
F_{200}	Cooling water flow rate	230.19	kg/min
T_{200}	Cooling water temperature inlet	25	°C
T_{201}	Cooling water temperature outlet	45.48	°C
Q_{200}	Condenser duty	330	kW

11.1.3 Active constraints and back-off

To achieve optimal operation we should control the active constraints (Maarleveld and Rijnsdorp, 1970). To find the active constraints we calculate the optimum for all possible disturbances and implementation errors, and we find that the product quality constraint (x_2) and the maximum steam pressure constraint (P_{100}) are always active. In addition, the evaporator pressure constraint (P_2) is active for a feed rate of $F_1 =$ 8 kg/min. Thus, the set of active constraints varies with the disturbances, violating the assumption that the set of active constraints must be active for all disturbances. For the moment we disregard this and assume that we control the steam pressure (P_{100}) and the product composition (x_2), leaving one degree of freedom left for self-optimizing control. Due to the implementation error in enforcing the active constraints, we back off from the optimal values (35% and 400 kPa respectively) to avoid violating the constraints. Thus, the nominal set points for the active constraints are as given in eq. (11.6).

$$\begin{aligned} c^s_{x_2} &= 36\% \\ c^s_{P_{100}} &= 390 kPa \end{aligned} \tag{11.6}$$

Using the above setpoints for the active constraints we re-optimize and find the backed-off optimal values which we use in the subsequent work.

11.2 Control structures for the evaporator case

11.2.1 Previously proposed control structures

Govatsmark (2003) ranks several possible self-optimizing control structures based on the singular value method (Skogestad and Postlethwaite, 1996; Halvorsen et al., 2003). The singular value method ranks candidates based on the smallest singular value (which corresponds to the absolute value in the SISO case) of the scaled steady-state gain $G(0)$. The most promising self-optimizing control structures as reported by Govatsmark (2003) are given in Table 11.3. As seen from Table 11.3, candidates that require

Table 11.3: *Most promising alternative sets of controlled variables based on the singular value method*

Rank	c_1	c_2	c_3	$\lvert G(0)\rvert$
1	x_2	P_{100}	T_{201}	0.0150
2	x_2	P_{100}	F_{200}/F_1	0.0135
3	x_2	P_{100}	F_{200}	0.0108
4	x_2	P_{100}	P_2	0.0044
5	x_2	P_{100}	T_2	0.0042
6	x_2	P_{100}	T_3	0.0042
7	x_2	P_{100}	F_3	0.0018
-	x_2	P_{100}	$T_{201} - T_{200}$	0.0181[a]

[a]Not included by Govatsmark (2003)

direct disturbance information (F_1) are included. Cao (2003) found, by differentiation, that a promising controlled variable, in addition to the ones already mentioned, were $T_{201} - T_{200}$, the temperature difference on the cold side in the condenser. This candidate controlled variable was found by inspecting the gradient function, which for this simple example, is possible to derive analytically. Note that the candidate proposed by Cao (2003) also require direct measurement of the disturbance (T_{200}) and based on the singular value rule should be the best self-optimizing controlled variable.

The goal here is to use the null space method of Chapter 3 to synthesize self-optimizing control structures without requiring direct disturbance information, and compare these with the previously proposed structures.

11.2.2 Measurement selection and controlled variables using the null space method

Following the procedure for selecting the best subset of measurements for the null space method as given in Section 4.4, we linearize the model equations around the backed-off nominal optimal point (remember, this is a constrained linear model where we enforce the active constraints). The resulting model is

$$\Delta \mathbf{y}_0 = \mathbf{G}^{y_0}\Delta u + \Delta \mathbf{G}_d^{y_0}\Delta \mathbf{d} \tag{11.7}$$

where u is the unconstrained input (F_{200}), $\mathbf{y}_0$ is the vector of all available measurements as given by eq. (11.5). The minimum number of measurements required for the null space method is

$$n_y \geq n_u + n_d = 1 + 4 = 5 \tag{11.8}$$

where n_y is the number of selected measurements, n_u the number of unconstrained inputs and n_d the number of disturbances. The measurement selection procedure of Section 4.4 suggests to select the subset of measurements that maximize the minimum singular value of the scaled augmented plant matrix ($\tilde{\mathbf{G}}^y = [\mathbf{G}^y \ \mathbf{G}_d^y]$). Following this rule, the five most promising sets of measurements are shown in Table 11.4. From Table

Table 11.4: *Most promising sets of measurements based on maximizing the minimum singular value of the scaled augmented process matrix*

Rank	y_1	y_2	y_3	y_4	y_5	$\underline{\sigma}(\tilde{\mathbf{G}})^y$
1	F_2	F_3	P_2	F_{200}	T_{201}	0.178
2	F_2	F_3	T_2	F_{200}	T_{201}	0.173
3	F_2	F_3	T_3	F_{200}	T_{201}	0.169
4	F_2	P_2	F_{100}	F_{200}	T_{201}	0.140
5	F_2	P_2	Q_{100}	F_{200}	T_{201}	0.140

11.4, note that even though F_2 by it self has zero gain (not shown), this measurement is included in all candidate sets due to high disturbance gain. All five sets of measurements have similar minimum singular value, and show very similar self-optimizing performance. Therefore, only the first candidate is included in the following analysis. The controlled variable for the null space method is the optimal combination given by $\Delta\mathbf{c} = \mathbf{H}\Delta\mathbf{y}$ where the vector $\mathbf{H}$ is given by requiring $\mathbf{HF} = 0$ where $\mathbf{F}$ is the optimal sensitivity from disturbances to the measurements $\Delta\mathbf{y}^{opt} = \mathbf{F}\Delta\mathbf{d}$. For the most promising set of measurements we get

$$\Delta c_{ns} = \mathbf{H}\Delta\mathbf{y} = \begin{bmatrix} -0.84465 & -0.0028331 & -0.24302 & 0.10253 & 0.46582 \end{bmatrix} \begin{bmatrix} \Delta F_2' & \Delta F_3' & \Delta P_2' & \Delta F_{200}' & \Delta T_{201}' \end{bmatrix}^T \tag{11.9}$$

where the nominal setpoint is $c^s_{ns} = 29.874$.

11.3 Loss evaluation with nominal set points

The losses, defined as the difference in objective function value for the constant setpoint policy and the true optimal value, for the most promising candidates using a nominal setpoint policy, are shown in Table 11.5. We also include the loss for the re-optimized case, in which we keep the constraints at the backed off setpoint while re-optimizing for each disturbance, assuming no implementation error in implementing the last degree of freedom ("the benchmark structure"). We also include the best candidates that require disturbance information as discussed above.

For the loss calculations it is assumed that only one disturbance d_i or measurement error n^y_j may occur at any time. The last column of Table 11.5 shows the average loss for all measurement errors.

As is evident from the loss data, the dominating contribution to the loss is due to the backoff from the constraints, since all structures show losses comparable in magnitude to the re-optimized case. As seen from Table 11.5, controlling the last input at its nominal setpoint (CS 9 or CS 11) yields a higher loss for a disturbance in the feed flow F_1. Of the two, controlling F_{200} (CS 9) shows the best performance. This implies that the objective function is flat with respect to F_{200} as illustrated in Figure 11.2. As seen from Table 11.5, none of the candidates are feasible for all disturbances using

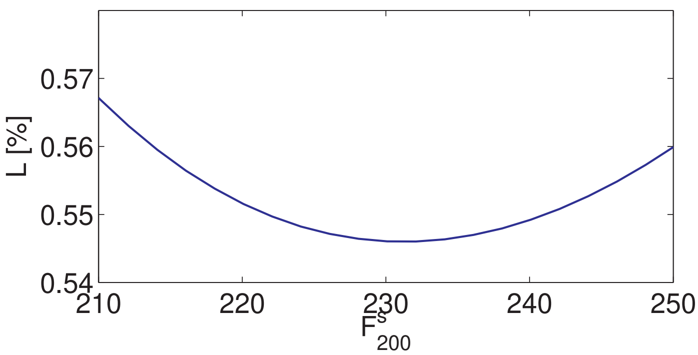

Figure 11.2: *Loss in percent with respect to the input F_{200} at the nominal disturbance.*

nominal set points due to the pressure constraint on P_2 becoming active. Feasible operation for all disturbances may be achieved using robust optimization or flexible back-off, see Govatsmark (2003) for more details. Alternatively, one can implement a cascade structure where the setpoint of P_2 is used as an input and use a min/max selector where we limit the signal to stay within the allowable range (Cao, 2003), see Section 11.5.3 for details.

Table 11.5: *Percentage loss for different disturbances and average loss for the implementation error for different candidate control structures. $d_j^{\pm}$ denote disturbance j with its low value marked by '$-$' and high value marked by '$+$' where $d^T = [F_1\ x_1\ T_1\ T_{200}]$.*

$CS\ \#$	c_3	note	$L_{d_1^-}$	$L_{d_1^+}$	$L_{d_2^-}$	$L_{d_2^+}$	$L_{d_3^-}$	$L_{d_3^+}$	$L_{d_4^-}$	$L_{d_4^+}$	L_n^{avg}
-	re-optimized	[b]	0.5318	0.5563	0.4398	0.6597	0.5383	0.5540	0.5479	0.5454	0.5397
1	c_{ns}	[a]	inf	0.5564	0.4398	0.6597	0.5383	0.5540	0.5479	0.5454	0.5498
2	$T_{201} - T_{200}$	[a], [c]	inf	0.5568	0.4402	0.6602	0.5383	0.5540	0.5479	0.5455	0.5493
3	T_{201}	[a]	inf	0.5568	0.4402	0.6602	0.5383	0.5540	0.6526	0.7157	0.5438
4	F_{200}/F_1	[a], [c]	inf	0.5568	0.4406	0.6606	0.5383	0.5540	0.5479	0.5455	0.5807
5	P_2	[a]	1.5426	inf	0.5116	0.7160	0.5383	0.5540	0.9065	inf	0.5461
6	T_2	[a]	1.5426	inf	0.5116	0.7160	0.5383	0.5540	0.9065	inf	0.5498
7	T_3	[a]	1.5426	inf	0.5116	0.7160	0.5383	0.5540	0.9065	inf	0.5497
8	F_3/F_1	[a], [c]	1.5426	inf	0.7204	0.8255	0.5502	0.5646	0.9065	inf	inf
9	F_{200}	[a]	inf	0.6459	0.4406	0.6606	0.5383	0.5540	0.5479	0.5455	0.5496
10	F_{100}/F_1	[a], [c]	1.5426	inf	inf	inf	inf	1.2347	0.9065	inf	inf
11	F_3	[a]	2.9367	inf	0.7204	0.8255	0.5502	0.5646	0.9065	inf	0.6695
12	F_{100}	[a]	inf	inf	inf	inf	inf	1.2347	0.9065	inf	inf
13	Q_{100}	[a]	inf	inf	inf	inf	inf	1.2347	0.9065	inf	inf
14	c_{ns}^2	[d]	inf	0.5582	0.4401	0.6600	0.5383	0.5540	0.6498	0.7099	0.5447
15	c_{ns}^3	[e]	inf	0.5563	0.4403	0.6602	0.5383	0.5540	0.5572	0.5543	0.5471

[a] inf means infeasible

[b] Re-optimized corresponds to re-optimizing for a new disturbance while keeping a constant back-off for the active constraints

[c] Controlled variables with feed-forward information of disturbances

[d] Using two measurements P_2 and T_{201}

[e] Using three measurementes F_3, T_2 and F_{200}

If we compare the candidates, controlling c_{ns} (CS 1) shows the same loss performance as the re-optimized case, which implies that controlling c_{ns} implicitly tracks the true optimal value, without any direct measurement of the disturbances. Compared to the other candidates that have no direct disturbance information, controlling T_{201} and F_{200} show comparable loss performance. Controlling T_{201} yields a higher loss for a disturbance in the cooling water temperature, while for disturbance F_{200} we get a slightly higher loss for a positive perturbation of the feed disturbance (F_1).

Compared to the control structures utilizing direct disturbance information, we see that controlling the temperature difference $T_{201} - T_{200}$ and the ratio F_{200}/F_1 give almost as good loss performance as the c_{ns} candidate. Overall, while the differences between the candidates are minor, the candidate synthesized using the null space method show the lowest losses, and is preferred from a steady-state point of view. Only the structures with no direct disturbance information will be considered in the following analysis.

11.3.1 Disturbance lumping

As seen from Table 11.5, some of the disturbances have a small effect on the loss. This is true for disturbance T_1, and is partially true for disturbance F_1 (if one disregard the infeasibility) which may indicate an opportunity for reducing the disturbances into a subset of pseudo-disturbances, thus reducing the number of measurements needed for the null space method. Following the rules for disturbance discrimination in Section 5.3.2, we check if using a smaller number of measurements (lumping disturbances) in the null space method is acceptable. A singular value decomposition of $\mathbf{G}_d^y$ (scaled with respect to the expected disturbances) yields the following singular values:

$$\sigma_1 = 28.25, \quad \sigma_2 = 8.00, \quad \sigma_3 = 6.03, \quad \sigma_4 = 2.67 \tag{11.10}$$

There is a leap in the singular values from σ_1 to σ_2, with a ratio of $\sigma_1/\sigma_2 \approx 3.5$. Based on this observation, two new candidates are proposed:

1. The first candidate (c_{ns}^2) using only two measurements (reducing the disturbances from four to one pseudo disturbance) and
2. the second candidate (c_{ns}^3) using three measurements (reducing the disturbances from four to two pseudo-disturbances).

The same procedure for selecting the best subset of measurements are applied as for the candidate using five measurements. Table 11.6 summarize the best set of measurements and the resulting coefficient vector $\mathbf{H}$.

The losses for these candidates are shown in the last two rows of Table 11.5. For candidate c_{ns}^2 the loss with respect to a disturbance in the feed flow rate is as low as candidate c_{ns}, while the loss for a disturbance in T_{200} is higher (approximately the same as for candidate T_{201}). Thus, lumping four disturbances into one does have a penalty. On the other side, using three measurements (candidate c_{ns}^3) the candidate has as good self-optimizing properties as candidate c_{ns} and shows that for this case

Table 11.6: *Best subset of measurements, the coefficients vector* **H** *for the null space method using two and three measurements. The nominal setpoints are included in the last column.*

Candidate	y_1	y_2	y_3	h_1	h_2	h_3	$c_{ns}^{i,s}$
c_{ns}^2	P_2	T_{201}	-	-0.0145	0.9998	-	44.656
c_{ns}^3	F_3	P_2	F_{200}	-0.71031	-0.54379	0.44694	51.751

three measurements are sufficient for acceptable self-optimizing properties using the null space method.

To conclude, these simulations show that the major contribution to the loss is due to the backoff from the constraints, and that there are only small differences between the candidates. The candidates using the null space method (c_{ns} and c_{ns}^3) have marginally better self-optimizing properties.

11.4 Dynamic comparison of the economically most promising control structures

Here, the most economically promising structures are compared dynamically. One of the possible disadvantages of the null space method is that the controlled variable does not have any physical interpretation; it is a linear combination of several measurements from different parts of the plant. Thus, this may give rise to more complex dynamic behavior. In the following section, three promising candidates, namely CS 1, CS 3 and CS 9 from Table 11.5 are compared. Note that candidate CS 15 is not included since it shows very similar dynamic properties as candidate CS 1 (not shown). For all structures the level in the separator (L_2) is stabilized using the product flow rate (F_2) and a decentralized control structure with PI-controllers is used.

11.4.1 Control structure analysis CS 1

The Relative Gain Array (RGA) is used to pair the inputs and outputs. For this structure we have

$$\begin{bmatrix} x_2 \\ P_{100} \\ c_{ns} \end{bmatrix} = G_{CS\ 1} \begin{bmatrix} P_{100} \\ F_{200} \\ F_3 \end{bmatrix} \tag{11.11}$$

and the steady-state RGA and the corresponding pairing are:

$$RGA_{CS\ 1}(0) = \begin{bmatrix} 0 & 0.0382 & 0.9618 \\ 1 & 0 & 0 \\ 0 & 0.9618 & 0.0382 \end{bmatrix} \quad \Rightarrow \quad \begin{array}{ccc} c & & u \\ \hline c_{ns} & \leftrightarrow & F_{200} \\ P_{100} & \leftrightarrow & P_{100} \\ x_2 & \leftrightarrow & F_3 \end{array} \tag{11.12}$$

Note that $RGA_{CS\ 1}^{2,1} = 1\ \forall\ \omega$, so it is sufficient to look at one element from the RGA since all columns and row sums up to one (Skogestad and Postlethwaite, 1996). Figure

11.3 shows the $RGA^{1,3}_{CS\ 1}$-element with respect to frequency and we see that the same pairing applies for frequencies near the cross-over frequency. With the level stabilized, all poles and zeros are in the left half plane (LHP, not shown), so no fundamental control limitations are expected.

11.4.2 Control structure analysis CS 3

For candidate CS 3 the same pairing applies with respect to the active constraints as seen by the steady-state RGA shown in eq. (11.14) and from the plot in Figure 11.3

$$\begin{bmatrix} x_2 \\ P_{100} \\ T_{201} \end{bmatrix} = G_{CS\ 3} \begin{bmatrix} P_{100} \\ F_{200} \\ F_3 \end{bmatrix} \tag{11.13}$$

we have the following steady-state RGA and pairing:

$$RGA_{CS\ 3}(0) = \begin{bmatrix} 0 & 0.0622 & 0.9378 \\ 1 & 0 & 0 \\ 0 & 0.9378 & 0.0622 \end{bmatrix} \quad \Rightarrow \quad \begin{array}{ccc} c & & u \\ \hline T_{201} & \leftrightarrow & F_{200} \\ P_{100} & \leftrightarrow & P_{100} \\ x_2 & \leftrightarrow & F_3 \end{array} \tag{11.14}$$

All poles and zeros are in the left half plane, so no fundamental limitations for control should be expected.

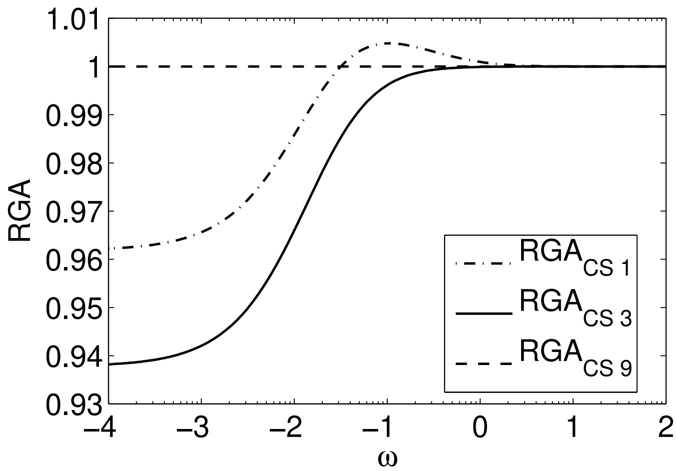

Figure 11.3: *Plot of $RGA^{1,3}$ for control structure CS 1, CS 3 and CS 9 with respect to frequency*

11.4.3 Control structure analysis CS 9

Controlling F_{200} as a self-optimizing variable, implies fixing one additional input (already fixed P_{100} and x_2) and the resulting RGA (independent of frequency) and corresponding pairing are:

$$RGA_{CS\ 9}(\omega) = \begin{bmatrix} 0 & 0 & 1 \\ 1 & 0 & 0 \\ 0 & 1 & 0 \end{bmatrix} \Rightarrow \begin{array}{ccc} c & & u \\ \hline F_{200} & \leftrightarrow & F_{200} \\ P_{100} & \leftrightarrow & P_{100} \\ x_2 & \leftrightarrow & F_3 \end{array} \tag{11.15}$$

11.5 Dynamic simulations using non-linear model

For the three candidates, a decentralized control structure was designed using PI controllers tuned with Skogestad's IMC tuning rules (Skogestad, 2003). The sequential disturbance signal shown in Figure 11.4 was imposed. The disturbance signal is modeled as step signals passing through a first order filter with time constant τ_{d_i} and a duration T_{d_i}, see Table 11.7 for data on each disturbance. The measurement lag is assumed to be modeled as a first-order process with a time constant of $\tau = 0.1$ and it is assumed no measurement error.

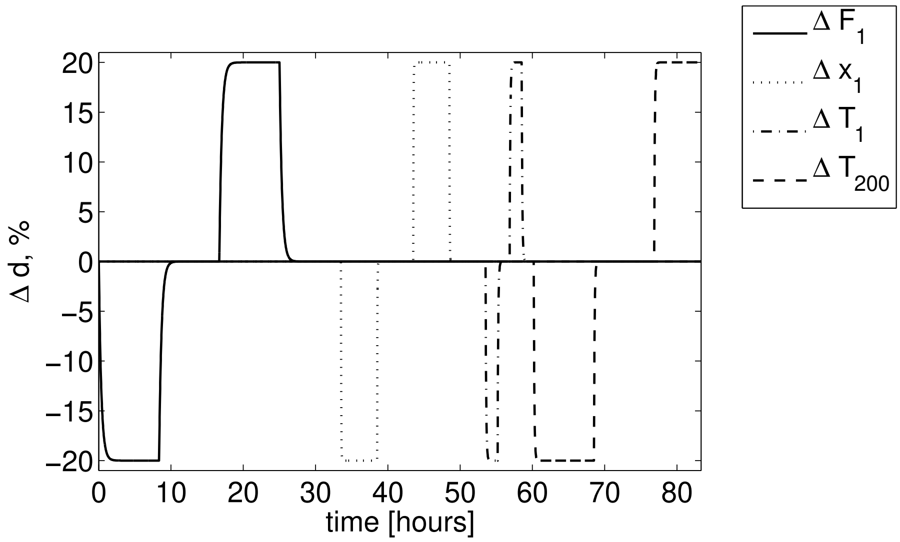

Figure 11.4: *Plot of imposed disturbance signal (all variables in percent of nominal value).*

Table 11.7: *Step duration and time constant for the disturbance signal*

d	T_{d_i} [min]	τ_{d_i} [min]
F_1	500	20
x_1	300	2
T_1	100	5
T_{200}	500	5

11.5.1 Dynamic cost for the candidates

Figure 11.5 shows the dynamic objective function value for all three control structures. The resulting average dynamic operating cost is given in Table 11.8. The dynamic

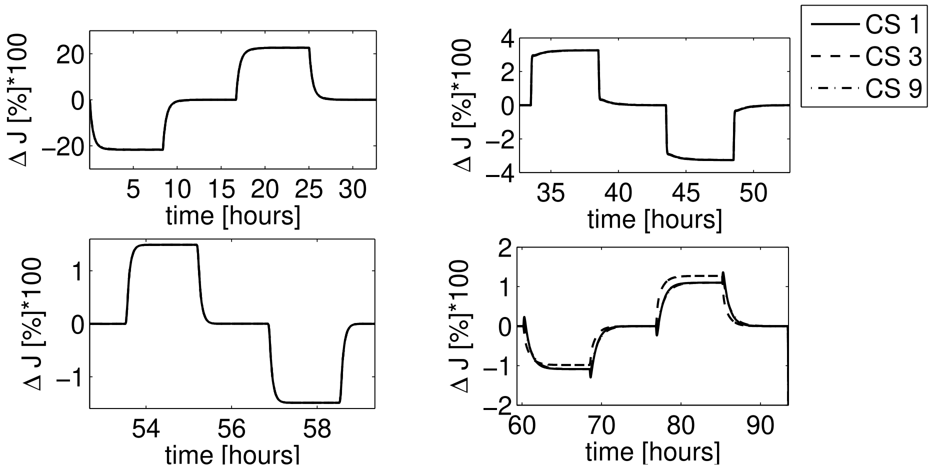

Figure 11.5: *Plot of objective (percentage relative change from the nominal objective value* $\frac{J-J^*}{J^*}100[\%]$*) for control structures* CS 1 *(*c_{ns}*),* CS 3 *(*T_{201}*) and* CS 9 *(*F_{200}*).*

Table 11.8: *Average dynamic cost for the self-optimizing control structures*

$CS\#$	Average cost $[/hour]$
1	6199.8
9	6200.7
3	6201.3

Table 11.9: *Average cost in period when disturbance* T_{201} *is active*

$CS\#$	Average cost $[/hour]$
1	6195.5
9	6195.5
3	6199.7

economic performance for all structures are similar as seen from Table 11.8, which confirms the stead-state results of Table 11.5, with CS 1 having a slightly better performance. As seen from Figure 11.5 and 11.6 the largest deviations between the candidates with respect to the operating cost is for the disturbances F_1 and T_{200}. For a disturbance in T_{200} (the lower right plot in Figure 11.5) the steady-state cost is higher for candidate CS 3 than CS 1 and CS 9. The average dynamic cost for the same period is shown in Table 11.9 which confirms this. For a disturbance in F_1, the loss is higher for CS 9 than for CS 1 and CS 3, see Figure 11.6, which confirm the findings in Table 11.5. For the other disturbances, all candidates show the same dynamic loss. The similar overall losses illustrate two points. First, the results show that there are no limitations in controlling the linear combination of measurements, since the performance is as good as controlling only one variable. This is of course not a general result, but for this case it applies. Second, these results show that the lower

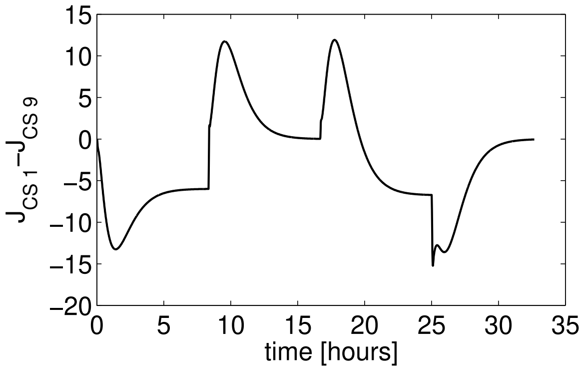

Figure 11.6: *Plot of the difference in cost ($J_{CS\ 1} - J_{CS\ 9}$) for the disturbance in F_1*

losses for the candidate CS 1 are minor, and a simpler structure (e.g. fixing F_{200}) may be preferable from an implementation point of view.

11.5.2 Constraints

Figure 11.7 plots the concentration of the product x_2 for all three structures. All structures keep the concentration above the constraint. Minor differences are observed for a disturbance in T_{200}, where controlling T_{201} gives a somewhat faster response, and for a disturbance in F_1 where candidate CS 9 shows longer rise time. Figure 11.8 shows

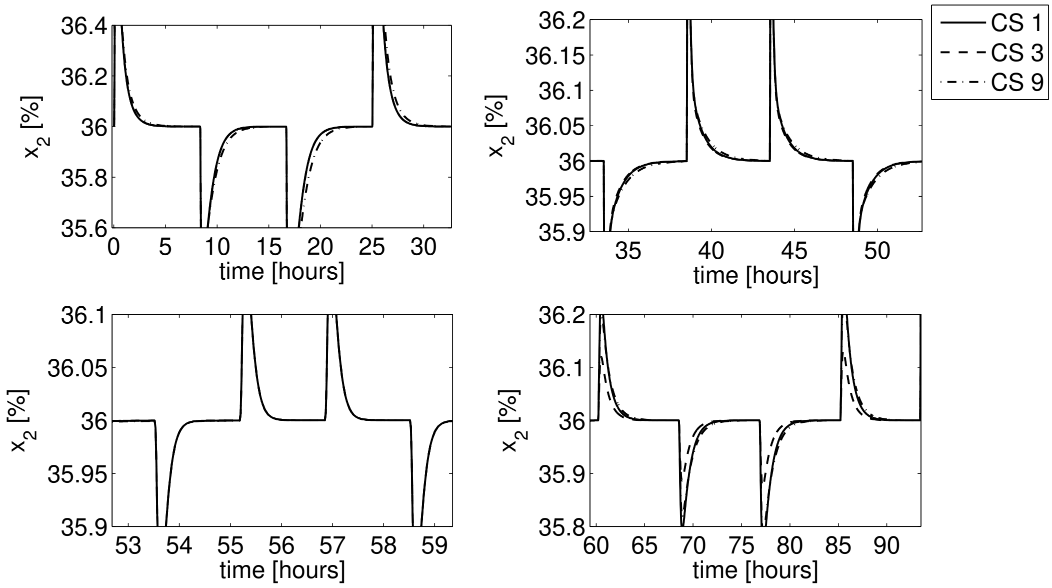

Figure 11.7: *Plot of the product composition (x_2) for the three control structures. Note that the scaling on the ordinate axis is different for the four sub-plots*

the pressure in the evaporator (P_2) for all candidates. For control structures CS 1 and

CS 3, the performance are similar and both structures violate the minimum allowed pressure for the feed disturbance as pointed out earlier. For the disturbance T_{201} the variation in P_2 is smaller for CS 3. Control structure CS 9 shows a larger constraint violation in P_2 and also touches the upper constraint. When including measurement

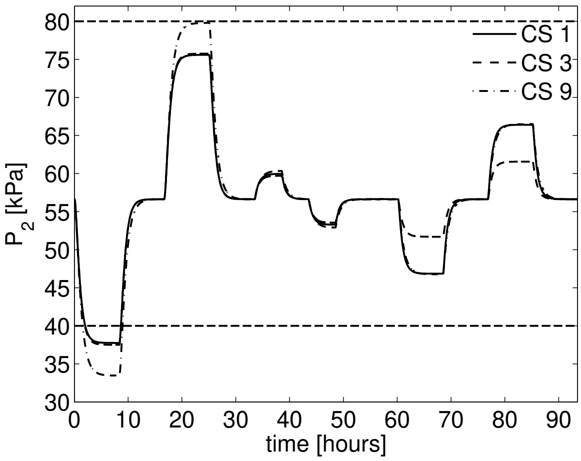

Figure 11.8: *Plot of evaporator pressure (P_2) for the three control structures*

Table 11.10: *Average dynamic cost for all structures including disturbances and noise*

$CS\#$	Average cost $[/hour]$
1	6199.8
9	6200.7
3	6201.3

error, all candidates show the same performance. The steady-state loss is shown in Table 11.5 and the corresponding dynamic cost is shown in Table 11.10. As seen from Table 11.10, including measurement error does not affect the economic performance to a great extent nor does it alter the rank between the candidates.

11.5.3 Cascade structure for self-optimizing control

As proposed by Cao (2003), one approach to avoid constraint violation is to use a cascade control structure as illustrated in Figure 11.9. The inner loops correspond to

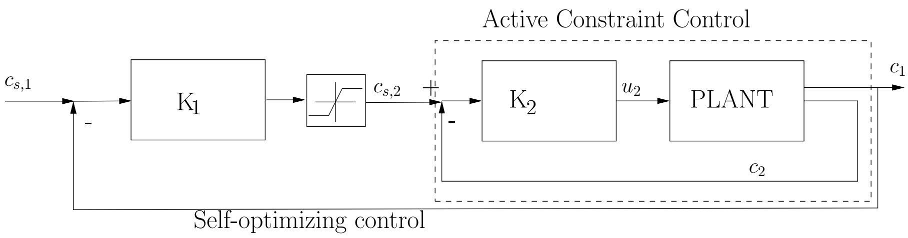

Figure 11.9: *Cascade structure for implementing active and partially active constraints, including saturation block for the input to the inner loop.*

the active constraints, i.e. controlling P_2, x_2 and P_{100}. For active or partially active constraints, we close these loops using the available inputs. The set points ($c_{s,2}$) for the controlled variables in the inner loops are the outputs from the controller in the outer loop. Normally, some constraints are always active for all disturbances and should be controlled without any change of the setpoints by the outer loop. Some constraints may be partially active and the setpoint for that loop is given by the outer loop when not active. We use the saturation block to override the self-optimizing loops when these constraints become active. This structure has been implemented for the pressure in the evaporator (P_2) which is partially active for one the feed flow disturbances. For the inner loops (the active constraints) we have the following manipulated and controlled variables

$$\begin{bmatrix} x_2 \\ P_{100} \\ P_2 \end{bmatrix} = G_{AC} \begin{bmatrix} P_{100} \\ F_{200} \\ F_3 \end{bmatrix} \tag{11.16}$$

The steady state RGA is

$$RGA_{AC} = \begin{bmatrix} 0 & 0.357 & 0.643 \\ 1 & 0 & 0 \\ 0 & 0.643 & 0.0357 \end{bmatrix} \tag{11.17}$$

and the frequency dependent RGA (not shown) gives the same pairing. Based on the RGA, the following pairing is proposed:

$$\begin{array}{ccc} c & & u \\ \hline P_2 & \leftrightarrow & F_{200} \\ P_{100} & \leftrightarrow & P_{100} \\ x_2 & \leftrightarrow & F_3 \end{array} \tag{11.18}$$

After closing the inner loops, the set point $c_s^{P_2}$ is used as the manipulated variable for the self-optimizing control loop. All loops are closed using PI-controllers tuned with Skogestad IMC tuning rules. The cascade structure ensures near optimal operation for all disturbances if the self-optimizing controlled variable (which is active when not all degrees of freedom are used in controlling the active constraints) shows good self-optimizing properties. The disturbance signal in Figure 11.4 (the same as in the previous simulation) is imposed. The average dynamic cost for the cascade structure is shown in Table 11.11 and as seen from Figure 11.10 the constraint on P_2 is not violated. Note that the effect on the average loss is small, but the system remains feasible for all disturbances. To conclude, the candidate synthesized using the null space method shows the best steady-state and dynamic self-optimizing properties, and is the best candidate for control. Since the improvement in performance is minor, a simpler structure such as $CS9$, where we keep the last input constant, may be favorable.

11.6 Conclusions

Here we study control structure selection for an evaporator example. The new proposed structure, using the null space method, has improved self-optimizing properties as

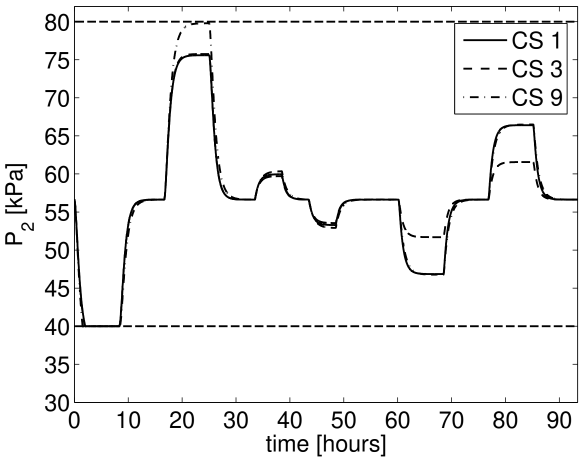

Figure 11.10: *Plot of evaporator pressure (P_2) for all candidate control structures using cascade.*

Table 11.11: *Average cost for all structures for the cascade structure.*

$CS\#$	Average cost [$/hour$]
1	6199.9
9	6200.5
3	6201.4

compared to previously proposed structures. The idea of disturbance discrimination in the null space method has also been illustrated. We find that it is possible to lump disturbances together, reducing the number of measurements needed in the null space method without any penalty on the loss.

Bibliography

Cao, Y. (2003). Self-optimizing control structure selection via differentiation. *in European Control Conference (ECC 2003)*, pages 445–453. In CDROM.

Govatsmark, M. (2003). *Integrated optimization and control*. PhD thesis, Norwegian University of Science and Technology.

Govatsmark, M. and Skogestad, S. (2001). Control structure selection for an evaporation process. *European Symposium on Computer Aided Process Engineering, May 27-30, 2001, Kolding, Denmark*, 9:657–662. See C01-1, Volume 1, HS2001-6.

Halvorsen, I., Skogestad, S., Morud, J., and Alstad, V. (2003). Optimal selection of controlled variables. *Ind. Eng. Chem. Res.*, 42(14):3273–3284.

Maarleveld, A. and Rijnsdorp, J. (1970). Constraint control on distillation columns. *Automatica*, 6(1):51–58. 1.

Newell, R. and Lee, P. (1989). *Applied process control - A Case study*. Prentice Hall.

Skogestad, S. (2003). Simple analytic rules for model reduction and PID controller tuning. *J. Proc. Control,*, 13:291–309.

Skogestad, S. and Postlethwaite, I. (1996). *Multivariable Feedback Control*. John Wiley & Sons.

Wang, F. and Cameron, I. (1994). Control studies on a model evaporation process - Constraint state driving with conventional and higher relative degree systems. *J. Proc. Control*, 4(2):59–75.

Chapter 12

Concluding remarks and further work

12.1 Concluding remarks

This thesis has dealt with the selection of controlled variables that are self-optimizing. The simplicity of the self-optimizing control structure, where we can achieve acceptable economic operation with constant setpoints, is the main motivation for this thesis. We have proposed a new method, the null space method, for the selection of controlled variables as measurement combinations, $\mathbf{c} = \mathbf{H}\mathbf{y}$. Let $\mathbf{F}$ be the optimal sensitivity matrix $\Delta\mathbf{y}^{opt} = \mathbf{F}\Delta\mathbf{d}$ and we propose to select the coefficient matrix $\mathbf{H}$ such that $\mathbf{H}\mathbf{F} = 0$ (the left null space). In forming the controlled variables, we need as many measurements as there are unconstrained inputs and disturbances.

We generalized the null space method to include measurement errors, and proposed a procedure for selecting the best subset of measurements to reduce the effects of measurement error on the loss. The procedure is split in two. First, we select the minimum required number of measurements (to reduce the effect of measurement error) based on maximizing the minimum singular value of the steady-state augmented plant. Second, we combine the measurements using the null space method (to reduce the effect of the disturbance), and form controlled variables as $\mathbf{c} = \mathbf{H}\mathbf{y}$. We applied the procedure to a case study of the Petlyuk column, and we found measurements that are insensitive to measurement errors.

The null space method has been applied to several case studies. For a Petlyuk distillation column, we found that we could achieve acceptable steady-state economic performance when fixing one of the unconstrained degrees of freedom (R_V) and controlling a combination of temperatures using the last unconstrained degree of freedom (R_L). The disturbance loss is small and the dynamic performance is acceptable. We compared this structure with previously proposed structures (the DT_S) and found that the structure using the null space method gave the best self-optimizing performance. We also used the singular value method of Skogestad and Postlethwaite (1996) to synthesize a self-optimizing control structure, and we found a structure with almost as good self-optimizing properties as the one using the null space method. We found that failing to utilize the remaining unconstrained degrees of freedom yields large losses and is not recommended. .

We have shown that using non-optimal setpoints do not affect the internal ranking of candidate controlled variables. In fact, we found that the average increase in loss is independent of what we select to control. However, if the loss is not acceptable we must put effort into finding a better estimate on the nominal optimal point.

For the Petlyuk distillation column we found that it is optimal to over-fractionate one of the product streams to save energy. We derived explicit expressions for the possible savings using the Underwood equations (Underwood, 1948). The physical explanation for this is that when the required separation work in the top and bottom of the main column is different, we can use the "extra" energy to over-fractionate the non-limiting section. Additional savings is possible by bypassing some of the feed and mix it with the over-fractionated product stream. This requires that we can accept all three components in one of the products.

The gas-lift case considers the optimal distribution of lift-gas for increased oil production. We found that controlling the total gas flow rate at the outlet of the process at the constraint, is most important for good economic performance. The additional savings for using the null space method for the design of the controlled variables, are in the range $1.8 - 3.6$ million \$/year. The second case study considered a special type of reservoir, where the ratio of gas and oil from the reservoir depends on the rate of production. We found that by using practically available measurements we could achieve acceptable operation using the null space method as compared to other candidates using flow measurements from each well. We found that controlling the choke valves (keeping the inputs constant) yield unacceptable operation, and is not recommended.

In the evaporator process, we compared the singular value method (Skogestad and Postlethwaite, 1996; Halvorsen et al., 2003) with the null space method. We found that we could achieve good self-optimizing control by controlling a combination of three measurements with the same performance as previously proposed structures that required direct disturbance information ($T_{201} - T_{200}$ and F_{200}/F_1). To remain feasible using nominal setpoints, we used a cascade structure as proposed by (Cao, 2004).

12.2 Directions for further work

12.2.1 Model uncertainty

The effect of model uncertainty when selecting controlled variables based on economics should be studied in more detail. We have shown that *parametric uncertainty* can be handled in the null space method. However, it is unclear how *structural model uncertainty* would affect the loss for structures synthesized using the null space method. Structural model uncertainty is difficult to describe mathematically. One way to handle structural model uncertainty is through the measurement error. However, then the measurement errors are correlated and we must find methods for describing the correlation.

12.2.2 Experimental verification

Controlling measurement combinations should be verified by experiments. A promising case study would be the Petlyuk column, where the potential losses are large if not operating close to the optimal point. The Petlyuk column is also interesting from a dynamic point of view. It has been stated in the literature that in order to achieve good dynamic performance, a model based controller such as MPC is necessary (Adrian et al., 2004), which should be investigated in more detail. The simulations in this thesis show that acceptable operation can be achieved using a decentralized control structure.

12.2.3 Disturbance discrimination

The methods for disturbance discrimination presented here are crude, and better methods for finding what disturbances to include in the design and analysis of self-optimizing control structures should be studied in more detail.

12.2.4 More case studies

More cases should be studied using the existing tools for selecting self-optimizing controlled variables. Focus should be on large scale systems, see for example (Luyben et al., 1998).

12.2.5 Active constraints

One important limitation of self-optimizing control is the assumption of a constant set of active constraints. This limits the applicability for systems with many constraints and where they change depending on the value of the disturbances. The methods of (Cao, 2004) should be studied in more detail.

12.3 Case studies

12.3.1 Case studies in Chapter 10

The models used in the study of the gas-lift optimization and the rate-dependent GOR in Chapter 10 should be improved. In the work here, we used a simple pseudo-one phase assumption on flow equations, and a simple thermodynamic model.

Bibliography

Adrian, T., Schoenmakers, H., and Boll, M. (2004). Model predictive control of integrated unit operations: Control of a divided wall column. *Chem. Eng. Process*, 43:347–355.

Cao, Y. (2004). Controlled variable selection for static self-optimising control. *in the IFAC Symposium on Advanced Control of Chemical Processes (ADCHEM) 2003, (Hong Kong)*, pages 63–71. In CDROM.

Halvorsen, I., Skogestad, S., Morud, J., and Alstad, V. (2003). Optimal selection of controlled variables. *Ind. Eng. Chem. Res.*, 42(14):3273–3284.

Luyben, W., Tyreus, B., and Luyben, M. (1998). *Plantwide process control.* McGraw-Hill.

Skogestad, S. and Postlethwaite, I. (1996). *Multivariable Feedback Control.* John Wiley & Sons.

Underwood, A. (1948). Fractional distillation of multi-component mixtures. *Chem. Eng. Prog.*, 44(8):603–614.

Appendix A

Extended null space method

Manuscript in preparation

Here we extend the null space method of Chapter 3 to a more general class of models and we derive explicit solutions for the optimal inputs parameterized in the disturbances $\mathbf{d}$. We derive controlled variables parameterized in $\mathbf{d}$ that when kept at constant setpoint yield optimal operation. We need explicit disturbance information by means of direct measurement of inferred by other measurements. The extended method for selecting controlled variables is illustrated on a simple continuous-stirred-tank reactor.

A.1 Introduction

Increasing demands on more economical and environmental operation of process plants, have introduced more focus on the optimal operation. In Chapter 2, we listed several alternative methods for ensuring optimal operation:

1. Optimal control
2. Real time optimization
3. Self-optimizing control

Here we extend the ideas of the null space method of Alstad and Skogestad (2004), in which controlled variables are selected as linear combinations of the measurements. The extension is to include the uncertain parameters (disturbances) explicitly in the controlled variables, while retaining the self-optimizing properties of the null space method. The idea of the null space method is to map the optimality condition onto the measurement space. Mathematically, the method proposed in Alstad and Skogestad (2004) assume a linear relation between the optimal outputs and the disturbances

$$\Delta\mathbf{y}^{opt} = \mathbf{F}\Delta\mathbf{d} \tag{A.1}$$

where $\Delta\mathbf{y}^{opt}$ is a $n_y \times 1$ vector and we select controlled variables $c_i = \mathbf{h}_i\mathbf{y}$ where $\mathbf{h}_i$ is a $1 \times n_y$ vector and selected to be in the left null space of $\mathbf{F}$. This implies a perfect self-optimizing structure for small perturbation of the disturbance around the optimal nominal point. The performance of the self-optimizing control structure depends on the degree of non-linearity of the problem where a highly non-linear system may be poorly described by the linear relation of eq. (A.1) which may result in poor self-optimizing properties.

To address this, we extend the null space method to include non-linearity with respect to the disturbances, and we limit the work to a special class of models. For the moment, assume that the relation between the optimal change of the outputs and the disturbances are given by eq. (A.2)

$$\Delta \mathbf{y}^{opt} = \mathcal{F}(\mathbf{d}) \tag{A.2}$$

and we would select controlled variables such that $\mathbf{h}_i$ is in the null space of $\mathcal{F}(\mathbf{d})$.

A.2 Optimal operation

Typically, optimal operation is formulated as a mathematical programming problem where the purpose is to minimize some time average of the objective (J) of the plant (Biegler et al., 2002)

$$\min_{\mathbf{x}_0 \in \mathcal{X}_0, \mathbf{u}_0 \in \mathcal{U}_0, \mathbf{d} \in \mathcal{D}} \int_{t \in T} J_0(t, \mathbf{x}_0, \mathbf{u}_0, \mathbf{d}) \mathrm{d}t \tag{A.3}$$

s.t.

$$\frac{\mathrm{d}\mathbf{x}_0}{\mathrm{d}t} = \mathbf{f}(t, \mathbf{x}_0, \mathbf{u}_0, \mathbf{d}) \tag{A.4}$$

$$\mathbf{p}(t, \mathbf{x}_0, \mathbf{u}_0, \mathbf{d}) = 0 \tag{A.5}$$

$$\mathbf{g}(t, \mathbf{x}_0, \mathbf{u}_0, \mathbf{d}) \leq 0 \tag{A.6}$$

where $\mathbf{x}_0$ is the vector of states, $\mathbf{u}_0$ the inputs, $\mathbf{d}$ the parameters (disturbances), $\mathbf{f}$ is the right-hand side of the differential equations, $\mathbf{p}$ is the algebraic equations, and $\mathbf{g}$ defines the inequality constraints that need to be fulfilled. For a given disturbance trajectory $\mathbf{d}(t)$, the problem of eq. (A.3) can be solved using regular NLP solvers (often variations of Successive Quadratic Programming (SQP) methods). Due to the computationally complexity of solving problems of this type and the need for a disturbance prediction model (or feedback from the process for estimating the parameters $\mathbf{d}$), a pseudo-steady state assumption is often made, resulting in:

$$\min_{\mathbf{x}_0 \in \mathcal{X}_0, \mathbf{u}_0 \in \mathcal{U}_0, \mathbf{d} \in \mathcal{D}} J(\mathbf{x}_0, \mathbf{u}_0, \mathbf{d}) \tag{A.7}$$

s.t.

$$\mathbf{f}'(\mathbf{x}_0, \mathbf{u}_0, \mathbf{d}) = 0 \tag{A.8}$$

$$\mathbf{g}(\mathbf{x}_0, \mathbf{u}_0, \mathbf{d}) \leq 0 \tag{A.9}$$

where $\mathbf{f}'^T = [\mathbf{f}^T \ \mathbf{p}^T]$. For a given disturbance $\mathbf{d}$, the problem in eq. (A.7) can be solved and the optimal inputs ($\mathbf{u}_0^{opt}$) implemented in the plant resulting in the optimal states ($\mathbf{x}_0^{opt}$). If the disturbances do not vary with time, this could be performed off-line once and the process would be operating optimally. New setpoints are calculated and implemented in an open-loop fashion, only if product specifications change. In most systems, the disturbances vary and keeping the operation at the nominal optimal value may lead to non-optimal operation and resulting economic loss. In order to address this, some sort of feedback from the process is necessary: Key steps in ensuring optimality are:

1. Detect that a change in the disturbances has happened.
2. Update the underlying model using available measurements (information) in the plant.
3. Redo the optimization with the updated model.
4. Implement new optimal values in the control system and start over.

One approach for ensuring optimality is Real-Time Optimization (RTO) (Cutler and Perry, 1983; Marlin and Hrymak, 1997). RTO is a much used method for ensuring optimal operation in presence of varying disturbances. In the RTO framework, new setpoints for the control layer are calculated on-line and implemented by the underlying control layer. An illustration of a typical RTO system is given in Figure A.1 (Marlin and Hrymak, 1997). The RTO framework uses online measurements as feedback in

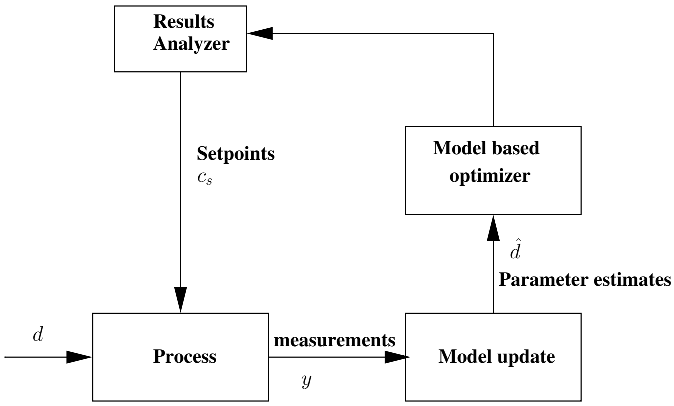

Figure A.1: *Illustration of a typical RTO structure*

order to update the models of the plant used for optimization. An optimization is carried out, and the result is analyzed, before implemented in the process. The RTO can be fully automated or semi-automated, depending on the complexity of the system and the details of the model.

As compared to RTO, the self-optimizing control framework tries to incorporate the identification and the optimization in the control layer by selecting controlled variables that when kept at constant setpoints give near optimal operation. Thus, the local feedback loop ensures optimal operation, which implies that no model needs to be updated online. In order for self-optimizing control to be an alternative, the set of active constraints (the subset of the inequality constraints $\mathbf{g}$ that is active) must be constant for all disturbances (see Section 11.5.3 for a method to relax this assumption). Mathematically, this implies that a subset $\mathbf{g}' \in \mathbf{g}$ is active such that $\mathbf{g}' = 0 \; \forall \; \mathbf{d} \in \mathcal{D}$.

The resulting optimization problem has only equality constraints where we use a subset of the inputs $\mathbf{u}_0$ to enforce the active inequality constraints.

$$\mathbf{f}'' = \begin{bmatrix} \mathbf{f}' \\ \mathbf{g}' \end{bmatrix} \tag{A.10}$$

For many chemical processes, this prerequisite is valid, at least for small perturbations of the disturbance. Typically, production is constrained by the capacity of the plant, which translates into the situation that many of the degrees of freedom are used for active constraints. Implementation in such cases is often simple, by which we can utilize the ideas of active constraint control (Maarleveld and Rijnsdorp, 1970). As pointed out by Govatsmark (2003), normally it is possible to assign a single measured (or estimated) variable y related to each constraint and use the relation

$$g_i = y_i - y_{i,max} \quad \text{or} \quad g_i = y_{i,min} - y_i \tag{A.11}$$

depending on the constraint being a maximum or a minimum. We here assume that the constraints can be measured or inferred from indirect measurements. In the following we simplify the notation and let $\mathbf{f}$ denote all equality constraints (including the active inequality constraints).

A.2.1 Mapping of the optimality condition on the measurement space

The idea of self-optimizing control (Skogestad, 2000) is to find controlled variables that when kept at constant setpoints, indirectly give optimal operation. This correspond to finding feedback controlled variables that, when a disturbance enters the plant, result in the (near) optimal inputs as given by:

$$(\mathbf{x}_0^{opt}(\mathbf{d}), \mathbf{u}_0^{opt}(\mathbf{d})) = arg\left[\min_{\mathbf{x}_0,\mathbf{u}_0} \; J(\mathbf{x}_0, \mathbf{u}_0, \mathbf{d})\right] \tag{A.12}$$

s.t.

$$\mathbf{f}(\mathbf{x}_0, \mathbf{u}_0, \mathbf{d}) = 0 \tag{A.13}$$

$$\mathbf{g}(\mathbf{x}_0, \mathbf{u}_0, \mathbf{d}) \leq 0 \tag{A.14}$$

The optimal point $\left(\mathbf{x}_0^{opt}(\mathbf{d}), \mathbf{u}_0^{opt}(\mathbf{d})\right)$, depends on the disturbance $\mathbf{d}$ and the idea is to map the optimality condition onto the output space and by using feedback control, indirectly keep the system optimal.

To illustrate, assume that the optimal objective is given as in Figure A.2 and that we map the optimality into the measurement space. For each disturbance, this corresponds to the optimal output vector $\mathbf{y}^{opt}(d)^T = [y_1^{opt}(d) \; y_2^{opt}(d) \; y_3^{opt}(d)]$ which is a point in the measurement space. We see from Figure (A.2) that the objective is smooth with respect to the disturbances, and that the mapping is smooth.

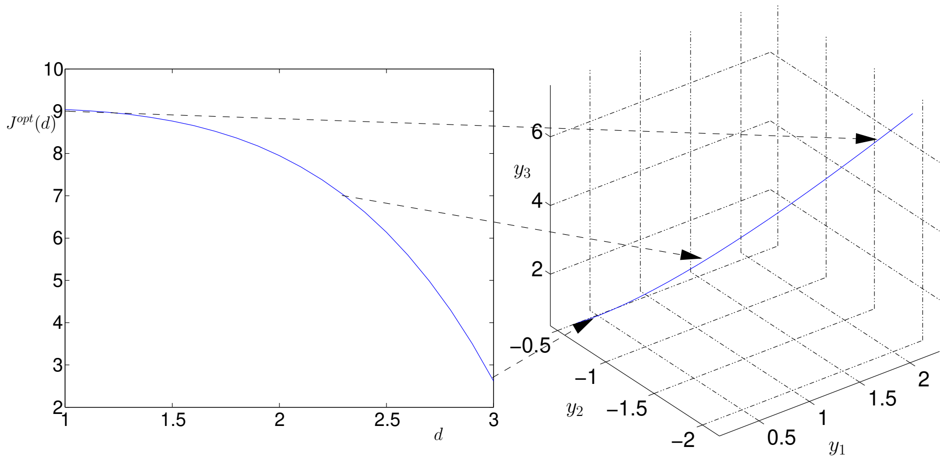

Figure A.2: *Optimal objective value $J^{opt}(d)$ with respect to the disturbance d and the mapping into output space.*

A.3 Optimality condition and class of models

Consider the simplified problem where we have assumed that all active inequality constraints are enforced.

$$\min_{\mathbf{x},\mathbf{u}} J = J(\mathbf{x}, \mathbf{u}, \mathbf{d}) \tag{A.15}$$

$$\text{s.t.} \quad \mathbf{f}(\mathbf{x}, \mathbf{u}, \mathbf{d}) = 0 \tag{A.16}$$

where $\mathbf{u}$ is the remaining degrees of freedom. The goal here is to derive explicitly how the optimal input depends on the disturbances.

A.3.1 First order optimality condition

With the objective function and model as given by eqs. (A.15) and (A.16), the first order optimality condition is given by (considering $\mathbf{d}$ as a parameter) (Stengel, 1993):

$$\frac{\partial J}{\partial \mathbf{u}} + \frac{\partial \mathbf{x}^T}{\partial \mathbf{u}} \frac{\partial J}{\partial \mathbf{x}} = 0 \tag{A.17}$$

where

$$\frac{\partial \mathbf{f}}{\partial \mathbf{u}^T} + \frac{\partial \mathbf{f}}{\partial \mathbf{x}^T} \frac{\partial \mathbf{x}}{\partial \mathbf{u}^T} \tag{A.18}$$

and

$$\mathbf{f}(\mathbf{x}, \mathbf{u}, \mathbf{d}) = 0 \tag{A.19}$$

Assuming that $\left(\frac{\partial \mathbf{f}}{\partial \mathbf{x}^T}\right)$ is invertible yields

$$\frac{\partial \mathbf{x}}{\partial \mathbf{u}^T} = -\left[\frac{\partial \mathbf{f}}{\partial \mathbf{x}^T}\right]^{-1} \frac{\partial \mathbf{f}}{\partial \mathbf{u}^T} \tag{A.20}$$

which yields the first order optimality condition

$$\frac{\partial J}{\partial \mathbf{u}} - \left[\left[\frac{\partial \mathbf{f}}{\partial \mathbf{x}^T} \right]^{-1} \frac{\partial \mathbf{f}}{\partial \mathbf{u}^T} \right]^T \frac{\partial J}{\partial \mathbf{x}} = 0 \tag{A.21}$$

The n_u equations in eq. (A.21) is used to find $\mathbf{u}$, while eq. (A.19) gives n_x equations to define the state variables ($\mathbf{x}$). Assume that

1. no state information is available (in general this assumption may be relaxed using an estimator) and that
2. the disturbances can be measured directly or inferred from indirect measurements.

This limits the class of problems, both with respect to the form of the objective function and the model equations. The class of problems treated here is:

1. The objective function (J) can be second order with respect to the states ($\mathbf{x}$) , the inputs ($\mathbf{u}$) and the disturbances ($\mathbf{d}$).
2. The equality constraint equations $\mathbf{f}$ must be linear with respect to the states ($\mathbf{x}$) and inputs ($\mathbf{u}$).

If the original problem does not fit this class of models, a Taylor series expansion of the system yields the assumed form. Next, we formulate a second order accurate expression of the objective function.

A.3.2 Second order accurate Taylor series expansion of the objective function

First, consider the Taylor series expansion of the objective function and the process model as given by eqs. (A.15) and (A.16) around the nominal optimal point $(x^{opt}(d^*), u^{opt}(d^*)) = (x^*, u^*)$ where $\mathbf{d}^*$ is the nominal disturbance (Morud, 1995).

$$J \approx J_0 + \mathbf{J}_{\mathbf{x}}^T \Delta\mathbf{x} + \mathbf{J}_{\mathbf{u}}^T \Delta\mathbf{u} + \mathbf{J}_{\mathbf{d}}^T \Delta\mathbf{d} + \frac{1}{2} \begin{bmatrix} \Delta\mathbf{x}^T & \Delta\mathbf{u}^T & \Delta\mathbf{d}^T \end{bmatrix} \mathbf{H}_J \begin{bmatrix} \Delta\mathbf{x}^T & \Delta\mathbf{u}^T & \Delta\mathbf{d}^T \end{bmatrix}^T \tag{A.22}$$

where all partial derivatives are evaluated at the nominal optimal point. Similarly, for a general function $\mathbf{f}(\mathbf{x}, \mathbf{u}, \mathbf{d}) = 0$ we have the second-order Taylor series expansion:

$$0 \approx \Delta\mathbf{f} = \mathbf{f}_x^T \Delta\mathbf{x} + \mathbf{f}_u^T \Delta\mathbf{u} + \mathbf{f}_d^T \Delta\mathbf{d} + \frac{1}{2} \begin{bmatrix} \Delta\mathbf{x}^T & \Delta\mathbf{u}^T & \Delta\mathbf{d}^T \end{bmatrix} \mathbf{H}_f \begin{bmatrix} \Delta\mathbf{x}^T & \Delta\mathbf{u}^T & \Delta\mathbf{d}^T \end{bmatrix}^T \tag{A.23}$$

again with all partial derivatives evaluated at the nominal optimal point. Multiplying eq. (A.23) with λ^T, the Lagrangian multiplier yields

$$J \approx J_0 + \mathbf{L}_x^T \Delta\mathbf{x} + \mathbf{L}_u^T \Delta\mathbf{u} + \mathbf{L}_d^T \Delta\mathbf{d} + \frac{1}{2} \begin{bmatrix} \Delta\mathbf{x}^T & \Delta\mathbf{u}^T & \Delta\mathbf{d}^T \end{bmatrix} \mathbf{H}_L \begin{bmatrix} \Delta\mathbf{x}^T & \Delta\mathbf{u}^T & \Delta\mathbf{d}^T \end{bmatrix}^T \tag{A.24}$$

where $L \equiv J + \lambda^T \mathbf{f}$ is the Lagrangian function and $\mathbf{H}_L$ is the Hessian of the Lagrangian function.

$$\mathbf{H}_L = \begin{bmatrix} \mathbf{H}_{L,\mathbf{xx}} & \mathbf{H}_{L,\mathbf{xu}} & \mathbf{H}_{L,\mathbf{xd}} \\ \mathbf{H}_{L,\mathbf{ux}} & \mathbf{H}_{L,\mathbf{uu}} & \mathbf{H}_{L,\mathbf{ud}} \\ \mathbf{H}_{L,\mathbf{dx}} & \mathbf{H}_{L,\mathbf{du}} & \mathbf{H}_{L,\mathbf{dd}} \end{bmatrix} \tag{A.25}$$

At the nominal optimal point, $\mathbf{L_x} = 0$ and $\mathbf{L_u} = 0$ due to the first order conditions, so the second order accurate expansion may be written as

$$J \approx J_0 + \mathbf{L}_d^T \Delta\mathbf{d} + \frac{1}{2} \begin{bmatrix} \Delta\mathbf{x}^T & \Delta\mathbf{u}^T & \Delta\mathbf{d}^T \end{bmatrix} \mathbf{H}_L \begin{bmatrix} \Delta\mathbf{x}^T & \Delta\mathbf{u}^T & \Delta\mathbf{d}^T \end{bmatrix}^T \tag{A.26}$$

As pointed out by Morud (1995) this give an second order accurate representation of the objective function. Similar derivation is made in Morari et al. (1980) but they use a first order model of the process, and the resulting Taylor series expansion is not second order accurate.

A.3.3 Optimal inputs

Assume that the model equations are on the form

$$\mathbf{f} = \mathbf{A}(\mathbf{d})\mathbf{x} + \mathbf{B}(\mathbf{d})\mathbf{u} + \mathbf{e}(\mathbf{d}) = 0 \tag{A.27}$$

where $\mathbf{A}(\mathbf{d})$, $\mathbf{B}(\mathbf{d})$ and $\mathbf{e}(\mathbf{d})$ depend on $\mathbf{d}$. The process model is linear with respect to the states and the inputs, while non-linear with respect to the disturbances $\mathbf{d}$. To simplify notation we skip the explicit dependency on the disturbance vector $\mathbf{d}$. The restriction on the model class is necessary, in order to avoid the need of direct state information. In addition, we seek an explicit expression for the optimal inputs with respect to the disturbances, which requires linearity with respect to the inputs. Note that if the system can be modeled as in eq. (A.27), the Taylor series expansion above is simplified. If the model does not fit the model class, we can use the Taylor series expansion as given by eq. (A.23) where we truncate the expansion after first order terms for the states and the inputs, while we for the disturbances may have as high order as necessary (bit with no cross terms). Eq. (A.20) yields:

$$\frac{\partial \mathbf{x}}{\partial \mathbf{u}^T} = -[\mathbf{A}(\mathbf{d})]^{-1}\mathbf{B}(\mathbf{d}) \tag{A.28}$$

where we assume that $\mathbf{A}(\mathbf{d})$ is invertible for all $\mathbf{d}$. Assume that the objective function is given by eq. (A.26) which yields

$$\frac{\partial J}{\partial \Delta\mathbf{u}} = \frac{\partial J}{\partial \mathbf{u}} = \mathbf{H}_{L,\mathbf{uu}}\Delta\mathbf{u} + \mathbf{H}_{L,\mathbf{ux}}\Delta\mathbf{x} + \mathbf{H}_{L,\mathbf{ud}}\Delta\mathbf{d} \tag{A.29}$$

$$= \mathbf{H}_{L,\mathbf{uu}}\mathbf{u} + \mathbf{H}_{L,\mathbf{ux}}\mathbf{x} + \mathbf{H}_{L,\mathbf{ud}}\mathbf{d} + \mathbf{k_u}(\mathbf{d}^*) \tag{A.30}$$

and

$$\frac{\partial J}{\partial \Delta\mathbf{x}} = \frac{\partial J}{\partial \mathbf{x}} = \mathbf{H}_{L,\mathbf{xx}}\Delta\mathbf{x} + \mathbf{H}_{L,\mathbf{xu}}\Delta\mathbf{u} + \mathbf{H}_{L,\mathbf{xd}}\Delta\mathbf{d} \tag{A.31}$$

$$= \mathbf{H}_{L,\mathbf{xx}}\mathbf{x} + \mathbf{H}_{L,\mathbf{xu}}\mathbf{u} + \mathbf{H}_{L,\mathbf{xd}}\mathbf{d} + \mathbf{k_x}(\mathbf{d}^*) \tag{A.32}$$

where

$$\mathbf{k_u} = \mathbf{H}_{L,\mathbf{uu}}\mathbf{u}^* + \mathbf{H}_{L,\mathbf{ux}}\mathbf{x}^* + \mathbf{H}_{L,\mathbf{ud}}\mathbf{d}^* \tag{A.33}$$

$$\mathbf{k_x} = \mathbf{H}_{L,\mathbf{xx}}\mathbf{x}^* + \mathbf{H}_{L,\mathbf{xu}}\mathbf{u}^* + \mathbf{H}_{L,\mathbf{xd}}\mathbf{d}^* \tag{A.34}$$

are constant values given the nominal disturbance d^*. Substituting eq. (A.30) and (A.32) into (A.21) and solving for $\mathbf{u}^{opt}$ yields:

$$\begin{aligned}\mathbf{u}^{opt} = &-\left[\mathbf{H}_{L,\mathbf{uu}} - \left[\mathbf{A}(\mathbf{d})^{-1}\mathbf{B}(\mathbf{d})\right]^T \mathbf{H}_{L,\mathbf{xu}}\right]^{-1} \Big(\left[\mathbf{H}_{\mathbf{L},\mathbf{ux}} - \left[\mathbf{A}(\mathbf{d})^{-1}\mathbf{B}(\mathbf{d})\right]^T \mathbf{H}_{L,\mathbf{xx}}\right]\mathbf{x}^{opt} + \\ &\left[\mathbf{H}_{L,\mathbf{dd}} - \left[\mathbf{A}(\mathbf{d})^{-1}\mathbf{B}(\mathbf{u})\right]^T \mathbf{H}_{L,\mathbf{xd}}\right]\mathbf{d} + \left[\mathbf{k_u} - \left[\mathbf{A}(\mathbf{d})^{-1}\mathbf{B}(\mathbf{d})\right]^T \mathbf{k_x}\right]\Big) \\ = &-\mathcal{B}^{-1}\left[\mathcal{A}\mathbf{x}^{opt} + \mathcal{E}\mathbf{d} + \mathbf{k}\right]\end{aligned} \tag{A.35}$$

where

$$\mathcal{B} = \mathbf{H}_{L,\mathbf{uu}} - \left[\mathbf{A}(\mathbf{d})^{-1}\mathbf{B}(\mathbf{d})\right]^T \mathbf{H}_{L,\mathbf{xu}} \tag{A.36}$$

$$\mathcal{A} = \mathbf{H}_{\mathbf{L},\mathbf{ux}} - \left[\mathbf{A}(\mathbf{d})^{-1}\mathbf{B}(\mathbf{d})\right]^T \mathbf{H}_{L,\mathbf{xx}} \tag{A.37}$$

$$\mathcal{E} = \mathbf{H}_{L,\mathbf{dd}} - \left[\mathbf{A}(\mathbf{d})^{-1}\mathbf{B}(\mathbf{u})\right]^T \mathbf{H}_{L,\mathbf{xd}} \tag{A.38}$$

$$\mathbf{k} = \mathbf{k_u} - \left[\mathbf{A}(\mathbf{d})^{-1}\mathbf{B}(\mathbf{d})\right]^T \mathbf{k_x} \tag{A.39}$$

where we have assumed that $\mathcal{B}$ has full rank. Solving eq. (A.27) for $\mathbf{x}^{opt}$ yields

$$\mathbf{x}^{opt} = -\mathbf{A}(\mathbf{d})^{-1}\left[\mathbf{B}(\mathbf{d})\mathbf{u}^{opt} + \mathbf{e}(\mathbf{d})\right] \tag{A.40}$$

which inserted into eq. (A.35) and solved for $\mathbf{u}^{opt}$ gives

$$\mathbf{u}^{opt} = -\left[\mathcal{B} - \mathcal{A}\mathbf{A}(\mathbf{d})^{-1}\mathbf{B}(\mathbf{d})\right]^{-1}\left[\mathcal{E}\mathbf{d} - \mathcal{A}\mathbf{A}(\mathbf{d})^{-1}\mathbf{e}(\mathbf{d}) + \mathbf{k}\right] \tag{A.41}$$

which is explicit in $\mathbf{d}$. Using eq. (A.41) and (A.40) have an explicit expression for the optimal inputs and states with respect to the disturbances. The expression for the optimal input in eq. (A.41) resembles the expression for the optimal inputs as given by Halvorsen et al. (2003)

$$\Delta\mathbf{u}^{opt} = -\mathbf{J}_{uu}^{-1}\mathbf{J}_{ud}\Delta\mathbf{d} \tag{A.42}$$

if $\mathbf{e}(\mathbf{d})$ is a linear term. Thus, the major difference from the previous work is that we allow the process model to include non-linear terms with respect to the disturbances in the process model.

A.4 Optimal outputs

Based on the above explicit expressions for the inputs and states, we can calculate the optimal outputs. Assume that the measurement vector $\mathbf{y}$ is given by (the non-linear vector function)

$$\mathbf{y} = \mathbf{f}_y(\mathbf{x}, \mathbf{u}, \mathbf{d}) \tag{A.43}$$

and by inserting eq. (A.40) and (A.41) the optimal change for the measurements from the nominal disturbance $\mathbf{d}^*$ to a disturbance $\mathbf{d}$ is

$$\Delta\mathbf{y}^{opt} = \mathbf{y}^{opt}(\mathbf{d}) - \mathbf{y}^{opt}(\mathbf{d}^*) = \mathcal{F}(\mathbf{d},\mathbf{d}^*) = \\ \mathbf{f}_y\left(\mathbf{x}^{opt}(\mathbf{d}),\mathbf{u}^{opt}(\mathbf{d}),\mathbf{d}\right) - \mathbf{f}_y\left(\mathbf{x}^{opt}(\mathbf{d}^*),\mathbf{u}^{opt}(\mathbf{d}^*),\mathbf{d}^*\right) \quad \text{(A.44)}$$

which is generally a nonlinear vector function with respect to the disturbances. Below we illustrate the above derivations on a simple CSTR example.

Example A.1 *Consider an iso-thermal CSTR, with a first order reversible reaction*

$$A \rightleftharpoons B \quad \text{(A.45)}$$

with the following rate expression

$$r = k_1 C_A - k_2 C_B \quad \text{with} \quad k_i = C_i e^{\frac{-E_i}{RT}} \quad \text{(A.46)}$$

and component balances

$$\frac{\mathrm{d}C_a}{\mathrm{d}t} = \frac{1}{\tau}(C_{A,i} - C_A) - r \quad \frac{\mathrm{d}C_B}{\mathrm{d}t} = \frac{1}{\tau}(C_{B,i} - C_B) + r \quad \text{(A.47)}$$

where the states are $x^T = [C_A \quad C_B]$, the input $u = C_{A,i}$, and the disturbance $d = k_1$. The equations can be expressed on the form of eq. (A.27) where

$$\mathbf{A}(k_1) = \begin{bmatrix} -\frac{1}{\tau} - k_1 & k_2 \\ k_1 & -\frac{1}{\tau} - k_2 \end{bmatrix} \quad \mathbf{B} = \begin{bmatrix} \frac{1}{\tau} \\ 0 \end{bmatrix} \quad \mathbf{e} = \begin{bmatrix} 0 \\ \frac{C_{B,i}}{\tau} \end{bmatrix} \quad \text{(A.48)}$$

Solving for the states (assuming that $\mathbf{A}(d)$ is invertible) yields

$$\begin{bmatrix} C_A \\ C_B \end{bmatrix} = \frac{1}{1+\tau(k_1+k_2)} \begin{bmatrix} k_2\tau + 1 \\ k_1\tau \end{bmatrix} C_{A,i} + \frac{1}{1+\tau(k_1+k_2)} \begin{bmatrix} k_2\tau + C_{B,i} \\ C_{B,i}(1+k_1\tau) \end{bmatrix} \quad \text{(A.49)}$$

Assume that the objective of the plant operation is given by

$$J(u,\mathbf{x},d) = p_A C_A^2 + p_B C_B \quad \text{(A.50)}$$

where p_i is the price of the products. Here we assume that $p_A = -1 < 0$ and $p_B = 1 > 0$ such that there is a quadratic penalty for producing product with component A. The first order optimality condition in eq. (A.21) yields

$$\frac{\partial J}{\partial \mathbf{u}} - \left[\left[\frac{\partial \mathbf{f}}{\partial \mathbf{x}^T}\right]^{-1} \frac{\partial \mathbf{f}}{\partial \mathbf{u}^T}\right]^T \frac{\partial J}{\partial \mathbf{x}} = 0 + \frac{1}{1+\tau(k_1+k_2)} \begin{bmatrix} 1 + k_2\tau & k_1\tau \end{bmatrix} \begin{bmatrix} -2C_A \\ 1 \end{bmatrix} \quad \text{(A.51)}$$

Substituting for C_A from eq. (A.49) and solving for the optimal inputs ($C_{A,i}^{opt}$) gives

$$C_{A,i}^{opt} = -\frac{1}{2(1+k_2\tau)^2}\left[\tau k_2(k_2\tau + 2)C_{B,i} - \tau k_1(1 + k_1 + k_2\tau)\right] \quad \text{(A.52)}$$

and we have an explicit expression for the optimal inputs and states, which makes us able to find the optimal change in the outputs by substitution. Assume here, that the available measurements are $\mathbf{y} = [C_A \quad C_{A,i}]$*, then after some algebra:*

$$\begin{bmatrix} \Delta y_1^{opt} \\ \Delta y_2^{opt} \end{bmatrix} = \begin{bmatrix} C_A^{opt}(k_1) - C_A^{opt}(k_{10}) \\ C_{A,i}^{opt}(k_1) - C_{A,i}^{opt}(k_{10}) \end{bmatrix} = \begin{bmatrix} \frac{\tau}{2}\frac{k_1 - k_{10}}{k_2\tau+1} \\ \\ \frac{\tau^2}{2}\frac{k_1^2 - k_{10}^2}{(k_2\tau+1)^2} \end{bmatrix} \tag{A.53}$$

which correspond to the change in the optimal outputs for a change from k_{10} *to* k_1*. Note that the second element is nonlinear in* k_1*.*

A.5 Selection of controlled variables

In the framework of self-optimizing control, the optimal self-optimizing control variable is the one in which a change in the uncertain parameter (or disturbance) does not change the optimal value of the control variable (but may change the value of the controlled variable). This simple insight is used to find controlled variables that inhibits this property. In this work we consider the controlled variables on the form

$$\Delta \mathbf{c}(\mathbf{y}, \mathbf{u}, \mathbf{d}) = \sum_{i=1}^{n_u+n_d} \mathbf{h}_i(\mathbf{d}, \mathbf{d}^*)\Delta y_i(\mathbf{x}, \mathbf{u}, \mathbf{d}) \tag{A.54}$$

where the coefficient vector $\mathbf{h}_i$ depends on the disturbance vector $\mathbf{d}$. As discussed in Chapter 3, perfect self-optimizing control is achievable if

$$\Delta c_j^{opt} = \sum_{i=1}^{n_u+n_d} h_{ij}(\mathbf{d})\left(y_i^{opt}(\mathbf{d}) - y_i^{opt}(\mathbf{d}^*)\right) = \mathbf{h}_j(\mathbf{d})\Delta \mathbf{y}^{opt}(\mathbf{d}) = \mathbf{0} \tag{A.55}$$

where $\mathbf{h}_j = [h_{1j} \; h_{2j} \; \dots \; h_{n_y j}]$ is an $1 \times n_y$vector function and

$$\Delta \mathbf{y}^{opt} = [\Delta y_1^{opt} \; \Delta y_2^{opt} \; \dots \; \Delta y_{n_y}^{opt}]^T$$

which corresponds to selecting suitable weights for each measurement ($h_{ij}'s$) such that eq. (A.55) is fulfilled for all values of the uncertain parameters. For the simplest linear case ($\mathcal{F}$ is linear), a constant weight would be selected which corresponds to the null space method Alstad and Skogestad (2004). For the case of multiple controlled variables we have:

$$\Delta \mathbf{c}^{opt} = \mathcal{H}(\mathbf{d})\Delta \mathbf{y}^{opt}(\mathbf{d}) \tag{A.56}$$

where

$$\mathcal{H} = \begin{bmatrix} \mathbf{h}_j \\ \vdots \\ \mathbf{h}_{n_u} \end{bmatrix}$$

Below, we derive parameterized versions of the coefficient vector $\mathbf{h}$

A.5.1 Extended null space method

Assume for the moment that $\Delta\mathbf{y}^{opt} = \mathbf{F}\Delta\mathbf{d}$, where $\mathbf{F}$ is a constant matrix and $\mathbf{h}(\mathbf{d}) = \mathbf{H}$, a constant $n_c \times n_y$ matrix. Let $\mathbf{h_j}$ denote the j'th row of $\mathbf{H}$, then we see that we should select $\mathbf{h}_j$ such that they are in the left null space of $\mathbf{F}$ A

$$\mathbf{h}_j \in \mathcal{N}(\mathbf{F}^T), \quad j = 1..n_c \tag{A.57}$$

which yields $\mathbf{h}_j\mathbf{F} = 0$ for $i = 1..n_d$. For the general case, assume that $\Delta\mathbf{y}^{opt} = \mathcal{F}(\mathbf{d}) = [\mathcal{F}_1(\mathbf{d}) \ \ldots \ \mathcal{F}_{n_y}(\mathbf{d})]^T$, and we seek $\mathbf{h}_j(\mathbf{d})$ such that

$$\mathbf{h}_j\mathcal{F}(\mathbf{d}) = 0 \quad \forall j \Rightarrow h_{1j}\mathcal{F}_1(\mathbf{d}) + h_{2j}\mathcal{F}_2(\mathbf{d}) + \ldots + h_{n_yj}\mathcal{F}_{n_y}(\mathbf{d}) = 0 \tag{A.58}$$

Since direct disturbance information is available, in most cases one should add the corresponding disurbances to the measurement vector,

$$\mathbf{y}^T = \begin{bmatrix} y_1 & \ldots & y_{n_u} & d_1 & \ldots d_{n_d} \end{bmatrix} \tag{A.59}$$

so that

$$\mathbf{y}^{optT} = \begin{bmatrix} y_1^{opt} & \ldots & y_{n_u}^{opt} & d_1 & \ldots d_{n_d} \end{bmatrix} \tag{A.60}$$

It is clear that the number of measurements when requiring $\mathbf{h}\Delta\mathbf{y}^{opt} = 0$ is $n_y = n_u + n_d$. If we select to not include the disturbances in the measurements vector, we need $n_{y_t} = n_d + n_u + 1$ total measurements.

Remark. Number of measurements
To illustrate consider the following case, where $n_u = 2$, and let

$$\Delta y_1^{opt} = g_1 \quad \Delta y_2^{opt} = g_2 \quad \Delta y_3^{opt} = g_3 \tag{A.61}$$

Assume first that we want to use two measurements, then we have

$$h_1^1 g_1 + h_1^2 g_2 = 0 \Rightarrow h_1^1 = -h_1^2 \frac{g_2}{g_1} \tag{A.62}$$

$$h_2^1 g_1 + h_2^2 g_2 = 0 \Rightarrow h_2^2 = -h_2^1 \frac{g_1}{g_2} \tag{A.63}$$

which is equal to

$$\mathbf{H} = \begin{bmatrix} -h_1^2 \frac{g_2}{g_1} & h_1^2 \\ h_2^1 & -h_2^1 \frac{g_1}{g_2} \end{bmatrix} = \begin{bmatrix} -\frac{g_2}{g_1} & 1 \\ 1 & -\frac{g_1}{g_2} \end{bmatrix} \begin{bmatrix} -h_1^2 & 0 \\ 0 & h_2^1 \end{bmatrix} = 0 \tag{A.64}$$

which has rank equal 1. This implies that the two controlled variables are linearly dependent. Therefore, we must require the use of three measurements. Using three measurements, we get that

$$h_1^1 g_1 + h_1^2 g_2 + h_1^3 g_3 = 0 \Rightarrow h_1^1 = -h_1^2 \frac{g_2}{g_1} - h_1^3 \frac{g_3}{g_1} \tag{A.65}$$

$$h_2^1 g_1 + h_2^2 g_2 + h_2^3 g_3 = 0 \Rightarrow h_2^2 = -h_2^1 \frac{g_1}{g_2} - h_2^3 \frac{g_3}{g_2} \tag{A.66}$$

which corresponds to

$$\begin{bmatrix} -h_1^2 \frac{g_2}{g_1} - h_1^3 \frac{g_3}{g_1} & h_1^2 & h_1^3 \\ h_2^1 & -h_2^1 \frac{g_1}{g_2} - h_2^3 \frac{g_3}{g_2} & h_2^3 \end{bmatrix} = 0 \tag{A.67}$$

which has rank 2 (if $h_1^2 \vee h_1^3 \neq 0$ and $h_2^1 \vee h_2^3 \neq 0$).

We now revisit the CSTR example in order to find a self-optimizing control variable that inhibits the properties of eq. (A.55).

Example A.2 ***CSTR revisited***
For the CSTR example, we have that the optimal change in the measurements from the nominal optimal value k_{10} to k_1 is given by eq. (A.53) and further we have that

$$\begin{bmatrix}\Delta y_1^{opt}\\ \Delta y_2^{opt}\end{bmatrix} = \begin{bmatrix}C_A^{opt}(k_1) - C_A^{opt}(k_{10})\\ C_{A,i}^{opt}(k_1) - C_{A,i}^{opt}(k_{10})\end{bmatrix} = \begin{bmatrix}\frac{\tau}{2}\frac{k_1-k_{10}}{k_2\tau+1}\\ \\ \frac{\tau^2}{2}\frac{k_1^2-k_{10}^2}{(k_2\tau+1)^2}\end{bmatrix} \tag{A.68}$$

The requirement for a perfect self-optimizing variable is given in eq. (A.58), and we see that

$$\mathbf{h}\cdot\mathcal{F} = [h_1\ h_2]\cdot[\mathcal{F}_1\ \mathcal{F}_2]^T = h_1\mathcal{F}_1 + h_2\mathcal{F}_2 = 0 \Rightarrow h_1 = -\frac{h_2\mathcal{F}_2}{\mathcal{F}_1} \tag{A.69}$$

As is evident, the solution of eq. (A.69) has an infinite number of solution. One solution correspond to setting

$$h_2 = -1 \tag{A.70}$$

which leads to

$$[h_1\ h_2] = [\frac{(k_{10}+k_1)\tau}{k_2\tau+1} \quad -1] \tag{A.71}$$

The self-optimizing control variable is then

$$\Delta C_c = [\frac{(k_{10}+k_1)\tau}{k_2\tau+1} \quad -1][\Delta C_A \quad \Delta C_{A,i}]^T \tag{A.72}$$

and we need an estimate or measurement of the uncertain parameter k_1.

To illustrate, consider the plot of the dynamic response for a $\pm 1\%$ change in E_1 (assuming that the uncertainty in the parameter k_1 stems from E_1), see Figure A.3 for three different controlled variables, namely the self-optimizing variable as given by eq. (A.72) and controlling C_A and C_B at their respective nominal value. As is evident from Figure A.3 is that the proposed candidate, track the steady state optimality perfectly, with nominal optimal setpoint. The drawback is that the disturbances need to be measured directly or inferred from secondary measurements.

For this simple case, $\mathcal{F}$ are almost linear in the uncertain parameter k_1 so using a linearized version of eq. (A.68) yields similar self-optimizing properties. Alternatively, using $\mathbf{y}^T = [k_1\ C_A]$ as measurements (measuring the disturbance) we need $n_y = 2$ measurements and

$$\begin{bmatrix}\Delta y_1^{opt}\\ \Delta y_2^{opt}\end{bmatrix} = \begin{bmatrix}1\\ \frac{\tau/2}{k_2\tau+1}\end{bmatrix}(k_1 - k_{10}) \tag{A.73}$$

is linear in k_1 and the resulting in constant coefficients h_i.

By selecting controlled variables using the above methods, we need to ensure that the coefficient vector $\mathbf{h}$ is not singular (resulting in zero gain).

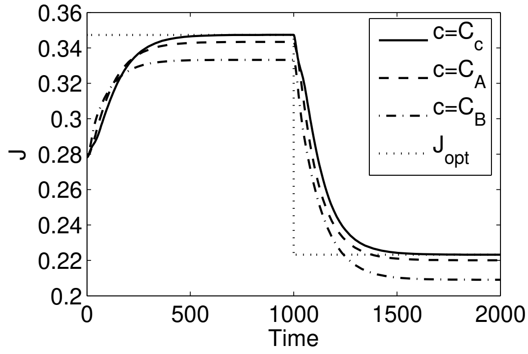

(a) Plot of the objective J for three different structures

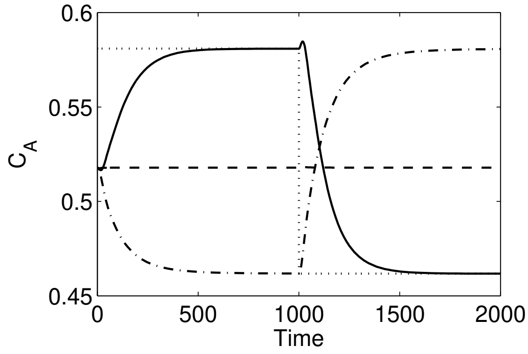

(b) Plot of composition of component A, C_A, for three different structures

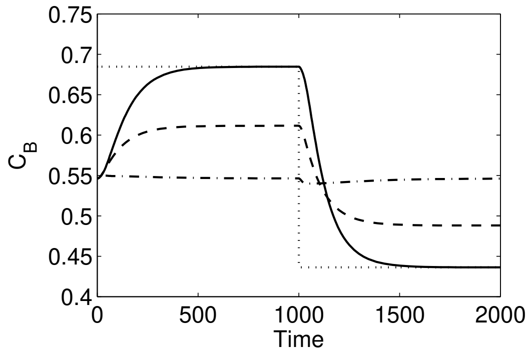

(c) Plot of composition of component B, C_B, for three different structures

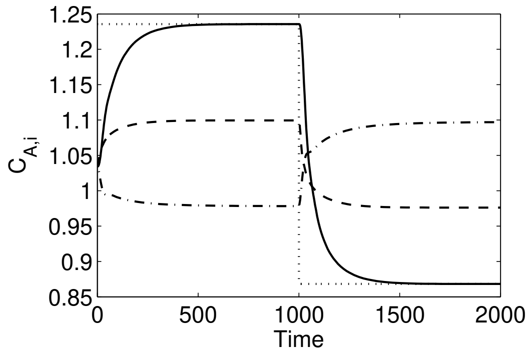

(d) Plot of composition of A in the input stream, $C_{A,i}$, for three different structures

Figure A.3: *Responses for a step in E_1 at $t = 0$ and at $t = 1000$ for three different candidate controlled variables. The steady-state optimal values correspond to the dotted lines.*

A.6 Conclusions

In this paper we extend the null space method. We assume that the objective function is second order in the states, inputs and disturbances, while the equality constraints are linear in the states and inputs, but non-linear in the uncertain parameters (disturbances). A method for selecting self-optimizing controlled variables are presented. The proposed ideas are illustrated on a simple CSTR-example.

Bibliography

Alstad, V. and Skogestad, S. (2004). Combinations of measurements as controlled variables; Application to a petlyuk distillation column. *in the IFAC Symposium on Advanced Control of Chemical Processes (ADCHEM) 2003, (Hong Kong).*

Biegler, L., Cervantes, A., and Wächter, A. (2002). Advances in simultaneous strategies for dynamic process optimization. *Chem. Eng. Sci.*, 57:575–593.

Cutler, C. and Perry, R. (1983). Real-time optimization with multivariable control is required to maximize profits. *Comput. Chem. Eng.*, 7(5):663–667.

Govatsmark, M. (2003). *Integrated optimization and control*. PhD thesis, Norwegian University of Science and Technology.

Halvorsen, I., Skogestad, S., Morud, J., and Alstad, V. (2003). Optimal selection of controlled variables. *Ind. Eng. Chem. Res.*, 42(14):3273–3284.

Maarleveld, A. and Rijnsdorp, J. (1970). Constraint control on distillation columns. *Automatica*, 6(1):51–58. 1.

Marlin, T. and Hrymak, A. (1997). Real-time optimization of continous processes. *American Institute of Chemical Engineering Symposium Series - Fifth International Conference on Chemical Process Control*, 93:85–112.

Morari, M., Stephanopoulos, G., and Arkun, Y. (1980). Studies in the synthesis of control structures for chemical processes. Part I: Formulation of the problem, process decomposition and the classification of the controller task. Analysis of the optimizing control structures. *AIChE Journal*, 26(2):220–232.

Morud, J. (1995). *Studies on the dynamics and operation of integrated plants*. PhD thesis, Norwegian Institute of Technology, Trondheim.

Skogestad, S. (2000). Plantwide control: The search for the self-optimizing control structure. *J. Proc. Control*, 10:487–507.

Stengel, R. (1993). *Optimal control and estimation*. Dover Publications Inc.

Appendix B

Taylor series expansion of the loss function

An alternative derivation of the Taylor series expansion of the loss function is presented here. In Halvorsen et al. (2003), a second order accurate Taylor series expression of the objective function was given as:

$$\begin{aligned} J(\mathbf{u},\mathbf{d}) = J^* + \mathbf{J}_u^T(\mathbf{u}-\mathbf{u}^*) + \mathbf{J}_d^T(\mathbf{d}-\mathbf{d}^*) + \frac{1}{2}(\mathbf{u}-\mathbf{u}^*)^T\mathbf{J}_{uu}(\mathbf{u}-\mathbf{u}^*) \\ + (\mathbf{d}-\mathbf{d}^*)^T\mathbf{J}_{du}(\mathbf{u}-\mathbf{u}^*) + \frac{1}{2}(\mathbf{d}-\mathbf{d}^*)^T\mathbf{J}_{dd}(\mathbf{d}-\mathbf{d}^*) + \mathcal{O}^3 \end{aligned} \tag{B.1}$$

where $\mathbf{J}_{uu}$ is the second derivative of the cost function with respect to $\mathbf{u}$, etc. and $(\mathbf{u}^*, \mathbf{d}^*)$ is the nominal point in which we expand around. Assume that the nominal point is optimal such that $(\mathbf{u}^*, \mathbf{d}^*) = \mathbf{u}^{opt}(\mathbf{d}^*), \mathbf{d}^*)$, then $\mathbf{J}_u = 0$. Further we have that the optimal input is given by

$$\frac{\partial J}{\partial \mathbf{u}^T} = \frac{\partial J}{\partial(\mathbf{u}-\mathbf{u}^*)^T} = 0 \tag{B.2}$$

then

$$\begin{aligned} \frac{\partial J}{\partial(\mathbf{u}-\mathbf{u}^*)^T} &= \frac{1}{2}\mathbf{J}_{uu}(\mathbf{u}^{opt}-\mathbf{u}^*) + \frac{1}{2}\mathbf{J}_{uu}^T(\mathbf{u}^{opt}-\mathbf{u}^*) + (\mathbf{d}-\mathbf{d}^*)^T\mathbf{J}_{du} \\ &= \mathbf{J}_{uu}(\mathbf{u}^{opt}-\mathbf{u}^*) + (\mathbf{d}-\mathbf{d}^*)^T\mathbf{J}_{du} = 0 \end{aligned} \tag{B.3}$$

since $\mathbf{J}_{uu} = \mathbf{J}_{uu}^T$. If we assume that the optimal point is unique, then in the case of minimum (or maxima in case of maximization) $\mathbf{J}_{uu}$ must be positive definite (negative definite), and we have that $\mathbf{J}_{uu} = \mathbf{J}_{uu}^T$. The objective function for the optimum input $\mathbf{u} = \mathbf{u}^{opt}$ is

$$\begin{aligned} J(\mathbf{u}^{opt},\mathbf{d}) = J^* + \mathbf{J}_d^T(\mathbf{d}-\mathbf{d}^*) + \frac{1}{2}(\mathbf{u}^{opt}-\mathbf{u}^*)^T\mathbf{J}_{uu}(\mathbf{u}^{opt}-\mathbf{u}^*) \\ + (\mathbf{d}-\mathbf{d}^*)^T\mathbf{J}_{du}(\mathbf{u}^{opt}-\mathbf{u}^*) + \frac{1}{2}(\mathbf{d}-\mathbf{d}^*)^T\mathbf{J}_{dd}(\mathbf{d}-\mathbf{d}^*) + \mathcal{O}^3 \end{aligned} \tag{B.4}$$

and the loss is given by the difference from eq. (B.1) and (B.4)

$$
\begin{aligned}
L(\mathbf{u},\mathbf{d}) &= J(\mathbf{u},\mathbf{d}) - J(\mathbf{u}^{opt},\mathbf{d}) \\
&= \mathbf{J}_d^T(\mathbf{d}-\mathbf{d}^*) + \frac{1}{2}(\mathbf{u}-\mathbf{u}^*)^T\mathbf{J}_{uu}(\mathbf{u}-\mathbf{u}^*) + (\mathbf{d}-\mathbf{d}^*)^T\mathbf{J}_{du}(\mathbf{u}-\mathbf{u}^*) \\
&\quad - \mathbf{J}_d^T(\mathbf{d}-\mathbf{d}^*) - \frac{1}{2}(\mathbf{u}^{opt}-\mathbf{u}^*)^T\mathbf{J}_{uu}(\mathbf{u}^{opt}-\mathbf{u}^*) - (\mathbf{d}-\mathbf{d}^*)^T\mathbf{J}_{du}(\mathbf{u}^{opt}-\mathbf{u}^*)
\end{aligned} \tag{B.5}
$$

By recognizing that $(\mathbf{x}-\mathbf{y})^T\mathbf{A}(\mathbf{x}-\mathbf{y}) = \mathbf{x}^T\mathbf{A}\mathbf{x} - \mathbf{x}^T\mathbf{A}\mathbf{y} - \mathbf{y}^T\mathbf{A}\mathbf{x} + \mathbf{x}^T\mathbf{A}\mathbf{x}$ we have

$$
\begin{aligned}
L(\mathbf{u},\mathbf{d}) &= \frac{1}{2}\left(\mathbf{u}^T\mathbf{J}_{uu}\mathbf{u} - \mathbf{u}^T\mathbf{J}_{uu}\mathbf{u}^* - \mathbf{u}^*\mathbf{J}_{uu}\mathbf{u} + \mathbf{u}^{*T}\mathbf{J}_{uu}\mathbf{u}^*\right) \\
&\quad - \frac{1}{2}\left(\mathbf{u}^{optT}\mathbf{J}_{uu}\mathbf{u}^{opt} - \mathbf{u}^{optT}\mathbf{J}_{uu}\mathbf{u}^* - \mathbf{u}^*\mathbf{J}_{uu}\mathbf{u}^{opt} + \mathbf{u}^{*T}\mathbf{J}_{uu}\mathbf{u}^*\right) + (\mathbf{d}-\mathbf{d}^*)^T\mathbf{J}_{du}\left(\mathbf{u}-\mathbf{u}^{opt}\right) \\
&= \frac{1}{2}\mathbf{u}^T\mathbf{J}_{uu}\mathbf{u} - \mathbf{u}^T\mathbf{J}_{uu}\mathbf{u}^* - \frac{1}{2}\mathbf{u}^{optT}\mathbf{J}_{uu}\mathbf{u}^{opt} + \mathbf{u}^{optT}\mathbf{J}_{uu}\mathbf{u}^* + (\mathbf{d}-\mathbf{d}^*)^T\mathbf{J}_{du}\left(\mathbf{u}-\mathbf{u}^{opt}\right)
\end{aligned} \tag{B.6}
$$

since $\mathbf{u}^T\mathbf{J}_{uu}\mathbf{u}^* = \mathbf{u}^{*T}\mathbf{J}_{uu}\mathbf{u}$ and $\mathbf{u}^{optT}\mathbf{J}_{uu}\mathbf{u}^* = \mathbf{u}^{*T}\mathbf{J}_{uu}\mathbf{u}^{opt}$. Using eq. (B.3) we have

$$
\begin{aligned}
L(\mathbf{u},\mathbf{d}) &= \frac{1}{2}\mathbf{u}^T\mathbf{J}_{uu}\mathbf{u} - \mathbf{u}^T\mathbf{J}_{uu}\mathbf{u}^* - \frac{1}{2}\mathbf{u}^{optT}\mathbf{J}_{uu}\mathbf{u}^{opt} + \mathbf{u}^{optT}\mathbf{J}_{uu}\mathbf{u}^* + (\mathbf{d}-\mathbf{d}^*)^T\mathbf{J}_{du}\left(\mathbf{u}-\mathbf{u}^{opt}\right) \\
&= \frac{1}{2}\mathbf{u}^T\mathbf{J}_{uu}\mathbf{u} - \mathbf{u}^T\mathbf{J}_{uu}\mathbf{u}^* - \frac{1}{2}\mathbf{u}^{optT}\mathbf{J}_{uu}\mathbf{u}^{opt} - \mathbf{u}^{optT}\mathbf{J}_{uu}\mathbf{u}^* - (\mathbf{u}^{optT}-\mathbf{u}^*)\mathbf{J}_{uu}(\mathbf{u}-\mathbf{u}^{opt}) \\
&= \frac{1}{2}\mathbf{u}^T\mathbf{J}_{uu}\mathbf{u} - \mathbf{u}^T\mathbf{J}_{uu}\mathbf{u}^* - \frac{1}{2}\mathbf{u}^{optT}\mathbf{J}_{uu}\mathbf{u}^{opt} - \mathbf{u}^{optT}\mathbf{J}_{uu}\mathbf{u}^* - \mathbf{u}^{optT}\mathbf{J}_{uu}\mathbf{u} \\
&\quad + \mathbf{u}^{optT}\mathbf{J}_{uu}\mathbf{u}^{opt} - \mathbf{u}^{*T}\mathbf{J}_{uu}\mathbf{u}^{opt} + \mathbf{u}^{*T}\mathbf{J}_{uu}\mathbf{u}^{opt}
\end{aligned} \tag{B.7}
$$

and we then have that

$$
\begin{aligned}
L(\mathbf{u},\mathbf{d}) &= \frac{1}{2}\mathbf{u}^T\mathbf{J}_{uu}\mathbf{u} + \frac{1}{2}\mathbf{u}^{optT}\mathbf{J}_{uu}\mathbf{u}^{opt} - \frac{1}{2}\mathbf{u}^{optT}\mathbf{J}_{uu}\mathbf{u} - \frac{1}{2}\mathbf{u}^T\mathbf{J}_{uu}\mathbf{u}^{opt} \\
&= (\mathbf{u}-\mathbf{u}^{opt})^T\mathbf{J}_{uu}(\mathbf{u}-\mathbf{u}^{opt})
\end{aligned} \tag{B.8}
$$

which is the same as given in Halvorsen et al. (2003). Thus, the expansion around a “moving optimal point” follows directly from the equations and using the optimality condition. In Halvorsen et al. (2003), a distinction was made between the Hessian from the expansion around the stationary nominal point $(\mathbf{u}^*, \mathbf{d}^*)$ and the “moving nominal point” $(\mathbf{u}^{opt}(\mathbf{d}), \mathbf{d})$. However, the derivation above shows that this distinction is not necessary when we assume that the nominal point is optimal. The same Hessian $\mathbf{J}_{uu}$ applies in both cases.

Bibliography

Halvorsen, I., Skogestad, S., Morud, J., and Alstad, V. (2003). Optimal selection of controlled variables. *Ind. Eng. Chem. Res.*, 42(14):3273–3284.

Appendix C

Perfect steady-state indirect control

Eduardo S. Hori, Sigurd Skogestad[1] and Vidar Alstad
Department of Chemical Engineering
Norwegian University of Science and Technology
N–7491 Trondheim Norway

Ind.Eng.Chem.Res., In press

Indirect control is commonly used in industrial applications where the primary controlled variable is not measured. This paper considers the case of "perfect indirect control" where one attempts to control a combination of the available measurements such that there is no effect of disturbances at steady-state. This is always possible provided the number of measurements is equal to the number of independent variables (inputs plus disturbances). It is further shown how extra measurements may be used to minimize the effect of measurement error. The results in this paper also provide a nice link to previous results on inferential control, perfect disturbance rejection and decoupling (DRD), and self-optimizing control.

C.1 Introduction

Indirect control (Skogestad and Postlethwaite, 1996) is used when we for some reason cannot control the "primary" outputs y_1. Instead, we aim at indirectly controlling y_1 by controlling the "secondary" variables c (often denoted y_2) (Skogestad and Postlethwaite, 1996). More precisely,

> **Indirect control** is when we aim at (indirectly) keeping the primary variables y_1 close to their setpoints y_{1s}, by controlling the secondary variables c at constant setpoints c_s.

[1]Corresponding author. E-mail: skoge@chemeng.ntnu.no; Fax: +47-7359-4080; Phone: +47-7359-4154

An example is control of temperature (c) in a distillation column, in order to indirectly achieve composition control (y_1).

A less obvious example of indirect control, is the selection of "control configurations" in distillation columns. The term "control configuration" here refers to which two flows or flow combinations are left as degrees of freedom after we have closed the stabilizing loops for the condenser and reboiler levels. Ideally, keeping the selected two flow combinations (c) constant will indirectly lead to good control of the product compositions (primary outputs, y_1). For example, in the LV-configuration the condenser and reboiler levels are controlled such that the flows L (reflux) and V (boilup) are left as free variables for the layer above. However, keeping these flows constant (selecting L and V as c's) gives large changes in the product compositions (y_1) when there are disturbances in the feed flowrate. Instead, one may use the L/D V/B-configuration. In this case, keeping L/D and V/B constant (c's) gives almost constant product compositions (good control of y_1) when there disturbances in the feed flowrate. However, the changes in the product composition are large (poor control of y_1) for feed composition disturbances (e.g. (Skogestad et al., 1990)). Häggblom and Waller (1990) looked for a flow combination that handles all disturbances, and proposed the "disturbance rejecting and decoupling" configuration. This partially motivated our work, and is discussed in more detail below.

In the following, we let the set y denote the "candidate" measured variables for indirect control. We will refer to the entire set y as "measurements", but note that we in this set also include the original manipulated variables (inputs) (e.g. L, V, D and B for the distillation example). In this paper, we select as "secondary" controlled variables c a linear combination of the variables y,

$$\Delta c = H \Delta y \tag{C.1}$$

In other words, we want to find a good choice for the matrix H. In the simplest case individual measurements y are selected as c's, and the matrix H consists of zeros and ones. However, more generally we allow for combinations (functions) of the available measurements y, and H is a "full" matrix with all entries nonzero. In the paper, we show that if we have as many measurements as there are independent variables (inputs plus disturbances), then we can always achieve at steady state "perfect indirect control" with perfect disturbance rejection and in addition with a decoupled response from the setpoints c_s (the "new" inputs) to the primary variables y_1.

Indirect control may be viewed as a special case of "self-optimizing control" (Halvorsen et al., 2003). This is clear from the definition:

> **Self-optimizing control** (Skogestad, 2000) is when we can achieve acceptable (economic) loss with constant setpoint values for the controlled variables c (without the need to re-optimize when disturbances occur).

In most cases the "loss" is an economic loss, but for indirect control it is the setpoint deviation, i.e. $L = \|y_1 - y_{1s}\|$. The implications of viewing indirect control as a special case of self-optimizing control are discussed later in the paper.

Another related idea is inferential control (Weber and Brosilow, 1972). However, in inferential control the basic idea is to use the measurements y to estimate the primary variables y_1, whereas the objective of indirect control is to directly control a combination c of the measurements y.

In the paper we only consider the steady-state behavior. The notation in this paper largely follows that used by Halvorsen et al. (2003).

C.2 Perfect indirect control

Consider a setpoint problem where the objective is to keep the "primary" controlled variables y_1 at their setpoints y_{1s}. We also have

u: Inputs (independent variables available for control of y_1)
d: Disturbances (independent variables outside our control)
y: Measurements (including u and possible measured d's)

Problem definition: *Find a set of (secondary) controlled variables $c = h(y)$ such that a constant setpoint policy ($c = c_s$) indirectly results in acceptable control of the primary outputs (y_1).*

We make the following assumptions

1. The number of secondary controlled variables c is equal to the number of inputs u ($n_c = n_u$), and they are independent such that it is possible to adjust u to get $c = c_s$.
2. We consider the local behavior based on linear models.
3. We only consider the steady-state behavior.
4. We neglect the control error (including measurement noise), that is, we assume that we achieve $c = c_s$ at steady state (this assumption is relaxed later).
5. We assume that the nominal operating point (u^*, d^*) is optimal, that is, at the nominal point (where $d = d^*$ and $c = c_s$) we have $y_1^* = y_{1s}$.

The linear models relating the variables are

$$\Delta y = G^y \Delta u + G_d^y \Delta d = \tilde{G}^y \begin{bmatrix} \Delta u \\ \Delta d \end{bmatrix} \tag{C.2}$$

$$\Delta y_1 = G_1 \Delta u + G_{d1} \Delta d = \tilde{G}_1 \begin{bmatrix} \Delta u \\ \Delta d \end{bmatrix} \tag{C.3}$$

$$\Delta c = G \Delta u + G_d \Delta d = \tilde{G} \begin{bmatrix} \Delta u \\ \Delta d \end{bmatrix} \tag{C.4}$$

where $\Delta u = u - u^*$, etc. From (C.4) we can obtain the inputs Δu needed to get a given change Δc:

$$\Delta u = G^{-1} \Delta c - G^{-1} G_d \Delta d$$

where G^{-1} exists because of assumption 1. Substituting this into (C.3) yields the corresponding change in the primary variables

$$\Delta y_1 = \underbrace{G_1 G^{-1}}_{P_c} \Delta c + \underbrace{(G_{d1} - G_1 G^{-1} G_d)}_{P_d} \Delta d \tag{C.5}$$

The "partial disturbance gain" P_d gives the effect of disturbances d on the primary output y_1 with closed-loop ("partial") control of the variables c, and P_c gives the effect on y_1 of changes in c (e.g., due to a setpoint change c_s).

The controlled variables c are combinations of the measurements, $\Delta c = H\Delta y$, and it follows from (C.2) and (C.4) that

$$G = HG^y; \quad G_d = HG_d^y; \quad \tilde{G} = H\tilde{G}^y \tag{C.6}$$

Ideally, we would like to choose H such that $P_d = 0$. Somewhat surprisingly, at least from a physical point of view, it turns out that this is always possible provided we have enough measurements y, and that we in fact have additional degrees of freedom left which we may use, for example, to specify P_c. For example, it may be desirable to have $P_c = I$, because this (at least at steady state) gives a decoupled response from c_s (which are our "new inputs") to the primary controlled variables y_1.

> **"Perfect indirect control" (refined problem definition):** *Find a linear measurement combination, $\Delta c = H\Delta y$, such that at steady state we have perfect disturbance rejection ($P_d = 0$) and a specified setpoint response (i.e. $P_c = P_{c0}$, where P_{c0} is given.)*

We make the following additional assumptions:

6. The number of primary outputs y_1 is equal to the number of secondary controlled variables c (i.e., $n_{y_1} = n_c$), such that P_{c0} is invertible.

7. The number of (independent) measurements y is equal to the number of inputs plus disturbances ($n_y = n_u + n_d$), such that the matrix $\tilde{G}^y$ is invertible (this assumption is relaxed later).

Solution to refined problem definition: We have $\Delta c = H\Delta y$ and want to find H such that

$$\Delta y_1 = P_{c0}\Delta c + 0 \cdot \Delta d$$

This gives $\Delta y_1 = P_{c0} H \Delta y$, and using (C.2) and (C.3) gives

$$\Delta y_1 = \tilde{G}_1 \begin{bmatrix} \Delta u \\ \Delta d \end{bmatrix} = P_{c0} H \tilde{G}^y \begin{bmatrix} \Delta u \\ \Delta d \end{bmatrix}$$

which gives $\tilde{G}_1 = P_{c0} H \tilde{G}^y$ or

$$H = P_{c0}^{-1} \tilde{G}_1 {\tilde{G}^y}^{-1} \tag{C.7}$$

which is the solution to the refined problem definition.

Extension 1. More generally, we may specify $P_d = P_{d0}$ (where P_{d0} is given and may be nonzero) and the resulting choice for H is

$$H = P_{c0}^{-1} \hat{G}_1 \tilde{G^y}^{-1} \tag{C.8}$$

where

$$\hat{G}_1 = \begin{bmatrix} G_1 & G_{d1} - P_{d0} \end{bmatrix} = \tilde{G}_1 - \begin{bmatrix} 0 & P_{d0} \end{bmatrix} \tag{C.9}$$

Extension 2. If the measurements y are not independent or closely correlated, then the matrix $\tilde{G^y}$ in (C.7) and (C.8) will be singular or close to singular, resulting in infinite or large elements in $\tilde{G^y}^{-1}$. In this case, one needs to consider another set of measurements y or use more measurements. This is discussed separately below.

C.3 Application to control configurations for distillation

The results of Häggblom and Waller (1990) on control configurations for "disturbance rejection and decoupling (DRD) of distillation" provide an interesting special case of the above results, and actually motivated their derivation. Häggblom and Waller (1990) showed that one could derive a DRD control configuration that achieved

1. Perfect disturbance rejection with the new loops closed (i.e. $P_d = 0$ in our notation).

2. Decoupled response from the new manipulators to the primary outputs (i.e. $P_c = I$ in our notation).

Häggblom and Waller (1990) derived this for distillation column models, and made no attempt of generalizing their results. However, they can be shown to be a special case of the above results when we introduce

$$y_1 = \begin{bmatrix} y_D \\ x_B \end{bmatrix}, \quad y = \begin{bmatrix} L \\ V \\ D \\ B \end{bmatrix}, \quad u = \begin{bmatrix} L \\ V \end{bmatrix}, \quad d = \begin{bmatrix} F \\ z_F \end{bmatrix} \tag{C.10}$$

Comments:

1. The primary outputs y_1 are the product compositions (bottoms and distillate product)

2. The measured variables are $y = u_0$ where $u_0 = \begin{bmatrix} L & V & D & B \end{bmatrix}^T$ (flows) are the original manipulated inputs for the distillation column.

3. The inputs u (a subset of u_0) are the remaining two inputs after satisfying the steady-state constraints of constant M_B and M_D (reboiler and condenser level have no steady-state effect). In (C.10) we have selected $u = \begin{bmatrix} L & V \end{bmatrix}^T$, but it actually does not matter which two variables we choose to include in u, as long as the variables in u are independent.

4. The disturbances d are feed flowrate and feed composition.

Note that we in (C.10) only allow for flows as measurements, $y = u_0$. This implies that we want to achieve indirect control by keeping flow combinations at constant values. This implicitly requires that the feed composition z_F has an effect on at least one of the flowrates. This will generally be satisfied in practice where u_0 represents mass or volumetric flows, but it will not be satisfied in the "academic" case where we use the "constant molar flows" assumption (simplified energy balance) and assume that we manipulate molar flows.

We want to use a combination $\Delta c = H\Delta y$ of the measurements y as controlled variables,

$$\Delta c_1 = h_{11}\Delta L + h_{12}\Delta V + h_{13}\Delta D + h_{14}\Delta B$$
$$\Delta c_2 = h_{21}\Delta L + h_{22}\Delta V + h_{23}\Delta D + h_{24}\Delta B$$

From (C.7) we derive the choice for H that gives "perfect indirect control" at steady state, and we find that it is identical to that of the DRD-configuration in Häggblom and Waller (1990).

As a specific example, consider the model of a 15-plate pilot-plant ethanol-water distillation column studied by Häggblom and Waller (1990). The steady-state model in terms of $u = \begin{bmatrix} L & V \end{bmatrix}^T$ (LV-configuration) is

$$\begin{bmatrix} \Delta y_D \\ \Delta x_B \end{bmatrix} = G_1 \begin{bmatrix} \Delta L \\ \Delta V \end{bmatrix} + G_{d1} \begin{bmatrix} \Delta F \\ \Delta z_F \end{bmatrix}$$

$$y = \begin{bmatrix} \Delta L \\ \Delta V \\ \Delta D \\ \Delta B \end{bmatrix} = G^y \begin{bmatrix} \Delta L \\ \Delta V \end{bmatrix} + G_d^y \begin{bmatrix} \Delta F \\ \Delta z_F \end{bmatrix}$$

with (Häggblom and Waller, 1990)

$$G_1 = \begin{bmatrix} -0.045 & 0.048 \\ -0.23 & 0.55 \end{bmatrix} \quad G_{d1} = \begin{bmatrix} -0.001 & 0.004 \\ -0.16 & -0.65 \end{bmatrix} \tag{C.11}$$

$$G^y = \begin{bmatrix} 1 & 0 \\ 0 & 1 \\ -0.61 & 1.35 \\ 0.61 & -1.35 \end{bmatrix} \quad G_d^y = \begin{bmatrix} 0 & 0 \\ 0 & 0 \\ 0.056 & 1.08 \\ 0.944 & -1.08 \end{bmatrix} \tag{C.12}$$

From (C.7) we derive that the following variable combination gives perfect disturbances rejection and decoupling (DRD):

$$H = \begin{bmatrix} -0.0427 & 0.0430 & 0.0025 & -0.0012 \\ -0.5971 & 1.3625 & -0.7281 & -0.1263 \end{bmatrix} \tag{C.13}$$

which is identical with the DRD-structure found in Häggblom and Waller (1990).

We note that our derivation is much simpler. In addition, our results generalize the results in Häggblom and Waller (1990) in two ways:

1. The results are generalized to other measurements than the choice $y = u_0$ (flows). For example, it is possible to derive a DRD-configuration based on keeping two combinations of four temperature measurements constant.

2. The results are generalized to other processes than distillation.

A further extensions is discussed next.

C.4 Extension 2: Selection of measurements and effect of measurement error

Above we assumed that the number of independent measurements was equal to the number of independent variables, i.e. $n_y = n_u + n_d$ (Assumption 7), and neglected the effect of measurement error (noise) and control error by assuming that we can achieve perfect control of c, i.e. $c = c_s$ at steady state (Assumption 4). These assumptions are related, since the violation of Assumption 7, will lead to sensitivity the measurement error neglected in Assumption 4.

Let n^y denote the measurement error associated with the measurements y. Since $\Delta c = H\Delta y$, the effect on the controlled variables c is $n^c = c - c_s = Hn^y$. This corresponding error in the primary outputs is then

$$\Delta y_1 = P_c H n^y \tag{C.14}$$

From (C.14) we have that the effect of measurement error is large if the norm of the matrix $P_c H$ is large. With "perfect indirect control" we have from (C.7) that $P_c H = \tilde{G}_1 {\tilde{G}^y}^{-1}$ which is large if the measurements are closely correlated since then $\tilde{G}^y$ is close to singular and the elements in ${\tilde{G}^y}^{-1}$ are large.

If we have extra measurements, $n_y > n_u + n_d$, then we may use these extra measurements to affect $P_c H$ and thus minimize the effect of the measurement noise. This may be done in two ways as discussed below:

(a) Select the best subset of all the measurements, ("use the most independent measurements").

(b) Use all the measurements and select the best combination ("average out the measurement error").

Method (b), where we use all the measurements, it always better mathematically, but method (a), where we use only a subset, may be preferred in practice because it uses fewer measurements. In addition, there may cases where we have too few or correlated measurements, so that it is impossible to achieve "perfect" disturbance rejection. We would then like to:

(c) Select (control) a combination of the available measurements so that the effect of disturbances on the primary variables is minimized.

(a) Best subset of measurements. This is the case discussed earlier where we select as many measurements as there are inputs and disturbances ($n_y = n_u + n_d$). The matrix $\tilde{G}^y$ is then invertible and from (C.7) we have for "perfect indirect control" that

$$P_c H = \tilde{G}_1 {\tilde{G}^y}^{-1} \tag{C.15}$$

The issue here is which subset of the measurements to select.

First, we note that the choice of P_c does not affect the sensitivity to measurement error $\tilde{G}_1 {\tilde{G}^y}^{-1}$, that is, the "degree of freedom" in selecting P_c is not useful in terms of measurement error. Also note that the choice of measurements y does not influences the matrix $\tilde{G}_1$. However, the choice of measurements y does affect the matrix $\tilde{G}^y$, and if we have extra measurements then we should select them such that the effect of measurement error is minimized, that is, such that $\tilde{G}_1 {\tilde{G}^y}^{-1}$ is minimized. To choose the best measurements we first need to scale the measured variables:

- Each measured variable y is scaled such that its associated measurement error n^y is of magnitude 1.

Since the induced 2-norm or maximum singular value of a matrix, $\bar{\sigma}$, provides the worst-case amplification in terms of the two-norm, we have from (C.14) and (C.15) that

$$\max_{\|n^y\|_2 \le 1} \|\Delta y_1\|_2 = \bar{\sigma}(\tilde{G}_1 {\tilde{G}^y}^{-1}) \le \bar{\sigma}(\tilde{G}_1)\bar{\sigma}({\tilde{G}^y}^{-1}) = \bar{\sigma}(\tilde{G}_1)/\underline{\sigma}(\tilde{G}^y) \tag{C.16}$$

This has the following implications:

1. (Optimal) In order to minimize the worst-case value of $\|\Delta y_1\|_2$ for all $\|n^y\|_2 \le 1$, select measurements such that $\bar{\sigma}(\tilde{G}_1 {\tilde{G}^y}^{-1})$ is minimized.
2. (Suboptimal) Recall that the measurement selection does not affect $\tilde{G}_1$. From the inequality in (C.16) it then follows that the effect of the measurement error n^y will be small when $\underline{\sigma}(\tilde{G}^y)$ (the minimum singular value of $\tilde{G}^y$) is large. It is therefore reasonable to select measurements y such that $\underline{\sigma}(\tilde{G}^y)$ is maximized. Here $\tilde{G}^y$ represents the effect of u and d on y.

(b) Best combination of all the measurements. Let $\tilde{G}^y_{\text{all}}$ represent the effect of the independent variables on all the available measurements. A derivation similar to (C.7) gives that "perfect indirect control" is achieved when

$$H\tilde{G}^y_{\text{all}} = P_{c0}^{-1}\tilde{G}_1 \tag{C.17}$$

However, we now have $n_y > n_u + n_d$, and (C.17) has an infinite number of solutions for H. We want to find the solution that minimizes the effect of measurement error on the primary outputs y_1. The solution that minimizes the 2-norm of y_1 is the one with the smallest 2-norm of P_cH, see (C.14). With $P_c = P_{c0} = I$ (decoupling) this is obtained from (C.17) by making use of the pseudo inverse:

$$H = \tilde{G}_1 {\tilde{G}^y_{\text{all}}}^{\dagger} \tag{C.18}$$

In this case ${G^y_{\text{all}}}^\dagger$ is the left inverse of G^y_{all}. With this choice the effect of measurement error is

$$P_c H = \tilde{G}_1 {\tilde{G}^{\tilde{y}}_{\text{all}}}^\dagger$$

(c) Few measurements. We here consider the case with fewer measurements than independent variables, i.e. $n_y < n_u + n_d$. In this case, (C.17) has no solution, so perfect disturbance rejection ($P_d = 0$) is not possible. One possibility, is to delete or combine disturbances such that (C.17) has a solution. Another possibility, is to use the pseudo inverse as shown in (C.18),

$$H = \tilde{G}_1 {\tilde{G}^{\tilde{y}}_{\text{all}}}^\dagger \tag{C.19}$$

but in this case the pseudo inverse is the right inverse. This corresponds to selecting H such $\|E\|_2$ is minimized, where $E = P_{c0}^{-1}\tilde{G}_1 - H\tilde{G}^y_{\text{all}}$. This seems reasonable as we can show that $P_d \Delta d = P_{c0}^{-1} E \begin{bmatrix} \Delta u \\ \Delta d \end{bmatrix}$, so a small value of E implies a small value of $P_d \Delta d$, and thus a small disturbance sensitivity.

Comment. It is appropriate at this point to make a comment about the pseudo inverse of a matrix. Above we are looking for the best solution for H that satisfies the equation set $H\tilde{G}^y_{\text{all}} = P_{c0}^{-1}\tilde{G}_1$. In general, we can write the solution of $HA = B$ as $H = BA^\dagger$ where

- $A^\dagger = (A^T A)^{-1} A^T$ is the left inverse for the case when A has full column rank (we have extra measurements). In this case there are an infinite number of solutions and we seek the solution that minimizes H.

- $A^\dagger = A^T (A A^T)^{-1}$ is the right inverse for the case when A has row column rank (we have too few measurements). In this case there is no solution and we seek the solution that minimizes the two-norm of $E = B - HA$ ("regular least squares").

- In the general case with extra measurements, but where some are correlated, A has neither full column or row rank, and the singular value decomposition may be used to compute the pseudo inverse.

C.5 Discussion: Link to previous work

Inferential control. If we choose $P_{c0} = I$, then we find, not unexpectedly, that (C.7) is the same as Brosilow's static inferential estimator; see eq. (2.4) in Weber and Brosilow (1972). To more clearly see the link, recall that the idea in inferential control is to first "infer" from the measurements Δy the inputs and disturbances, and from this estimate the primary output. From (C.2) the inferred input and disturbance is

$$\begin{bmatrix} \Delta u \\ \Delta d \end{bmatrix} = {\tilde{G}^y}^{-1} \Delta y$$

and from (C.3) the resulting estimated value of the primary output is

$$\Delta y_1 = \tilde{G}_1 \tilde{G^y}^{-1} \Delta y$$

On the other hand, in indirect control, the idea is to control a measurement combination, and from (C.7) with $P_c = I$ (that is, we want $\Delta y_1 = \Delta c$) the resulting measurement combination is

$$\Delta c = H \Delta y = \tilde{G}_1 \tilde{G^y}^{-1} \Delta y$$

which is identical to the estimated primary output found with inferential control. The advantage with the derivation in our paper is that it provides a link to control configurations, regulatory control, cascade control, indirect control and self-optimizing control, and also provides the generalization (C.8).

Self-optimizing control. The results in this paper on perfect indirect control provide a nice generalization of the distillation results of Häggblom and Waller (1990), but are themselves a special case of the work of Alstad and Skogestad (2002) on self-optimizing control with perfect disturbance rejection (Alstad and Skogestad, 2002) (Alstad and Skogestad, 2003). To see this link we need to write the cost function as

$$J = \frac{1}{2}(y_1 - y_{1s})^T (y_1 - y_{1s}) \tag{C.20}$$

Differentiation gives

$$J_u = (G_1 \Delta u + G_{d1} \Delta d)^T G_1, \ J_{uu} = G_1^T G_1, \ J_{ud} = G_1^T G_{d1} \tag{C.21}$$

and we can compute the matrix M in the exact method of Alstad and Skogestad (2002) and search for the optimal measurement combination. We find that:

- $P_d = 0$ ("perfect control" with zero sensitivity to disturbances) implies $M_d = 0$ (zero loss for disturbances). To prove this premultiply P_d by $G_1^\dagger$ and note that $G_1^\dagger G_1 = I$ since $G_1^\dagger$ is a left inverse.

- However, unless $n_{y_1} \leq n_u$ we do not have $G_1^\dagger G_1 = I$, so $M_d = 0$ (zero loss) does not generally imply $P_d = 0$ ("perfect control"). This is easily explained: We can only perfectly control as many outputs (y_1) as we have independent inputs (u).

C.6 Conclusions

Indirect control is commonly used in industrial applications where the primary controlled variable is not measured. In this paper we considered the case of "perfect steady-state indirect control" where one attempts to control a combination of the available measurements such that there is no effect of disturbances at steady-state. This is always possible provided the number of measurements is equal to the number of independent variables (inputs plus disturbances). It is further shown how extra measurements may be used to minimize the effect of measurement error. This paper generalizes the work of Häggblom and Waller (1990), but is itself a special case of the work of Halvorsen et al. (2003) and Alstad and Skogestad (2002) on self-optimizing control.

Bibliography

Alstad, V. and Skogestad, S. (2002). Robust operation by controlling the right variable combination. *2002 AIChE Annual Meeting, Indianapolis, USA. (Available from the home page of S. Skogestad).*

Alstad, V. and Skogestad, S. (2003). Combinations of measurements as controlled variables: Application to a petlyuk distillation column. *Preprints IFAC symposium Adchem'03, Hong Kong, June 2003 / Jan. 2004*.

Häggblom, K. and Waller, K. (1990). Control structures for disturbance rejection and decoupling in distillation. *AIChe J.*, pages 1107–1113.

Halvorsen, I., Skogestad, S., Morud, J., and V., A. (2003). Optimal selection of controlled variables. *Ind.Eng.Chem.Res.*, 42(14):3273–3284.

Skogestad, S. (2000). Plantwide control: the search for the self-optimizing control structure. *J. Proc. Control*, 10:487–507.

Skogestad, S., Lundström, P., and Jacobsen, E. (1990). Selecting the best distillation control configuration. *AIChE Journal*, 36(5):753–764.

Skogestad, S. and Postlethwaite, I. (1996). *Multivariable Feedback Control*. John Wiley & Sons.

Weber, R. and Brosilow, C. (1972). The use of secondary measurements to improve control. *AIChE J.*, pages 614–623.

Appendix D

Models and data for oil and gas examples

D.1 Model equations

Here we list the models used for the wells and transportation lines.

Continuity equations

One-dimensional steady-state assumption

$$\frac{\mathrm{d}}{\mathrm{d}x}(\rho u^2) = -\frac{\partial P}{\partial x} - \rho g \frac{\mathrm{d}z}{\mathrm{d}x} - \frac{2\rho u|u|}{D} f \tag{D.1}$$

where ρ is density, u velocity, P pressure, g gravity, D diameter, x axial direction (positive along the flow direction), z the vertical displacement and f the friction factor. Orthogonal collocation is used to discretized the equations. The friction factor f is modeled as (assuming turbulent flow)

$$f = 0.079 Re^{-0.25}/4 \tag{D.2}$$

where Re is the Reynolds number.

Well inflow

$$q = PI(P_r - P) \tag{D.3}$$

where q is the volumetric rate, PI is the production index, P_r is the reservoir pressures and P the pressure in the well.

PVT

Black oil PVT model (Golan and Whitson, 1996). Let m_o be mass of black oil, m_g mas of gas (free and dissolved) and m_s mass of dissolved gas. The amount of dissolved gas is

$$m_s = m_o GOR_s \tag{D.4}$$

where GOR_s is the GOR at standard conditions (stock tank conditions). Let GOR_r be gas oil ratio at reservoir conditions, then

$$GOR(P) = \frac{P - P_s}{P_r - P_s} GOR_r \tag{D.5}$$

where P_s is the standard pressure (stock tank pressure),P the pressure in the well and P_r the pressure in the reservoir. The gas is modeled as ideal gas.

Valve model

The valve is modeled as compressible flow of ideal gas (White, 1999).

$$\dot{m} = \frac{AP}{\sqrt{RT}} \sqrt{\frac{2k}{k-1} \left(\frac{P_s}{P}\right)^{2/k} \left[1 - \left(\frac{P_s}{P}\right)^{(k-1)/k}\right]} \tag{D.6}$$

where A is the area, P_s is the downstream pressure, P the upstream pressure, R the universal gas constant, T the upstream temperature and

$$k = \frac{C_p}{C_v} \tag{D.7}$$

where C_p and C_v are the specific heat capacity.

D.2 Data for Section 10.3

The data used in the simulations are shown in Table D.1

Bibliography

Golan, M. and Whitson, C. H. (1996). *Well perfomance.* Tapir, 2 edition.

White, F. (1999). *Fluid Mechanics.* McGraw-Hill.

Table D.1: *Data for the rate dependent GOR example*

Variable	Value	Units	Description
$\dot{m}_{g,tot}^{max}$	7.1720	kg/s	Max gas capacity
P_s	25	bar	Pressure separator
P_r	155.8	bar	Pressure reservoir all wells
T_r	100	℃	Temperature reservoir
T_s	50	℃	Temperature separator
ρ_o	890	kg/m^3	Black oil density
PI	0.0012	$m^3/s, bar$	Production index W_1
PI	0.0026	$m^3/s, bar$	Production index W_2
PI	0.0025	$m^3/s, bar$	Production index W_3
PI	0.0008	$m^3/s, bar$	Production index W_4
PI	0.0018	$m^3/s, bar$	Production index W_5
L_W	1240	m	Vertical height wells
D_W	0.15	m	Diameter wells
L_T	7500	m	Length transport line
D_T	0.254	m	Diameter transport line
α_T	3	°	Angle transportation line with horizontal
μ_o	0.15	Pa s	Viscosity oil
μ_g	1×10^{-3}	Pa s	Viscosity gas
k	1.4	-	Relative specific heat-capacity

Appendix E

Evaporator-Model equations

The model equations for the Evaporator process, shown in Figure E and as studied in Chapter 11, are given below.

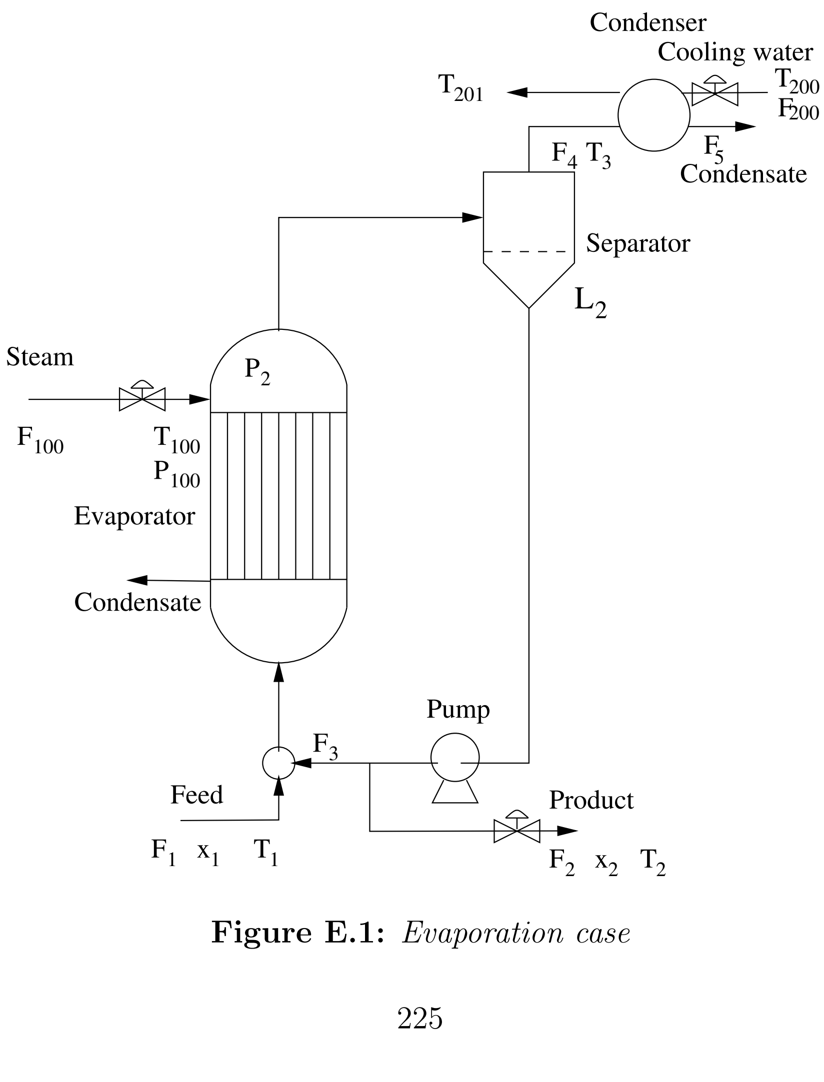

Figure E.1: *Evaporation case*

$$\frac{\mathrm{d}L_2}{\mathrm{d}t} = \frac{F_1 - F_4 - F_2}{20} \tag{E.1}$$

$$\frac{\mathrm{d}x_2}{\mathrm{d}t} = \frac{F_1 x_1 - F_2 x_2}{20} \tag{E.2}$$

$$\frac{\mathrm{d}P_2}{\mathrm{d}t} = \frac{F_4 - F_5}{4} \tag{E.3}$$

$$T_2 = 0.5516P_2 + 0.3126x_2 + 48.43 \tag{E.4}$$

$$T_3 = 0.507P_2 + 55 \tag{E.5}$$

$$F_4 = \frac{Q_{100} - 0.07F_1(T_2 - T_1)}{38.5} \tag{E.6}$$

$$T_{100} = 0.1538P_{100} + 90.0 \tag{E.7}$$

$$Q_{100} = 0.16(F_1 + F_3)(T_{100} - T_2) \tag{E.8}$$

$$F_{100} = \frac{Q_{100}}{36.6} \tag{E.9}$$

$$Q_{200} = \frac{0.9576F_{200}(T_3 - T_{200})}{0.14F_{200} + 6.84} \tag{E.10}$$

$$T_{201} = T_{200} + \frac{13.68(T_3 - T_{200})}{0.14F_{200} + 6.84} \tag{E.11}$$

$$F_5 = \frac{Q_{200}}{38.5} \tag{E.12}$$